BNL- 94830-2011

COMMARA-2.0 Neutron Cross Section Covariance Library

M. Herman, P. Obložinský, C.M. Mattoon[†)], M. Pigni,
S. Hoblit, S.F. Mughabghab, A. Sonzogni

National Nuclear Data Center, Brookhaven National Laboratory
PO Box 5000, Upton, NY 11973
[†)] Present address: Lawrence Livermore National Laboratory, Livermore, California, U.S.A.

P. Talou, M.B. Chadwick, G.M. Hale, A.C. Kahler,
T. Kawano, R.C. Little, P.G. Young

Los Alamos National Laboratory
Los Alamos, NM 87545

March 2011

National Nuclear Data Center
Brookhaven National Laboratory
P.O. Box 5000
Upton, NY 11973-5000
www.nndc.bnl.gov

U.S. Department of Energy
Office of Science, Office of Nuclear Physics

DISCLAIMER

COMMARA-2.0 Neutron Cross Section Covariance Library

Fuel Cycle Research & Development

M. Herman, P. Obložinský, C.M. Mattoon, M. Pigni,
S. Hoblit, S.F. Mughabghab, A. Sonzogni

National Nuclear Data Center, Brookhaven National Laboratory
PO Box 5000, Upton, NY 11973

P. Talou, M.B. Chadwick, G.M. Hale, A.C. Kahler,
T. Kawano, R.C. Little, P.G. Young

Los Alamos National Laboratory
Los Alamos, NM 87545

March 2011

Fuel Cycle Research & Development

SUMMARY

The COMMARA-2.0 covariance library has been developed by BNL-LANL collaboration for Advanced Fuel Cycle Initiative applications over the period of three years, 2008-2010. It contains covariances for 110 materials relevant to fast reactor R&D. The library is to be used together with the ENDF/B-VII.0 central values of the latest official release of US files of evaluated neutron cross sections.

COMMARA-2.0 library contains neutron cross section covariances for 12 light nuclei (coolants and moderators), 78 structural materials and fission products, and 20 actinides. Covariances are given in 33-energy groups, from 10−5 eV to 19.6 MeV, obtained by processing with LANL processing code NJOY using 1/E flux. In addition to these 110 files, the library contains 20 files with nu-bar covariances, 3 files with covariances of prompt fission neutron spectra (238,239,240-Pu), and 2 files with mu-bar covariances (23-Na, 56-Fe).

Over the period of three years several working versions of the library have been released and tested by ANL and INL reactor analysts. Useful feedback has been collected allowing gradual improvements of the library. In addition, QA system was developed to check basic properties and features of the whole library, allowing visual inspection of uncertainty and correlations plots, inspection of uncertainties of integral quantities with independent databases, and dispersion of cross sections between major evaluated libraries.

The COMMARA-2.0 beta version of the library was released to ANL and INL reactor analysts in October 2010. The final version, described in the present report, was released in March 2011.

Table of Contents

COMMARA-2.0 COVARIANCE LIBRARY

1. INTRODUCTION

The cross section covariance library has been under development by BNL-LANL collaborative effort over the last three years. The project builds on two covariance libraries developed earlier, with considerable input from BNL and LANL. In 2006, international effort under WPEC Subgroup 26 produced BOLNA covariance library by putting together data, often preliminary, from various sources for most important materials for nuclear reactor technology. This was followed in 2007 by collaborative effort of four US national laboratories to produce covariances, often of modest quality – hence the name low-fidelity, for virtually complete set of materials included in ENDF/B-VII.0.

The present project is focusing on covariances of 4-5 major reaction channels for 110 materials of importance for power reactors. The work started under Global Nuclear Energy Partnership (GNEP) in 2008, which changed to Advanced Fuel Cycle Initiative (AFCI) in 2009. With the 2011 release the name has changed to the Covariance Multigroup Matrix for Advanced Reactor Applications (COMMARA) version 2.0. The primary purpose of the library is to provide covariances for AFCI data adjustment project, which is focusing on the needs of fast advanced burner reactors. Responsibility of BNL was defined as developing covariances for structural materials and fission products, management of the library and coordination of the work; LANL responsibility was defined as covariances for light nuclei and actinides.

During the period of FY2008-FY2010 the following releases of the GNEP/AFCI/COMMARA covariances library were made:

- GNEP-1.0, October 2008, 108 materials, starter files mostly based on the low-fidelity covariance estimates;
- GNEP-1.1, April 2009, 110 materials, improved files across the board, improvements of minor actinides based on Maslov analysis, revisited low-fidelity files;
- GNEP-1.2, September 2009, improved minor actinides, added fission neutron spectra and mu-bars. This version of the library is described in the extensive BNL report [1];
- AFCI-1.3, April 2010, new evaluations for major structural materials, improved actinides, initial covariance QA system implemented;
- AFCI-2.0beta, October 2010, consistent set of structural materials, improved actinides, improved QA web-based system developed and extensive review of the library performed.

It should be noted that COMMARA-2.0 covariances refer to central values given in the 2006 release of the US neutron evaluated library ENDF/B-VII.0 [2]. This explicit requirement was formulated in the middle of 2010 as a strict rule, causing certain problems with several LANL evaluations in both light nuclei region (16-O) and actinides (238,240-Pu). The point is that these LANL evaluations were conceived as new evaluations where both central values and covariances are evaluated simultaneously and hence the new central values deviate from ENDF/B-VII.0.

The testing version of the library, AFCI-2.0beta, was provided to ANL-INL reactor analysts in October 2010. Based on their feedback, BNL-LANL adopted several changes and produced official version of the library, COMMARA-2.0, which was released in March 2011. Description of this library is subject of the present report.

The report is organized as follows. In Chapter 2 we briefly summarize evaluation methodology. This is followed by Chapter 3 where we describe the contents of the library, including basic information about each individual file. Then, in Chapter 4 we describe our Quality Assurance procedure. Conclusions are given in Chapter 5. An important part of the report is the **Appendix** where we provide NJOY-produced plots of covariances for each file in the library.

The present report is an updated version of the report prepared in October 2010 for DOE Nuclear Energy, Fuel Cycle Research & Development.

2. COVARIANCE METHODOLOGY

Covariance evaluation methodology evolved considerably over the last several years due to intensive work both in the United States (BNL, LANL and ORNL) and abroad. Initial US advances were achieved during 2005-2007. Thus, in 2006 as a part of ENDF/B-VII.0 library release 12 sample covariance evaluations were completed [2]. In 2007, WPEC Subgroup 26 produced BOLNA library with input from several laboratories including extensive BNL contribution [3]. This was followed by the United States inter-laboratory low-fidelity covariance project funded by the DOE Nuclear Criticality Safety Program in FY2007 [4]. Since then, considerable advances in methodology were made by both BNL and LANL.

Useful description of BNL and LANL covariance methodology can be found in several papers and reports published in 2008. References [5, 6] provide summary of LANL methodologies for light nuclei and actinides, while summary of BNL methodologies developed primarily for structural materials and fission products can be found in Refs. [7, 8]. In 2009-2010, further advances were made by both BNL and LANL. Notably, BNL developed new procedure for the resonance region based on kernel approximation and LANL improved methods for covariances of prompt fission neutron spectra [17].

2.1 Light nuclei

Light nuclei are defined here as materials from 1-H to 19-F. For these materials covariance methodology was based on two distinct methods, each of them covering full energy range. These distinct methods span the most sophisticated R-matrix methodology on one side and simple estimate on the other side:

- R-matrix methodology incorporated in the code EDA, for the most recent description see Ref. [5]. This method was developed and used by G. Hale, LANL for several priority materials. It should be noted that considerable effort is needed to produce full evaluation using this method.
- Simple estimate based on comparison of the ENDF/B-VII.0 cross sections with the experimental data in EXFOR library. This method is described in Ref. [6] and was used by T. Kawano, LANL to those materials where sophisticated R-matrix evaluations were not available.

2.2 Structural materials and fission products

For the purposes of the present project this category includes materials from 23-Na to 209-Bi. BNL methodology covers the whole energy range using one set of approaches for the resonance region and another one for fast neutron region.

In the resonance region two methods were broadly used:

- Resonance region – kernel approximation. Our central idea for the thermal and resonance region was to use uncertainty data in the Atlas of Neutron Resonances by S. Mughabghab [9] and propagate resonance parameter uncertainties into cross section uncertainties. Over the period of last 6 years we examined several possibilities how to achieve this goal. A summary of these approaches can be found in extensive report [8]. These earlier methods, even though partly useful, suffered from variety of drawbacks. In the final analysis we opted for the new method based on the idea of kernel approximation [10]. Major strengths of the kernel approximation are its transparency, its capability to treat level-level correlations and its capability to incorporate uncertainties related to potential elastic scattering. The kernel approximation was used for most important structural materials, for examples see Ref. [11] and Ref. [12].

- Resonance region – integral approximation. This simple, yet reasonable approach was originally developed for the purposes of low-fidelity covariance project [4]. The method approximates covariances by two uncorrelated uncertainties, one in the thermal region and another one in the low energy part of the resonance region. These uncertainties are supplied by thermal cross sections and by resonance integrals, which works pretty well for capture. For elastic scattering use was made of uncertainties of thermal cross sections and those of scattering radii. For the present project the method was mostly used for materials of lower priority, primarily fission products.

In the fast neutron region the following methods were used:

- Fast neutron region – EMPIRE/KALMAN method. This approach, described in detail Ref. [7] published in 2008, uses well known reaction model code EMPIRE coupled to RIPL library for *priors* and gets *posteriors* by including experimental data with the Bayesian code KALMAN [13]. The method has been recently improved by incorporation of model parameter uncertainties and accounting for model uncertainties through the marginalization of the so-called 'nuisance' parameters. Concept on marginalization of the nuisance parameters is critical for accounting for model uncertainties, and systematic uncertainties in the experimental data. This technique makes use of the model parameters, which scale certain parts of the reaction calculations. These parameters are not used in the analysis of the experimental data but their 'a priori' assigned uncertainty is used in the final propagation of parameter uncertainties to the cross section covariances.
- Fast neutron region – dispersion analysis. This approach, suitable for materials where independent evaluations are available, compares central values in major evaluated nuclear data libraries and infers estimate of cross section uncertainties from dispersion between these cross sections.
- Fast neutron region – propagation of model parameter uncertainties. This method uses code EMPIRE, accounts for assessment of model parameter uncertainties such as given in RIPL-3 library, and propagates them into cross section covariances. For more details see the recent paper by Pigni *et al*. [14]. The method was used for mass producing covariances included in the low-fidelity covariance library.

2.3 Actinides – cross sections

Covariance data for actinides consist of three types, reaction cross sections, prompt fission neutron multiplicity and prompt fission neutron spectra, each of them being evaluated independently. Covariance methodology for reaction cross sections used approaches of different complexity depending on the material priority:

- Major actinides – full scale evaluation for ENDF/B-VII.0. Central values for major actinides were evaluated already for VII.0, but covariances were completed after VII.0 release. Thus, covariances for major actinides can be viewed as stemming from simultaneous evaluations combining LANL fast region, with resonances supplied by ORNL. In the fast region, fission is obtained from detailed analysis of experimental data, while other reaction channels are evaluated mostly by nuclear reaction model code GNASH with experimental data included through the Bayesian code KALMAN. In the resonance region ORNL evaluations are based either on full scale SAMMY analysis or retroactive SAMMY analysis.
- Minor actinides – three methods of different complexity, depending on the material priority and the laboratory supplying covariances:
  - Full scale evaluation retrofitted to ENDF/B-VII.0. Simultaneous evaluations performed for VII.1 library by LANL and ORNL, with covariances retrofitted to account for discrepancies between VII.1 and VII.0 central values
  - Limited evaluation. Evaluation performed by BNL with EMPIRE-KALMAN using parameterization reproducing VII.0 central values.
  - Simple estimates. Estimates based on dispersion analysis performed for BNL by Maslov [15].

2.4 Actinides – nubars and fission spectra

LANL is developing code package aimed at analyzing and predicting prompt fission neutron spectrum and multiplicity. With this new tool, it is possible to analyze any experimental data set regarding the average prompt fission neutron spectrum matrix $\chi(E_{inc},E_{out})$, average prompt neutron multiplicity $<\nu>(E_{inc})$, average first moment $<E_{out}>$, etc. Experimental data can be compared directly to evaluated data files, and default model calculations, using the Los Alamos or Madland-Nix model, can be performed using model input parameter systematics. Sensitivity calculations can be performed on the model input parameters to assess the impact of any parameter on the calculated spectrum and multiplicity. The KALMAN module is included in the package, making it relatively straightforward to produce associated covariance matrices

For COMMARA-2.0 library covariances for nubars were evaluated independently from other data:

- Nubars - LANL methodology. Based on detailed analysis and fit of experimental data; used by LANL for six most important actinides. Similar method was used by Obninsk for 232-Th evaluation already included in ENDF/B-VII.0 library.
- Nubars - BNL methodology. Based on dispersion analysis, including experimental data, by Maslov [15]; used by BNL for 13 minor actinides.

For COMMARA-2.0 library covariances for prompt fission neutron spectra were evaluated independently from other data:

- Prompt fission neutron spectra – LANL methodology. The method is based on model prediction based on Madland-Nix model, combined with experimental data using code KALMAN.

3. CONTENTS OF THE COMMARA-2.0 LIBRARY

This section summarizes covariances available in the COMMARA-2.0 library. We start with brief overview of files and format and proceed with short description of covariances for individual materials dividing them into light nuclei, structural and fission products, and actinides. At the end we recapitulate on nu-bars, mu-bars and prompt fission neutron spectra. We use red color to highlight the priority materials. Covariance plots for each material including relative uncertainties and correlation matrices can be found in **Appendices**.

3.1 Files

The COMMARA-2.0 library contains covariances for most important reaction channels and few other selected quantities organized into 135 files as follows:

- 110 files with neutron cross section covariances (12 light nuclei, 78 structural materials and fission products, 20 actinides). Detailed lists of materials are provided later in the present report.
- 20 files with nu-bar covariances (20 actinides).
- 3 files with prompt fission neutron spectra covariances (238,239,240-Pu).
- 2 files with mu-bar (average scattering cosine) covariances (23-Na, 56-Fe).

In terms of ENDF-6 format nomenclature cross section covariances for the following nuclear reaction channels are provided:

- MT = 2, 4, 16, 102 (elastic, nn', n2n, capture) for all materials for which these reactions are energetically possible. MT1 is viewed as redundant and, in general, it is not provided.
- MT = 22, 103, 104, 107 (nn'α, np, nd, nα) for some light nuclei.
- MT = 18 (total fission) for actinides.

It should be noted that some priority evaluations, performed by sophisticated methods, do provide cross-reaction correlations which can be extracted from ENDF-6 formatted files by NJOY. In general, however, this information is not included in the library.

3.2 Format

All covariance files are provided in the same format, in multigroup representation using 33-energy groups covering the energy range from 19.6 MeV down to 10^{-5} eV. Whenever ENDF-6 formatted files were available, these 33-energy group files were obtained by processing with the LANL code NJOY using 1/E neutron flux. Definition of 33-energy group structure is given in Table 1.

Table 1. 33-energy group structure used for COMMARA-2.0 covariance library.

Given are group numbers, along with upper and lower energies for each group.

No.	E_{upper}	E_{lower}	No.	E_{upper}	E_{lower}	No.	E_{upper}	E_{lower}
1	19.6 MeV	10.0 MeV	12	67.3 keV	40.8 keV	23	304 eV	148 eV
2	10.0 MeV	6.06 MeV	13	40.8 keV	24.7 keV	24	148 eV	91.6 eV
3	6.06 MeV	3.67 MeV	14	24.7 keV	15.0 keV	25	91.6 eV	67.9 eV

4	3.67 MeV	2.23 MeV	15	15.0 keV	9.11 keV	26	67.9 eV	40.1 eV
5	2.23 MeV	1.35 MeV	16	9.11 keV	5.53 keV	27	40.1 eV	22.6 eV
6	1.35 MeV	820 keV	17	5.53 keV	3.35 keV	28	22.6 eV	13.7 eV
7	820 keV	497 keV	18	3.35 keV	2.03 keV	29	13.7 eV	8.31 eV
8	497 keV	301 keV	19	2.03 keV	1.23 keV	30	8.31 eV	4.00 eV
9	301 keV	183 keV	20	1.23 keV	748 eV	31	4.00 eV	0.54 eV
10	183 keV	111 keV	21	748 eV	454 eV	32	0.54 eV	0.01 eV
11	111 keV	67.3 keV	22	454 eV	304 eV	33	0.01 eV	10-5 eV

3.3 Light nuclei (12 materials)

All light nuclei covariances were produced by LANL. They were mostly completed in 2008 and already included into the low-fidelity covariance library [4]. It should be noted that covariances for several materials were determined by the most sophisticated methods, while the rest is mostly based on simple estimates. In summary:

- Four materials (1H, 4He, 6Li, 10B) were analyzed in terms of the R-matrix formalism. It should be noted that 16O was evaluated for ENDF/B-VII.1, but not retro-fitted for ENDF/B-VII.0. Hence this new evaluation is not included in COMMARA-2.0.
- One material (7Li), taken over from ENDF/B-VII.0, was partially obtained from the least-squares analysis of experimental data.
- Covariances for the remaining seven materials, including 16O, result from a simple comparison of the ENDF/B-VII.0 cross sections with the experimental data. The only changes compared to these low-fidelity data are corrections introduced during the Quality Assurance procedure at BNL. In particular, in some cases the off-diagonal elements of the correlation matrices were modified to eliminate large negative eigenvalues leading to the violation of the positive definiteness of the correlation matrix.

Two more comments should be made:

- Several reactions on light nuclei listed here serve as neutron cross section standards, namely 1H(n,el), 6Li(n,t), 10B(n,α0), 10B(n,α1) and 12C(n,el). Therefore, these cross sections are well determined, implying small uncertainties.
- Radiative capture cross sections for light nuclei are in general very small. Consequently radiative capture uncertainties for virtually all light nuclei should be fairly high.

1-H (material no.1)

Covariances were obtained at LANL by full scale R-matrix analysis of more than 5000 experimental data (chi-square per degree of freedom of 0.83) [5]. The major channel in this case is elastic scattering, often labeled also as *n-p* scattering. Elastic scattering serves as neutron cross section standard from 1 keV to 20 MeV, with cross sections well determined. Uncertainties for elastic scattering rise from values well below 1%, reach maximum at about 8 MeV, then gradually decrease with increasing energy. In addition to elastic scattering, covariances are supplied for radiative capture.

2-H (no.2)

Covariances are supplied for elastic, (n,2n) and radiative capture. Covariances were estimated at LANL based on a brief analysis of experimental data and their agreement with the ENDF/B-VII.0 central values.

4-He (no.3)

Covariances are provided for elastic scattering, often labeled as n-4He scattering or n-α scattering. The evaluation done originally by Nisley in 1973 has been updated to include the results of a more recent R-matrix analysis. This newer analysis (August 2006) is a multi-channel fit to data for the n-alpha and d-t reactions that extends to about 24 MeV excitation energy in the ^{5}He system. Although this is well above the d+t threshold, for the present library we give n-α data only over the original range up to 20 MeV, where it is single channel scattering. However, the results below the d+t threshold are constrained by the data at higher energies through the R-matrix parameterization, and they are therefore better determined than those of a single-channel analysis.

In addition, the covariance matrix for the elastic channel (MF=33, MT=2) was calculated from the parameter covariances and derivatives from the ^{5}He analysis. It should be noted that while the rank of this covariance matrix is 115, corresponding to the number of free parameters in the fit, it is given at 152 energies. This means that in principle some of the zero eigenvalues could have small negative values due to the limited precision of the numbers in the file and the matrix is not guaranteed to be positive semi-definite.

6-Li (no.4)

Covariances are supplied for several reaction channels, two strong channels are obtained by sophisticated method, the rest stems from simple estimate.

Elastic scattering (n+6Li scattering) and 6Li(n,t)4He reaction were obtained at LANL by state of the art R-matrix analysis [5] of the 7-Li system. This system contains data for all possible reactions among t+4He and n+6Li at energies extending from the t+4He threshold (well below the n+6-Li threshold) up to energies corresponding to 4 MeV incident neutrons. Also included are n+6Li* channels to simulate the effects of n+d+α breakup. A very good fit is obtained to the more than 3300 data points, with a chi-square per degree of freedom of 1.164.

Of particular note is the excellent fit to the t+4He scattering data, which have very small uncertainties. This is true in particular at energies near the obvious resonance structure in the 6-Li(n,t) reaction. These high-precision charged-particle elastic scattering measurements put stringent constraints on fitting the neutron data through the unitarity of the scattering matrix.

7-Li (no.5)

Covariances, supplied for several reaction channels, were taken over from the current ENDF/B-VII.0 evaluation. The original evaluation was done by Phil Young, LANL and dates back to 1988. The covariances are combination of experimental data analysis with the generalized least squares code GLUCS and ‘ad hoc’ estimates based on the spread of experimental data and their uncertainties.

9-Be (no.6)

Covariances were estimated at LANL based on a brief analysis of experimental data and their agreement with the ENDF/B-VII.0 central values.

10-B (no.7)

Covariances result from the full R-matrix analysis similar to those performed for 1H and 6Li. For MT=107, 800 and 801 the international neutron cross section standards were incorporated into the evaluation. Therefore, 10B covariances should be considered to be of high quality. We note that the uncertainties for the standards (n,α) reaction are below 1% or somewhat above 1%.

11-Be (no.8)

Covariances were estimated at LANL based on a brief analysis of experimental data and their agreement with the ENDF/B-VII.0 central values.

12-C (no.9)

Covariances were estimated at LANL based on a brief analysis of experimental data and their agreement with the ENDF/B-VII.0 central values. An exception is elastic scattering which serves as neutron cross section standard from 10 eV up to 1.8 MeV, with uncertainties below 1%.

15-N (no.10)

Covariances were estimated at LANL based on a brief analysis of experimental data and their agreement with the ENDF/B-VII.0 central values.

16-O (no.11)

Covariances are based on simple estimate performed by T. Kawano, LANL in 2008, even though new detailed R-matrix analysis has been completed at LANL by G. Hale late in 2010. The reason for adopting simple estimate for COMMARA-2.0 library is that central values stemming from this new evaluation differ from the ENDF/B-VII.0 cross sections to the extent that invalidates application of the new uncertainties to the ENDF/B-VII.0 cross sections. Hence, simple low-fidelity estimates were preserved in COMMARA-2.0 library. It is understood, however, that the new evaluation including both central values and covariances should be included into the forthcoming ENDF/B-VII.1 library.

19-F (no.12)

Covariances were taken from ENDF/B-VII.0 for all reaction channels where this library offered covariances. For the remaining reaction channels, namely elastic scattering and radiative capture, covariances were estimated at LANL based on a brief analysis of experimental data and their agreement with the ENDF/B-VII.0 central values.

3.4 Structural materials and fission products (78 materials)

BNL was responsible for producing covariances for structural materials and fission products. This category of materials contains altogether 78 materials, of which about one half are structural materials. Among them are 18 materials that are considered of high priority (marked in red in the following) because of their usage as structural materials or as a coolant (23Na). Priority materials received more attention and were usually subject to more detailed analysis than the remaining ones. These remaining materials were often taken from the low-fidelity library revisited by BNL in 2009. This revision usually extended the resonance region from 5 keV used in the low-fidelity to values more appropriate for the individual isotopes; in addition, elastic uncertainties were limited to 20% to avoid unrealistically high uncertainties resulting from propagating uncertainties of optical model parameters at low energies. Final corrections could also result from the Quality Assurance, see Chapter 4. In the following, we group these materials by element since the applied covariance methodology was often (albeit not always) the same for all isotopes of a given element.

Kernel method for covariances in the resonance region was first applied to 55Mn [10], then to major structural materials 52Cr, 56Fe and 58Ni [11], remaining 5 structural materials in the Cr-Fe-Ni range, to 5 materials in the Pb-Bi range, as well as to several other materials of some priority (Mg, Al, Si and Zr).

We note that various degrees of complexity and attention to details were adopted in the evaluations of following 40 materials, dictated by the importance of materials for AFCI applications:

- 24-Mg; 27-Al; 28-Si, 29-Si, 30-Si
- 50-Cr, 52-Cr, 53-Cr; 55-Mn; 54-Fe, 56-Fe, 57-Fe; 58-Ni, 60-Ni
- 90-Zr, 91-Zr, 92-Zr, 93-Zr, 94-Zr, 95-Zr, 96-Zr
- 92-Mo, 94-Mo, 95-Mo, 96-Mo, 97-Mo, 98-Mo, 100-Mo
- 109-Ag; 133-Cs, 135-Cs; 141-Pr

- 143-Nd, 145-Nd, 146-Nd, 148-Nd
- 204-Pb, 206-Pb, 207-Pb, 208-Pb; 209-Bi

Covariances for remaining 38 materials were taken over from the low-fidelity library released in 2008, after revisiting performed by BNL in 2009.

23-Na (material #1)

Sodium has been evaluated at BNL in the frame of the ongoing "Consistent Adjustment Project" by BNL, INL and ANL aiming in developing the methodology for shifting the adjustment procedure from group-wise cross sections down to the nuclear reaction model parameters. This exercise consisted of the full evaluation of cross sections with simultaneous determination of the covariances in both the resonance and the fast neutron regions.

The resonance module of EMPIRE was used both at the thermal energy and in the resonance region up to 985 keV. Uncertainties for parameters of 38 resonances (including the bound state) were retrieved from the electronic version of the Atlas of Neutron Resonances [9]. The KALMAN filter technique was used to adjust parameter uncertainties so that the uncertainties of the thermal values were reproduced. This adjustment created correlations between parameters of a few low-energy resonances and generated changes in the parameter uncertainties.

In the fast neutron region the sensitivity calculations were performed with the EMPIRE code. The spherical optical model provided total cross sections and neutron scattering, Hauser-Feshbach statistical model described the bulk of particle emission, and the exciton pre-equilibrium model described major features of fast particle emission at higher incident energies. Altogether, 21 model parameters were varied. The Bayesian update procedure was performed by the KALMAN code [3] by taking into account the sensitivity calculations and selected experimental data.

More details regarding the procedure can be found in the AFCI-1.2 report [1].

24-Mg, 25-Mg, 26-Mg (#2-4)

24-Mg. Covariances for 24-Mg in the resonance region were estimated using the kernel approach, which covers the range of the resonance region up to 520 keV. In this region, Mughabghab values given in Atlas were used. Differences between absolute values of data in Atlas of Neutron Resonances and ENDF/B-VII.0 have been taken into account, leading to enhanced cross section uncertainties.

24-Mg covariances at higher energies were treated as the fast neutron range. These fast neutron covariances were obtained at BNL using EMPIRE calculated sensitivities and KALMAN code to incorporate experimental data. Both elemental and isotopic data are available for total cross sections on 24-Mg. Some of them, below about 7 MeV, had to be filtered out, or the matrix would be too large for the KALMAN filter. Above 8 MeV, uncertainties come from the EMPIRE/KALMAN approach. In between these energies the uncertainties are based on the Bonner experimental uncertainty. For inelastic and capture there are only sparse and inconsistent data so the covariance estimates are essentially model-based.

25-Mg and 26-Mg. Covariances were adopted from the low-fidelity files revisited at BNL in 2009.

27-Al (#5)

New BNL estimates of the covariances in the resonances region were obtained using kernel approach up to 845 keV. Uncertainties of neutron resonance parameters as well as the scattering radius R' were taken from Atlas of Neutron Resonances.

In the fast neutron region new covariances were prepared using experimental uncertainties below 8 MeV and EMPIRE/KALMAN approach above. There are many experimental data for total cross sections, far too many for the KALMAN filter to handle. However, the ENDF/B-VII.0 follows the fluctuating experimental data all the way up to ~8 MeV. The fluctuations are still easy to follow in this region, and several different experiments are in good agreement. It was decided to treat this region (for total and elastic) with one correlated block, with uncertainty of 3% (suggested systematic uncertainty of normalization for both Cierjacks

and Schwartz experiments). Above 8 MeV, uncertainties come from EMPIRE/KALMAN.

Other channels do not have very much experimental data. For inelastic scattering and capture the data are inconsistent or discrepant and it was decided to use purely model-based covariances for these channels (no including experimental data). Thus capture uncertainties are based on EMPIRE/KALMAN from 845 keV up.

28-Si, 29-Si, 30-Si (#6-8)

New BNL estimates in the resonances region were obtained with the kernel approach. We note that resonance region for Si extends to fairly high energies, in particular for 28-Si up to 2.7 MeV. Included in our evaluation were resonance parameter uncertainties taken over from Atlas of Neutron Resonances. Dominant contribution to elastic scattering uncertainties comes from the uncertainty of the scattering radius R'.

Covariances in the resonance region were merged with the covariances in the fast neutron region taken from the ENDF/B-VI.8. We reviewed the latter data and concluded that they are reasonable with the exception of MT=104 covariances which were considered to be problematic and hence they have been removed.

50-Cr, 52-Cr, 53-Cr (#9-11)

Covariances in the resonance region for these three materials were estimated in terms of the kernel method. The resonance region for Cr isotopes extends to high energies of about 1 MeV. In view of the importance of Cr materials these evaluations were done rather carefully. To illustrate amount of work put in this evaluation we refer the reader to Ref. [11] for the detailed description of the kernel analysis of 52-Cr and to Ref. [12] for 50,53-Cr.

In the fast neutron region our covariances used the ENDF/B-VI.8 evaluation as the starting point. The reason was that both the basic files (adopted by ENDF/B-VII.0) and covariances were produced by the highly experience ORNL group, Hetrick et al (1991). We restored these covariances although CSEWG decided to drop them from ENDF/B-VII.0. In case of Cr the justification for dropping was relatively weak and mostly concerned the resonance region. At inelastic scattering threshold region, the original ENDF/B-VI.8 uncertainties were increased based on the dispersion analysis of existing evaluations. Similarly, capture cross sections uncertainties at high energies were increased to values that were deemed to be more realistic.

55-Mn (#12)

At BNL, covariances were originally produced using the resonance parameters and uncertainties tabulated in the Atlas of Neutron Resonances. Information from the Atlas was used in the covariance module of EMPIRE in order to create an ENDF file with resonance parameters (MF2) and uncertainties (MF32, the resonance parameter covariance matrix). Using the covariance module, an adjustment was also made to the experimental thermal uncertainty for the (n,γ) and (n,elastic) reaction channels. This adjustment effectively generated correlations or anti-correlations between the bound resonance(s) and positive-energy resonances, modifying the thermal uncertainty to the desired value.

Due to the difficulties with inclusion of level-level correlations and important role of scattering radius uncertainty which could not be adequately treated under MF32 approach, for COMMARA-2.0 we switched to MF33 representation and kernel approximation. These latter covariances were then adopted by COMMARA-2.0 library. Detailed account of 55-Mn evaluation in the resonance region using kernel approach can be found in Ref. [10].

Fast neutron covariances were estimated using EMPIRE/KALMAN approach by calculating sensitivity of the cross sections to the reaction model parameters and combining model calculations with the experimental data using the KALMAN code and propagating parameter covariances onto cross section covariances.

54-Fe, 56-Fe, 57-Fe (#13-15)

Evaluation of covariances in the resonance region for 54-Fe, 56-Fe and 57-Fe is based on kernel approximation and data from the Atlas of Neutron Resonances. The resonance region extends to high energies, for 56-Fe up to 850 keV. Similar to Cr isotopes described above, elastic scattering uncertainty was largely determined by contribution from potential scattering via the uncertainty of the scattering radius R'.

This work was again done fairly carefully and we refer to the reader to BNL reports for the detailed description of the kernel analysis of 56-Fe [11] and of 54,57-Fe [12].

In the fast region, the ENDF/B-VI.8 covariances were used as the basis. After review, uncertainties were increased in the threshold region following dispersion analysis (see AFCI-1.2 report [1]). We gave due consideration to users' comments on elastic and inelastic uncertainties and tended towards conservative estimates whenever possible. The same approach was also applied for the remaining 54-Fe and 57-Fe.

58-Ni, 60-Ni (#16, 17)

BNL produced covariances both in the resonance and in the fast neutron region. As in the case of Cr and Fe isotopes, the combination of kernel approach in the resonance region with revisited data from ENDF/B-VI.8 in the fast neutron range was used.

Evaluation in the resonance region was done fairly carefully and detailed reports were produced to document all details of the procedure [11,12]. Dominant contribution to elastic scattering uncertainty comes from the potential scattering via the uncertainty of the scattering radius R'.

Covariances in the fast region were obtained using the same approach as for Cr and Fe materials described above. Thus, as the staring point we used ENDF/B-VI.8 covariances which resulted from simultaneous evaluation by highly experienced ORNL group. Then, these data were subject to dispersion analysis, leading to certain modifications of uncertainties, while correlations were left unchanged.

90-Zr, 91-Zr, 92-Zr, 93-Zr, 94-Zr, 95-Zr, 96-Zr (#18-24)

In thermal and resolved resonance region we made use of the covariance formalism based on the kernel approximation along with data in the Atlas of Neutron Resonances. When data were not available, i.e. 95-Zr, estimates were provided by S.F. Mughabghab.

In fast neutron region up to 20 MeV covariance estimates were calculated using the nuclear reaction code EMPIRE and the Bayesian code KALMAN. The KALMAN code along with selected experimental data was used to determine the correlation matrix of the model parameters. Furthermore, additional parameters scaling total and absorption cross sections were included to prevent the unrealistic drop in the cross-section uncertainties and, in some instance, to cover the spread of the experimental data. In cases such as 93-Zr and 95-Zr, for which central value of the cross sections calculated by EMPIRE considerably differed from those in ENDF/B-VII.0 evaluations, we applied dispersion analysis. For all zirconium isotopes the total cross-section uncertainties were computed as the sum of elastic, inelastic, (n2n), and capture.

95-Nb (#25)

Covariances were adopted from the low-fidelity file revisited at BNL in 2009.

92-Mo (#26)

New set of covariances was obtained at BNL in 2010 using kernel approach in the resonance region and EMPIRE/KALMAN analysis of experimental data in the fast neutron region.

Dispersion analysis of the evaluated libraries was not very helpful since all major libraries are virtually identical. ROSFOND disagrees somewhat, but only capture (15% above 10 MeV) shows significant disagreement. Fairly complete isotopic experimental data are available, but only a few points for capture, thus elemental data were also used. In KALMAN fitting, we used uncertainties of total and absorption scaling factors to account for systematic uncertainties.

94-Mo, 95-Mo, 96-Mo, 97-Mo (#27-30)

New sets of covariances were obtained at BNL in 2010 using kernel approach in the resonance region and EMPIRE/KALMAN analysis of experimental data in the fast neutron region.

Dispersion analysis provided expected uncertainties of the order of 10% for total, elastic and capture with tendency to increase above 10 MeV. Some isotopic data are available for all channels but the results still

depend heavily on elemental data. The EMPIRE/KALMAN analysis was performed using 'nuisance' parameters scaling total and reaction cross sections to account for systematic uncertainties.

98-Mo (#31)

New sets of covariances were obtained at BNL in 2010 using kernel approach in the resonance region and EMPIRE/KALMAN analysis of experimental data in the fast neutron region.

Dispersion analysis of the evaluated libraries does not bring much insight since all major libraries are virtually identical. Only ROSFOND differs from other major libraries suggesting 15% uncertainty for elastic above 1 MeV and 50% for capture above 10 MeV. The isotopic data are available for total, elastic and capture so there was no need to resort to elemental measurements. The EMPIRE/KALMAN analysis was performed using 'nuisance' parameters scaling total and reaction cross sections to account for systematic uncertainties and meet dispersion guidelines.

100-Mo (#32)

New sets of covariances were obtained at BNL using kernel approach in the resonance region and EMPIRE/KALMAN analysis of experimental data in the fast neutron region.

Dispersion analysis of the evaluated libraries suggest uncertainties less than 10% for the total, up to 15% for elastic above 1 MeV and 50% for capture above 1 MeV. The isotopic data are available for total, elastic (n,2n) and capture so the elemental measurements were not used. The EMPIRE/KALMAN analysis was performed using 'nuisance' parameters scaling total and reaction cross sections to account for systematic uncertainties and meet dispersion guidelines. In addition, 15% uncertainty on the gamma-strength scaling factor was assumed.

99-Tc (#33)

BNL covariance estimates from ENDF/B-VII.0 were adopted.

101-Ru, 102-Ru, 103-Ru, 104-Ru, 106-Ru (#34-38)

Covariances were adopted from the low-fidelity file revisited at BNL in 2009.

103-Rh (#39)

Covariances were adopted from the low-fidelity file revisited at BNL in 2009.

105-Pd, 106-Pd, 107-Pd, 108-Pd (#40-43)

Covariances were adopted from the low-fidelity file revisited at BNL in 2009.

109-Ag (#44)

New covariances in the fast neutron region were produced at BNL using EMPIRE/KALMAN approach and merged with the revised Low-fidelity estimates in the resonance region.

The experimental data are available for total, elastic and capture. The dispersion analyses of available evaluations provided guidelines for the minimum uncertainties in the major reaction channels. The two 'nuisance' parameters scaling total and absorption (generally set to 6%) were used to adjust uncertainties to meet dispersion guidance.

127-I, 129-I (#45, 46)

Covariances were adopted from the low-fidelity file revisited at BNL in 2009.

131-Xe, 132-Xe, 134-Xe (#47-49)

Covariances were adopted from the low-fidelity file revisited at BNL in 2009.

133-Cs, 135-Cs (#50, 51)

New covariances in the fast neutron region were produced at BNL in 2010 using EMPIRE/KALMAN

approach and merged with the revised low-fidelity estimates in the resonance region.

The dispersion analysis was invoked to provide guidelines on minimum uncertainties. Then, 'nuisance' factors scaling total and reaction cross sections were used to meet these limits.

139-La (#52)

Covariances were adopted from the low-fidelity file revisited at BNL in 2009.

141-Ce (#53)

Covariances were adopted from the low-fidelity file revisited at BNL in 2009.

141-Pr (#54)

New covariances in the fast neutron region were produced at BNL in 2010 using EMPIRE/KALMAN approach and merged with the revised low-fidelity estimates in the resonance region.

Experimental data are available for all reaction channels. For total cross sections only single set by Carlson was used in the analysis. This set was also used in the elastic estimates together with an additional elastic measurement. The final uncertainties were increased by adding 5% systematic uncertainty to all channels. In addition, (n,2n) was increased further by 10% to account for the spread in experimental data.

143-Nd, 145-Nd, 146-Nd, 148-Nd (#55-58)

New covariances in the fast neutron region were produced at BNL using EMPIRE/KALMAN approach and merged with the revised Low-fidelity estimates in the resonance region.

The reaction channels were treated separately, i.e., cross-reaction correlations were not taken into account except of correlation between the total and elastic. In most cases, all experimental data were taken into account in the analysis. Tuning factors scaling the total cross section and the Multistep Direct response functions were used to account for the model deficiencies and to simulate correlations among the experiments.

147-Pm (#59)

Covariances were adopted from the low-fidelity file revisited at BNL in 2009.

149-Sm, 151-Sm, 152-Sm (#60-62)

Covariances were adopted from the low-fidelity file revisited at BNL in 2009.

153-Eu, 155-Eu (#63, 64)

Covariances were adopted from the low-fidelity file revisited at BNL in 2009.

155-Gd, 156-Gd, 157-Gd, 158-Gd, 160-Gd (#65-69)

Covariances from the ENDF/B-VII.0 library produced by ORNL-BNL collaboration were adopted. These covariances are based on retroactive SAMMY analysis in the resonance region, and on EMPIRE/KALMAN approach in the fast neutron region. In the case of 157-Gd thermal capture, ENDF/B-VII.0 uncertainty was increased to 8% to account for the new RPI measurement which differs by 10% from the absolute value recommended in ENDF/B-VII.0.

166-Er, 167-Er, 168-Er, 170-Er (#70-73)

Covariances were adopted from the low-fidelity file revisited at BNL in 2009.

204-Pb, 206-Pb, 207-Pb, 208-Pb (#74-77)

BNL performed new evaluation of covariances for a set of five Pb isotopes in the full energy range in 2010. In thermal and resolved resonance region we made use of the covariance formalism based on kernel approximation along with data in the Atlas of Neutron Resonances. We note that the resonance region for Pb isotopes extends to very high energies, notably for 208-Pb it goes up to 2.7 MeV. Elastic scattering uncertainty in the resonance region was largely determined by potential scattering contribution via the uncertainty of the

scattering radius R'.

In the fast neutron region up to 20 MeV covariance estimates were produced using the nuclear reaction code EMPIRE and the Bayesian code KALMAN. The KALMAN code along with selected experimental data was used to determine the correlation matrix of the model parameters. Furthermore, additional parameters scaling total and absorption cross sections were included to prevent the unrealistic drop in the cross-section uncertainties and, in some instance, to cover spread of the experimental data. For all lead isotopes, the elastic cross-section uncertainties were computed as difference of total and absorption reaction channel.

209-Bi (#78)

BNL performed new evaluation of covariances in the full energy range in 2010. In thermal and resolved resonance region we made use of the covariance formalism based on kernel approximation along with data in the Atlas of Neutron Resonances. Elastic scattering uncertainty was largely determined by potential scattering contribution via the uncertainty of the scattering radius R'.

In fast neutron region up to 20 MeV covariance estimates were produced using the nuclear reaction code EMPIRE and the Bayesian code KALMAN. The KALMAN code along with selected experimental data was used to determine the correlation matrix of the model parameters. Furthermore, additional parameters scaling total and absorption cross section were included to prevent the unrealistic drop in the cross-section uncertainties and, in some cases, to cover spread of experimental data. The elastic cross-section uncertainties were computed as difference of total and absorption reaction channel.

3.5 Actinides – cross sections (20 materials)

LANL has responsibility for covariances of actinides, focusing mostly on major actinides and several priority minor actinides. Remaining minor actinides were contributed by BNL, while 232Th was taken over from ENDF/B-VII.0.

LANL, 8 materials: Covariances for 233,235,238-U and 239-Pu were completed by LANL-ORNL collaboration in 2008-2009. These covariances were originally intended for ENDF/B-VII.0 library, but they were not completed in time for 2006 release. In 2010, LANL contributed new evaluations with covariances for 241-Am, 238-Pu and 240-Pu; the covariance matrix for the average prompt fission neutron multiplicity for 239-Pu was revised in order to eliminate the larger than expected uncertainties in the 1-100 keV range; the capture cross-section uncertainties in 235-U were reviewed; the 241-Pu neutron-induced fission cross-section was analyzed using experimental data only, and a covariance matrix was produced; LANL merged its new evaluation for 240-Pu with the ORNL file evaluated with SAMMY in the resolved and unresolved resonance ranges; all new evaluations come with a covariance matrix for the prompt fission neutron multiplicity, as well as spectrum given at 0.5 MeV of incident neutron energy.

BNL, 11 materials: BNL produced estimates of covariances for 11 minor actinides. Following the low-fidelity approach, the uncertainties in the low energy region are based on experimental uncertainties of thermal cross sections, uncertainties of the resonance integrals and uncertainty of the scattering radius. In the fast neutron region (above 1 keV) analysis by Maslov [15] was used.

232-Th (material #1)

Covariances were taken over from ENDF/B-VII.0 with some updates. Covariances as described in Ref. [2] are composed of contributions done by several parties: below 4 keV the covariance matrix for the resolved resonance parameters (MF=32) was generated by ORNL using the SAMMY code; unresolved resonance region was produced by Geel using purely experimental data; fast region covariances were produced by the IAEA using EMPIRE/GANDR system and experimental data from EXFOR; nu-bar covariances in the full energy range were produced by Obninsk.

In 2010 the IAEA revisited ENDF/B-VII.0 covariances and made updates to address some unrealistically low uncertainties. The major difference compared to ENDF/B-VII.0 is the 2% uncertainty added to the covariance

matrix of the elastic scattering.

233-U (#2)

233-U evaluation by ORNL and LANL is an update of ENDF/B-VII.0 file which added covariances to original central values. This new file, submitted as a candidate for ENDF/B-VII.1, qualifies for the COMMARA-2.0 since changes in the cross sections compared to the ENDF/B-VII.0 appear to be negligible.

Resonance parameter covariances were generated in the resolved energy region (1.0-5 eV to 600.0 eV) with SAMMY at ORNL. Uncertainty on nubar was also generated at ORNL. Experimental data and uncertainties were used to generate resonance parameter covariance in the MF=32 representation which was converted into the cross section (MF=33, MT=1, 2, 18, and 102) representation to reduce size of the file. Covariances in the unresolved resonance range were obtained by extending the fast neutron matrices generated at LANL.

Cross-section covariance matrices in the fast energy region were obtained through a combination of nuclear reaction sensitivity calculations using the GNASH code, and available information on experimental uncertainties for some of the cross sections. The sensitivity of GNASH results on the choice of model parameters was assessed, and the KALMAN code was used to merge sensitivity calculations with experimental uncertainties.

234-U (#3)

234-U covariances were contributed by BNL. Covariances are combination of the uncertainties recommended in the assessment of Ref. [15] and correlation matrices produced by the WPEC Subgroup 26 [3] which were converted to the AFCI 33-energy group structure. The initial estimates were obtained using EMPIRE/KALMAN system with default parameterization roughly adjusted to reproduce trends in the experimental data. The KALMAN code was run with default uncertainties assigned to the key model parameters to produce covariances. Following the low-fidelity approach, the uncertainties in the low energy region are based on experimental uncertainties of thermal cross sections, uncertainties of the resonance integrals and uncertainty of the scattering radius. The assessment of Ref. [15] set elastic uncertainty at 4%, confirmed SG 26 fission and (n,2n) uncertainties, modified inelastic, an slightly increased capture uncertainty.

235-U (#4)

Resonance parameter covariance was generated in the resolved energy region (1.0-5 eV to 2.25 keV) by ORNL with the computer code SAMMY using experimental data and their uncertainties. The covariance data for the parameters (MF=32 representation) were converted into the cross section covariances (MF=33, MT=1, 2, 18, and 102) to reduce size of the file.

Cross-section covariance matrices in the fast energy region were obtained through a combination of nuclear reaction sensitivity calculations using the GNASH code, and available information on experimental uncertainties for some of the cross sections. The sensitivity of GNASH results on the choice of model parameters was assessed, and the KALMAN code was used to merge sensitivity calculations with experimental uncertainties. For the fission cross section, the IAEA work on Standard cross sections was incorporated. Prompt (MT456) and total (MT452) neutron multiplicity covariance matrices were obtained from a generalized least-squares study of experimental data without any model calculations.

Although this file has been submitted as a candidate for ENDF/B-VII.1, it qualifies for the COMMARA-2.0 since changes to central values compared to the ENDF/B-VII.0 appear to be negligible.

236-U (#5)

236-U covariances were contributed by BNL. Covariances are combination of the uncertainties recommended in the assessment of Ref. [15] and correlation matrices produced by the WPEC Subgroup 26 [3] converted to the AFCI 33-energy group structure. The initial estimates were obtained using EMPIRE/KALMAN system with default parameterization roughly adjusted to reproduce trends in the experimental data. The KALMAN code was run with default uncertainties assigned to the key model parameters to produce covariances. Following the low-fidelity approach, the uncertainties in the low energy region are based on experimental

uncertainties of thermal cross sections, uncertainties of the resonance integrals and uncertainty of the scattering radius. The assessment of Ref. [3] set elastic uncertainty at 3%, confirmed fission uncertainty (except lowering it in the 4-6 MeV bin) and (n,2n), but altered uncertainties of inelastic.

238- U (#6)

Resonance parameter covariances were generated in the resolved energy region (1.0-5 eV to 20.0 keV) by ORNL with the computer code SAMMY using experimental data and their uncertainties. The resulting MF=32 representation was converted into the cross section covariances (MF=33, MT=1, 2, 18, and 102) representation to reduce computer storage.

Cross-section covariance matrices in the fast energy region were obtained through a combination of nuclear reaction sensitivity calculations using the GNASH code, and available information on experimental uncertainties for some of the cross sections. The sensitivity of GNASH results on the choice of model parameters was assessed, and the KALMAN code was used to merge sensitivity calculations with experimental uncertainties. Prompt (MT456) and total (MT452) neutron multiplicity covariance matrices were obtained from a generalized least-squares study of experimental data with no reference to any model calculations.

Although this file has been submitted as a candidate for ENDF/B-VII.1, it qualifies for the COMMARA-2.0 since central values appear to be the same as in the ENDF/B-VII.0.

237-Np (#7)

237-Np covariances were contributed by BNL. S. Mughabghab produced revisited low-fidelity estimates at low energies.

In the fast neutron region cross section covariances were obtained using EMPIRE/KALMAN approach (M. Pigni, BNL), with prior parameterization produced by Mihaela Sin (Bucharest). Three nuclear reaction models were adopted: (i) coupled-channels optical model (RIPL catalog number 2408), (ii) Hauser-Feshbach statistical model, and (iii) exciton pre-equilibrium model. Optical model allowed us to determine total and absorption cross sections, neutron direct elastic and inelastic scattering, as well as the transmission coefficients needed to calculate the compound-nucleus cross sections. Coupled-channels (CC) calculations were performed using five collective levels and three deformation parameters. For Hauser-Feshbach part of calculations adopted were EMPIRE-specific level densities. The treatment of the fission channel was carried out within the formalism developed by M. Sin. We varied inner and outer barrier heights and widths for the fissioning nuclei.

238-Pu (#8)

LANL has prepared a new evaluation for ENDF/B-VII.1, which contains a full set of covariances including prompt fission spectrum but differs considerably from ENDF/B-VII.0 as far as central values are concerned. COMMARA-2.0 covariances were produced by processing this new evaluation into 33-groups, followed by suitable scaling-up of some standard deviations to make them meaningful for ENDF/B-VII.0 central values.

The ENDF/B-VII.0 evaluation is very old, and some cross sections differ dramatically from the new LANL recommendations. Only in cases where both evaluations are based mostly on experimental data, one might use new uncertainties with ENDF/B-VII.0. This is the case for fission cross section (although moderate increase of the uncertainties is needed), as well as for the average prompt fission neutron multiplicity <v>, and average prompt fission neutron spectrum χ (at least at 0.5 MeV incident energy). To compensate for the differences in cross sections the ENDF/B-VII.1 uncertainties have to be considerably increased for elastic, inelastic, (n,2n) and capture.

Covariances in the thermal and resonance region are based on revisited low-fidelity estimates.

239-Pu (#9)

Covariances in the resonance region were produced by ORNL with the code SAMMY. Resonance parameter covariance matrix (MF32) was converted to cross section covariance matrix (MF33) by ORNL in order to

reduce the size of the matrix.

Cross-section covariance matrices in the fast energy region were obtained through a combination of nuclear reaction sensitivity calculations using the GNASH code, and available information on experimental uncertainties for some of the cross sections. The sensitivity of GNASH results on the choice of model parameters was assessed, and the KALMAN code was used to merge sensitivity calculations with experimental uncertainties.

Although this is an updated file submitted as a candidate for ENDF/B-VII.1, it can be used for the COMMARA-2.0 since the cross sections are unchanged compared to the ENDF/B-VII.0.

Special attention was given to evaluation of nubars. Compared to initial 239-Pu file present in the AFCI-1.3 covariance library, change was made to the average prompt and total fission neutron multiplicity $\langle\nu\rangle(E_{inc})$ covariance matrices. In the initial file, the uncertainties were evaluated based on experimental data only. In regions where few data existed, the final uncertainties remained dominated by large *prior* uncertainties. However, our understanding of the physics of prompt neutron emission leads to a relatively smooth behavior of $\langle\nu\rangle$ as a function of the neutron incident energy, adding significant constraints on the quantification of uncertainties and smoothing out the increased uncertainties in the 1-100 keV range.

240-Pu (#10)

LANL has prepared a new evaluation for ENDF/B-VII.1, which contains a full set of covariances including prompt fission spectrum and multiplicity but differs from ENDF/B-VII.0 as far as cross sections for several channels are concerned. The COMMARA-2.0 standard deviations were, therefore, scaled-up to compensate for discrepancies between ENDF/B-VII.0 and ENDF/B-VII.1.

In the fast region, the GLUCS generalized least-square code was used when experimental data better than model calculation are available. In all other cases, the GNASH-COH-KALMAN code package was used to obtain cross-sections and covariance matrices. The prompt fission neutron spectrum and multiplicity were obtained using the LANL PFNS code, which implements the Madland-Nix model. In the absence of spectrum experimental data, the model parameters were adjusted to reproduce the average multiplicity only, and estimates of spectrum uncertainties were used to obtain a reasonable covariance matrix.

Covariances in the thermal and resonance region are based on revisited low-fidelity estimates.

Applying the ENDF/B-VII.1 covariance matrices to the ENDF/B-VII.0 file, the situation for 240-Pu is much better than for 238-Pu, since for most cross sections of importance for COMMARA-2.0, deviations from ENDF/B-VII.0 are within the uncertainties evaluated for ENDF/B-VII.1. Only in cases of average prompt fission neutron multiplicity $\langle\nu\rangle$, average prompt fission neutron spectrum, and (n,2n) cross sections, the uncertainties should be increased, but correlation factors are deemed to be reasonable.

241-Pu (#11)

LANL has produced new covariance data for fission cross sections from 1 keV up to 30 MeV. Covariance analysis of 13 fission cross section data sets, including the most recent shape measurement by Tovesson at LANSCE, Los Alamos was, performed with the GLUCS code yielding standard deviations between 0.68% and 4.9%. Discrepancies below 0.9 MeV between Tovesson data and a majority of other data sets led LANL to discard the LANSCE data below this point. Some other data sets were also discarded, due to very large assumed uncertainties. Finally, an additional uncertainty was included to account for unknown systematic errors. Future work should lead to a better justification for this additional contribution. We are also developing new procedures to better account for discrepant data sets.

Covariances in the thermal and resonance region are based on revisited low-fidelity estimates.

242-Pu (#12)

242-Pu covariances were contributed by BNL.

Covariances in the thermal and resonance region are based on revisited low-fidelity estimates.

Estimates in the fast region were made using the EMPIRE/KALMAN approach. The estimate is based on a new EMPIRE input for 242-Pu prepared by M. Sin (Bucharest) in 2010. Sensitivities for each model input parameter were calculated using EMPIRE on a Linux cluster at the NNDC, and then the least-squares fitting code KALMAN was used to find an improved fit including covariances. Some experimental data were available and were included in the KALMAN fit including the most recent data by Tovesson (2009). Fluctuating experimental data below 200 keV were not taken into account, since such fluctuations are not handled by EMPIRE. Parameters varied in the EMPIRE fission input included: height and width of the first- and second-chance fission barriers, and level densities at the saddle point including their vibrational enhancement. In the main EMPIRE input, optical model parameters, level densities, and several tuning parameters were varied (generally by 1% or less).

Covariances for remaining reaction channels were taken over from the low-fidelity file.

241-Am (#13)

This is new evaluation, including quantification of uncertainties, performed recently by LANL. Since this new evaluation remains close to the ENDF/B-VII.0 values, the covariance matrices evaluated here can be used in association with the ENDF/B-VII.0 file.

ENDF/B-VII.0 resonance parameters which are the same as ENDF/B-VI.8 were replaced by the JENDL-4 resonance parameters. The energies of resolved resonances are almost identical to the values in ENDF/B-VI.8, but spins and widths show some differences. In the unresolved resonance range, we adopted LSSF=1, so that the dilute cross sections are given in MF3. The resonance parameter covariance matrix was taken directly from the JENDL-4.0 evaluated file.

In the fast region the neutron-induced fission cross section of 241-Am as well as its covariance matrix were obtained using the SOK code, which performs a generalized-least-square minimization of available experimental data. The energy boundary was lowered to 150 eV. The sub-threshold cross-sections are now given in File 3. The capture cross-section was re-evaluated with Hauser-Feshbach calculations using the CoH2 code, which reproduces the DANCE experimental data and an integral measurement. The covariance matrices for the total, inelastic, (n,2n), (n,3n), (n,4n), and capture cross sections were calculated with KALMAN, combining the statistical model calculations with available experimental data.

242m-Am (#14)

242m-Am covariances were supplied by BNL.

Covariances are combination of the uncertainties recommended in the assessment of Ref. [15] and correlation matrices produced by the WPEC Subgroup 26 [3] converted to the AFCI 33-energy group structure.

Following the low-fidelity approach, the uncertainties in the low energy region are based on experimental uncertainties of thermal cross sections, uncertainties of the resonance integrals and uncertainty of the scattering radius.

In the fast region the initial estimates [3] were obtained using EMPIRE/KALMAN system with default parameterization roughly adjusted to reproduce trends in the experimental data. The KALMAN code was run with default uncertainties assigned to the key model parameters to produce covariances. The assessment [15] of these initial estimates was based on the visual inspection of experimental data and dispersion of available evaluations. It led to considerable decrease of the elastic uncertainty and the inelastic uncertainty above 6 MeV, doubled fission uncertainty above 6 MeV, increased capture uncertainty in the whole fast neutron range and confirmed the nu-bar uncertainties.

243-Am (#15)

243-Am covariances were supplied by BNL.

Covariances are combination of the uncertainties recommended in the assessment of Ref. [15] and correlation matrices produced by the WPEC Subgroup 26 [3] converted to the AFCI 33-energy group structure.

Following the low-fidelity approach, the uncertainties in the low energy region are based on experimental uncertainties of thermal cross sections, uncertainties of the resonance integrals and uncertainty of the scattering radius.

In the fast region the initial estimates [3] were obtained using EMPIRE/KALMAN system with default parameterization roughly adjusted to reproduce trends in the experimental data. The KALMAN code was run with default uncertainties assigned to the key model parameters to produce covariances. The assessment [15] modified considerably elastic uncertainties, slightly increased fission uncertainties above 6 MeV, reduced those of inelastic, doubled (n,2n) uncertainties, and essentially confirmed capture and nu-bar uncertainties.

242-Cm (#16)

242-Cm covariances were supplied by BNL. It should be noted that ENDF/B-VII.0 evaluation is known to be of very poor quality, hence many COMMARA-2.0 uncertainties were set to the maximum possible value of 100%.

Following the low-fidelity approach, the uncertainties in the low energy region are based on experimental uncertainties of thermal cross sections, uncertainties of the resonance integrals and uncertainty of the scattering radius.

In the fast region covariances are combination of the uncertainties recommended in the assessment of Ref. [15] and correlation matrices produced by the WPEC Subgroup 26 [3] converted to the COMMARA 33-energy group structure. The initial estimates were obtained using EMPIRE/KALMAN system with default parameterization roughly adjusted to reproduce trends in the experimental data. The KALMAN code was run with default uncertainties assigned to the key model parameters to produce covariances.

243-Cm (#17)

243-Cm covariances were supplied by BNL.

Following the low-fidelity approach, the uncertainties in the low energy region are based on experimental uncertainties of thermal cross sections, uncertainties of the resonance integrals and uncertainty of the scattering radius.

Covariances are combination of the uncertainties recommended in the assessment of Ref. [15] and correlation matrices produced by the WPEC Subgroup 26 [3] converted to the AFCI 33-energy group structure. The initial estimates were obtained using EMPIRE/KALMAN system with default parameterization roughly adjusted to reproduce trends in the experimental data. The KALMAN code was run with default uncertainties assigned to the key model parameters to produce covariances. The assessment of Ref. [15] lowered considerably elastic and fission uncertainties, modified inelastic scattering uncertainty, and confirmed nu-bar uncertainties on the level of 1.3%.

244-Cm (#18)

243-Cm covariances were supplied by BNL.

Following the low-fidelity approach, the uncertainties in the low energy region are based on experimental uncertainties of thermal cross sections, uncertainties of the resonance integrals and uncertainty of the scattering radius.

In the fast region covariances are combination of the uncertainties recommended in the assessment of Ref. [13] and correlation matrices produced by the WPEC Subgroup 26 [3] converted to the AFCI 33-energy group structure. The initial estimates were obtained using EMPIRE/KALMAN system with default parameterization roughly adjusted to reproduce trends in the experimental data. The KALMAN code was run with default uncertainties assigned to the key model parameters to produce covariances. The assessment of Ref. [15] lowered considerably elastic uncertainties above 2 MeV (from about 10% down to about 3%), decreased fission and (n,2n) uncertainties, but increased slightly inelastic and dramatically capture uncertainties. The uncertainties of the prompt fission multiplicities have been increased slightly.

245-Cm (#19)

243-Cm covariances were supplied by BNL.

Following the low-fidelity approach, the uncertainties in the low energy region are based on experimental uncertainties of thermal cross sections, uncertainties of the resonance integrals and uncertainty of the scattering radius.

In the fast region covariances are combination of the uncertainties recommended in the assessment of Ref. [13] and correlation matrices produced by the WPEC Subgroup 26 [3] converted to the AFCI 33-energy group structure. The initial estimates were obtained using EMPIRE/KALMAN system with default parameterization roughly adjusted to reproduce trends in the experimental data. The KALMAN code was run with default uncertainties assigned to the key model parameters to produce covariances. The assessment of Ref. [15] reduced elastic uncertainties down to 3%, confirmed fission uncertainties, substantially reduced inelastic ones, dramatically modified capture uncertainties and left unchanged (n,2n) uncertainties. The nu-bar uncertainties were lowered from about 3% down to about 1.4% below 6 MeV and confirmed for energies above 6 MeV.

246-Cm (#20)

243-Cm covariances were supplied by BNL.

Following the low-fidelity approach, the uncertainties in the low energy region are based on experimental uncertainties of thermal cross sections, uncertainties of the resonance integrals and uncertainty of the scattering radius.

Covariances are combination of the uncertainties recommended in the assessment of Ref. [15] and correlation matrices produced by the WPEC Subgroup 26 [3] converted to the AFCI 33-energy group structure. The initial estimates were obtained using EMPIRE/KALMAN system with default parameterization roughly adjusted to reproduce trends in the experimental data. The KALMAN code was run with default uncertainties assigned to the key model parameters to produce covariances. These uncertainties have not been included in the Ref. [15] assessment.

3.6 Actinides - nu-bars (20 materials)

Procedures used for obtaining COMMARA-2.0 covariances for average neutron multiplicities, nu-bars, were in most cases described above. The ENDF/B-VII.0 library contains nu-bar covariances only for 232-Th and 235-U, while COMMARA-2.0 library contains nu-bar covariances for 20 materials. Out of these materials 2 were taken from ENDF/B-VII.0, 5 materials were supplied by LANL and remaining 13 materials by BNL:

- 232-Th and 235-U: nubar covariances were taken over from ENDF/B-VII.0
- 233,238-U and 239-Pu: nubar covariances stem from new evaluations completed by LANL. These evaluations were originally intended for ENDF/B-VII.0, but were not included into ENDF/B-VII.0 due to the lack of time.
- 238,240-Pu: nubar covariances represent new evaluations performed by LANL for the present project. We note that the new LANL evaluation for 238-Pu contains also nu-bar covariance consistent with the prompt fission neutron spectra. In the case of 240-Pu, nu-bar covariances have been obtained by LANL from the analysis of experimental data with the GLUCS code. **Note**: the 240-Pu nu-bar uncertainties are unusually large due to the differences between ENDF/B-VII.1 and ENDF/B-VII.0 that have been accounted for in the uncertainties.
- 234,236-U, 237-Np, 241,243-Pu, 241,242m,243-Am, 242,243,244,245,246-Cm: nu-bar covariances for these remaining 13 minor actinides were supplied by BNL. They are based on Maslov estimates of uncertainties using dispersion analysis and comparison with available experimental data [15]. Correlations were taken over from Ref. [3] and they based either on simple fits to data whenever possible or assumed to be the same as those of the appropriately selected neighboring nuclei.

3.7 Actinides – prompt fission neutron spectra (3 materials)

Covariance matrices for the prompt fission neutron spectra have been provided by LANL for 238-Pu, 239-Pu, and 240-Pu at incident neutron energy of 0.5 MeV. They were obtained following a method similar to the one employed for estimating cross-section uncertainties. The Madland-Nix approach was used to perform model calculations and the Bayesian updating code KALMAN was used to incorporate experimental data.

238-Pu (#1)

238-Pu prompt fission neutron spectra covariances were supplied by LANL as described above.

239-Pu (#2)

239-Pu prompt fission neutron spectra covariances were supplied by LANL as described above.

240-Pu (#3)

240-Pu prompt fission neutron spectra covariances were supplied by LANL as described above

3.8 mubars (2 materials)

Mu-bars are defined as average scattering cosines. The AFCI project requested mu-bar covariances for few most important materials, included in COMMARA-2.0 library are two prominent materials.

23-Na (#1)

The file was produced by BNL.

In major evaluated nuclear data libraries covariances for 23-Na mu-bars are available in JENDL-3.3 only. They are based on fairly simple optical model estimate. JENDL-3.3 does not provide mu-bar covariance matrix in an explicit way, it must be computed from MF34/MT2 using NJOY. We took this mubar covariance matrix as the basis and applied important modifications. In the region of 0.7 MeV - 2 MeV we rescaled JENDL-3.3 uncertainties by a factor of 3 to reflect the differences between basic values of mu-bars in JENDL-3.3 and ENDF/B-VII.0.

56-Fe (#2)

The file was produced by BNL.

In this case, a fairly robust evaluation of mu-bar is available that is fully based on experimental data. This evaluation was adopted by the recently released Russian library ROSFOND, based on the review of 56-Fe evaluations in major libraries performed by V. Pronyaev, Obninsk in 2006. Pronyaev recommended use of the original Russian evaluation developed for BROND-3. This in turn was taken over from the earlier mu-bar evaluation by Pronyaev-Vonach (1995) and adopted by JEFF-3.1. BNL reviewed this evaluation and decided to adopt it.

4. QUALITY ASSURANCE

The COMMARA-2.0 library has undergone Quality Assurance (QA) testing before release. This testing was designed to disclose formal deficiencies, enforce mathematical correctness and ensure that the uncertainties are reasonable, which is an essential condition for covariances to be useful to the end users. To this end, two dedicated QA tools have been developed at BNL:

- The unCor code, which performs several tests on the entire library in the AFCI format.
- A web-based visual system that allows performing a number of comparisons including cross sections, nu-bars, along with their uncertainties as well as uncertainties for integrated quantities.

4.1 Checking with unCor code

The BNL code unCor (uncertainties & correlations) was developed to check the AFCI-1.2 covariance library. The code has been gradually refined during the development of AFCI-1.3 and COMMARA-2.0 libraries. Using unCor, the entire COMMARA-2.0 library was subject to systematic tests applied to uncertainties and correlation coefficients. The testing suite raises warning upon encountering any of the following:

1. Uncertainties too high (>100%)
2. Uncertainties too low (total < 1%, elastic < 2%, capture < 2%, inelastic < 3%, fission < 0.7%, nubar < 0.7%, (n,2n) < 3%, other < 3%)
3. Uncertainty too low for small cross section (if cross section < 3 mb and uncertainty < 25%)
4. 0% uncertainties with non-zero cross sections
5. Sudden discontinuities and jumps in uncertainties (more than factor of 8)
6. Rows/columns of fission spectrum covariances (MF35) not summing to zero
7. Unphysical correlation coefficients (asymmetric matrices, coefficients not within -1 and +1, diagonal $\neq 1$)
8. Non-positive-definite matrices

The above criteria were used throughout the library to issue warnings. Some of these criteria, such as no. 6 and 7, were applied strictly while other were treated on a case-by-case basis. Accordingly, numerous cases of uncertainties bigger than 100% or smaller than the prescribed limits were corrected. As a result, the final number of warnings had been considerably reduced. We did not modify, however, low uncertainties obtained within the true R-matrix analysis of light nuclei, since overwriting these would require stronger arguments.

Special attention was paid to the positive-definiteness in all matrices. Non-positive-definite matrices appear either due to the limited precision (3 digits) used in the AFCI library or due to the oversimplified methodology employed in their generation or due to the processing of the original ENDF-6 formatted covariances into 33-group structure. Two techniques were used for fixing non-positive-definite matrices:

- large off-diagonal correlations were reduced slightly,
- matrix was diagonalized, all negative eigenvalues set to zero, and the resulting matrix written back with three significant digits.

The resulting correlation matrices are positive definite at the price of some change in the correlations produced by the processing codes.

4.2 Visual inspection and validation against integral quantities

The visual inspection Web-based covariance QA system, developed specially for testing COMMARA-2.0 library, is the essential tool for ensuring that the uncertainties in the library are reasonable. The system consists of two parts, the differential part designed to compare cross sections and the integral part allowing comparison of integral quantities. The system is using proven java-based programming capabilities largely employed and broadly tested in the NNDC neutron cross section retrieval and visualization tool Sigma. The system has been extensively used to review and update uncertainties primarily for structural materials in the final stage of the COMMARA-2.0 development.

The basic idea is to allow efficient inter-comparison of major evaluated data libraries, including experimental data and other suitable sources of information to help reviewer to perform two exercises. First, look into dispersion of central values as a possible indicator of precision reached by various evaluators and hence judge plausibility of COMMARA-2.0 covariances. Second, look into dispersion of suitable integral quantities along with their uncertainties as indicator of quality of COMMARA-2.0 covariances.

Comparison of differential quantities: The first part of the system is illustrated in Fig.1, showing somewhat controversial case of 241-Pu total fission cross sections. The reviewer has a choice and possibility of:

- comparing point-wise cross sections in ENDF/B-VII.0 with the selected experimental data including the uncertainty band taken from the selected version of the library,
- comparing cross sections in major nuclear data libraries processed into the AFCI 33-energy group structure,
- comparing uncertainties in the different releases of the AFCI library, and
- changing displayed energy range, scaling cross section range, choosing linear or logarithmic scale for both axes, selecting and unselecting individual experimental data sets.

The upper panel of Fig.1 shows pointwise 241-Pu fission sections with the corridor of the associated uncertainties which are almost non-visible. The system allows inclusion of experimental data from EXFOR and group-wise cross sections from major evaluated libraries, also shown in Fig.1. The bottom panel compares uncertainties in different versions of the AFCI library, showing that both AFCI-1.3 and COMMARA-2.0 uncertainties are fairly low. It should be noted that initial simple estimate included in AFCI-1.2 library complies with large dispersion between ENDF/B-VII.0 and new data by Tovesson (2010). Since, however, the most recent analysis by LANL evaluators determined that Tovesson data need to be carefully reviewed, they were not included into the analysis, yielding low COMMARA-2.0 uncertainties on the level of 1% or less.

Comparison of integral quantities: Inclusion of the integral quantities such as resonance integrals, Maxwellian averages, and californium spectrum averages along with their uncertainties provide a unique possibility of testing not only diagonals but, to some extent, also off-diagonal part of the covariance matrix. It should be emphasized that the off-diagonal part of the covariance matrix is included in the calculation of the integral uncertainties. Therefore, agreement with the measured integral quantity within quoted uncertainty is an indication that the covariance matrix as a whole reflects reality. The quantities compared by the system are elastic scattering, radiative capture, fission, and neutron multiplicities (total, prompt and delayed nu-bars).

An example can be seen in Fig.2 showing 241-Pu elastic and fission cross sections (Fig.2a), and also capture and nubars (Fig.2b). Fig. 2 displays all quantities as ratios to ENDF/B-VII.0 central values. Available are:

- thermal values,
- calculated resonance integrals,
- 30 keV Maxwellian and californium spectra averages,
- 14 MeV values, and also

- scattering radius R' in the case of elastic.

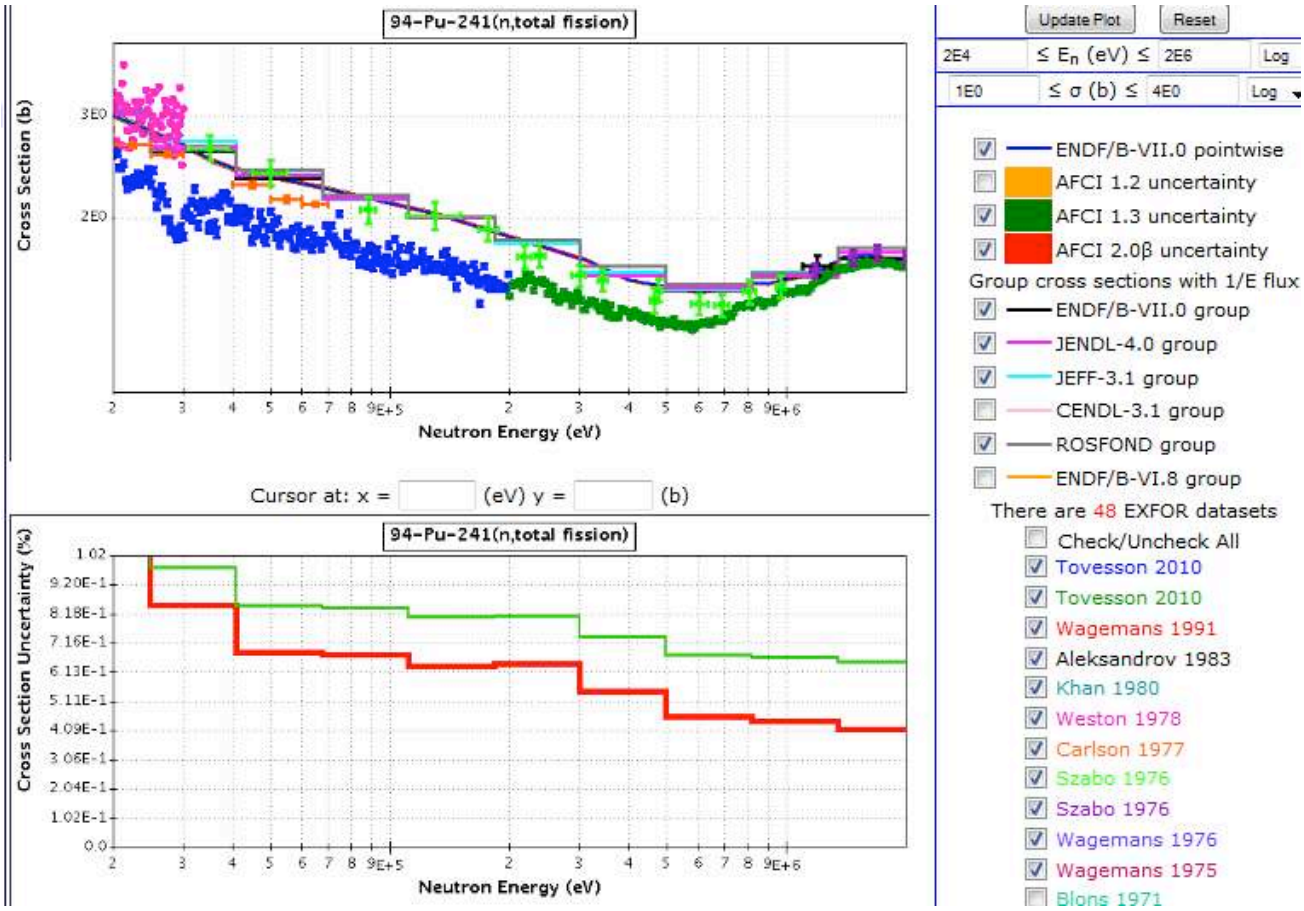

Figure 1: Screen-shot of the BNL Web-based QA review system with 241-Pu fission cross sections. The upper panel shows pointwise ENDF/B-VII.0 compared to more recent experimental data. Also shown are multigroup cross sections for major evaluated libraries, suggesting small dispersion between the libraries, in support of small AFCI uncertainties. Relative uncertainties can be seen in the bottom panel, AFCI-1.3 in green and COMMARA-2.0 in red. Important issue to be addressed in future is reliability of Tovesson 2010 data, which, if correct, would impact COMMARA-2.0 covariances considerably.

An evaluator can compare numerical values of these quantities resulting from different libraries and judge whether uncertainties of the integrals calculated from the library look plausible. If available, the experimental values and uncertainties from Atlas of Neutron Resonances and from KADoNiS astrophysical database [16] are also shown.

Fig.2a top panel displays 241-Pu elastic scattering integral quantities. Overall, our uncertainties are not unreasonable, though they are not without some issues. Comparison for thermal values, shown to the very left, suggests that COMMARA-2.0 uncertainty may look large (black bar) but this large value is justified by considerable discrepancy between ENDF/B-VII.0 value (black point) and the value in Atlas of Neutron Resonances (point in teal color with uncertainty bar). On the other hand, large dispersion between major libraries at 14 MeV indicates that COMMARA-2.0 uncertainty at the highest energies might be overoptimistic.

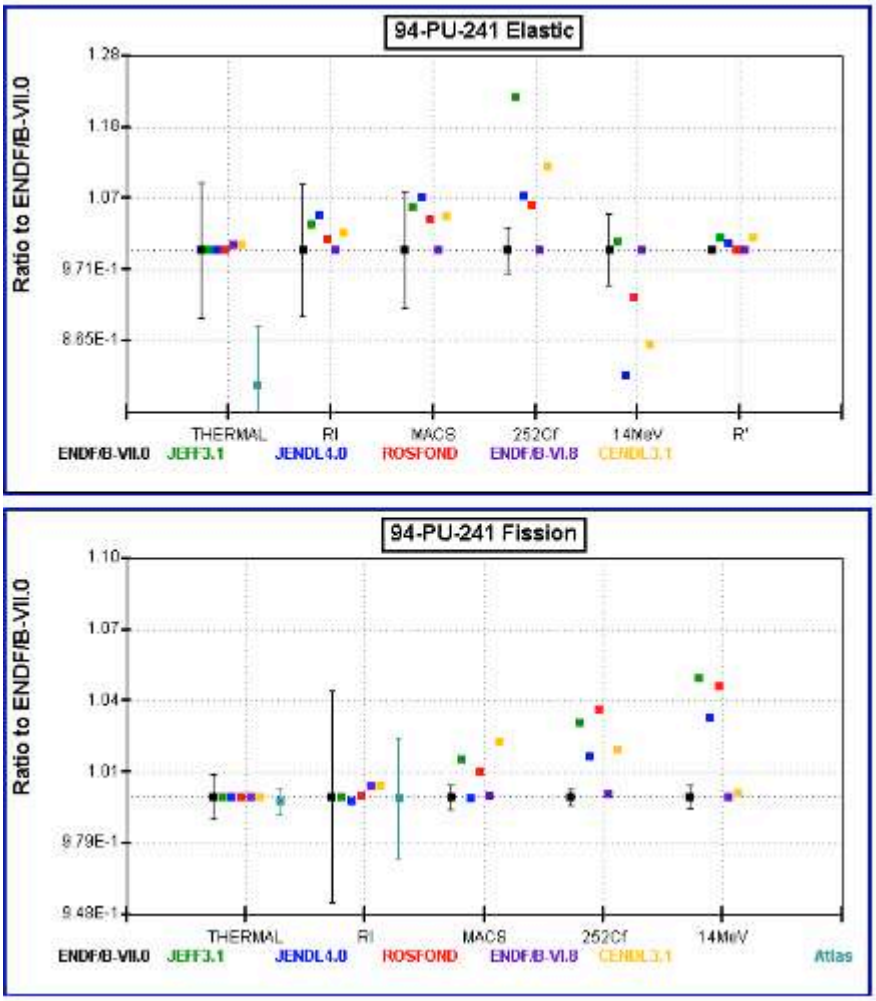

Figure 2a: Screen-shot of the BNL Web-based review system for 241-Pu integral quantities showing elastic scattering and fission cross sections relative to ENDF/B-VII.0. Compared are thermal values, resonance integrals (RI), 30 keV Maxwellian averages (MACS), 252-Cf spectrum averages and 14 MeV cross sections for major libraries. Shown are also central values and uncertainties given in Atlas of Neutron Resonances (light green) for thermal elastic, and for thermal fission and fission resonance integral.

Fig.2a bottom panel displays 241-Pu fission cross section integral quantities. Again, shown to the very left are thermal values, showing full agreement between major evaluated libraries, COMMARA-2.0 uncertainty of 1% being driven by the uncertainty in Atlas (light green point with uncertainty bar). Similar statement can be made about fission resonance integral, even though our 4% uncertainty looks a bit large compared to Atlas of Neutron Resonances. Both 30 keV Maxwellian and 252-Cf averages show that dispersion of major libraries exceeds COMMARA-2.0 uncertainty. This is also true for 14 MeV uncertainty, with ~0.5% of COMMARA-2.0 being much lower than ~4% of dispersion between 242-Pu fission cross sections in ENDF/B-VII.0 on one hand and fission cross sections in JEFF-3.1, JENDL-4.0 and ROSFOND on the other hand.

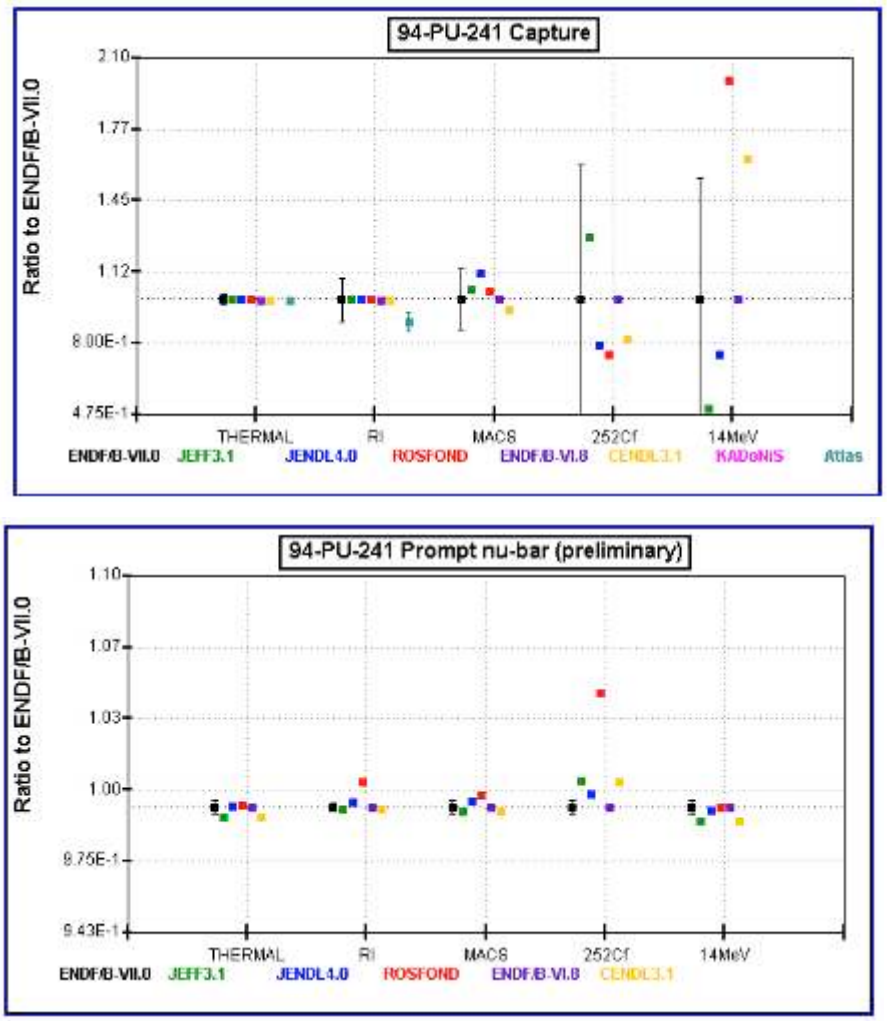

Figure 2b: Screen shot of the NNDC Web-based QA system for 241-Pu integral quantities showing capture cross sections and prompt nubars as ratios to ENDF/B-VII.0 central values. Shown are thermal values, resonance integrals (RI), 30-keV Maxwellian averages (MACS), 252-Cf averages and 14 MeV values. The upper panel displays capture in major libraries; shown are also values and uncertainties given in Atlas of Neutron Resonances, while KADoNiS [16] does not have data for 241-Pu. The bottom panel shows prompt nubars in major libraries.

Fig.2b top panel displays 241-Pu capture cross sections relative to ENDF/B-VII.0 central values. Shown are major evaluated nuclear data libraries and also data taken from Atlas of Neutron Resonances (points in teal color, with visible error bar for resonance integral). One can conclude that both the uncertainties given in Atlas (RI value) as well as uncertainties inferred from dispersion between major evaluated libraries support COMMARA-2.0 covariances.

Fig.2b bottom panel shows 241-Pu prompt nubars relative to ENDF/B-VII.0 central values. COMMARA-2.0 uncertainties are on the level of about 0.3% for all integral quantities shown here. This looks a bit too optimistic in particular for 252-Cf averages, suggesting that our estimates for prompt nubar uncertainties around 1 MeV might need some enhancement.

5. CONCLUSIONS

The COMMARA-2.0 neutron cross section covariance library has been developed by BNL-LANL collaboration for Advanced Fuel Cycle Applications during FY2008-FY2010. The primary role of COMMARA-2.0 is its use for developing adjusted multigroup library of neutron reaction data. COMMARA-2.0 library contains covariances for major reaction channels for 110 materials relevant to the fast reactor R&D and represents a solid step towards producing robust covariance information for AFCI applications. The library is to be used together with the ENDF/B-VII.0 central values of the latest official release of US files of evaluated neutron cross sections.

One of the most important issues that have been addressed is the quality of the covariance data. Development of adequate QA procedures and Web-based review tools is of key importance.

The COMMARA-2.0 beta version of the library was released to the reactor analysts at ANL and INL for testing in October 2010. Their feedback along with other comments was used to make final modifications of the library described in this report. As the next step, the library should be released to the international group of reactor analysts participating in the NEA-sponsored WPEC Subgroup 33 for testing their adjustment technology. COMMARA-2.0 should also serve as the basis for covariances to be included into the forthcoming release of ENDF/B-VII.1 library.

The present project provided huge challenge to US nuclear reaction data community. To produce covariance library for 110 materials of meaningful quality within 3 years was daunting task. Even though we managed to produce results that could and should be used by users broadly, we are fully aware that majority of our covariances were obtained by simplified methods and should be termed estimates rather than full scale evaluations. Hence, considerable further work is needed to produce robust covariances that could be used with confidence in reactor applications.

Acknowledgement

We are grateful to reactor analysts from ANL and INL for most useful feedback and numerous critical comments supplied to us in the course of this project. We owe special thank to ORNL evaluators for making available their covariances in the resonance region for several important actinides. Assistance of the NNDC staff in various stages of the project is gratefully acknowledged.

Development of the COMMARA-2.0 covariance library was sponsored by the United States Department of Energy, Office of Nuclear Energy as a part of Fuel Cycle R&D. This support is gratefully acknowledged.

REFERENCES

1. P. Obložinský et al., and P. Talou *et al*., "Progress on Nuclear Data Covariances: AFCI-1.2 Covariance Library," Report BNL-90897-2009, Brookhaven National Laboratory (2009).
2. M. Chadwick, P. Obložinský, M. Herman, et al*., "ENDF/B-VII.0: Next Generation Evaluated Nuclear Data Library for Nuclear Science and Techno*logy", *Nuclear Data Sheets* **107**, 2931 (2006).
3. D. Rochman, M. Herman, P. Obložinský, and S. F. Mughabghab, "Preliminary Cross Section Covariances for WPEC Subgroup 26," Report BNL-77407-2007-IR, Brookhaven National Laboratory (2007). See also addition to this report, "Preliminary nubar Covariances for ^{238,240}Pu and ^{242,243,244,245}Cm", Report BNL-77407-2007-IR-Suppl.1.
4. R.C. Little, T. Kawano, G.D. Hale, M.T. Pigni, M. Herman, P. Obložinský, M.L. Williams, M.E. Dunn, G. Arbanas, D. Wiarda, R.D. McKnight, J.N. McKamy, J.R. Felty, "Low-fidelity Covariance Project", *Nuclear Data Sheets*, **109**, 2828 (2008).
5. G. Hale, "Covariances from light-element R-matrix analyzes", *Nuclear Data Sheets,* **109**, 2812 (2008).
6. T. Kawano, P. Talou, P.G. Young, G. Hale, M.B. Chadwick, and R.C. Little, "Evaluation of Covariances for Actinides and Light Elements at LANL", *Nuclear Data Sheets* **109**, 2817 (2008).
7. M. Herman *et al*, "Development of Covariance Capabilities in EMPIRE code", *Nuclear Data Sheets* **109**, 2752 (2008).
8. M. Herman, R. Arcilla, C.M. Mattoon, S.F. Mughabghab, P. Obložinský, M.T. Pigni, B. Pritychenko, A.A. Sonzogni, "Covariance Evaluation Methodology for Neutron Cross Sections", Report BNL-81623-2008, Brookhaven National Laboratory (2008).
9. S. F. Mughabghab, "Atlas of Neutron Resonances: Thermal Cross Sections and Resonance Parameters", Elsevier, Amsterdam, 2006.
10. P. Obložinský, Y.-S. Cho, C.M. Mattoon, S.F. Mughabghab "Formalism for neutron cross section covariances in the resonance region using kernel approximation", Report BNL-91287-2010, Brookhaven National Laboratory (2010).
11. P. Obložinský, Y.-S. Cho, C.M. Mattoon, S.F. Mughabghab, "Neutron cross section covariances in the resonance region: ^{52}Cr, ^{56}Fe, ^{58}Ni," Report BNL-93903-2010, Brookhaven National Laboratory (2010).
12. P. Obložinský, Y.-S. Cho, C.M. Mattoon, S.F. Mughabghab, "Neutron cross section covariances in the resonance region: ^{50,53}Cr, ^{54,57}Fe, ^{60}Ni", Report BNL-94458-2010, Brookhaven National Laboratory (2010).
13. T. Kawano and K. Shibata, "Covariance Evaluation System", JAERI Data/Code, Japan Atomic Energy Research Institute, Tokai, Japan, 1997.
14. M. Pigni, M. Herman, P. Obložinský, "Extensive Set of Cross-Section Covariance Estimates in the Fast Neutron Region", Nucl. Sci. Eng. **162**, 25-40 (2009).
15. V.M. Maslov, P. Obložinský, M. Herman, "Review and Assessment of Neutron Cross Section and Nu-bar Covariances for Advanced Reactor Systems", Report BNL-81884-2008-IR, Brookhaven National Laboratory (2008).
16. I. Dillmann, M. Heil, F. Kappeler, R. Plag, "KADoNiS - Karlsruhe Astrophysical Database of Nucleosynthesis in Stars", www.kadonis.org, data retrieved in 2010.
17. P. Talou, T. Kawano, D.G. Madland, A.C. Kahler, D.K. Parsons, M.C. White, R.C. Little, and M.B. Chadwick, Nucl. Sci. Eng. **166**, 254 (2010).

Appendix A

AFCI 2.0 Covariance Plots

Light Nuclei

(12 materials)

^{1}H

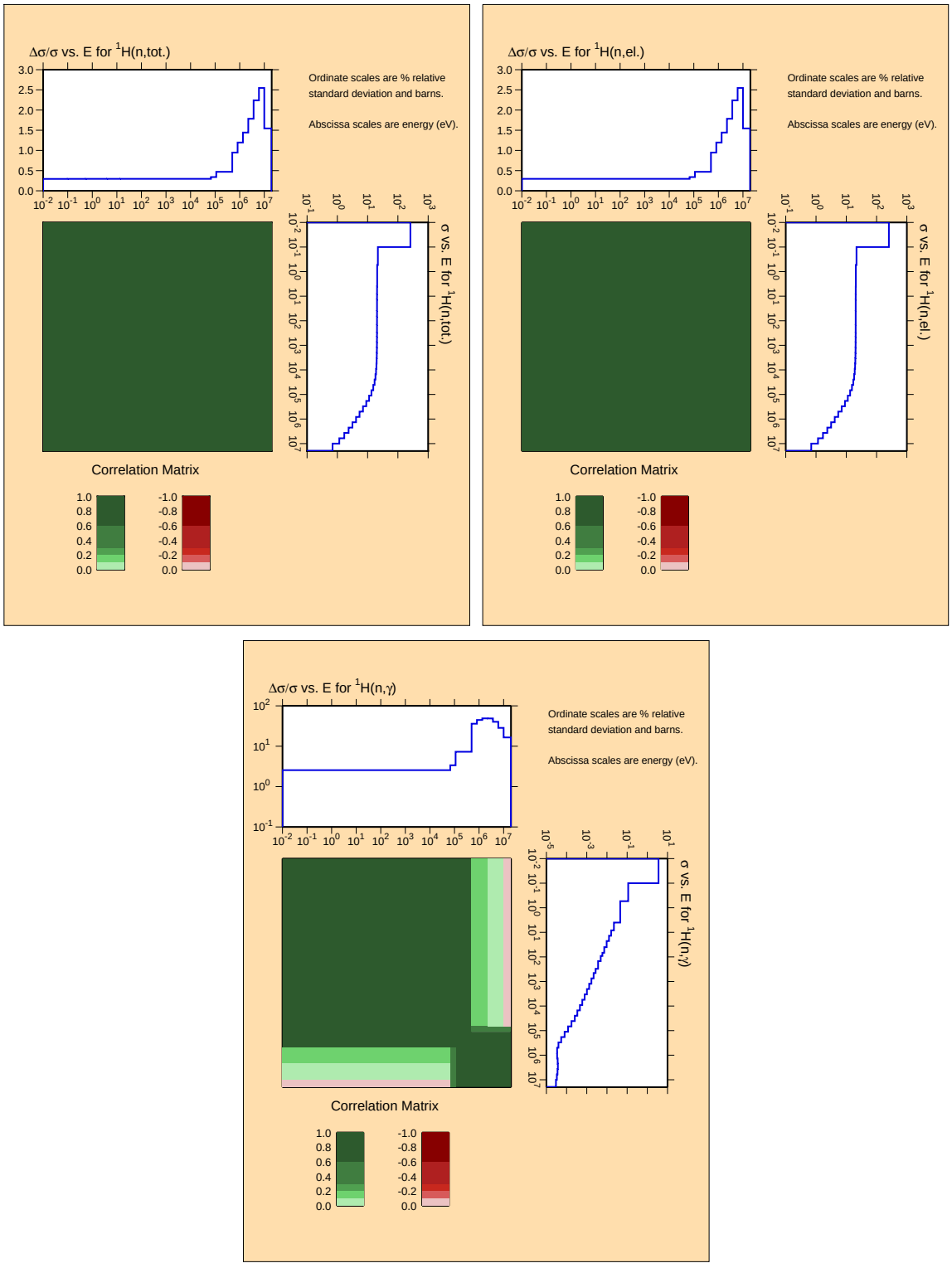

Figure A.1: Covariances for light nucleus ^{1}H.

^{2}H

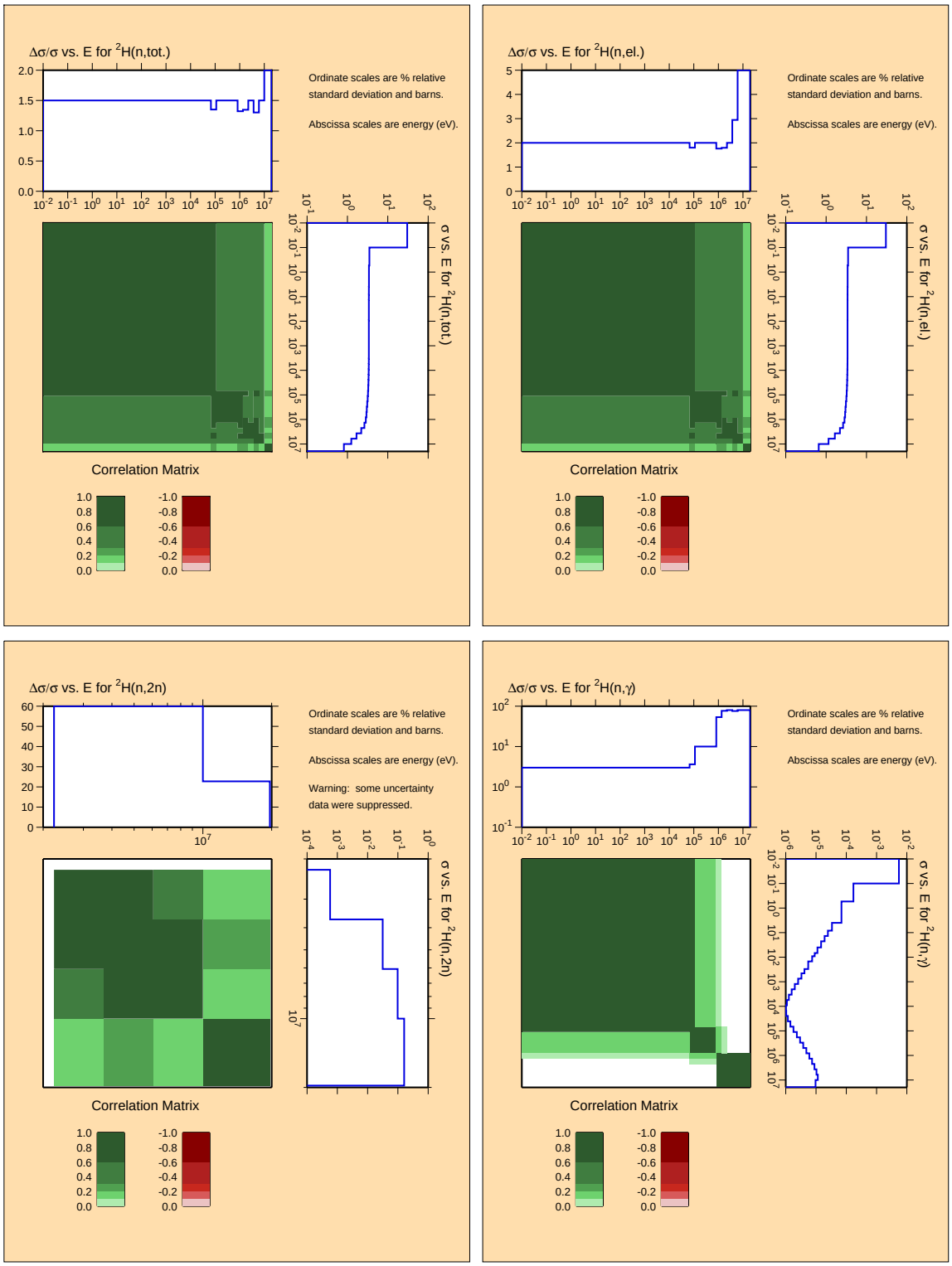

Figure A.2: Covariances for light nucleus ^{2}H.

^{4}He

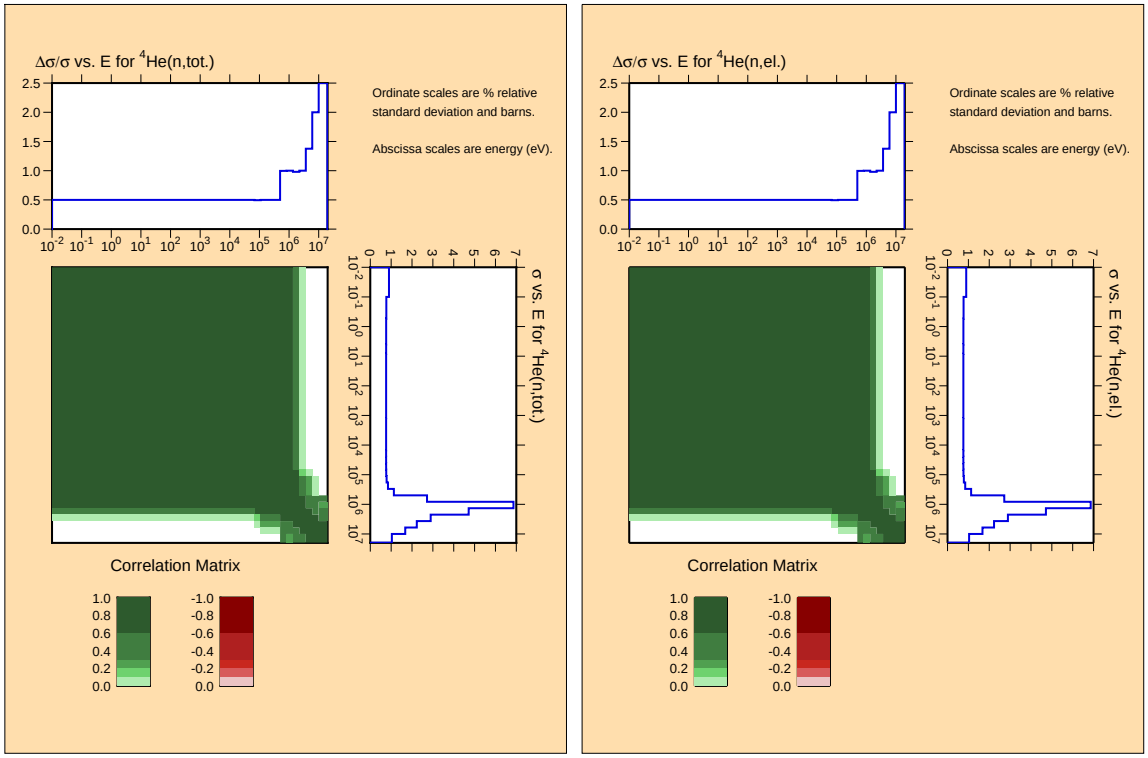

Figure A.3: Covariances for light nucleus ^{4}He.

^{6}Li

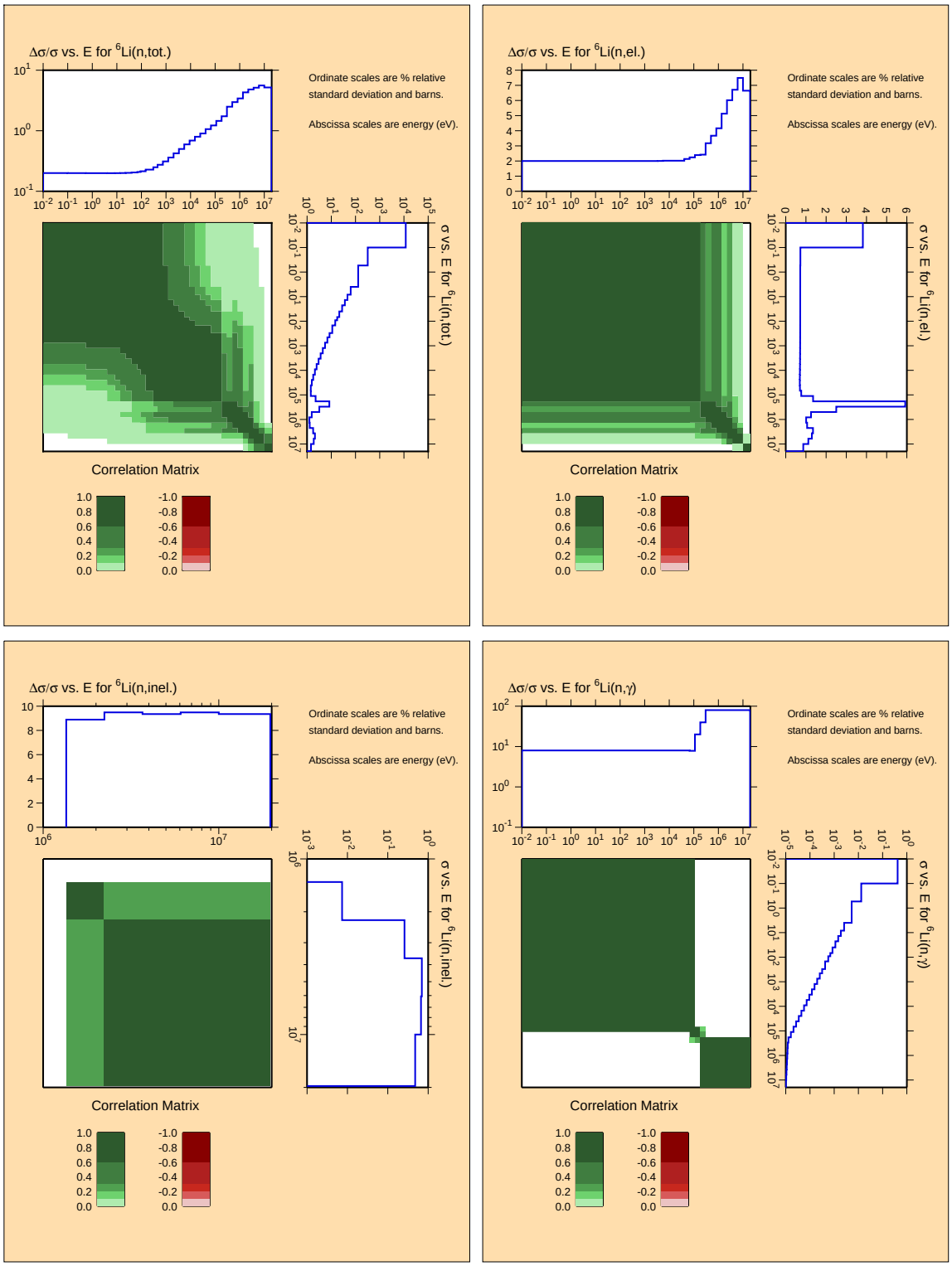

Figure A.4: Covariances for light nucleus ^{6}Li.

^{6}Li

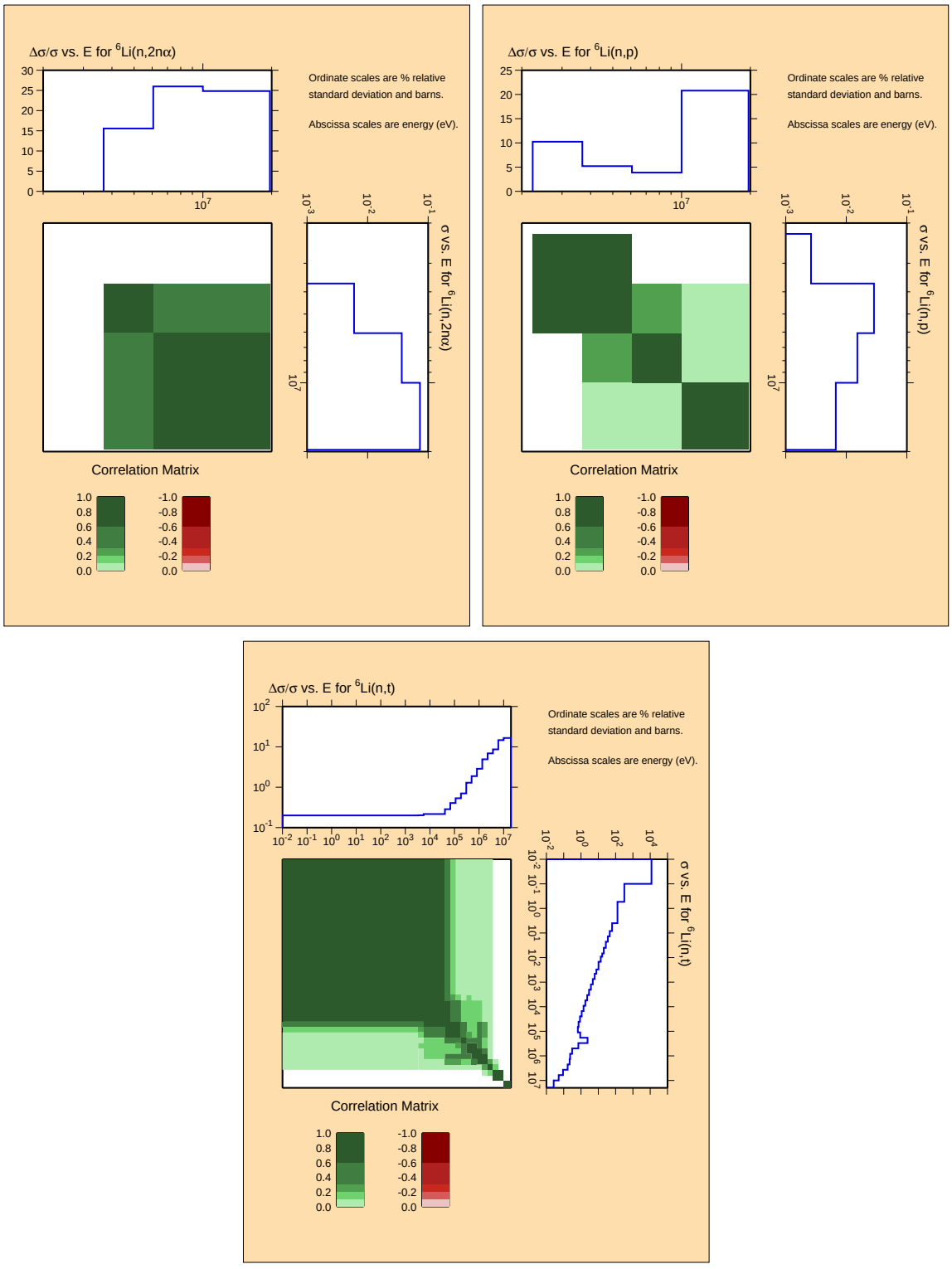

Figure A.5: Covariances for light nucleus ^{6}Li (continued).

^{7}Li

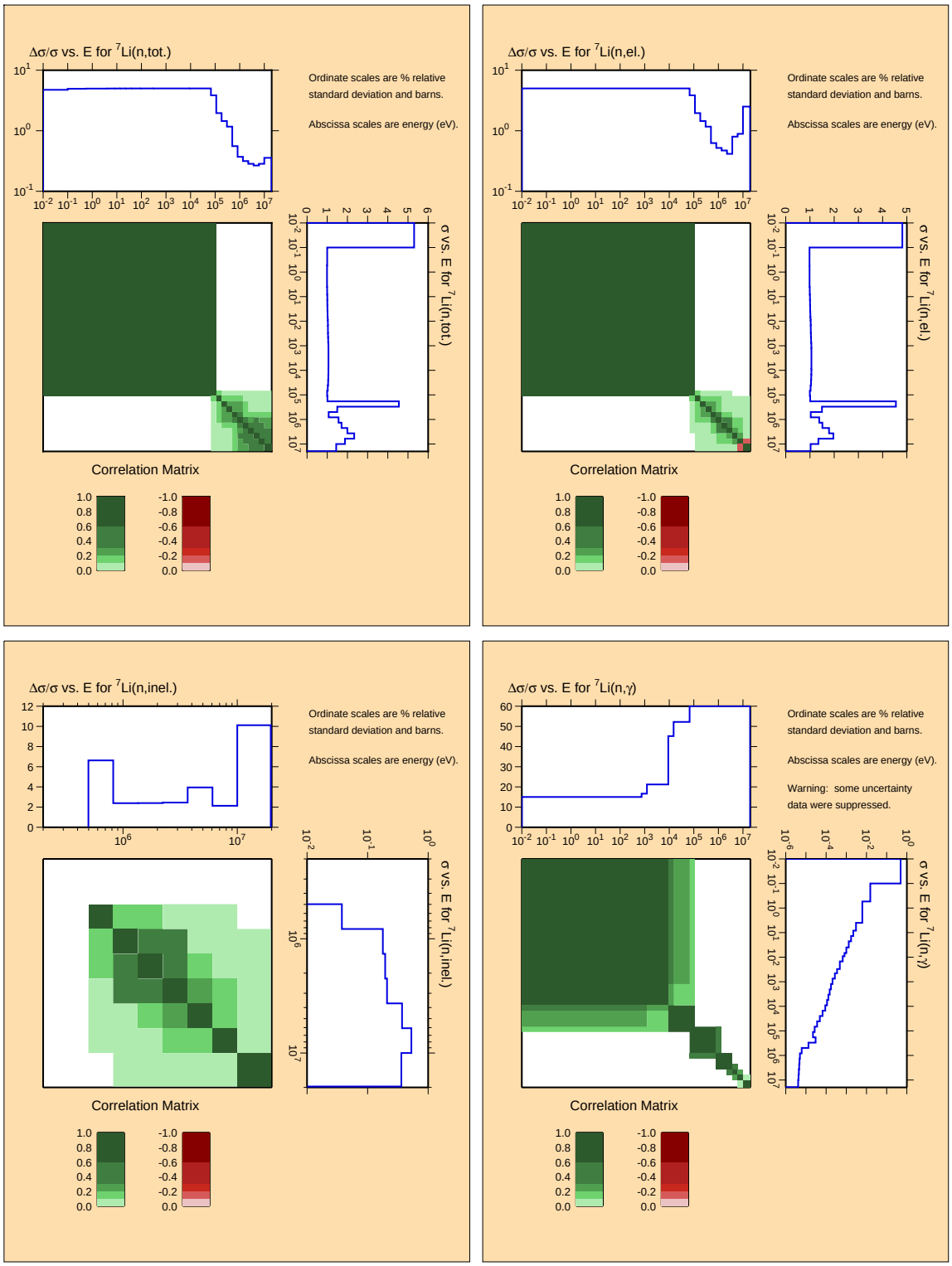

Figure A.6: Covariances for light nucleus ^{7}Li.

^{7}Li

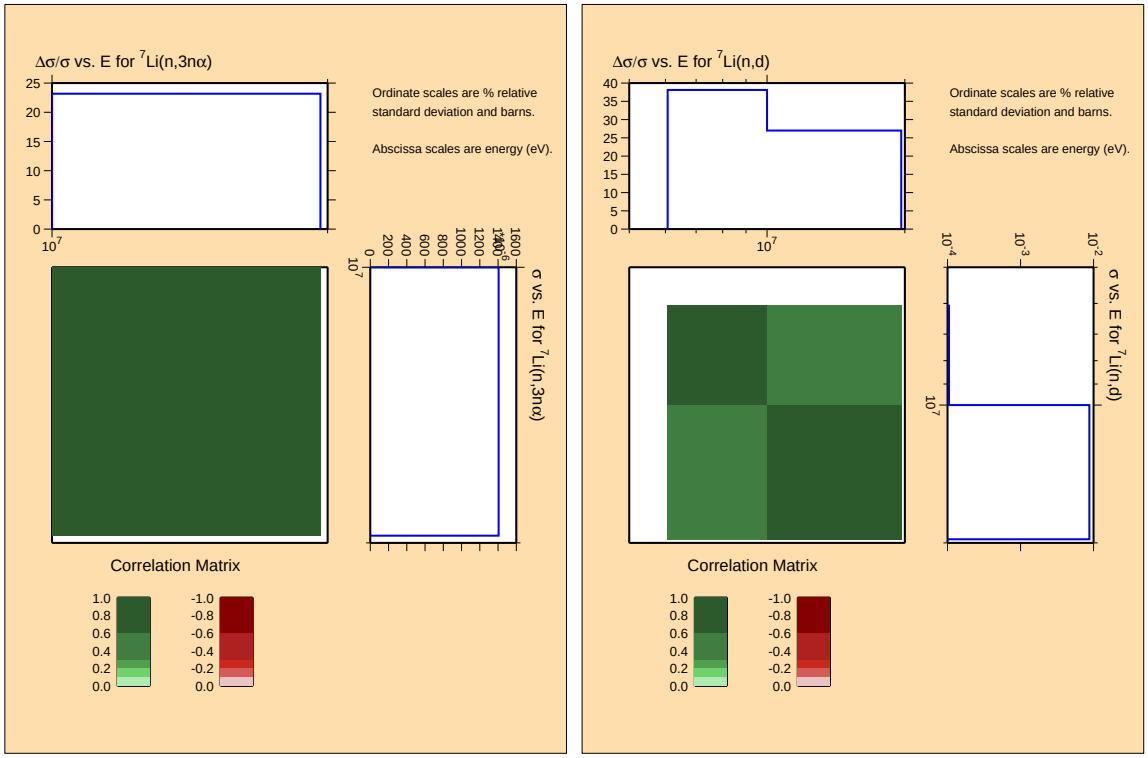

Figure A.7: Covariances for light nucleus ^{7}Li (continued).

^{9}Be

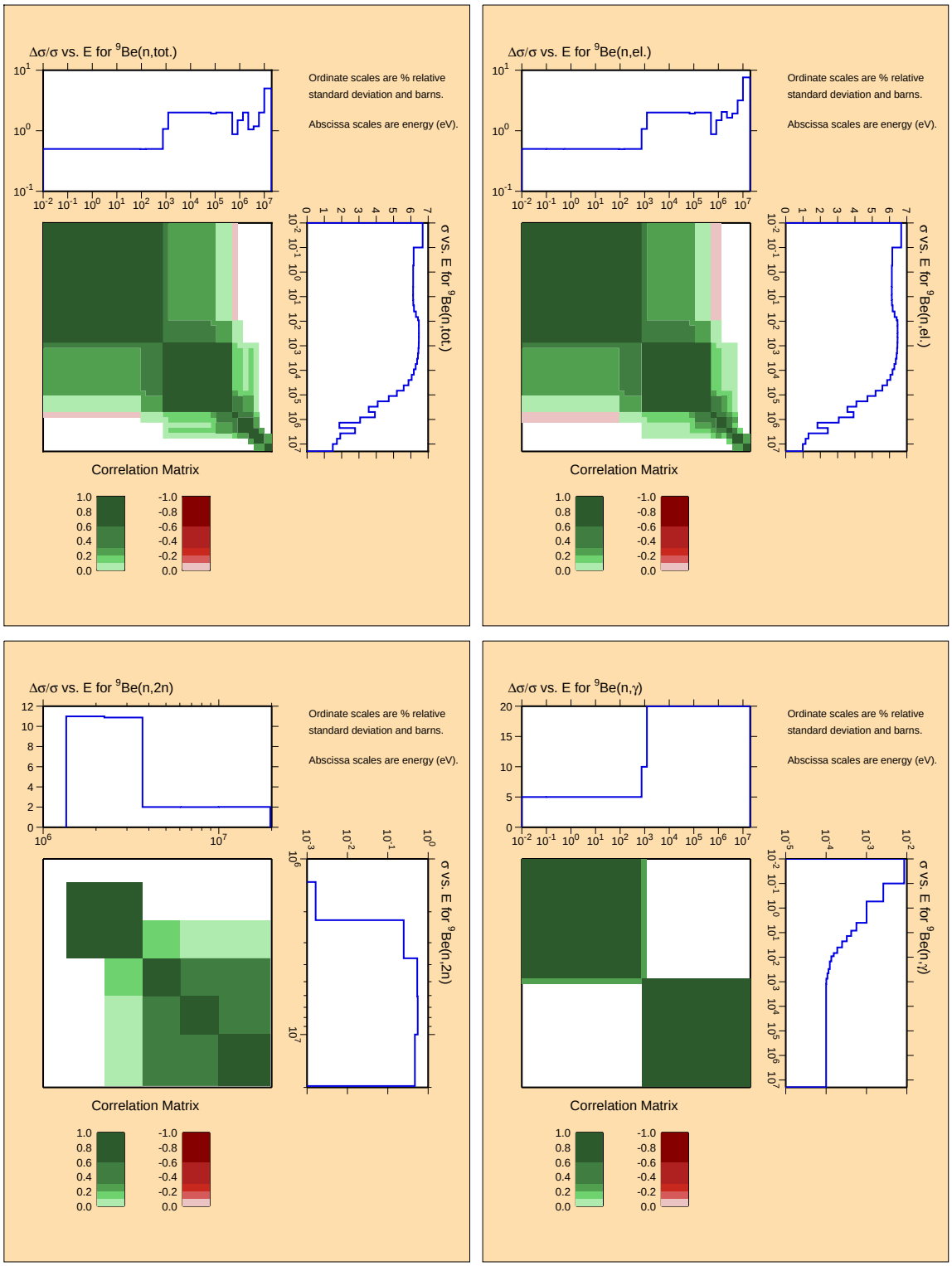

Figure A.8: Covariances for light nucleus ^{9}Be.

^{9}Be

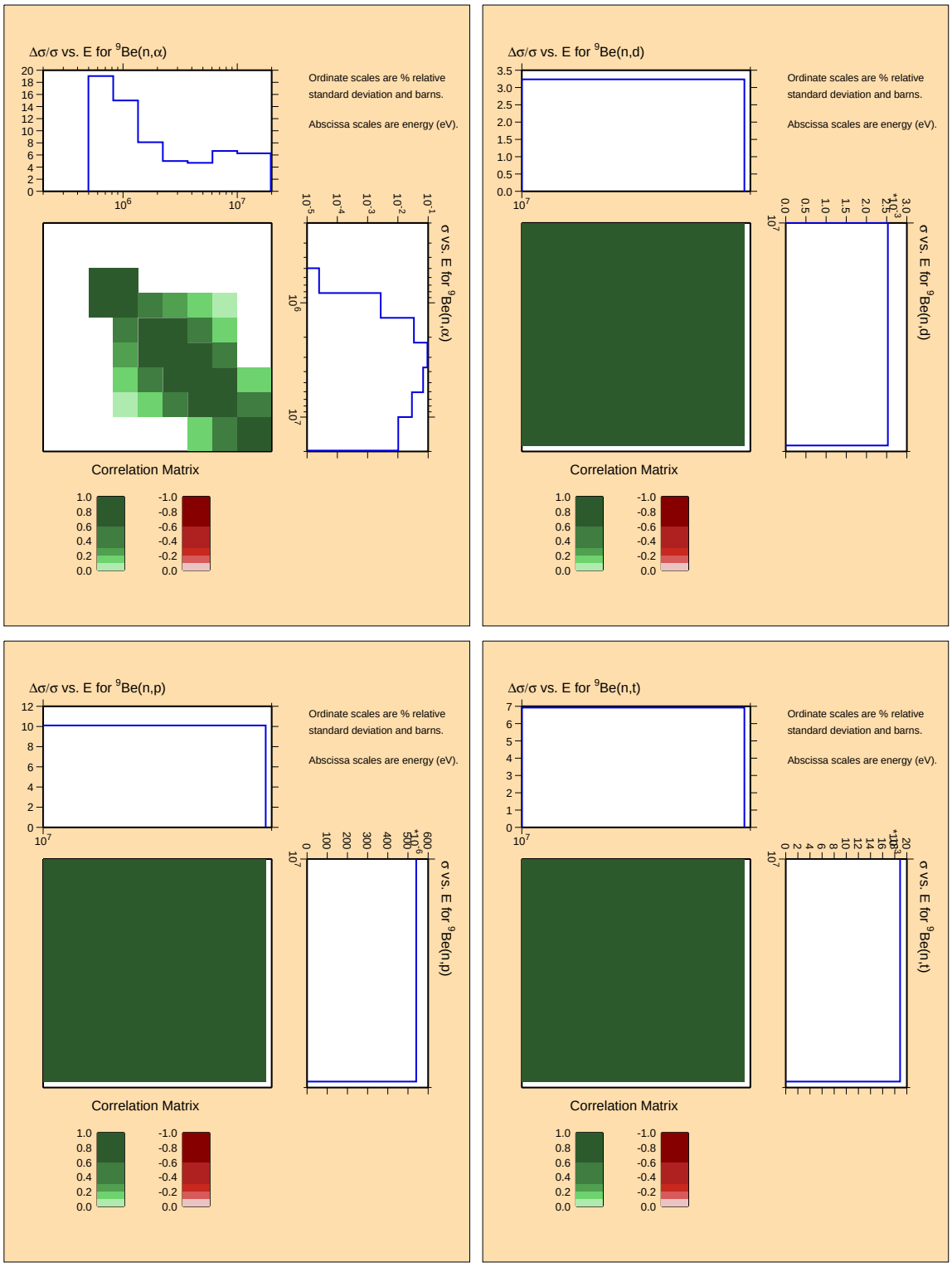

Figure A.9: Covariances for light nucleus ^{9}Be (continued).

^{10}B

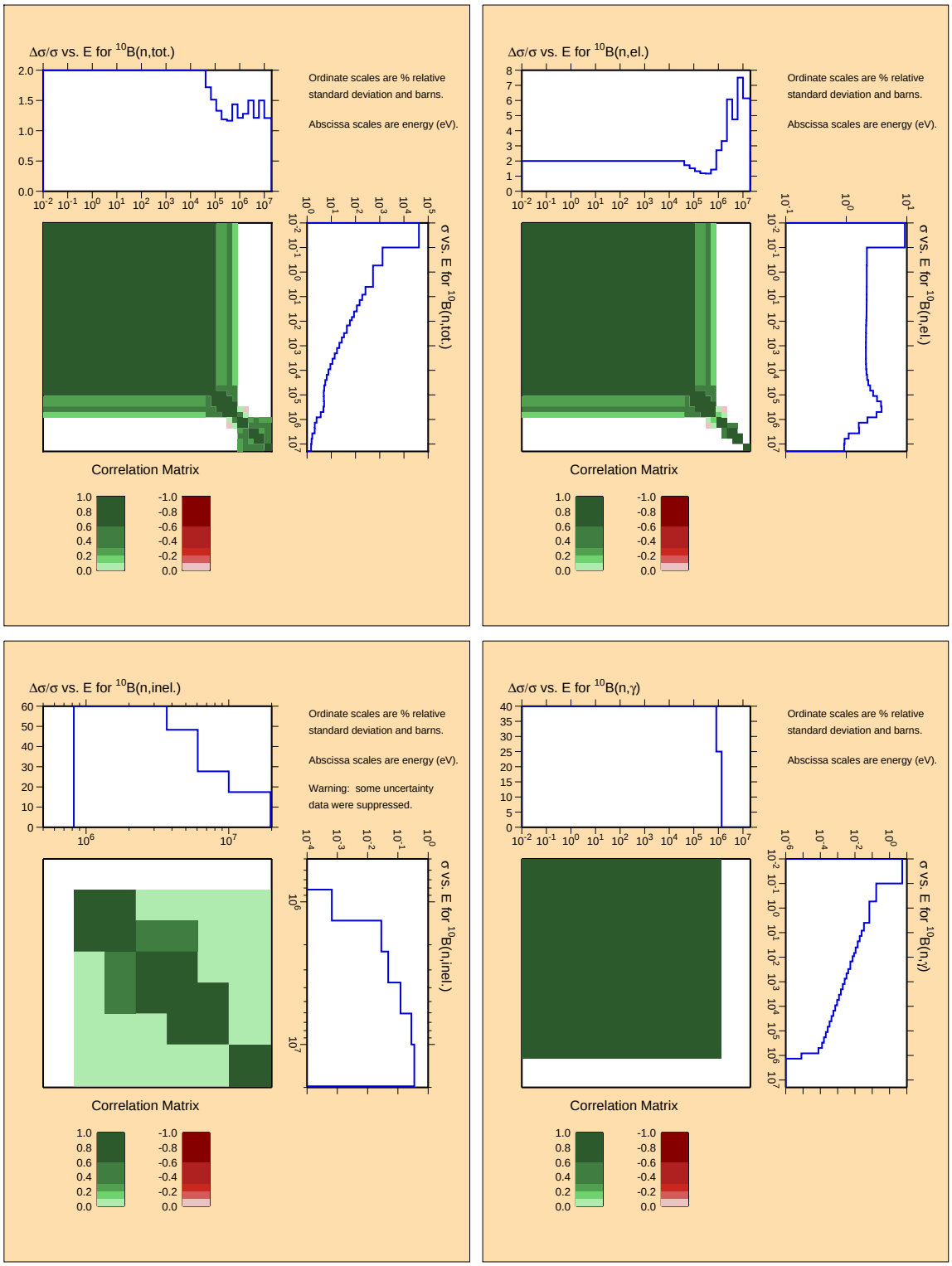

Figure A.10: Covariances for light nucleus ^{10}B.

^{10}B

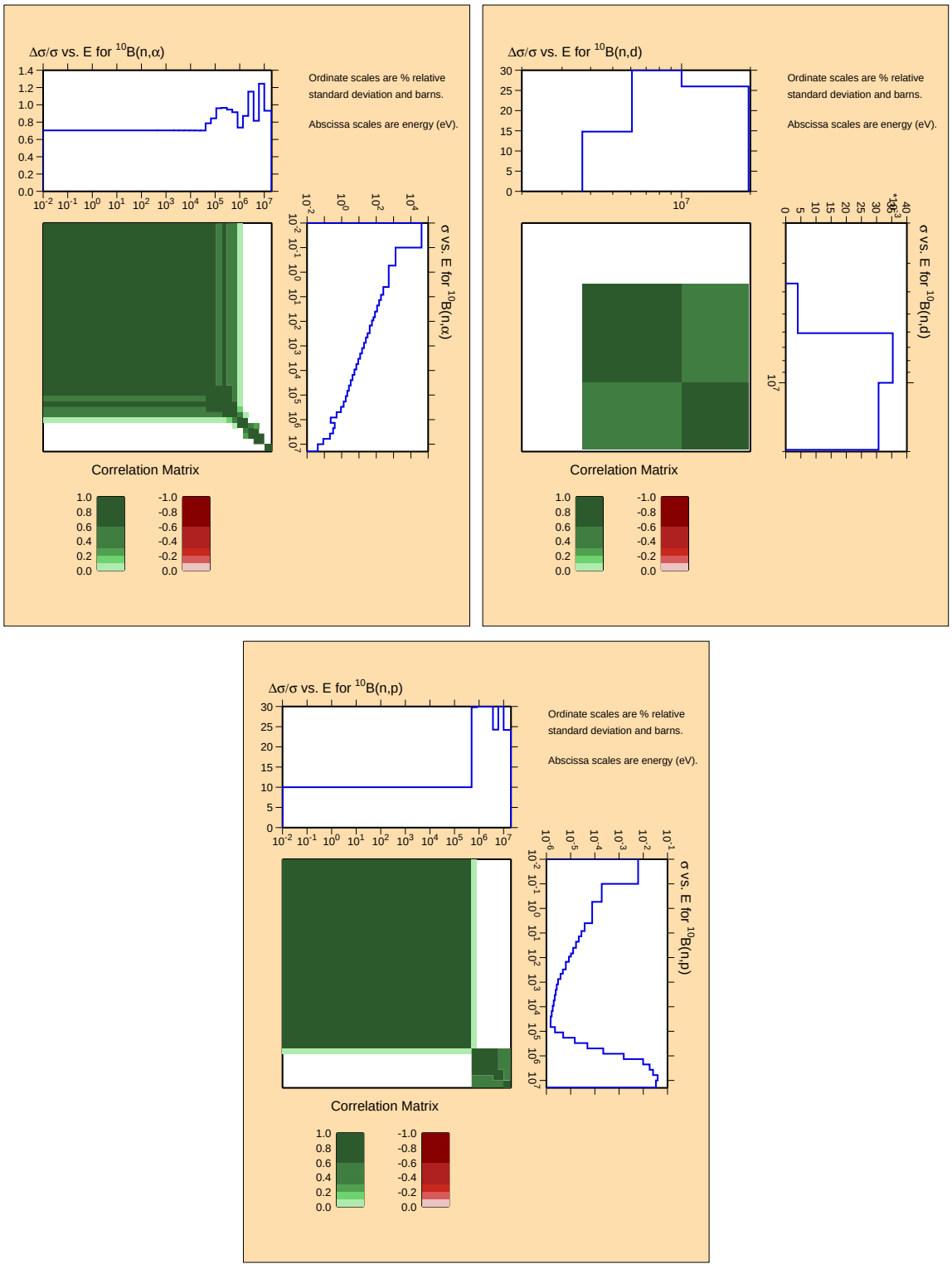

Figure A.11: Covariances for light nucleus ^{10}B (continued).

^{11}B

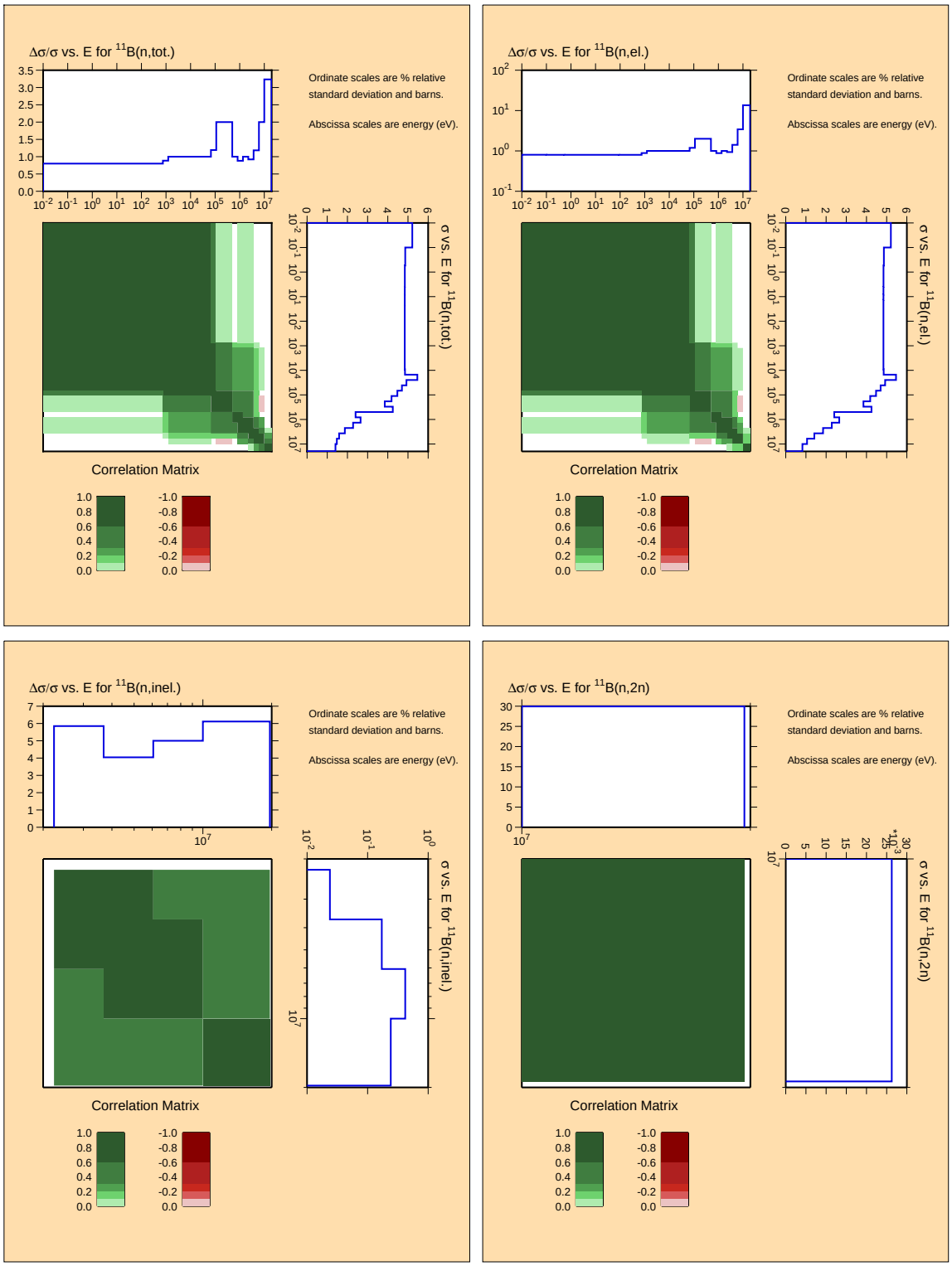

Figure A.12: Covariances for light nucleus ^{11}B.

^{11}B

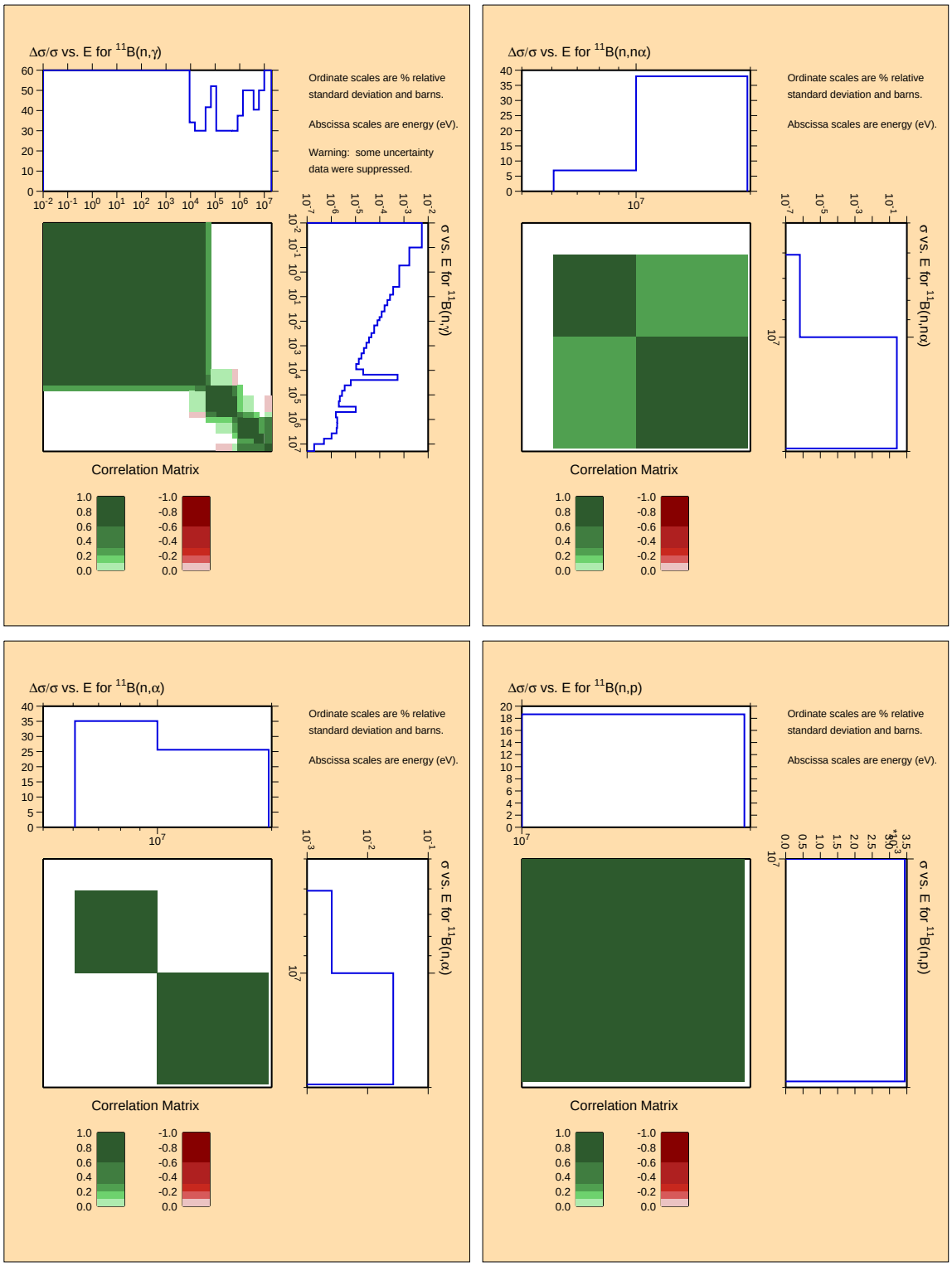

Figure A.13: Covariances for light nucleus ^{11}B (continued).

^{12}C

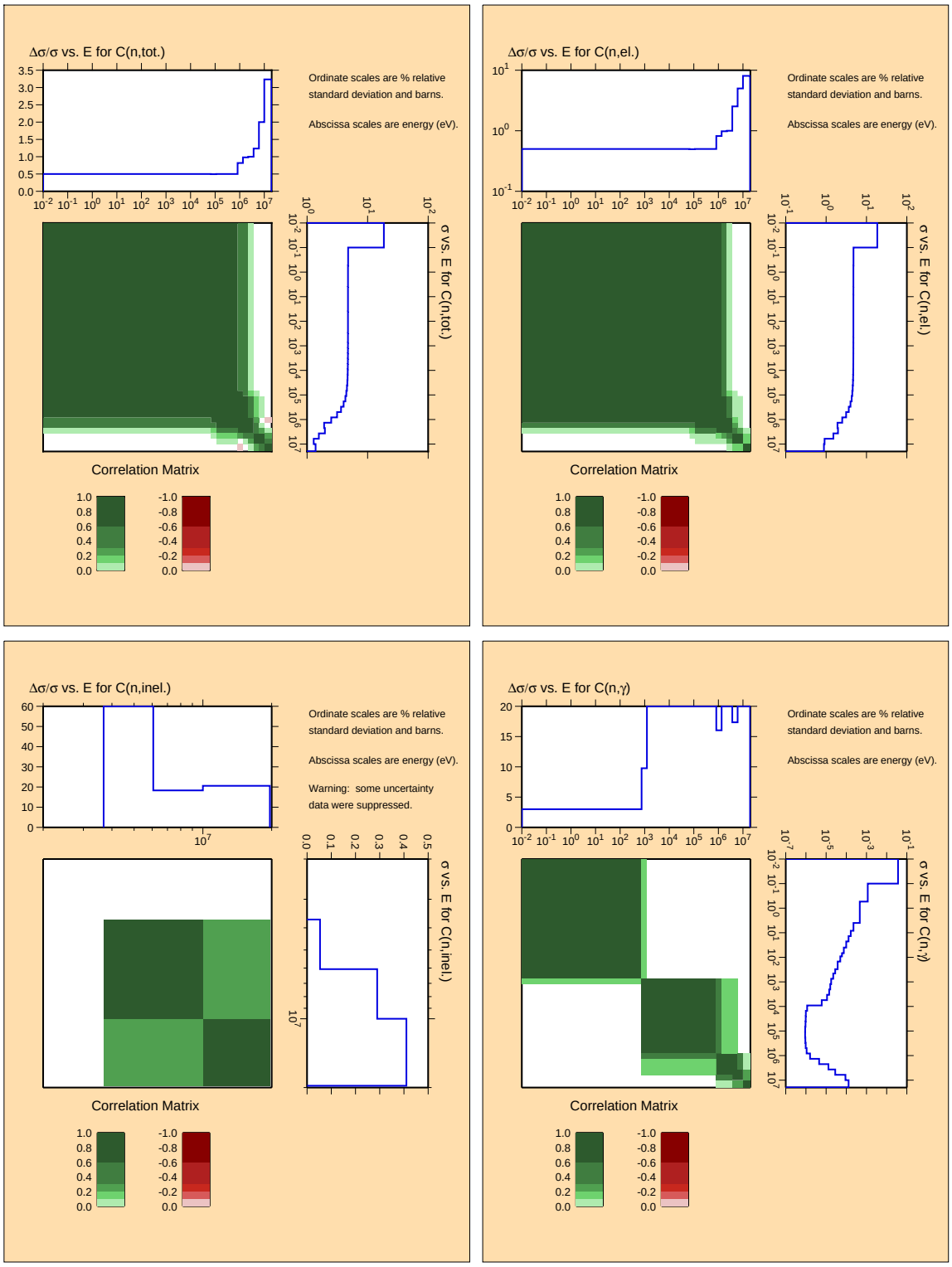

Figure A.14: Covariances for light nucleus ^{12}C.

^{12}C

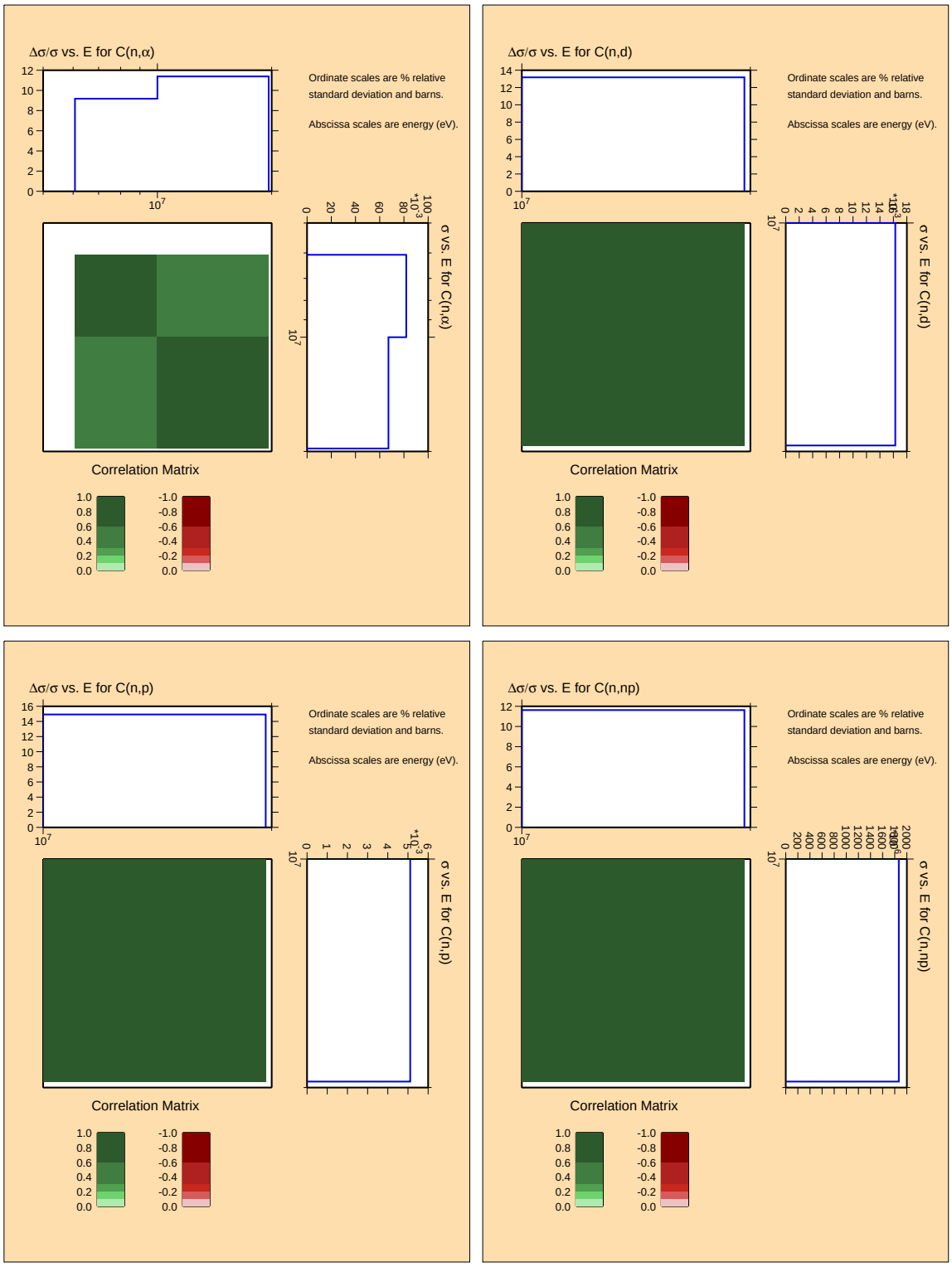

Figure A.15: Covariances for light nucleus ^{12}C (continued).

^{15}N

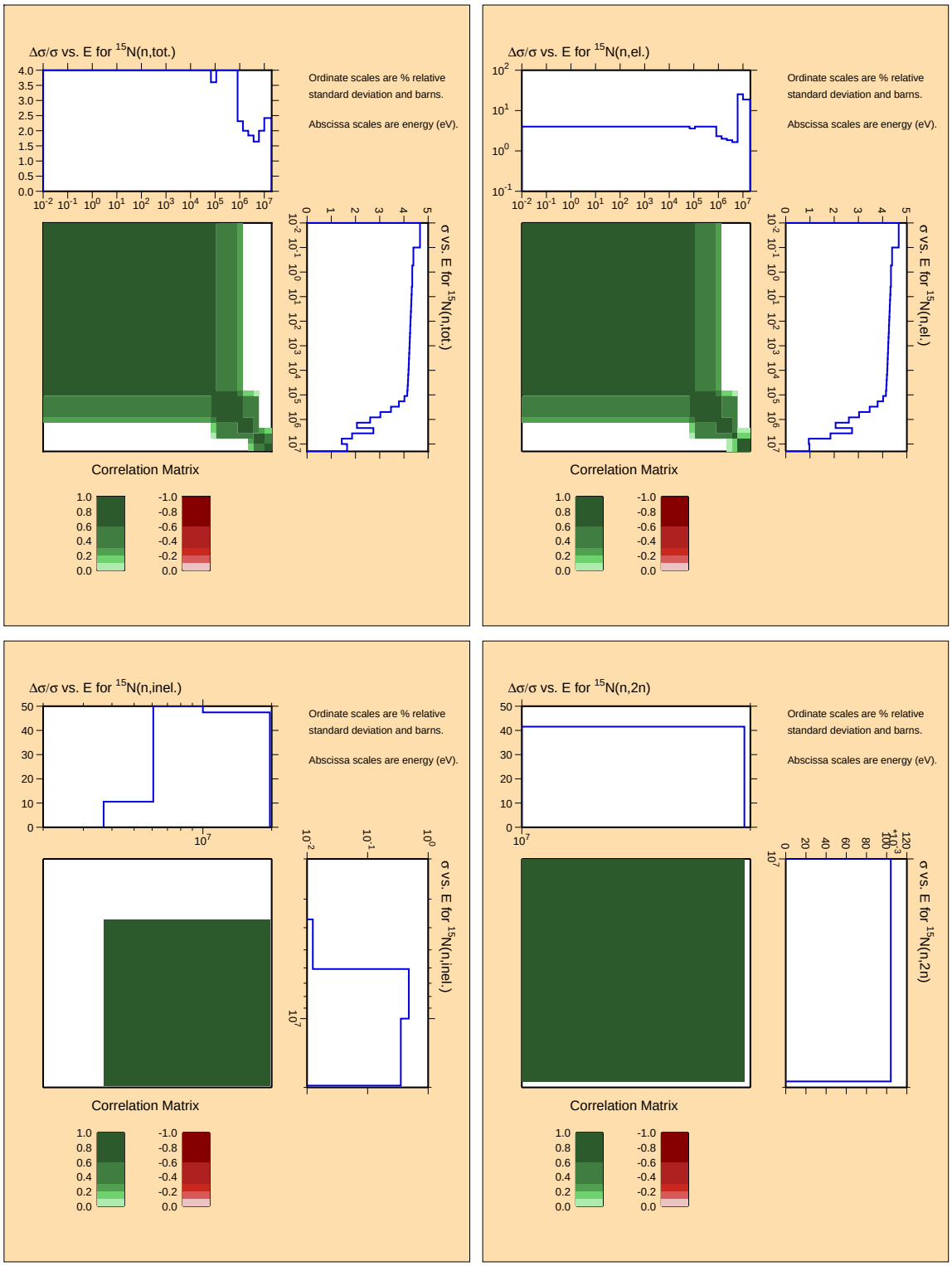

Figure A.16: Covariances for light nucleus ^{15}N.

^{15}N

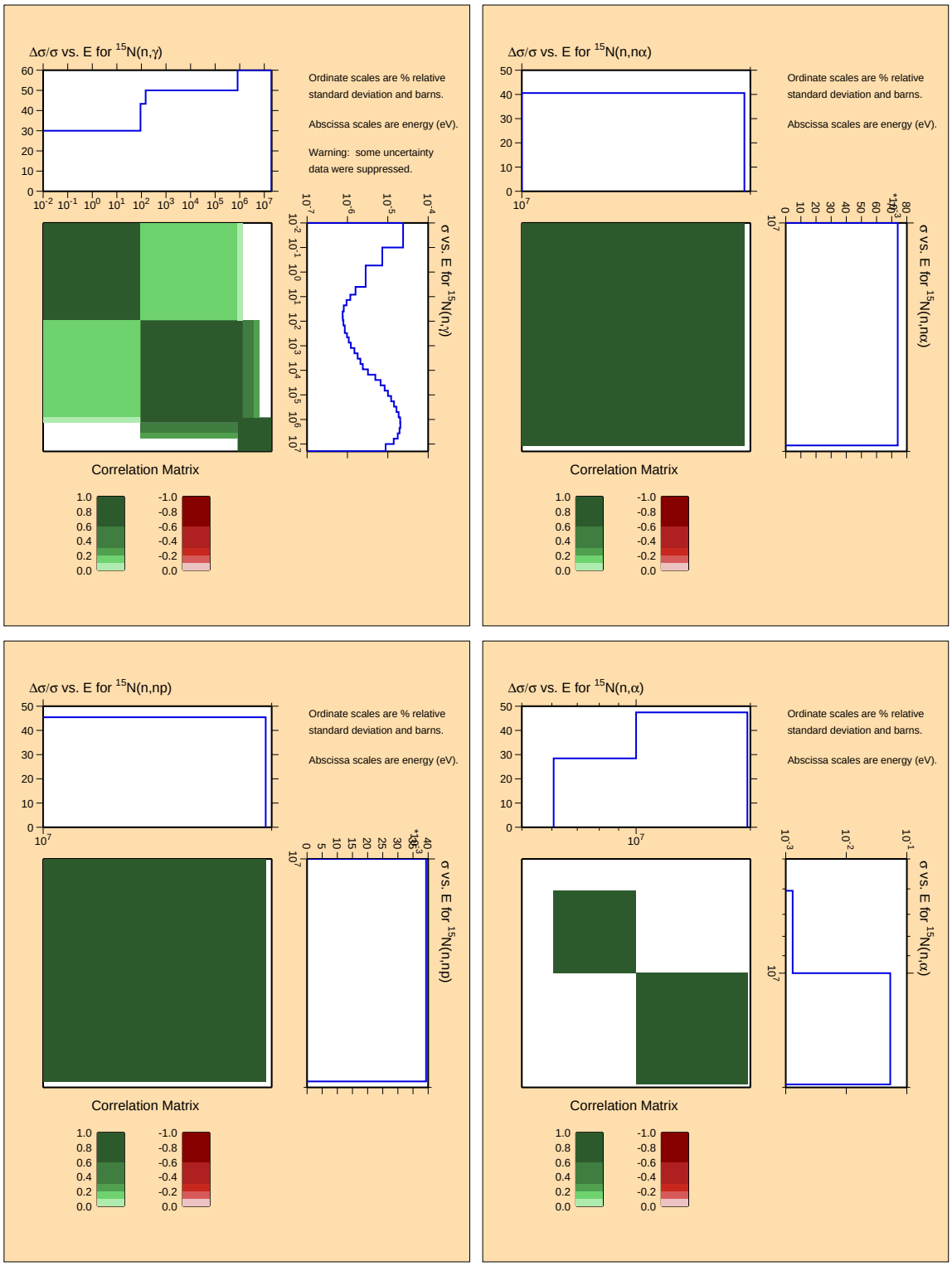

Figure A.17: Covariances for light nucleus ^{15}N (continued).

^{16}O

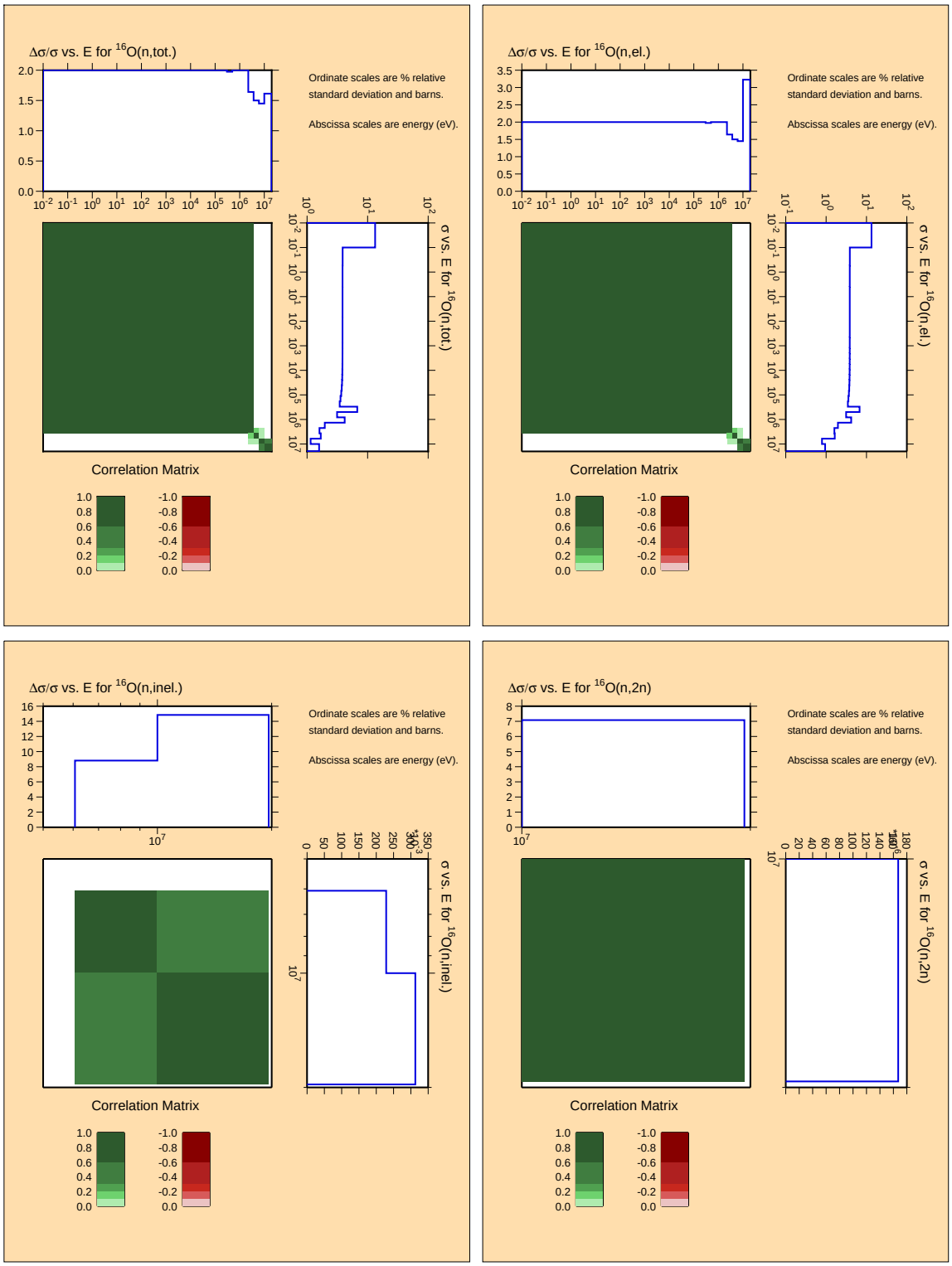

Figure A.18: Covariances for light nucleus ^{16}O.

^{16}O

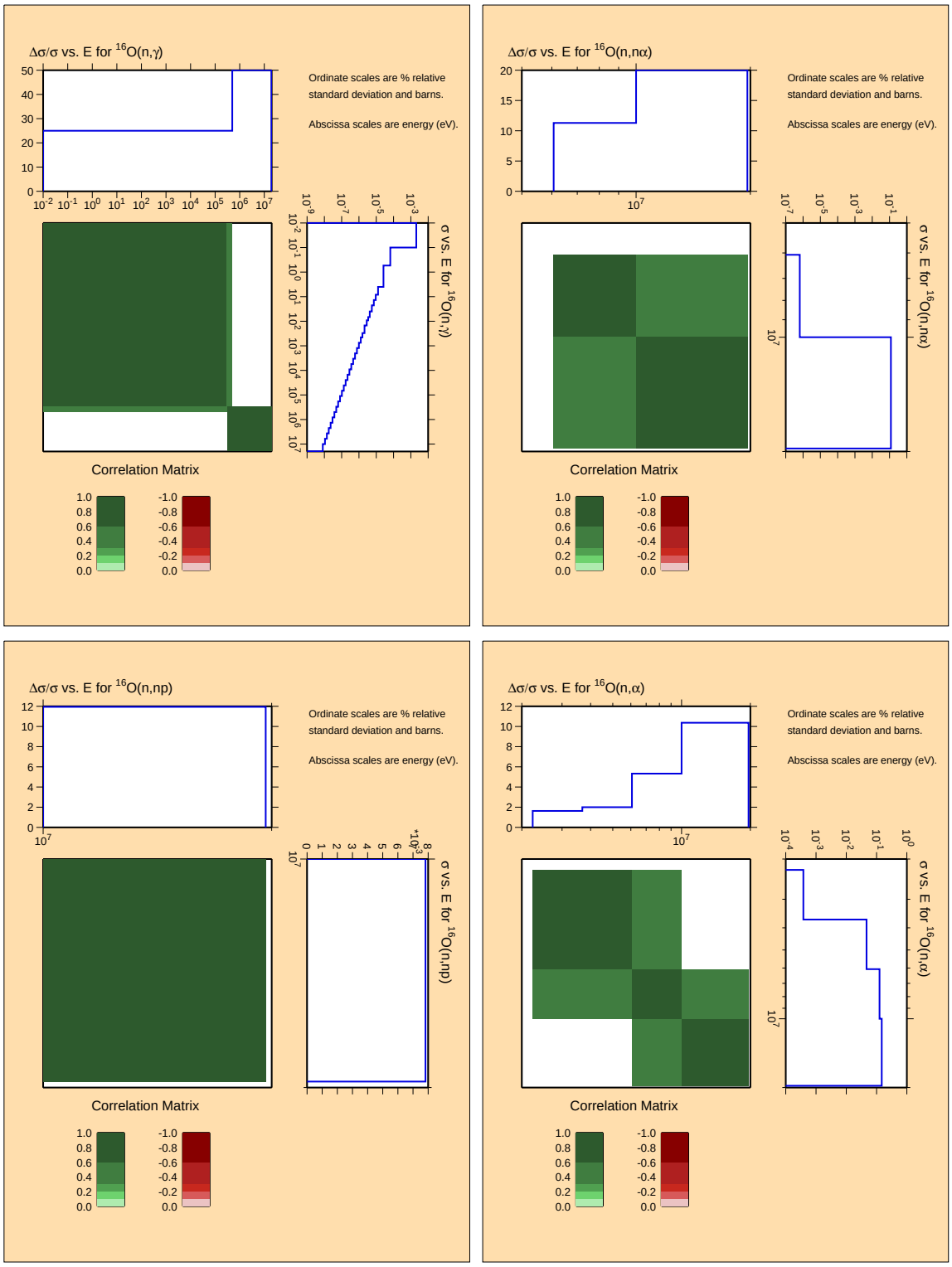

Figure A.19: Covariances for light nucleus ^{16}O (continued).

^{19}F

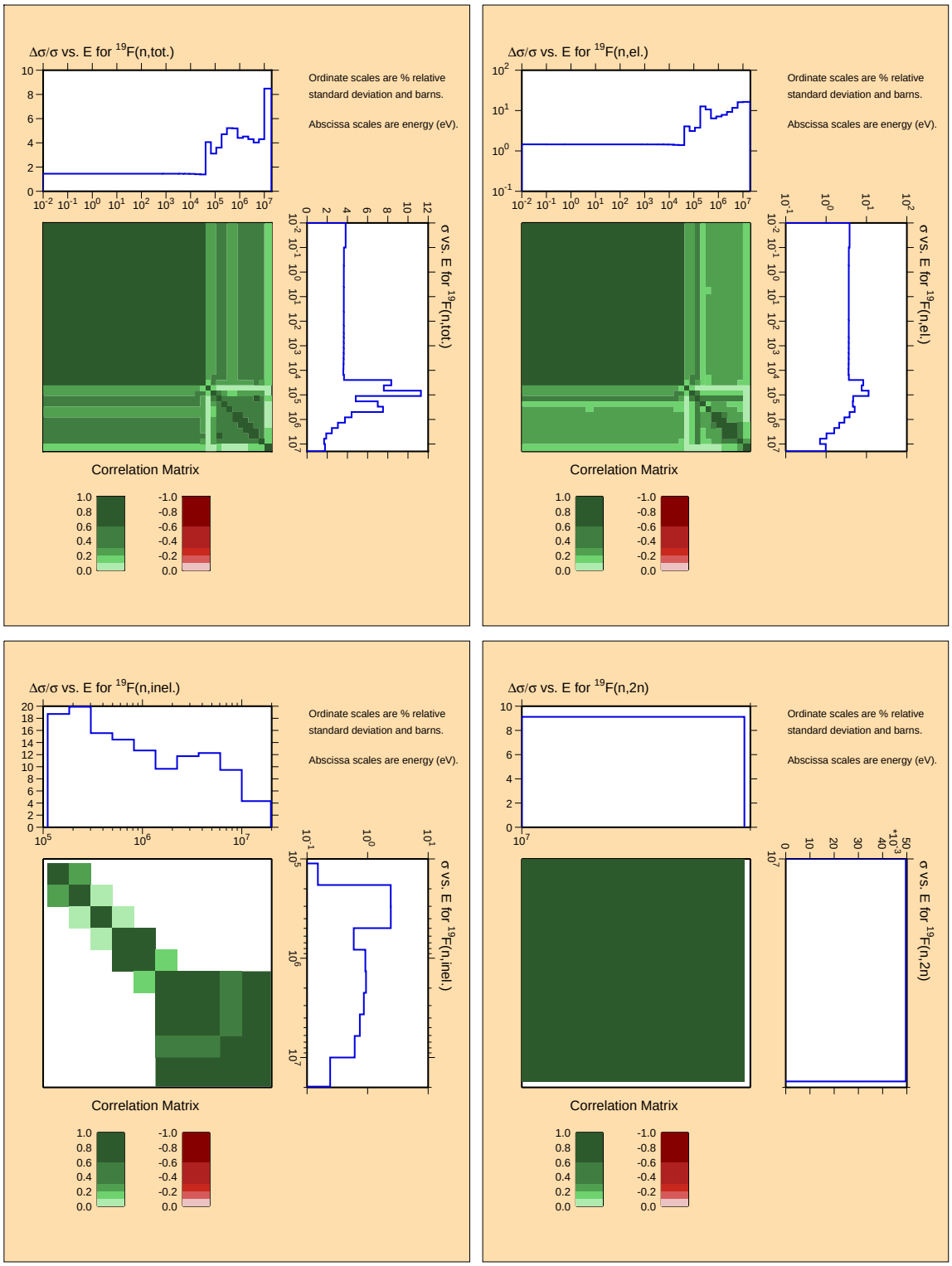

Figure A.20: Covariances for light nucleus ^{19}F.

^{19}F

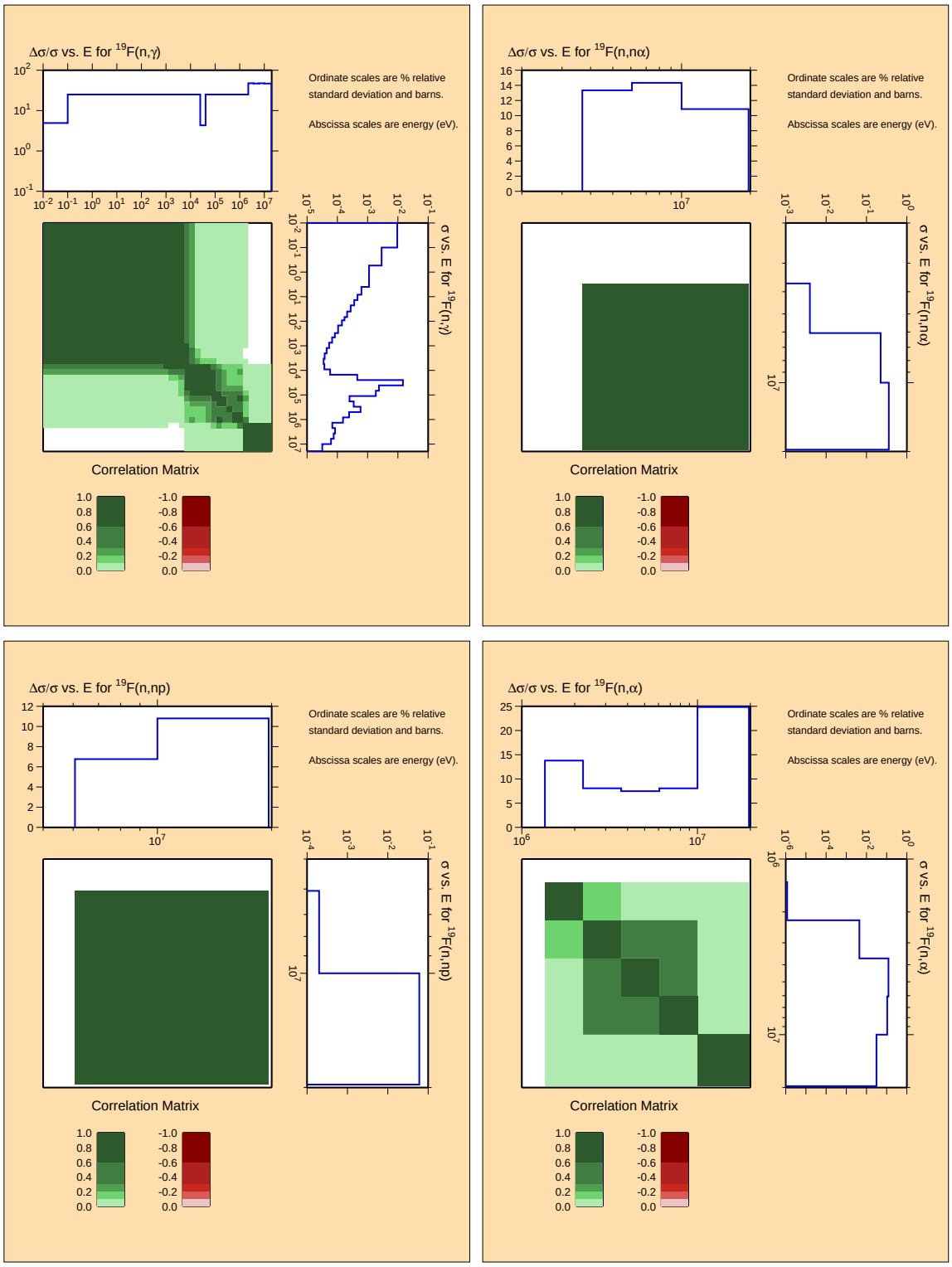

Figure A.21: Covariances for light nucleus ^{19}F (continued).

Appendix B

AFCI 2.0 Covariance Plots

Structural Materials and Fission Products

(78 materials)

^{23}Na

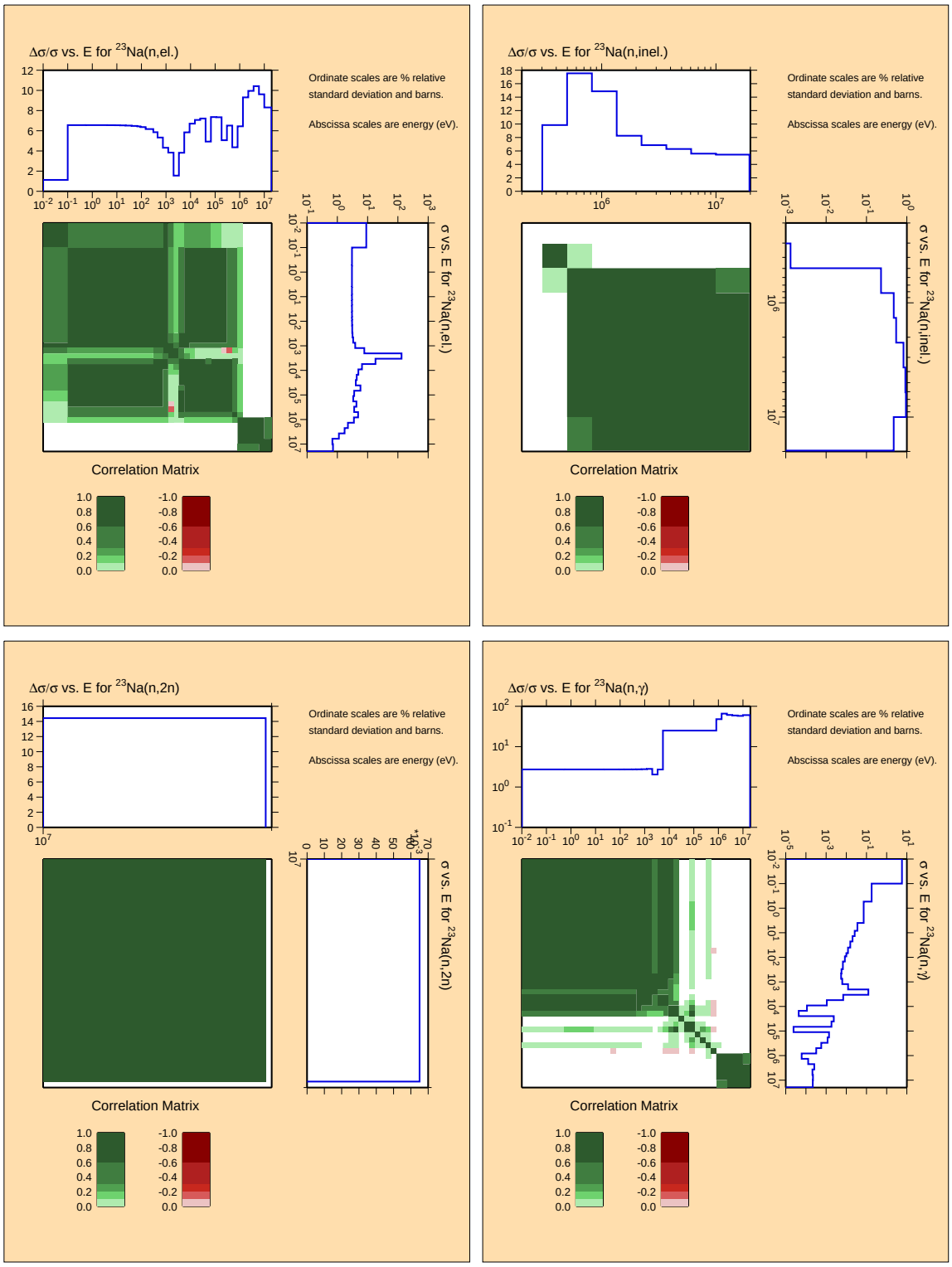

Figure B.1: Covariances for coolant ^{23}Na.

^{24}Mg

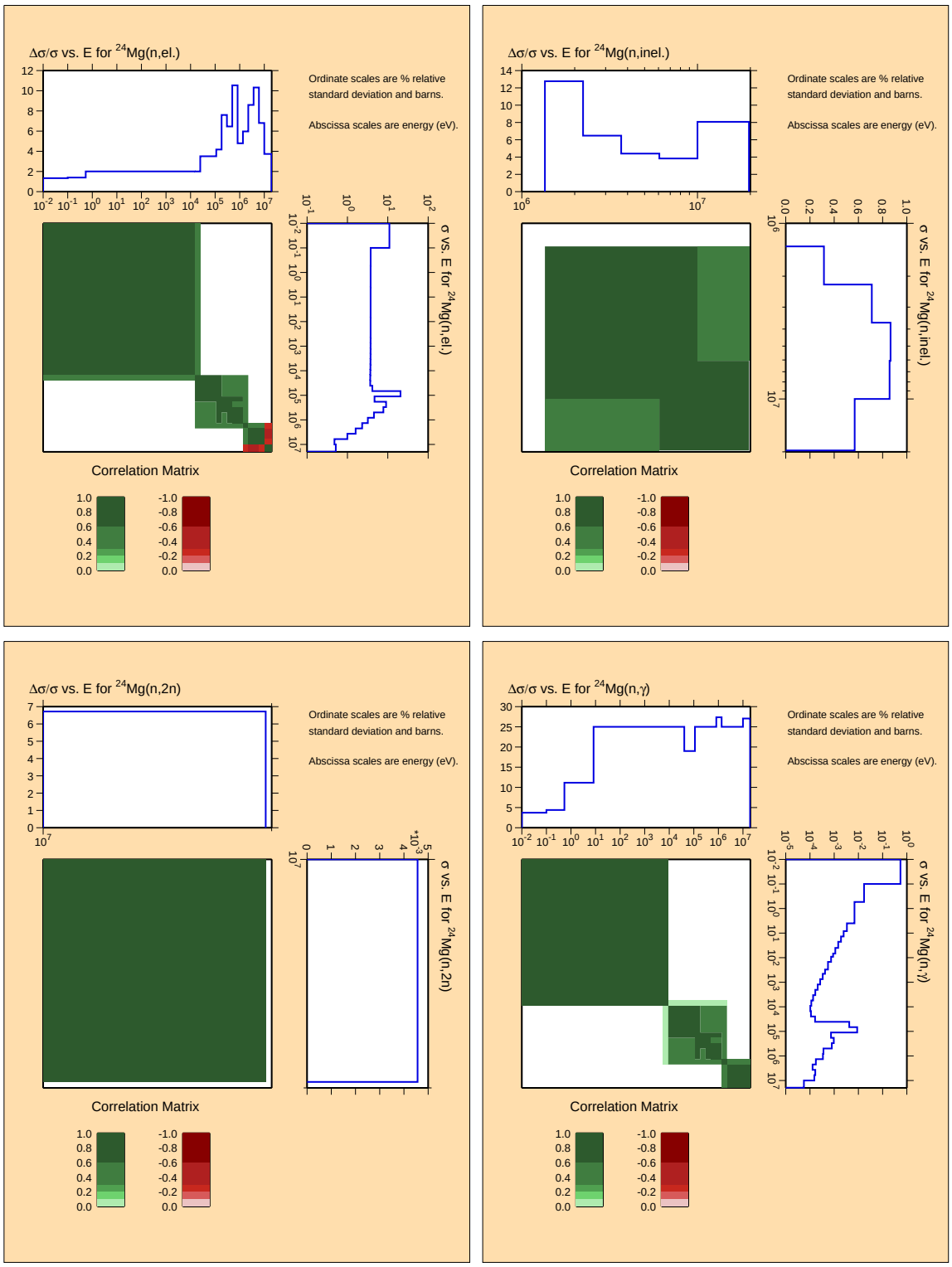

Figure B.2: Covariances for structural material ^{24}Mg.

^{25}Mg

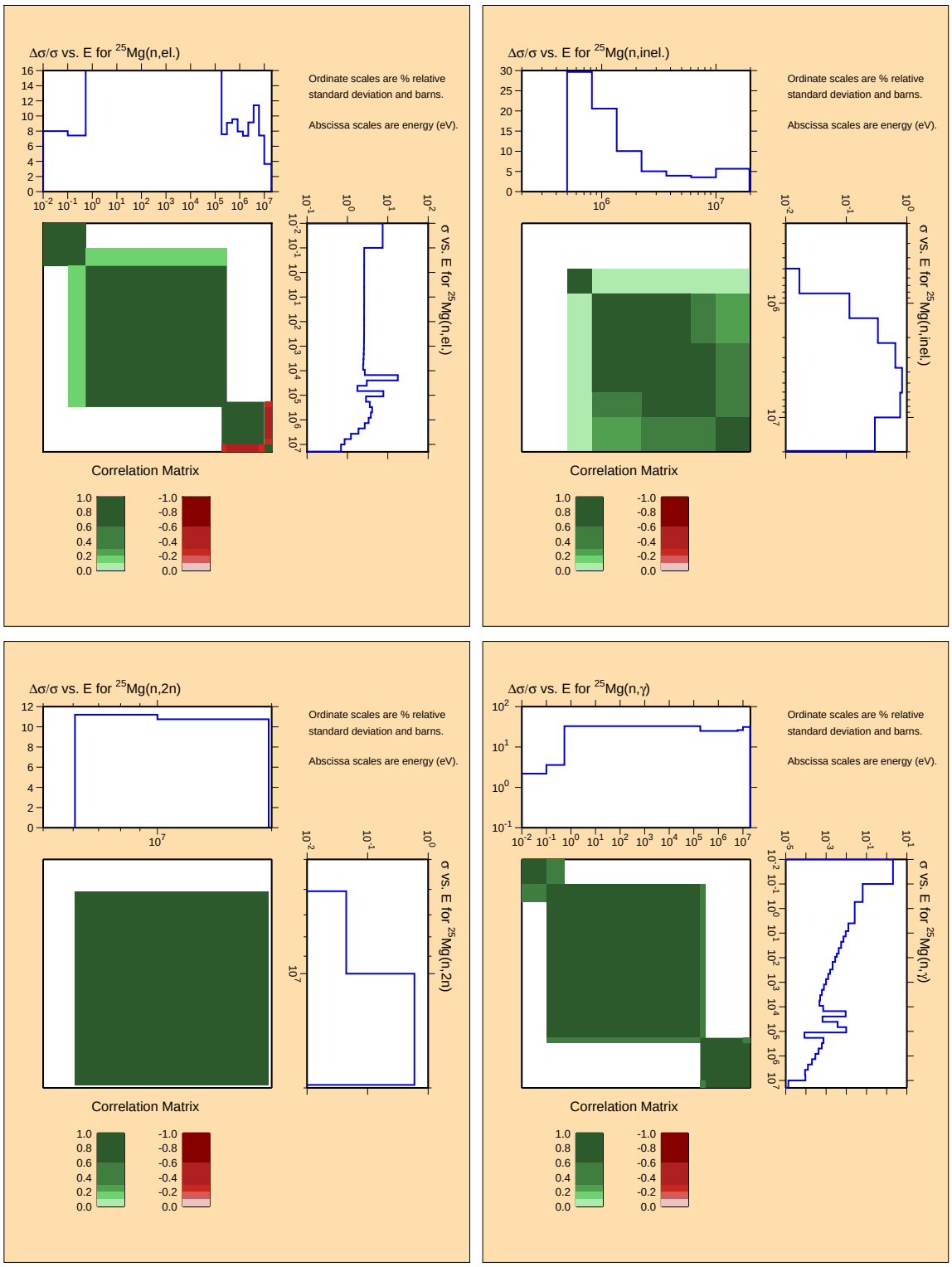

Figure B.3: Covariances for structural material ^{25}Mg.

^{26}Mg

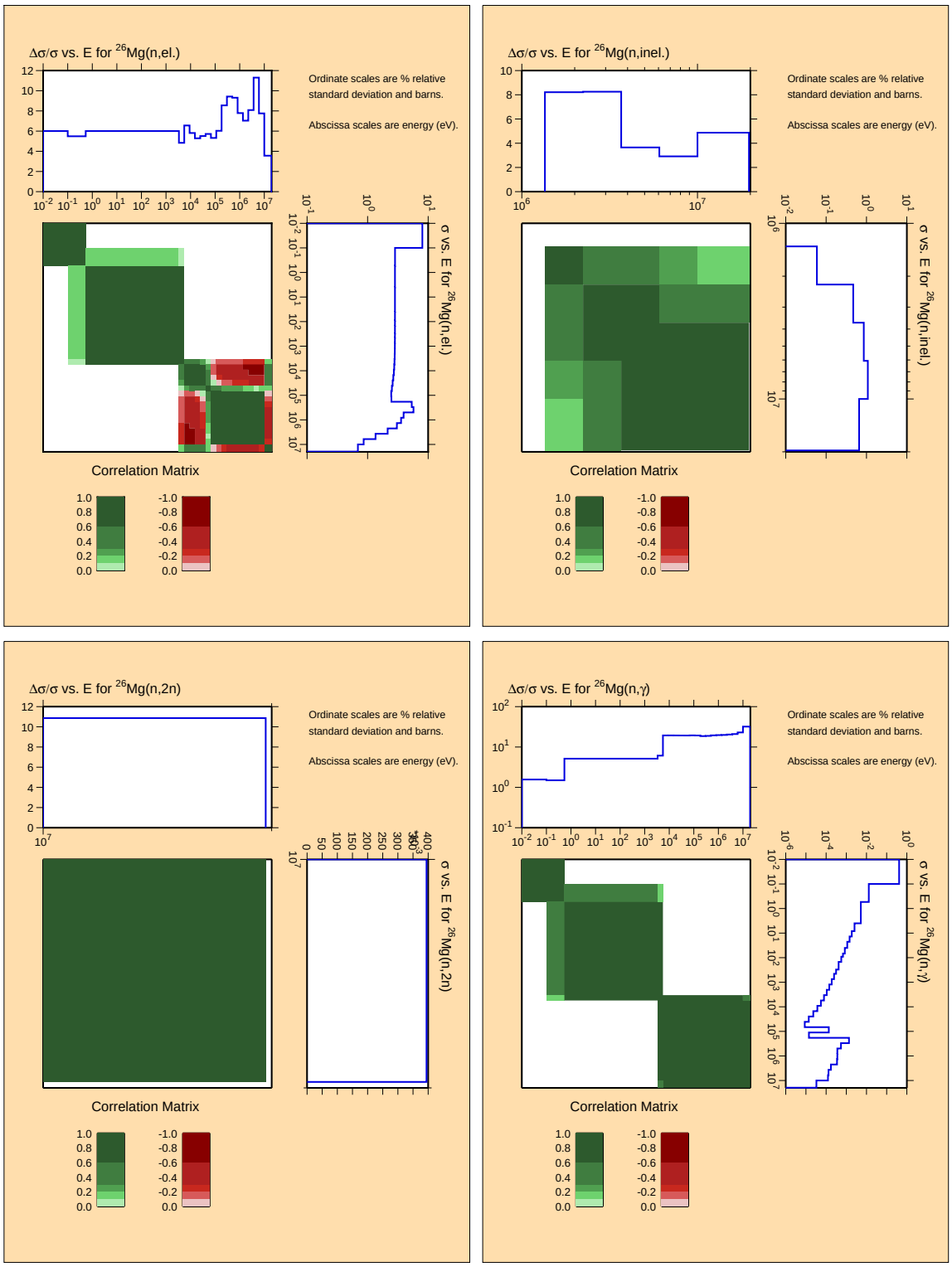

Figure B.4: Covariances for structural material ^{26}Mg.

^{27}Al

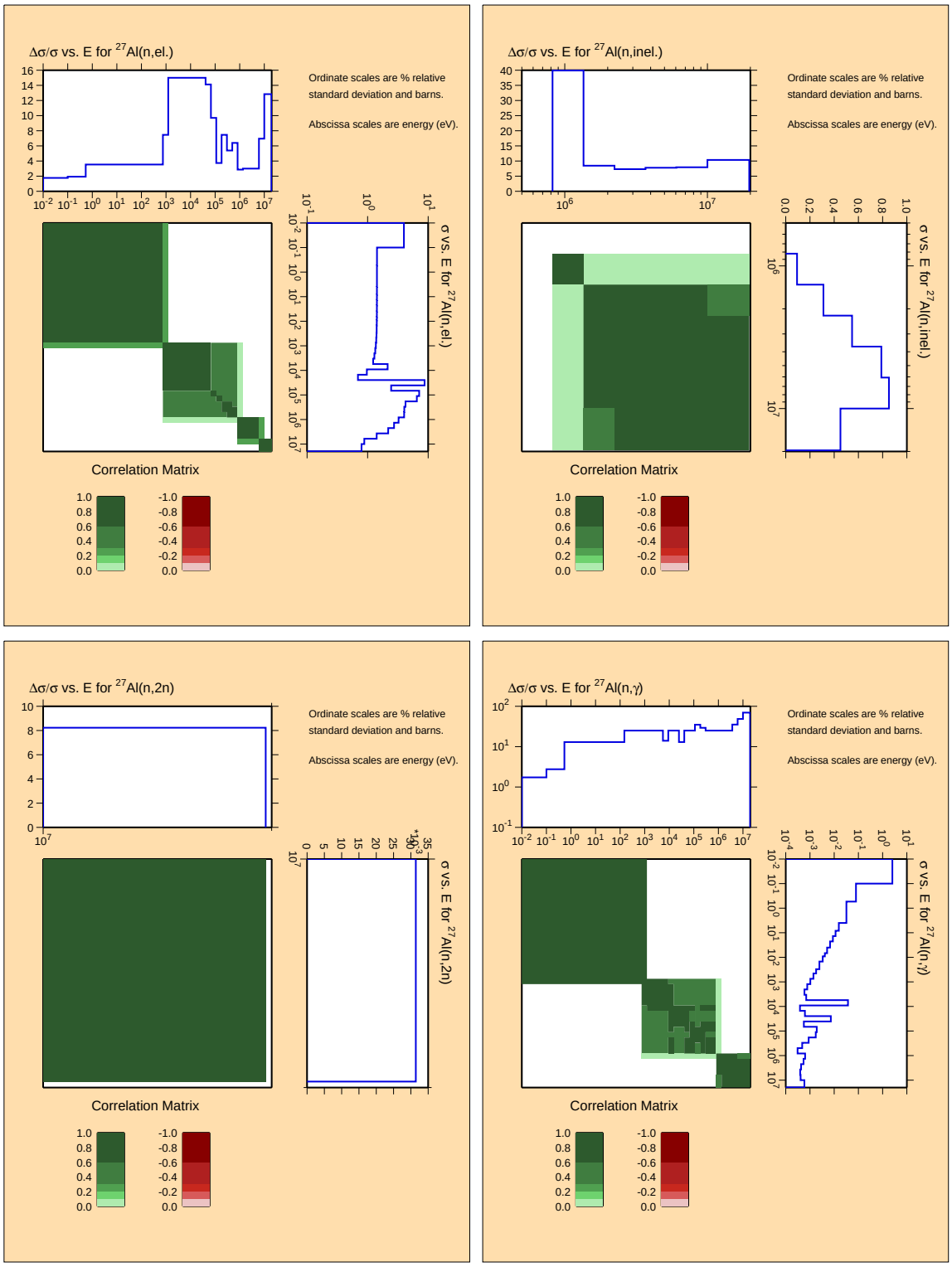

Figure B.5: Covariances for structural material ^{27}Al.

^{28}Si

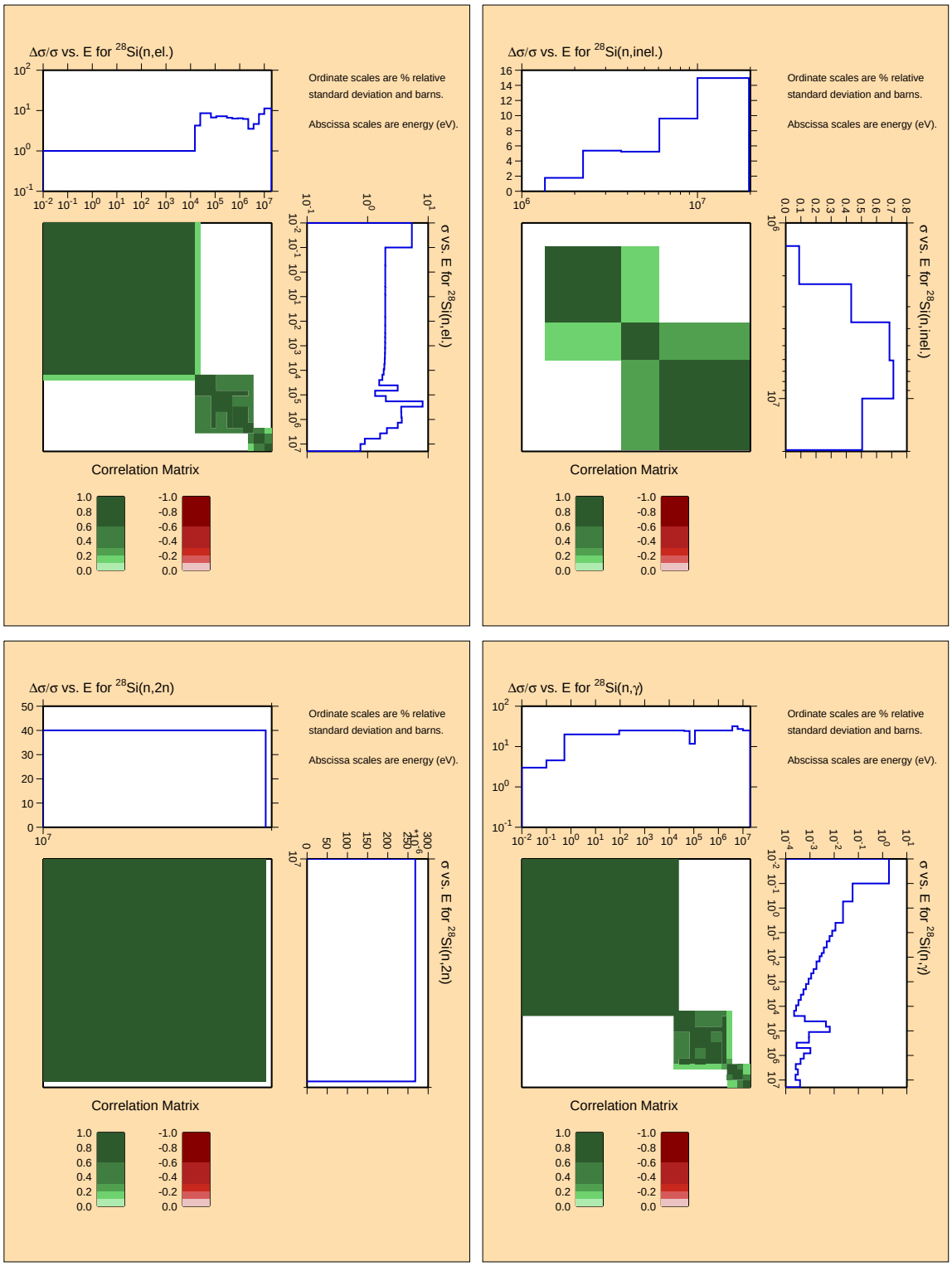

Figure B.6: Covariances for structural material ^{28}Si.

^{29}Si

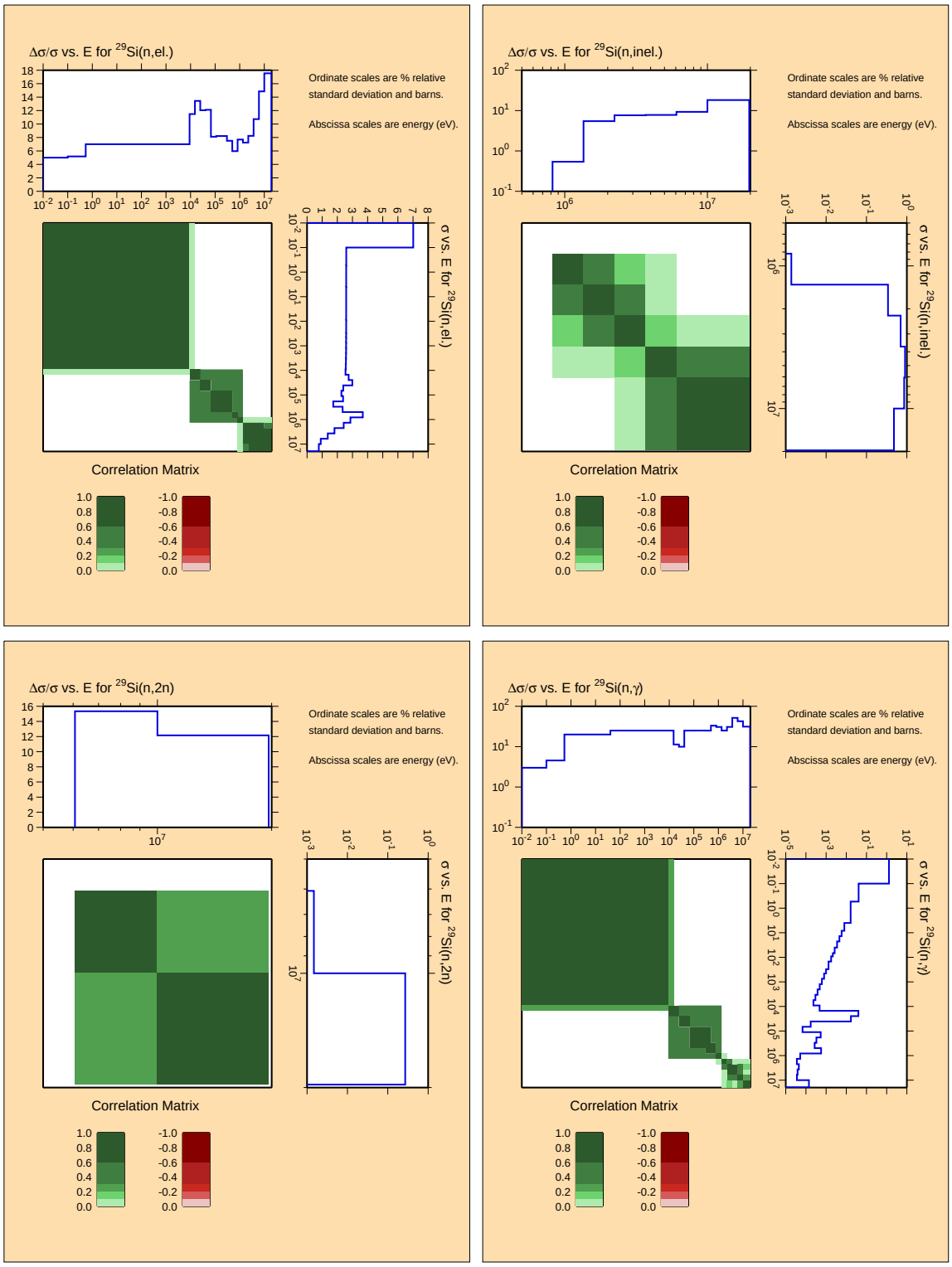

Figure B.7: Covariances for structural material ^{29}Si.

^{30}Si

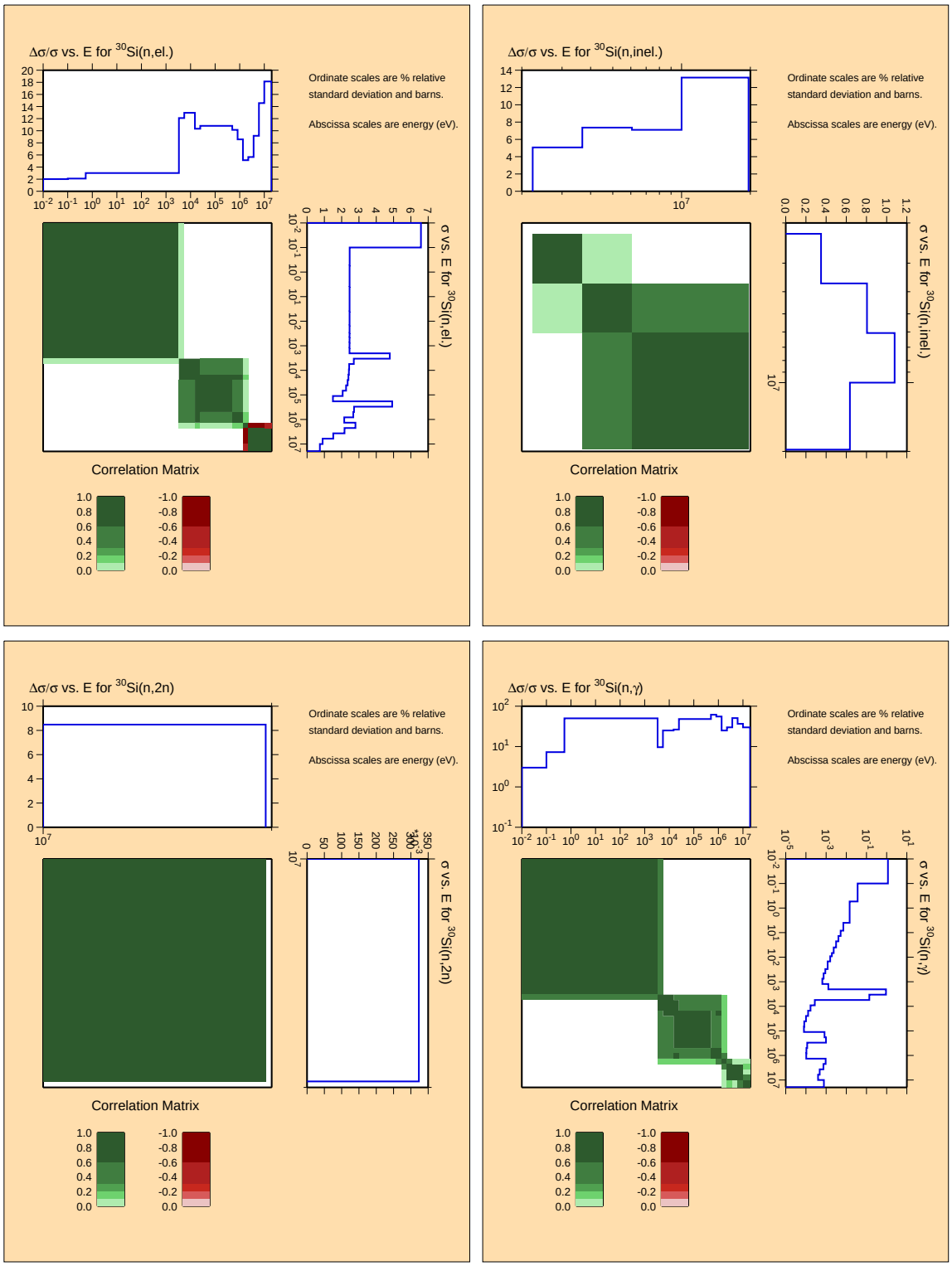

Figure B.8: Covariances for structural material ^{30}Si.

^{50}Cr

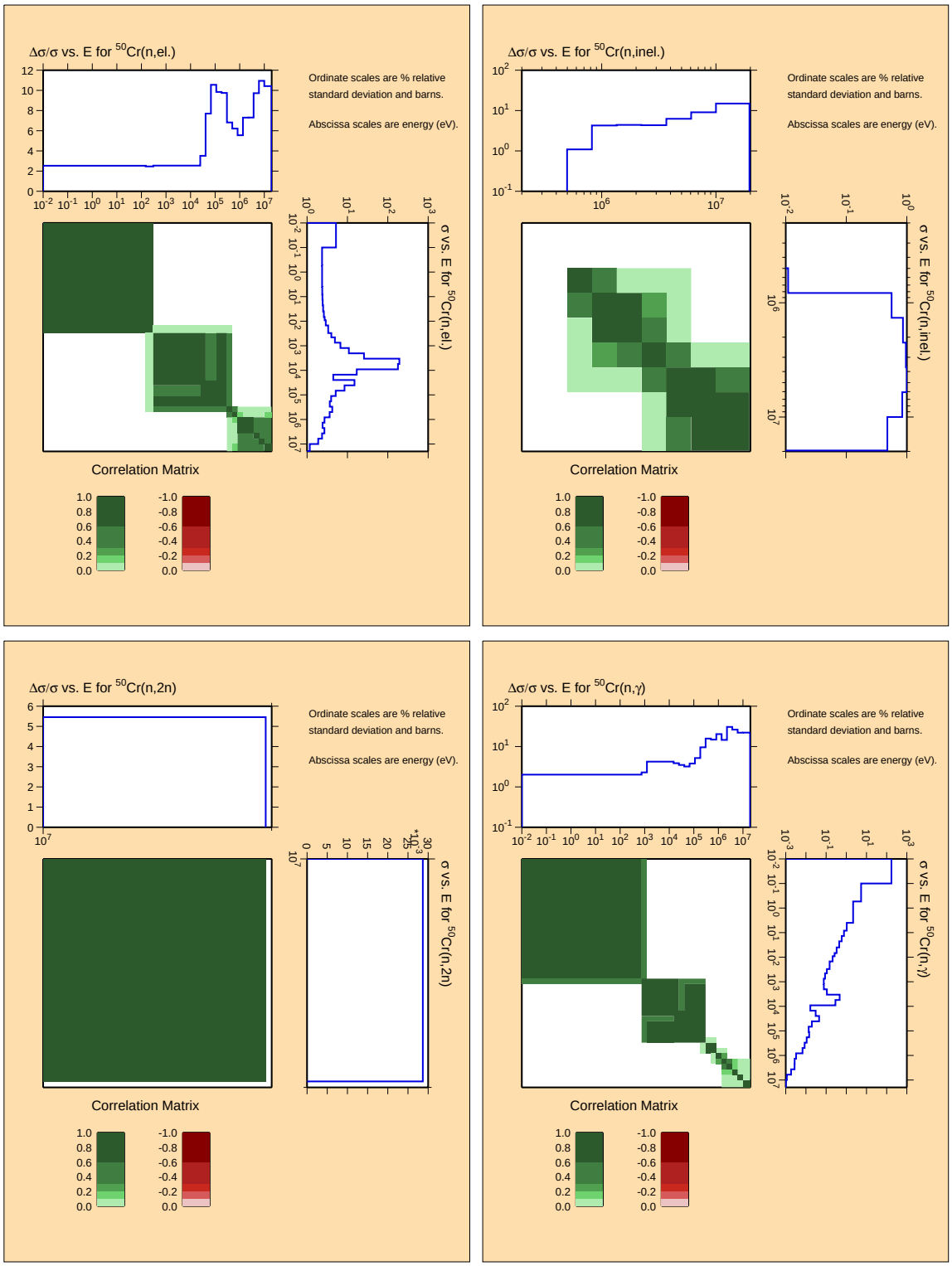

Figure B.9: Covariances for structural material ^{50}Cr.

^{52}Cr

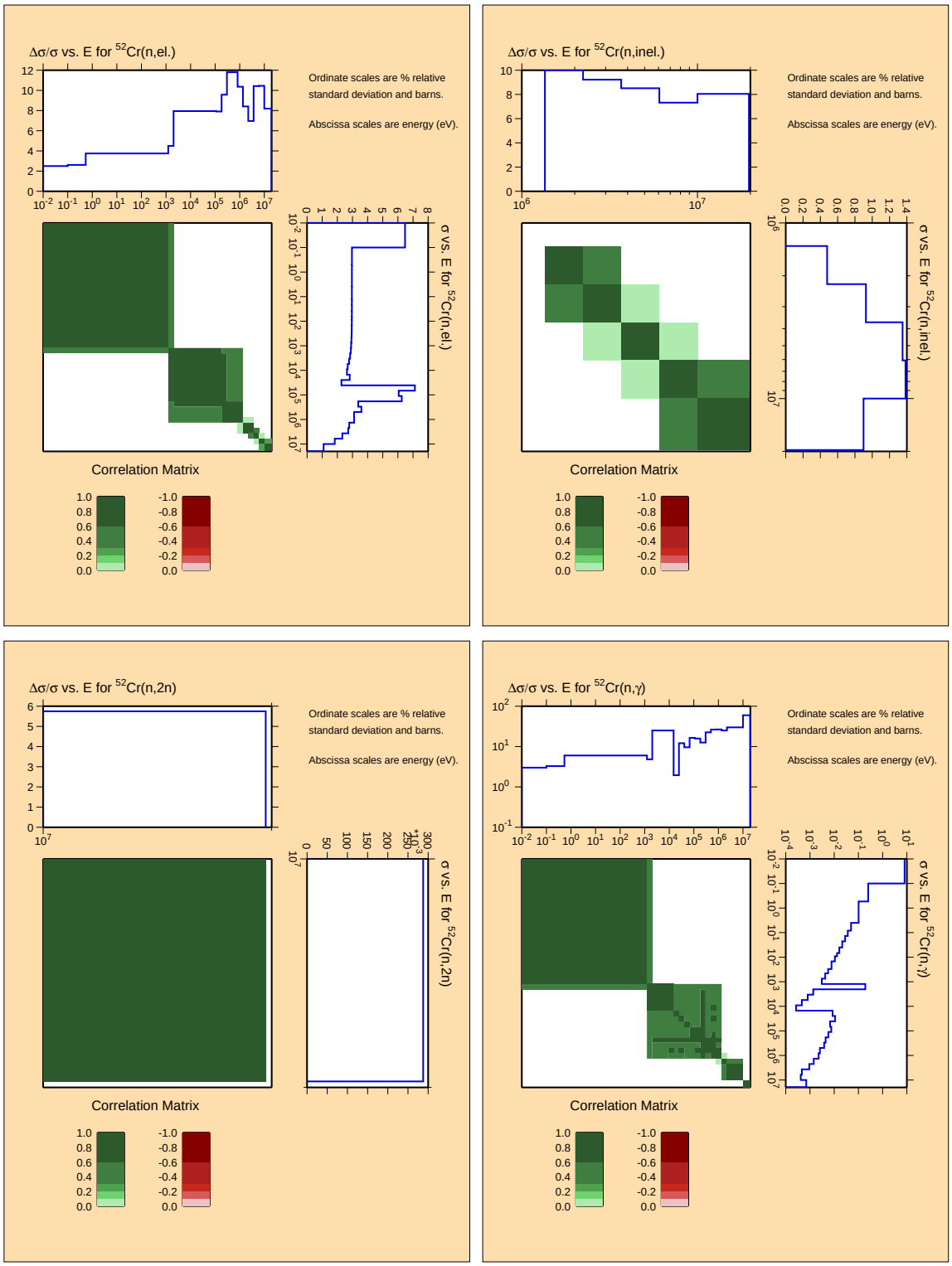

Figure B.10: Covariances for structural material ^{52}Cr.

^{53}Cr

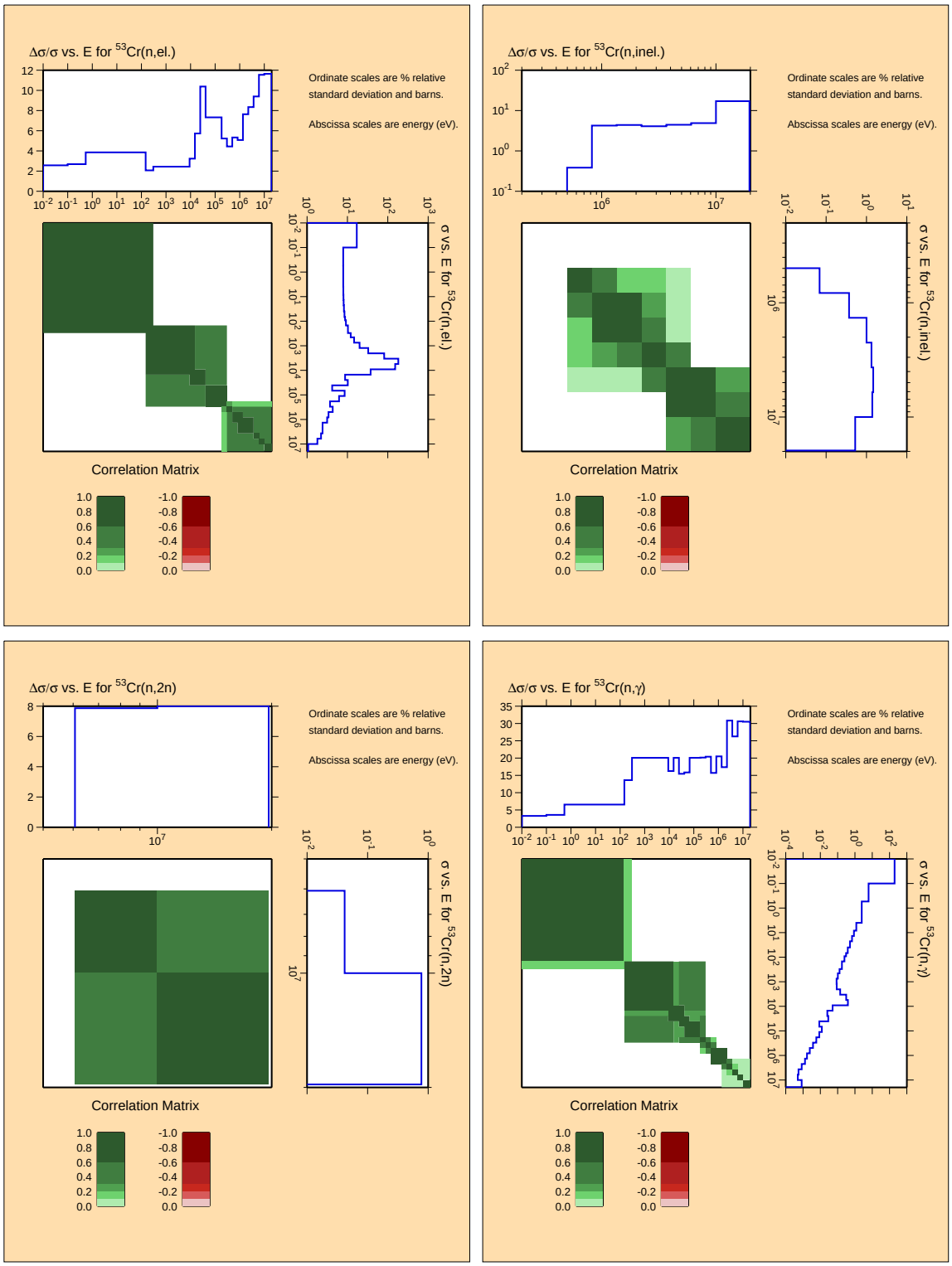

Figure B.11: Covariances for structural material ^{53}Cr.

^{55}Mn

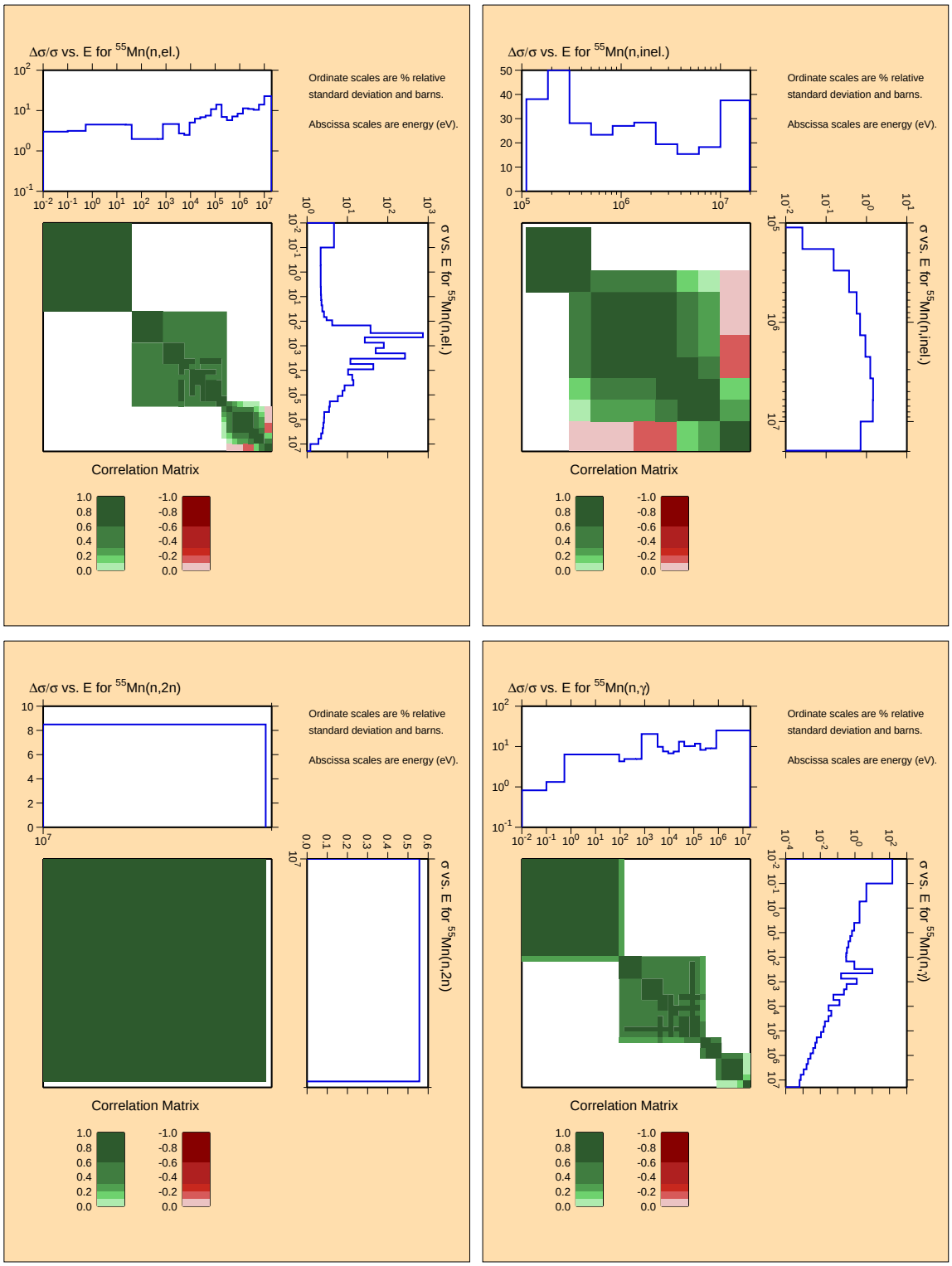

Figure B.12: Covariances for structural material ^{55}Mn.

^{54}Fe

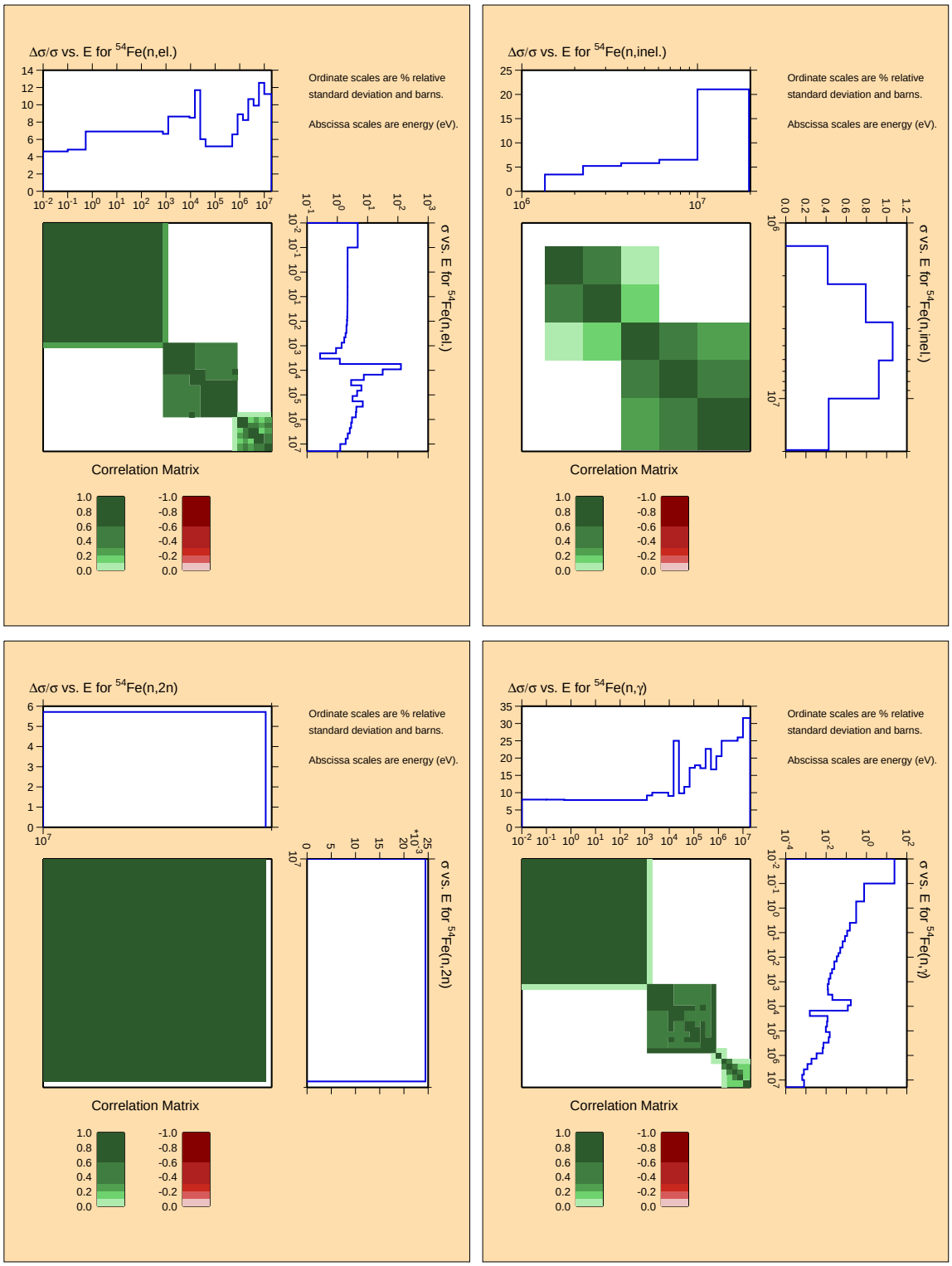

Figure B.13: Covariances for structural material ^{54}Fe.

^{56}Fe

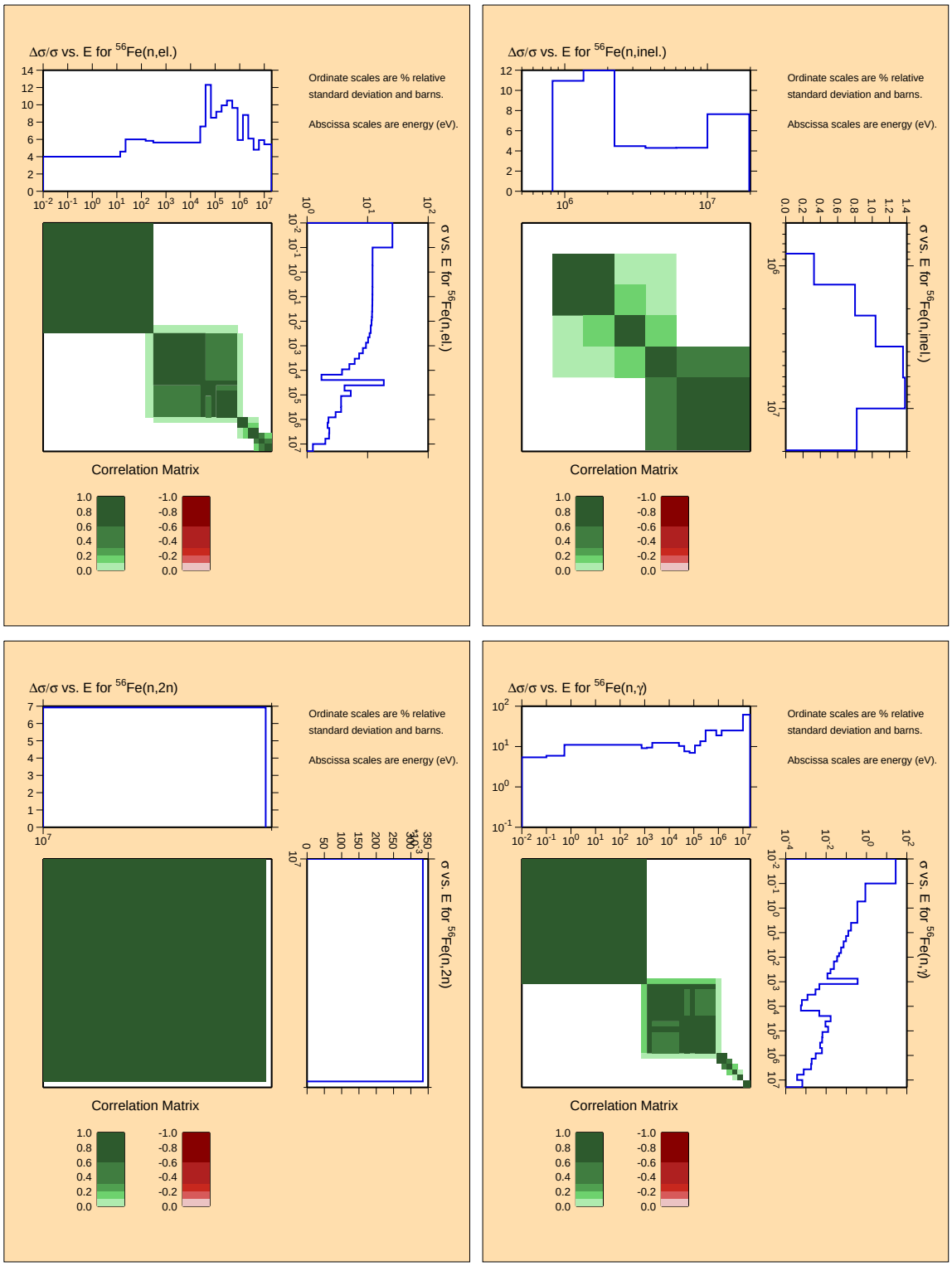

Figure B.14: Covariances for structural material ^{56}Fe.

^{57}Fe

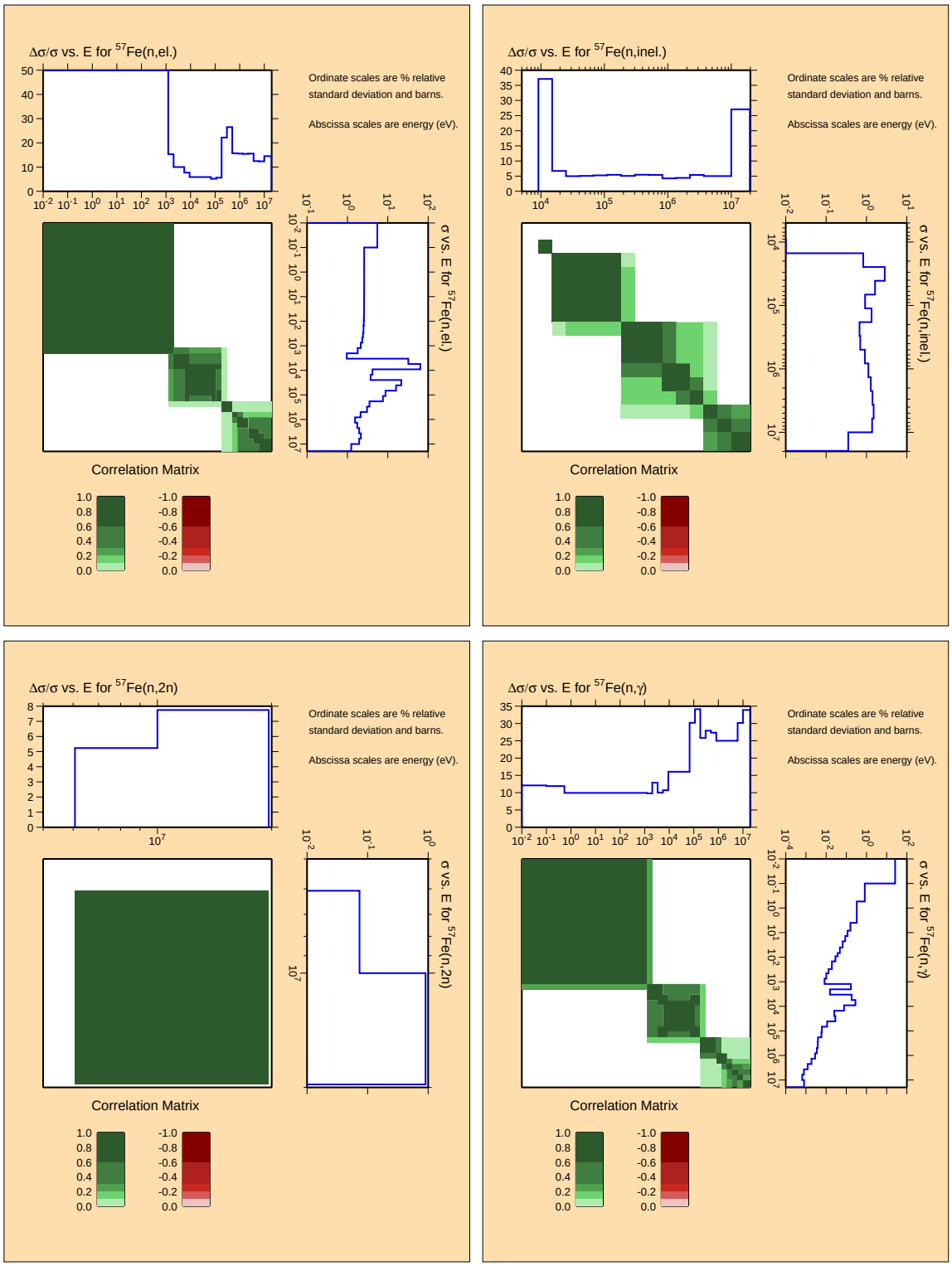

Figure B.15: Covariances for structural material ^{57}Fe.

^{58}Ni

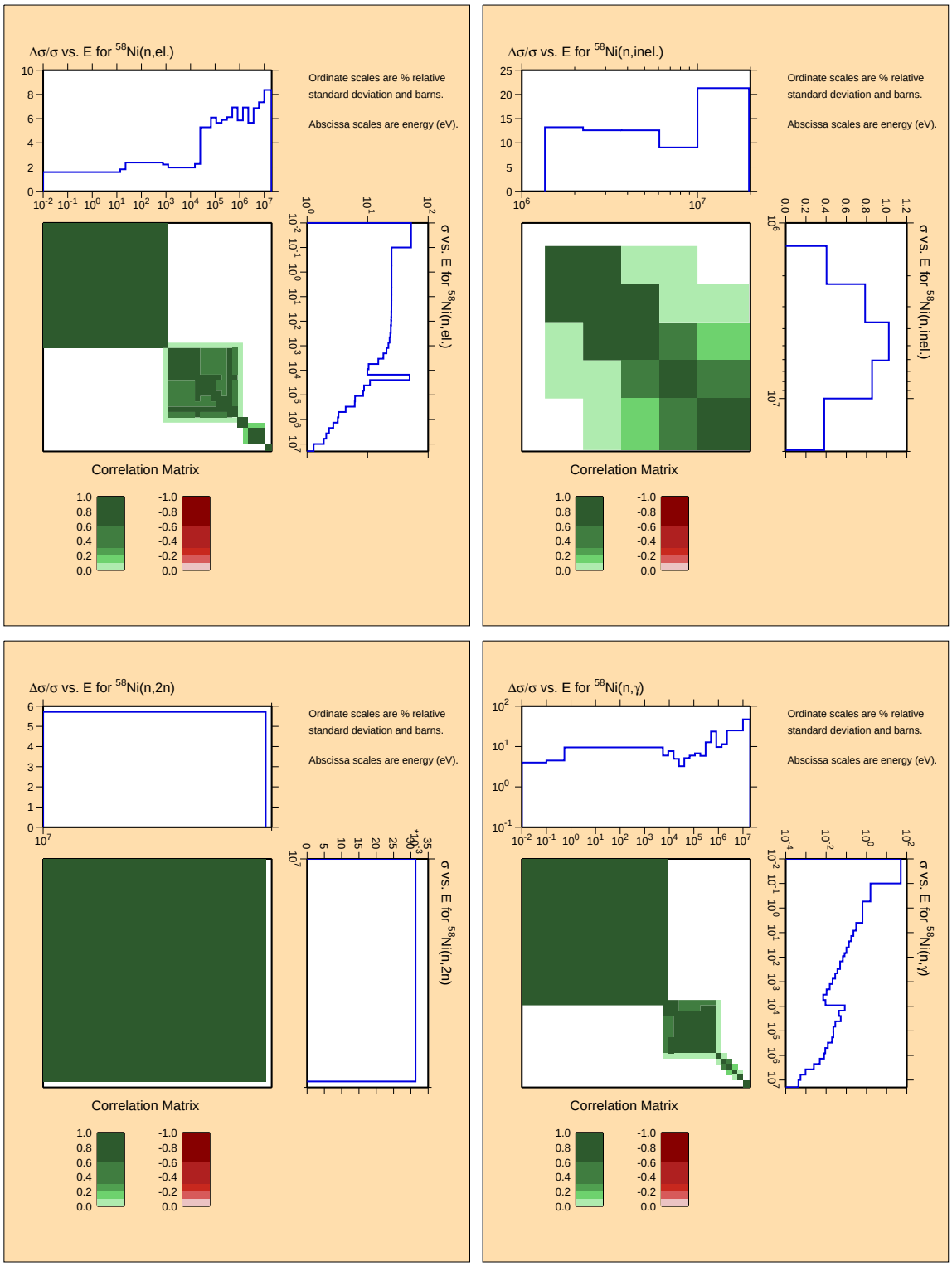

Figure B.16: Covariances for structural material ^{58}Ni.

^{60}Ni

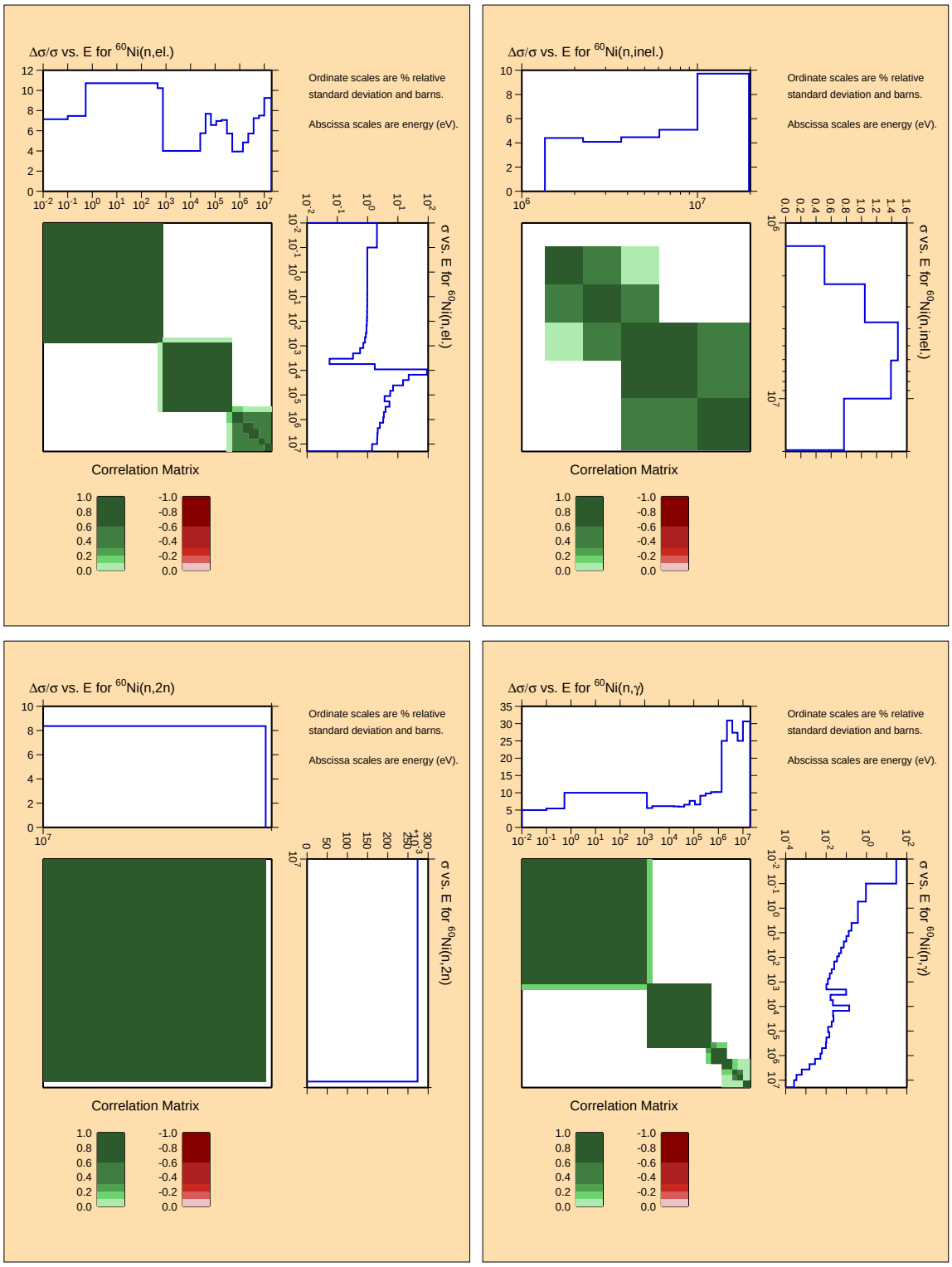

Figure B.17: Covariances for structural material ^{60}Ni.

^{90}Zr

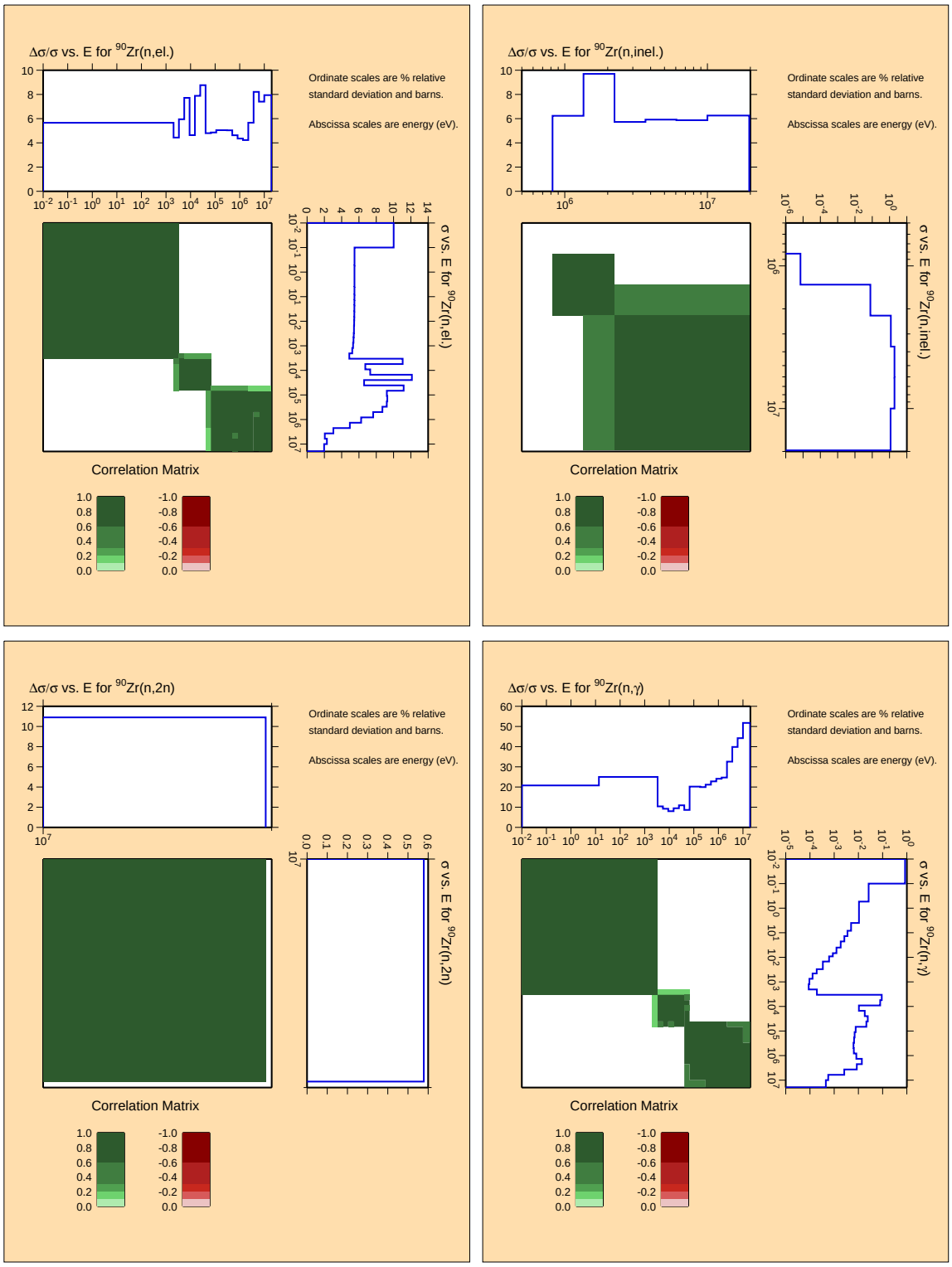

Figure B.18: Covariances for structural material ^{90}Zr.

^{91}Zr

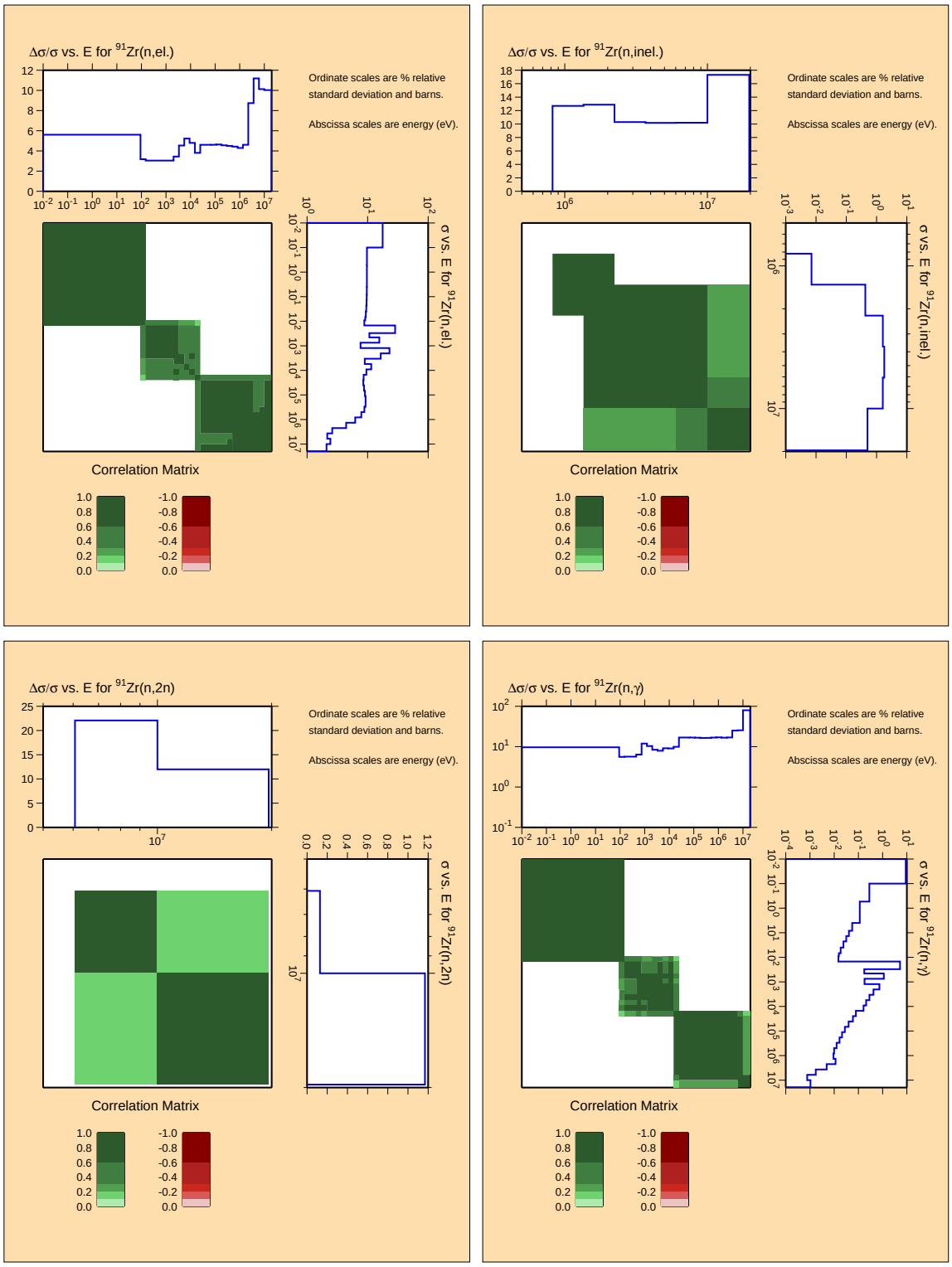

Figure B.19: Covariances for structural material ^{91}Zr.

^{92}Zr

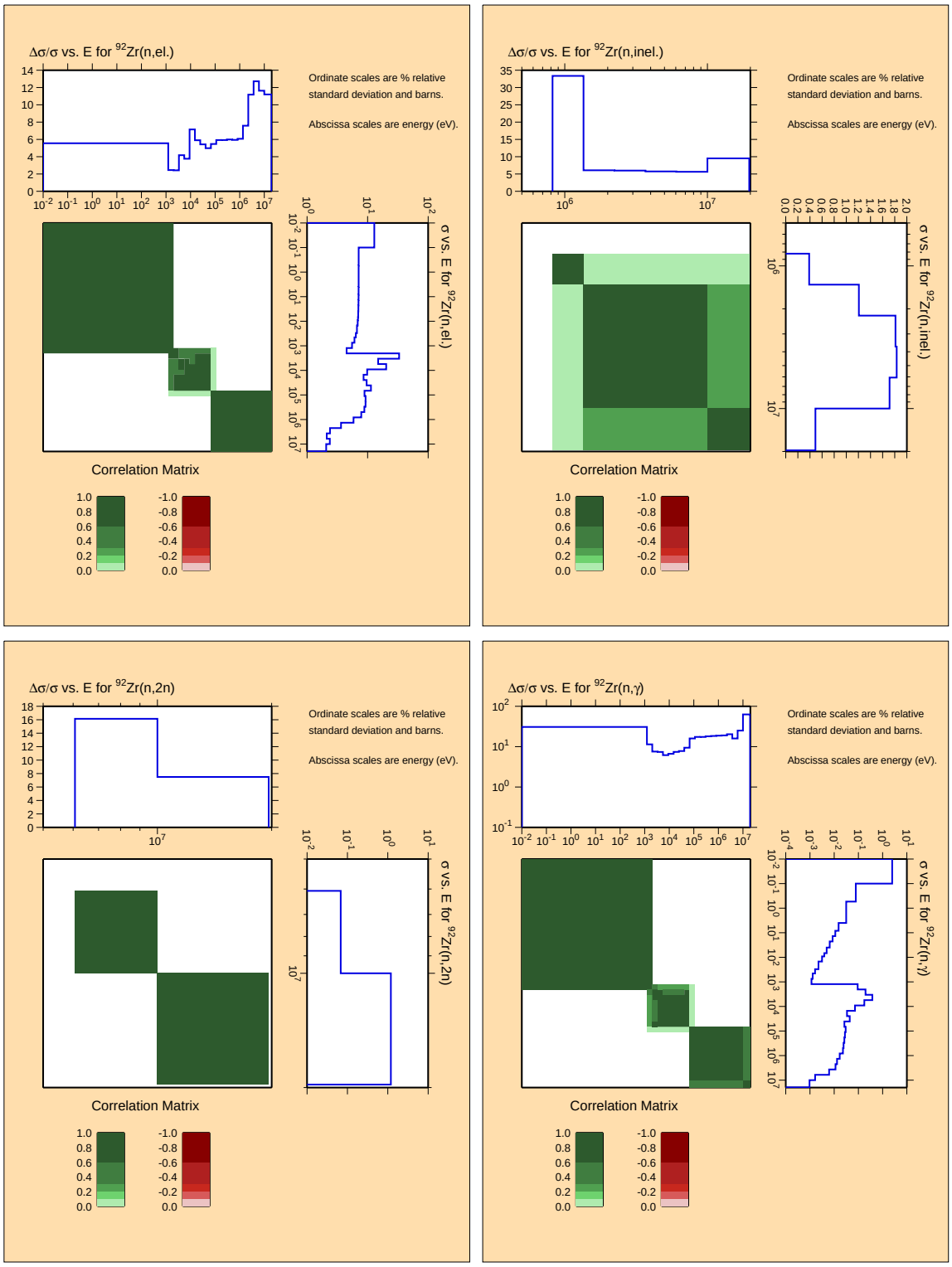

Figure B.20: Covariances for structural material ^{92}Zr.

^{93}Zr

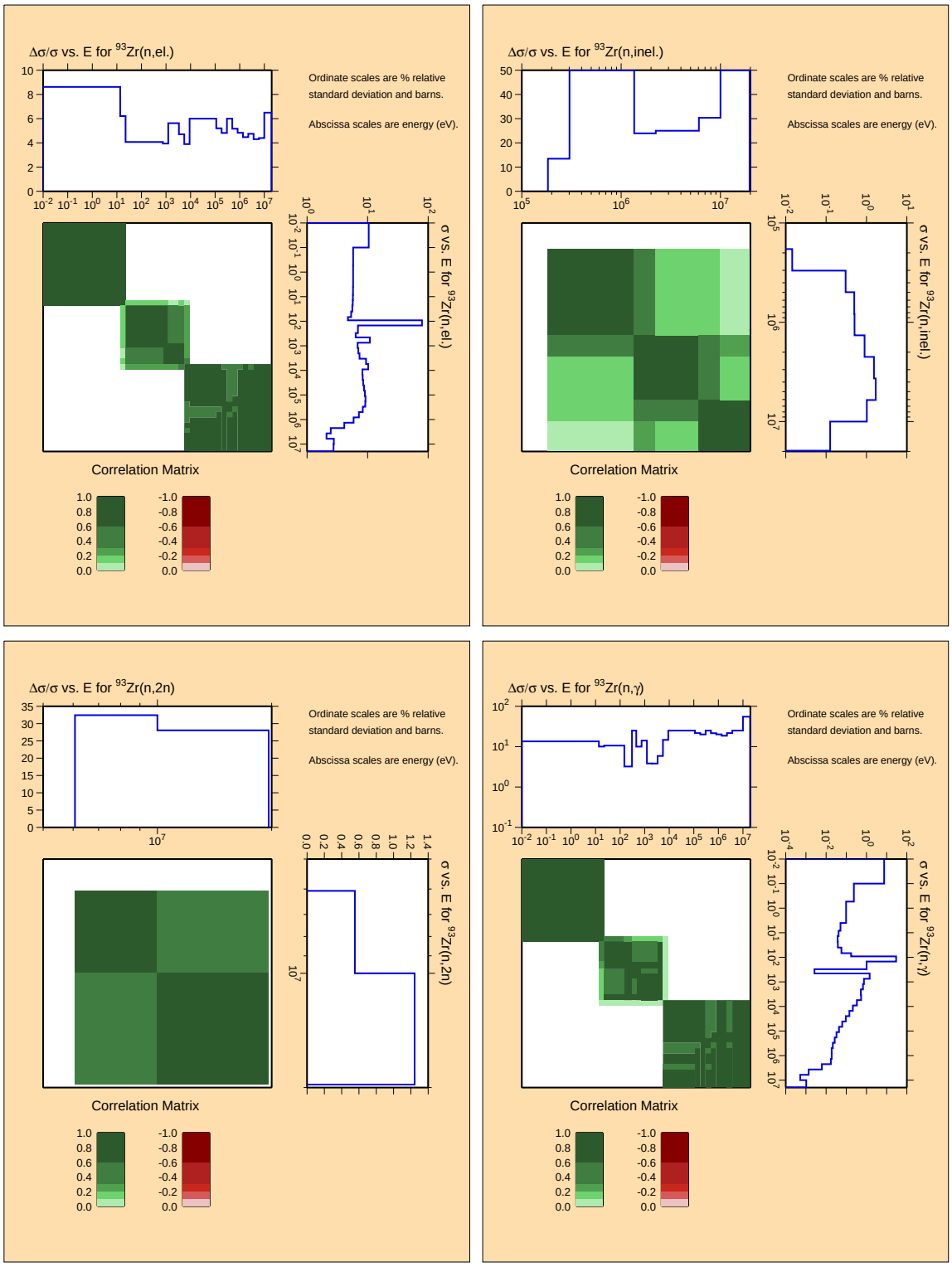

Figure B.21: Covariances for structural material ^{93}Zr.

^{94}Zr

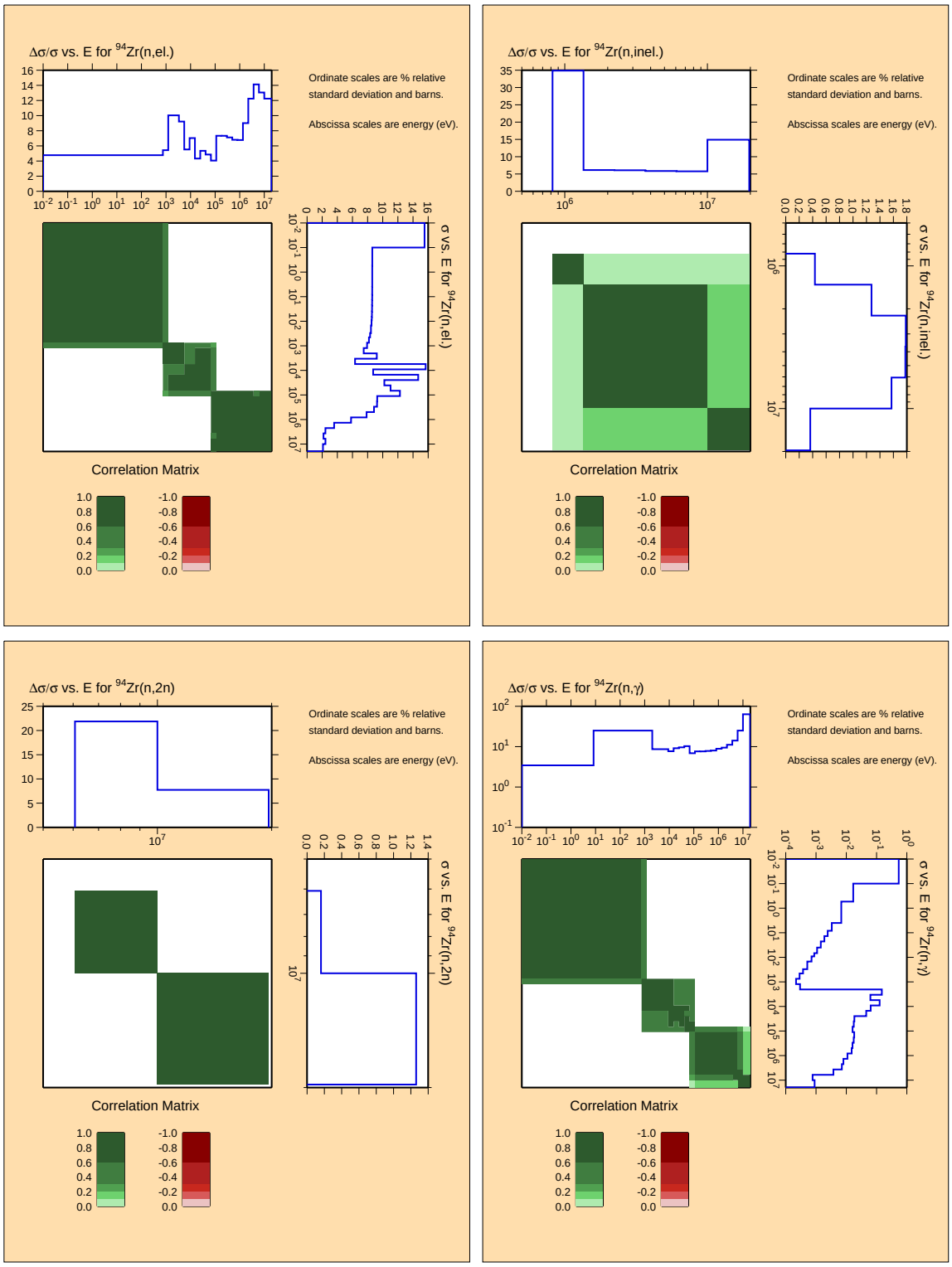

Figure B.22: Covariances for structural material ^{94}Zr.

^{95}Zr

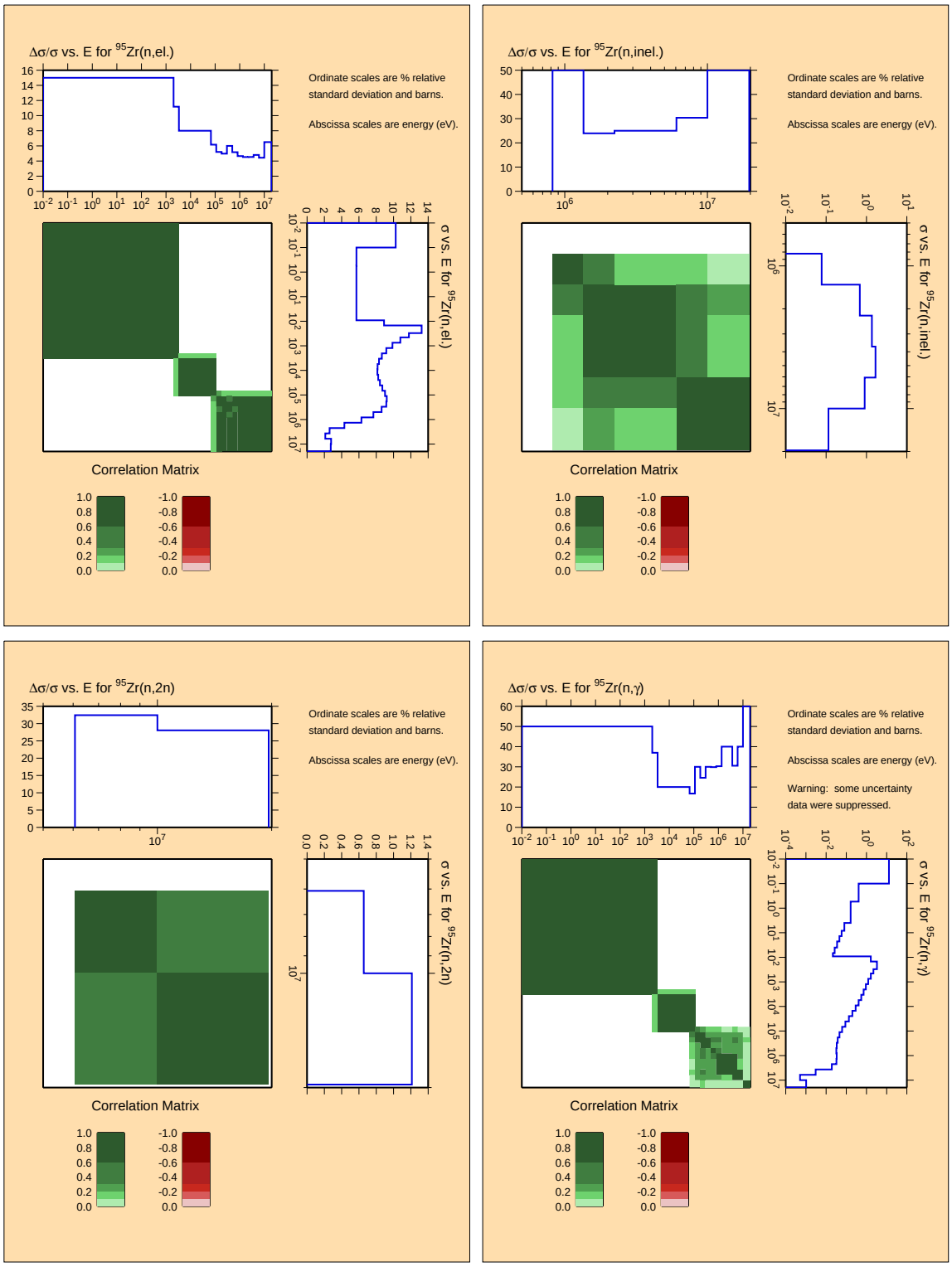

Figure B.23: Covariances for fission product ^{95}Zr.

^{96}Zr

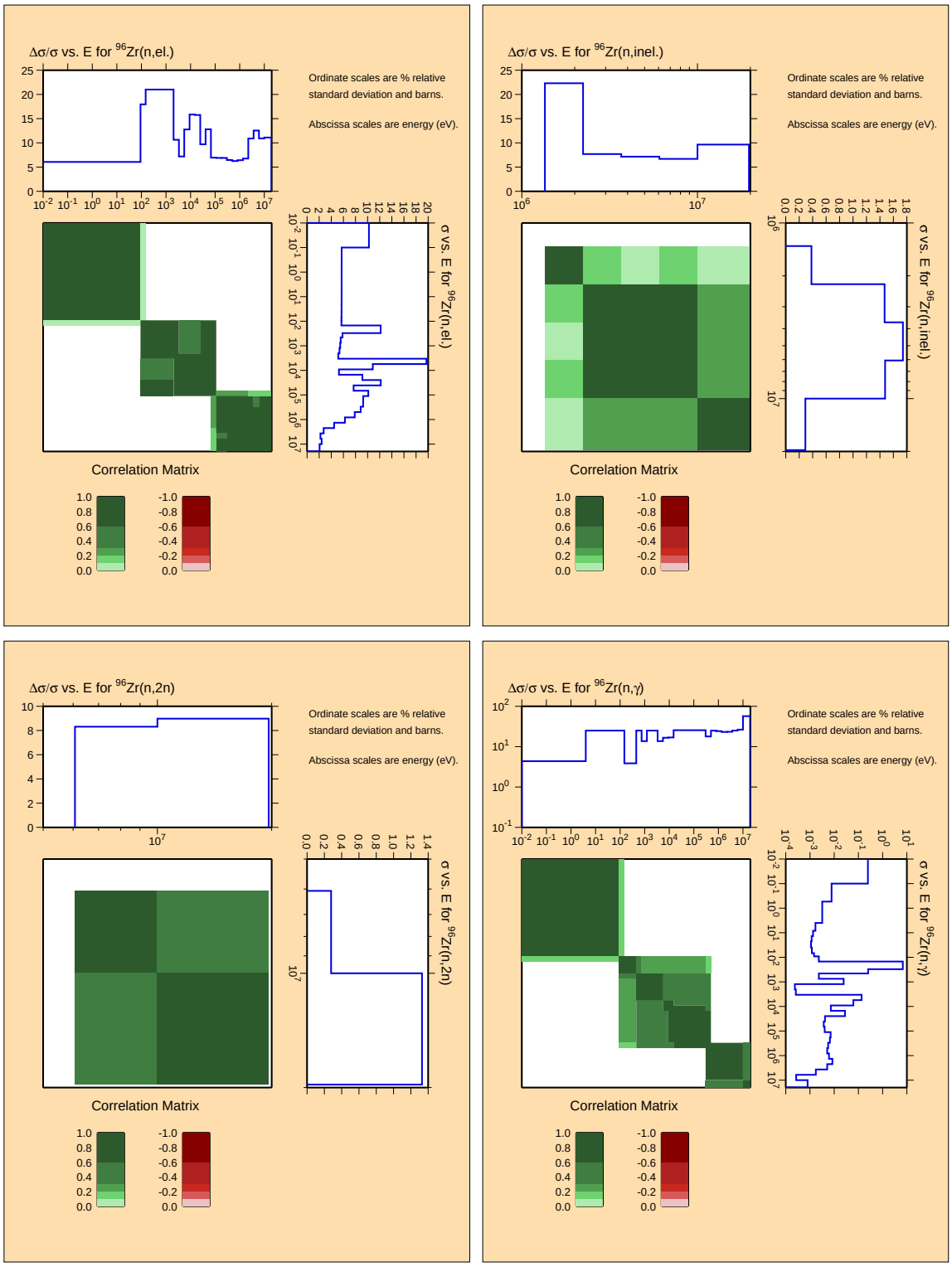

Figure B.24: Covariances for fission product ^{96}Zr.

^{95}Nb

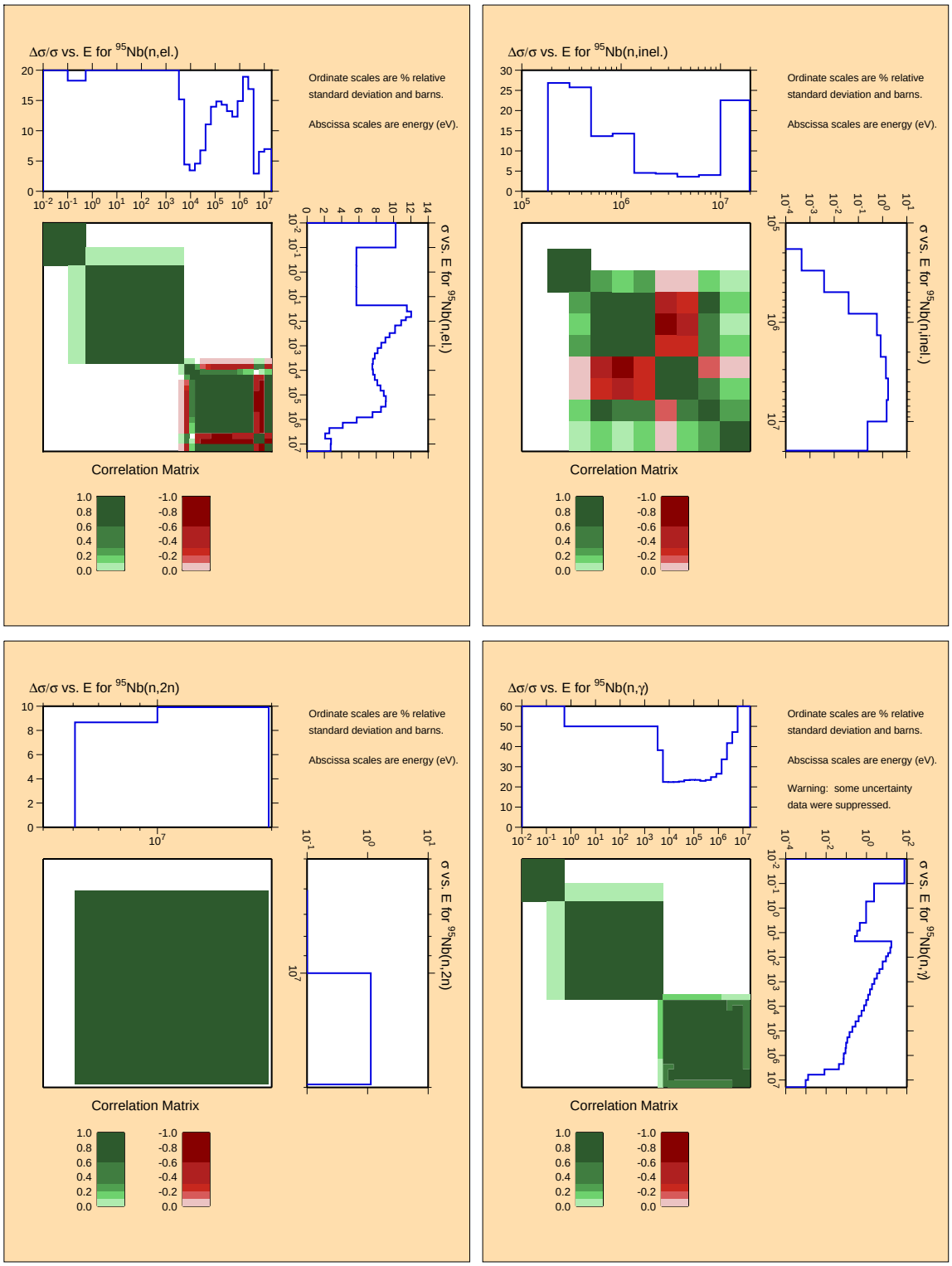

Figure B.25: Covariances for fission product ^{95}Nb.

^{92}Mo

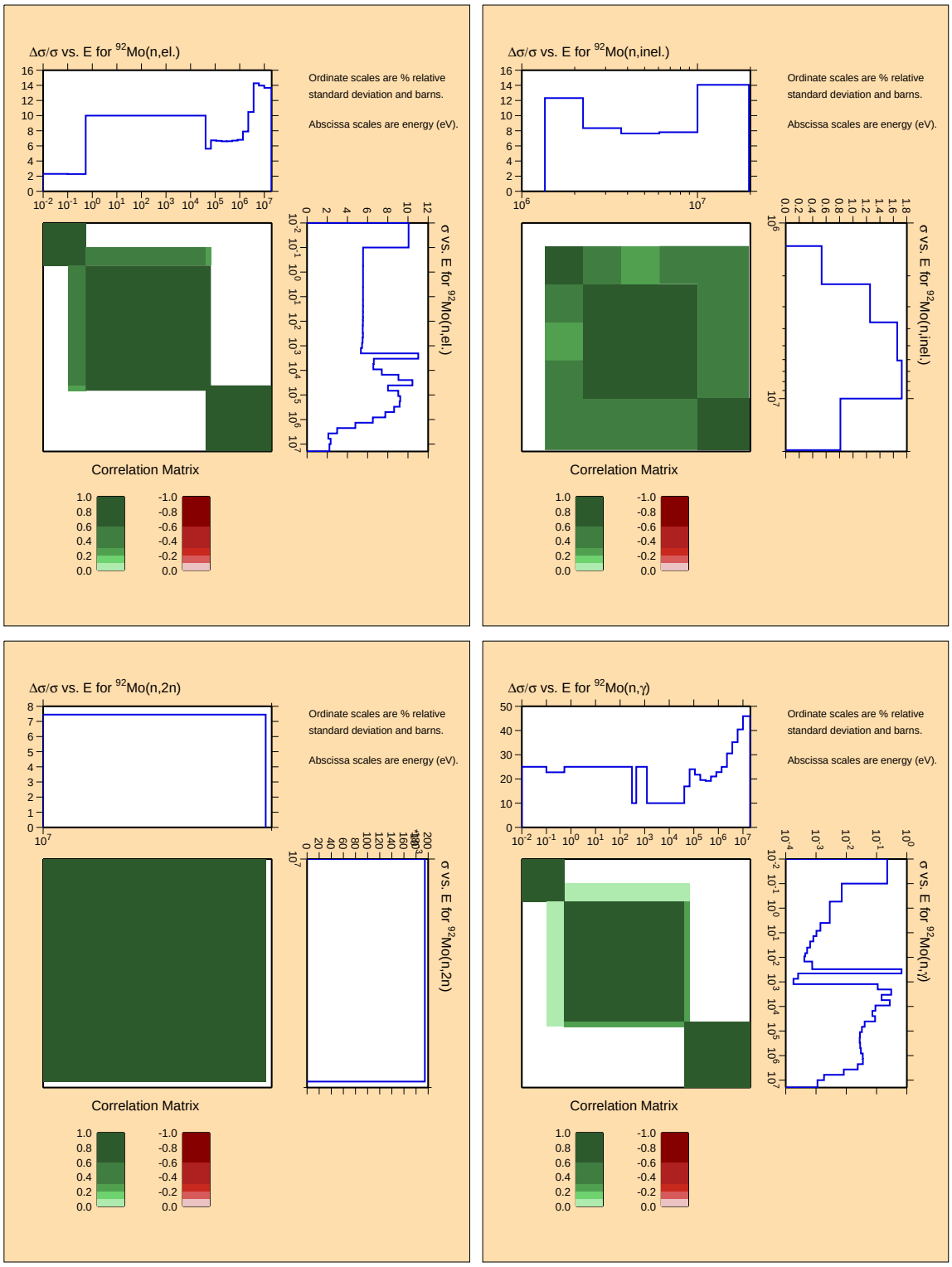

Figure B.26: Covariances for structural material ^{92}Mo.

^{94}Mo

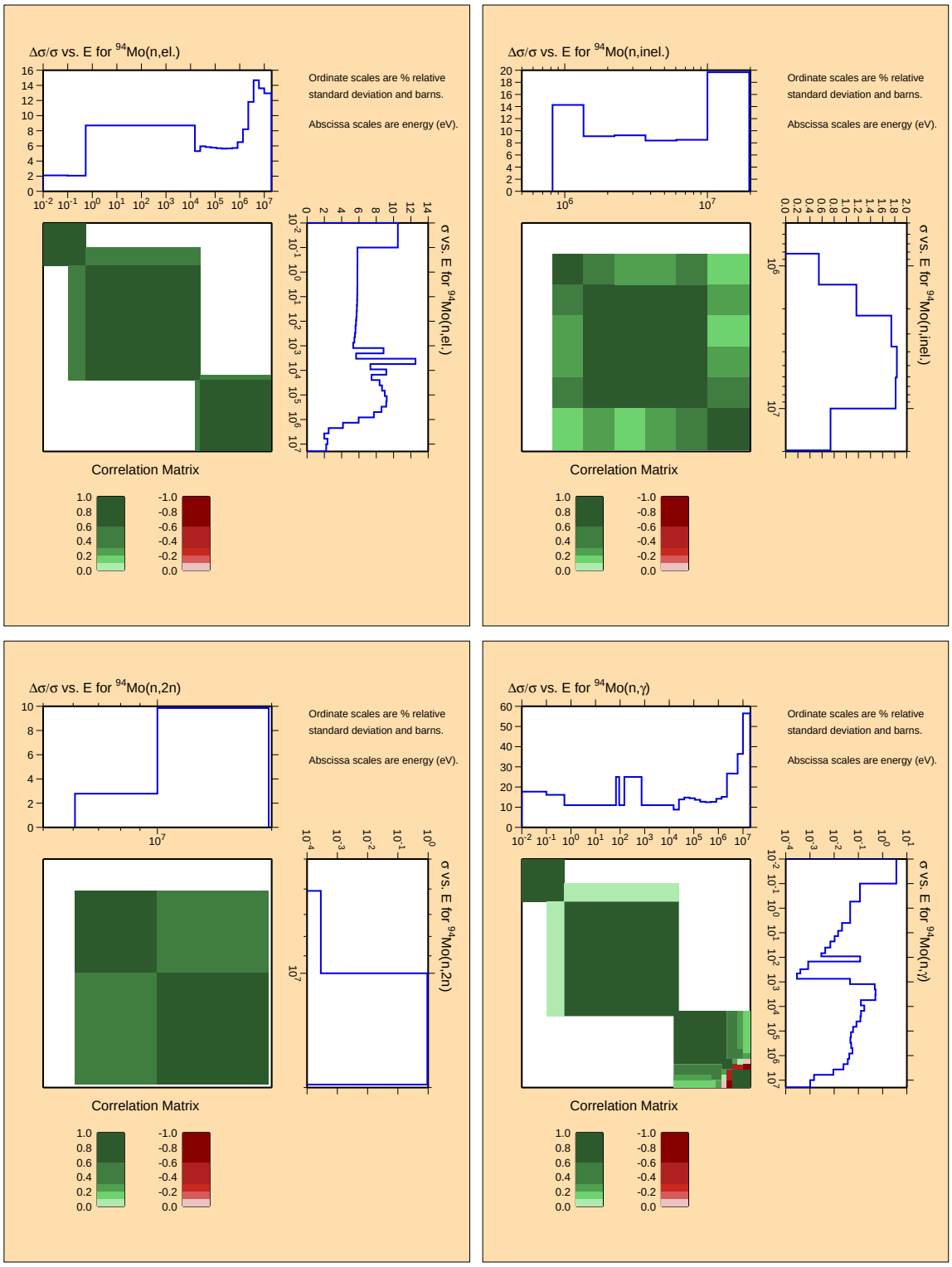

Figure B.27: Covariances for structural material ^{94}Mo.

^{95}Mo

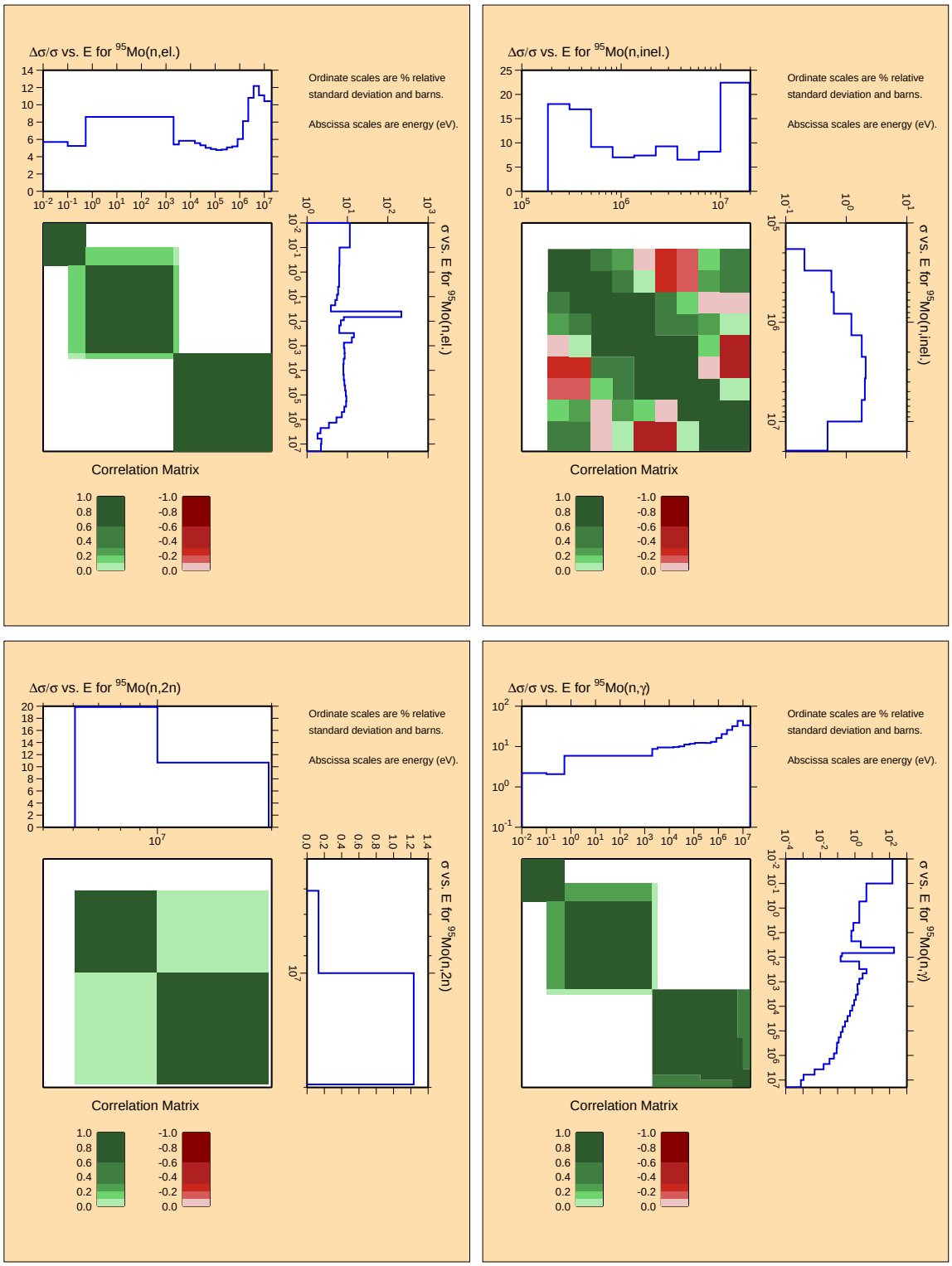

Figure B.28: Covariances for structural material ^{95}Mo.

^{96}Mo

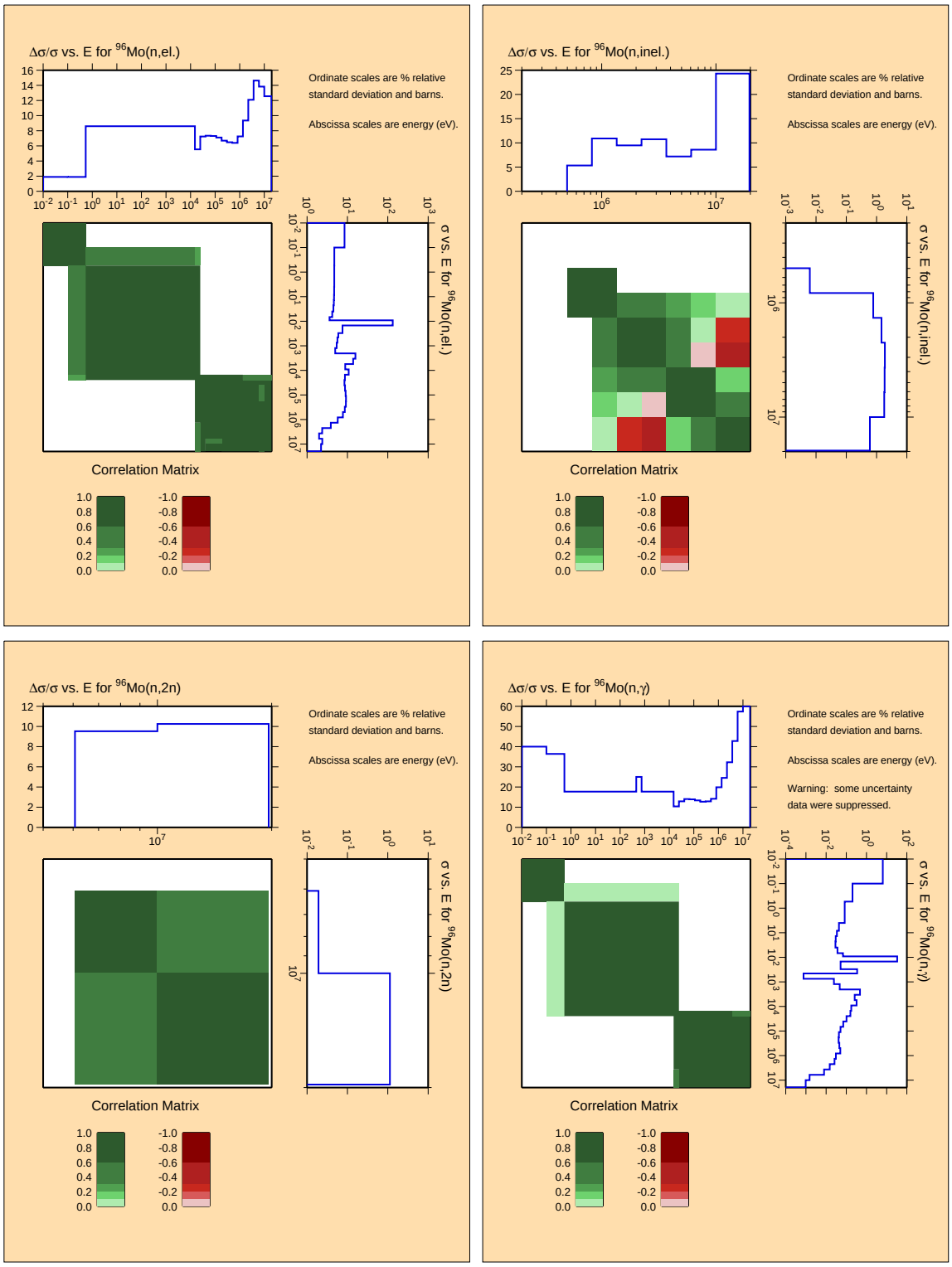

Figure B.29: Covariances for structural material ^{96}Mo.

^{97}Mo

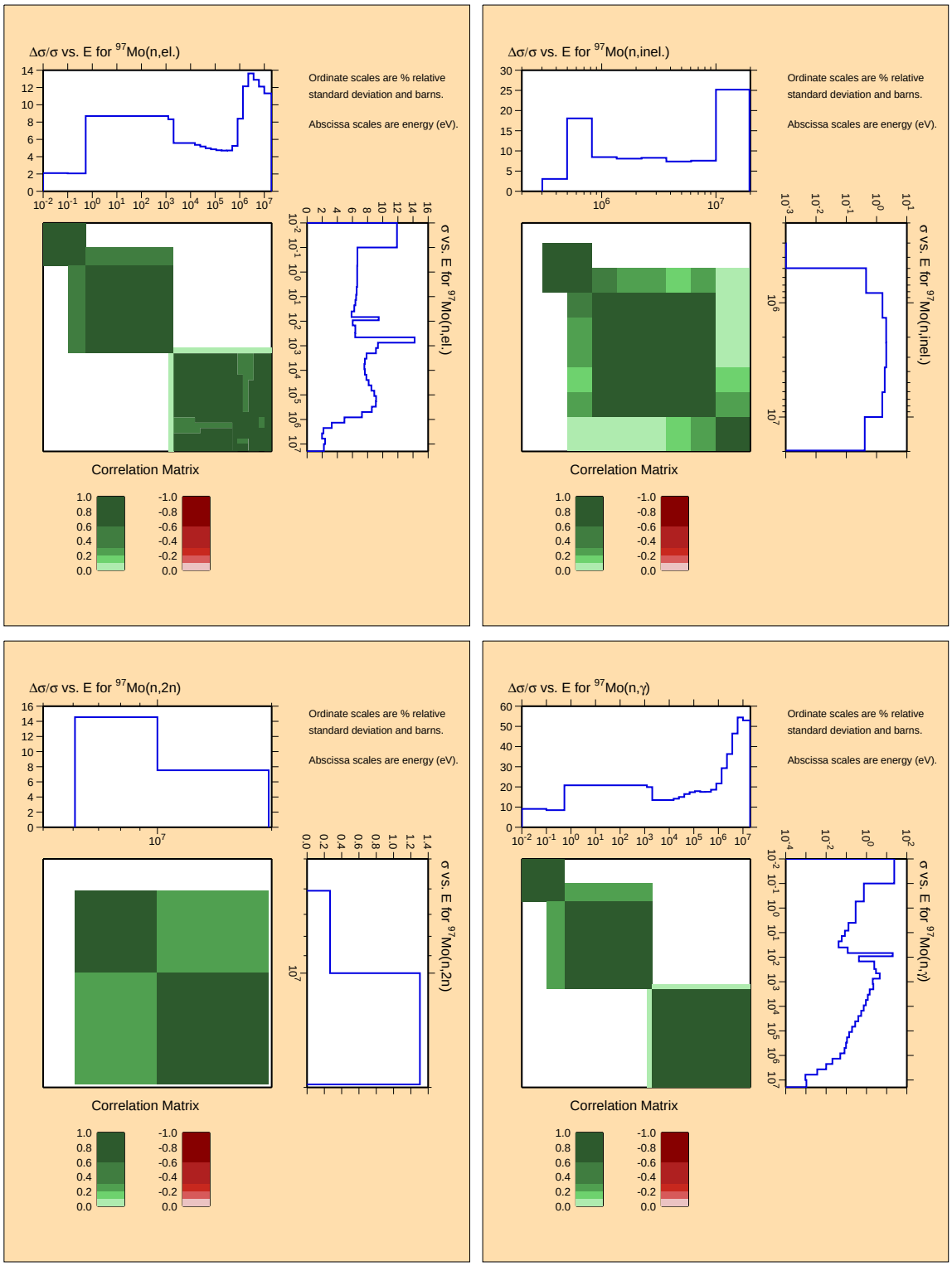

Figure B.30: Covariances for structural material ^{97}Mo.

^{98}Mo

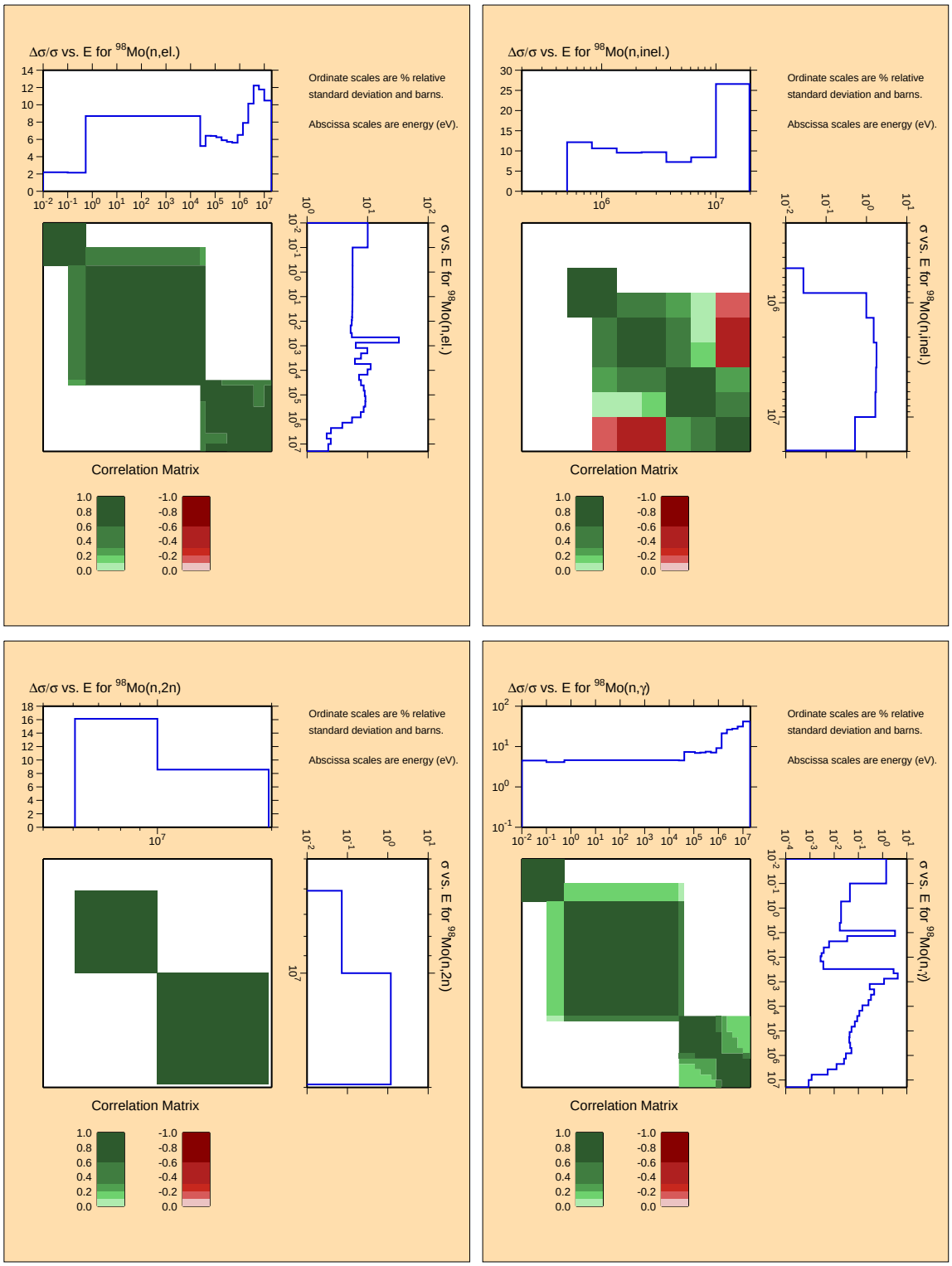

Figure B.31: Covariances for structural material ^{98}Mo.

^{100}Mo

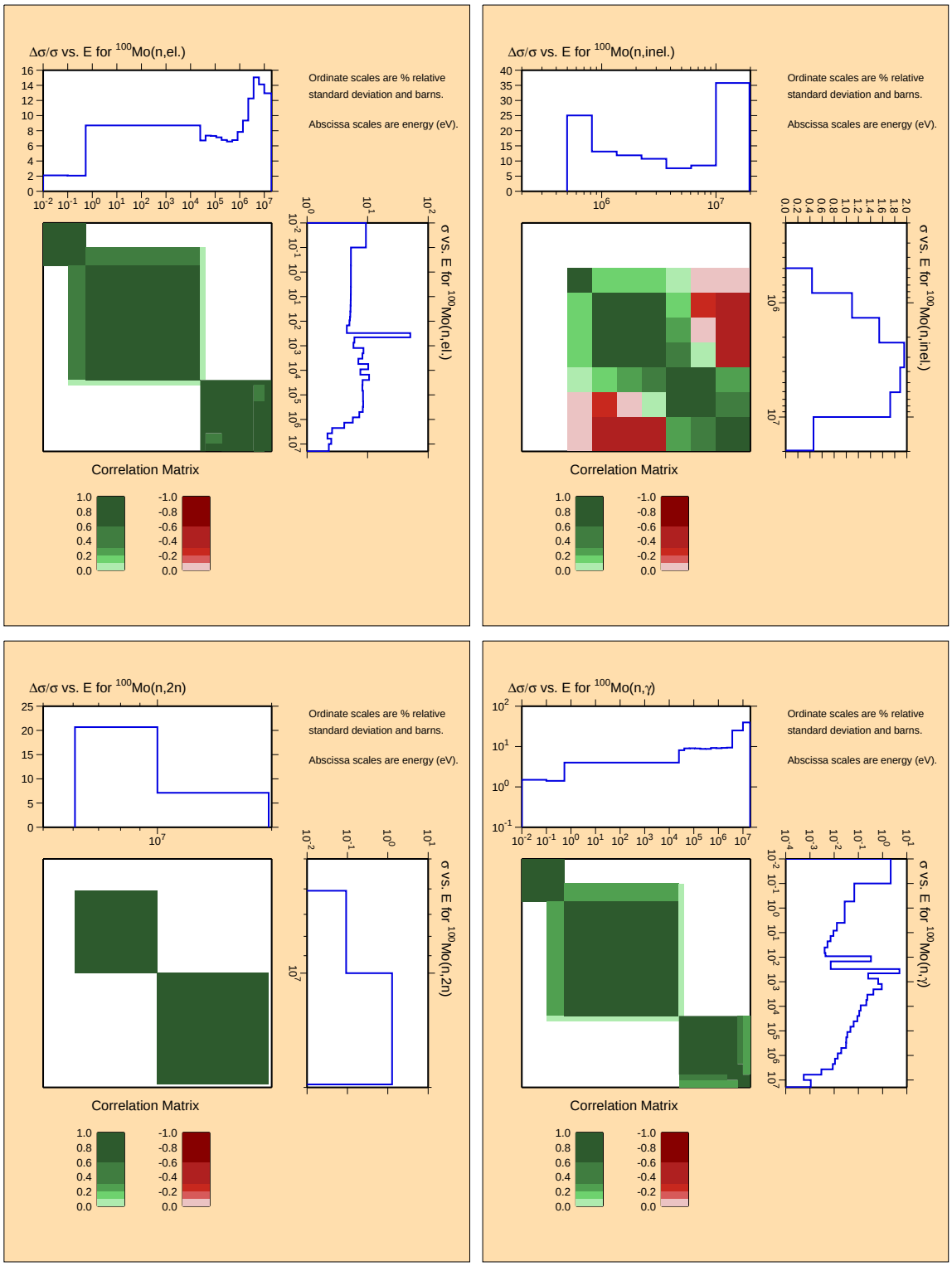

Figure B.32: Covariances for structural material ^{100}Mo.

^{99}Tc

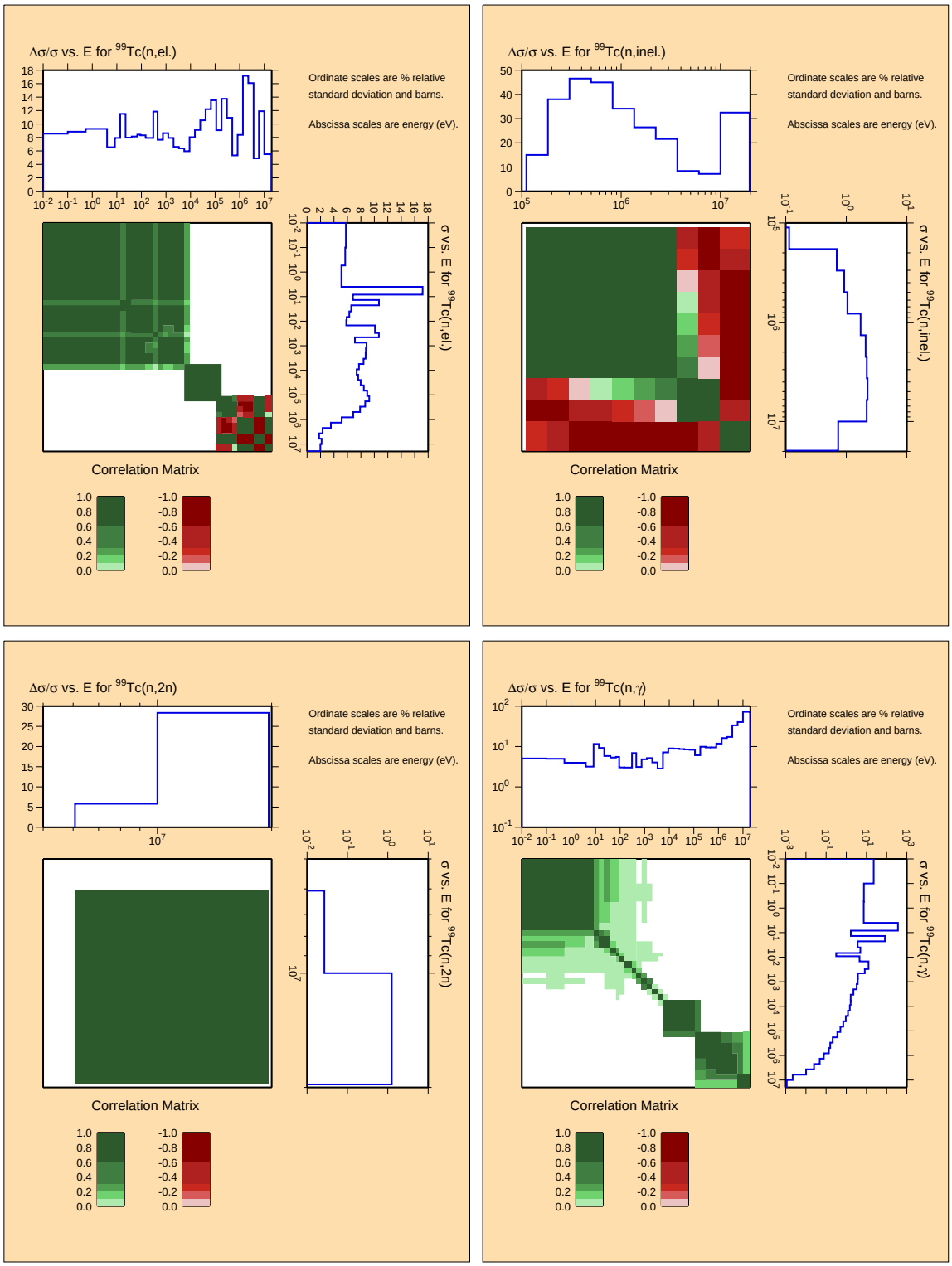

Figure B.33: Covariances for fission product ^{99}Tc.

^{101}Ru

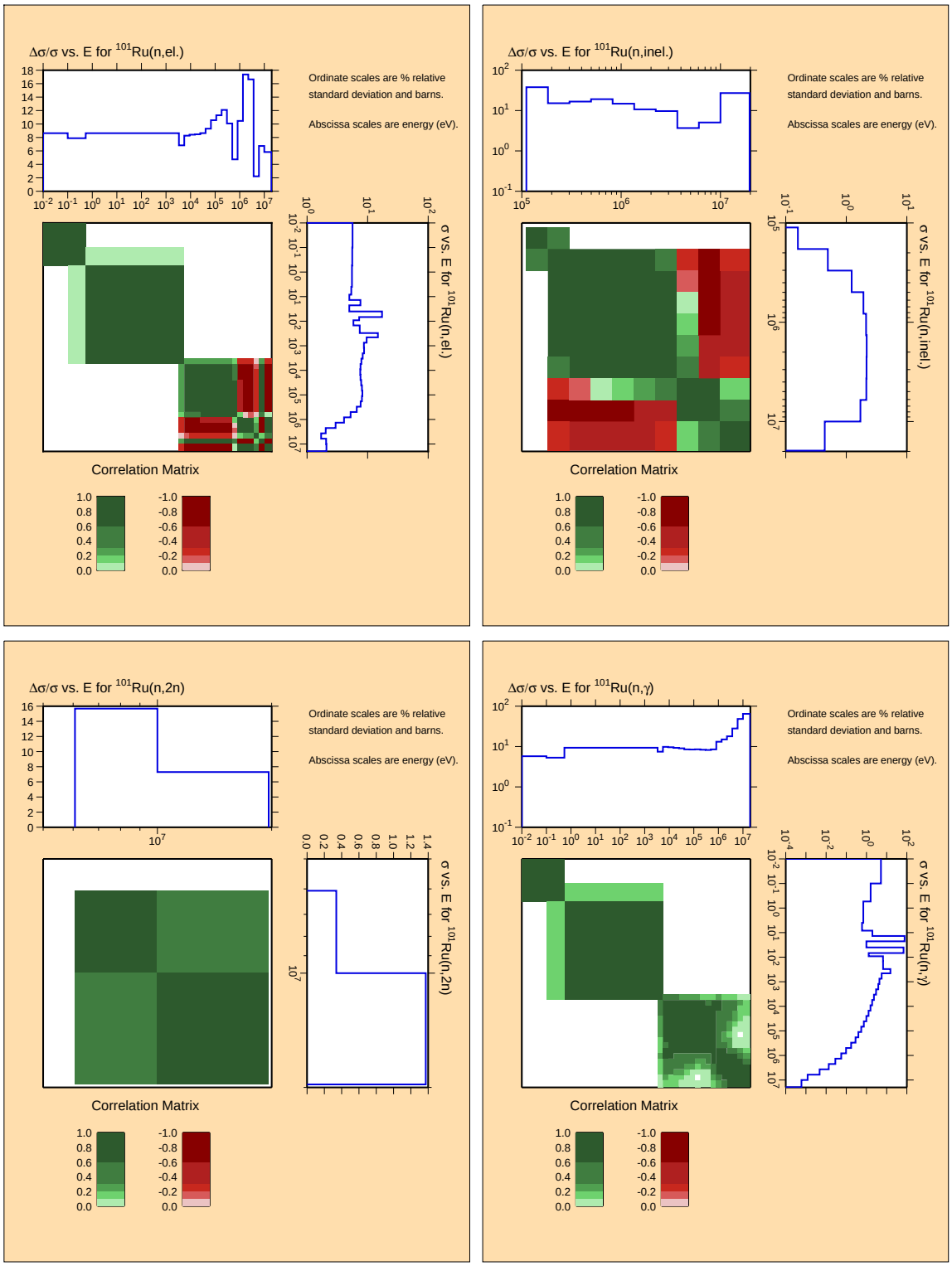

Figure B.34: Covariances for fission product ^{101}Ru.

^{102}Ru

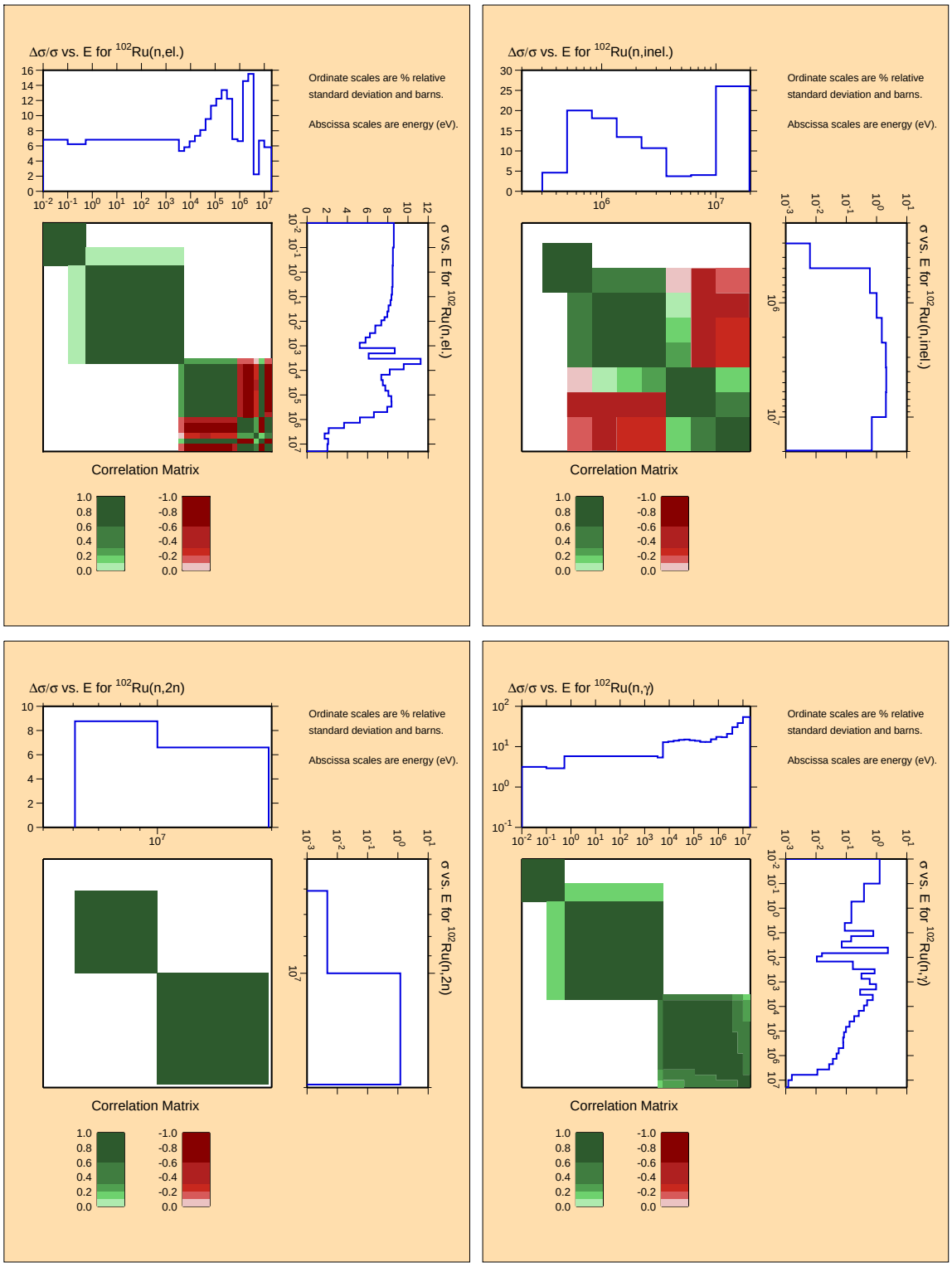

Figure B.35: Covariances for fission product ^{102}Ru.

^{103}Ru

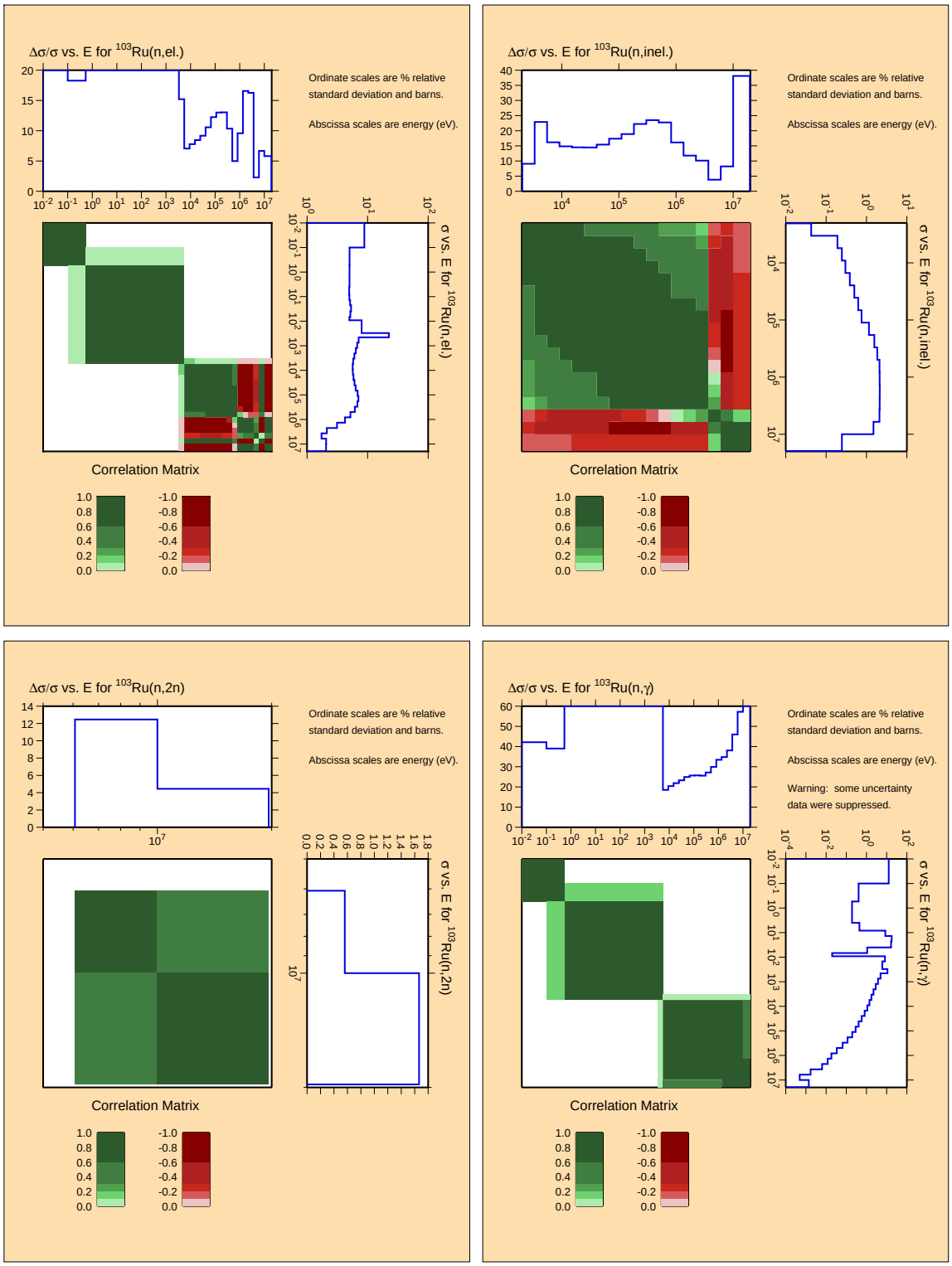

Figure B.36: Covariances for fission product ^{103}Ru.

^{104}Ru

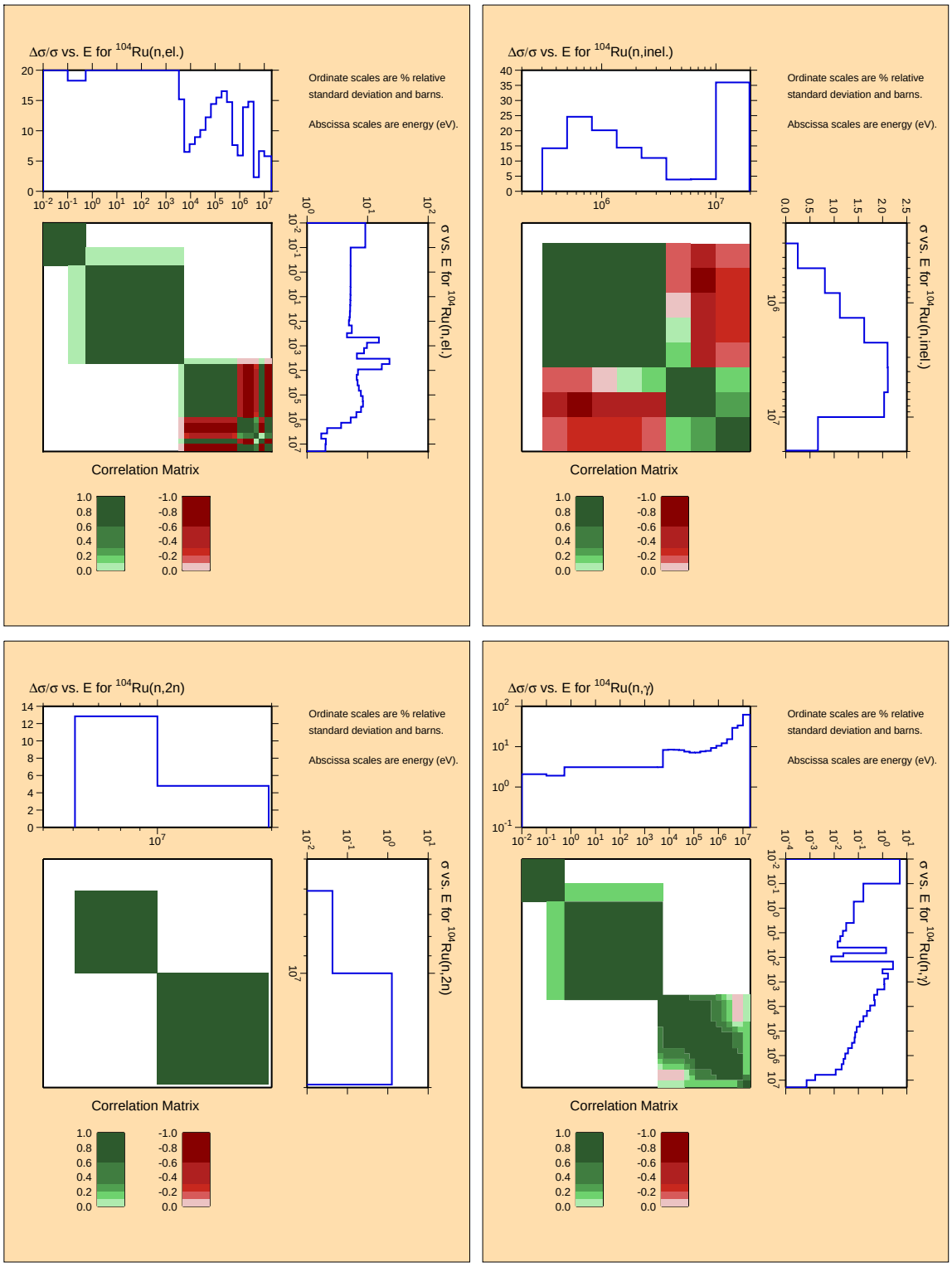

Figure B.37: Covariances for fission product ^{104}Ru.

^{106}Ru

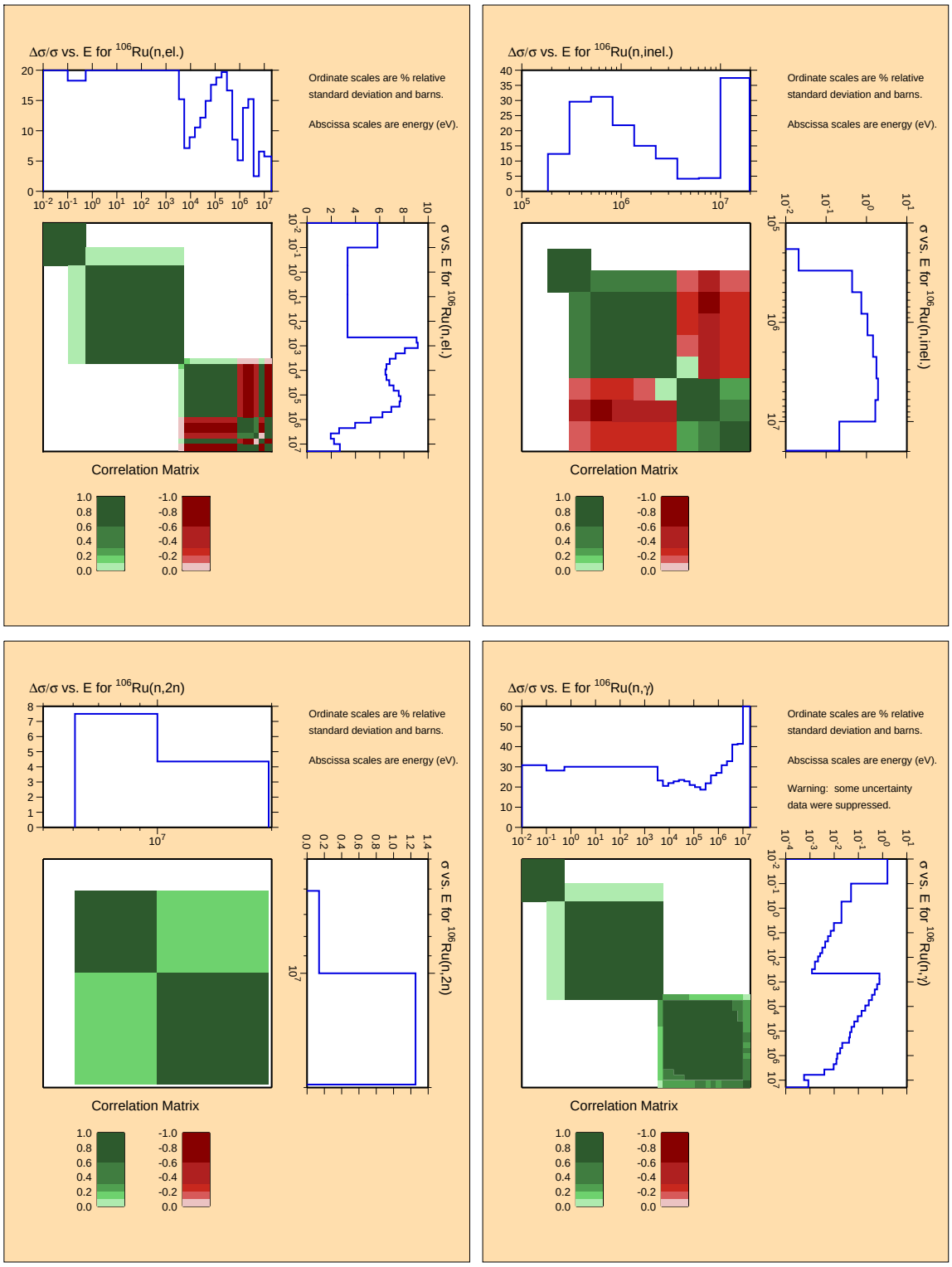

Figure B.38: Covariances for fission product ^{106}Ru.

^{103}Rh

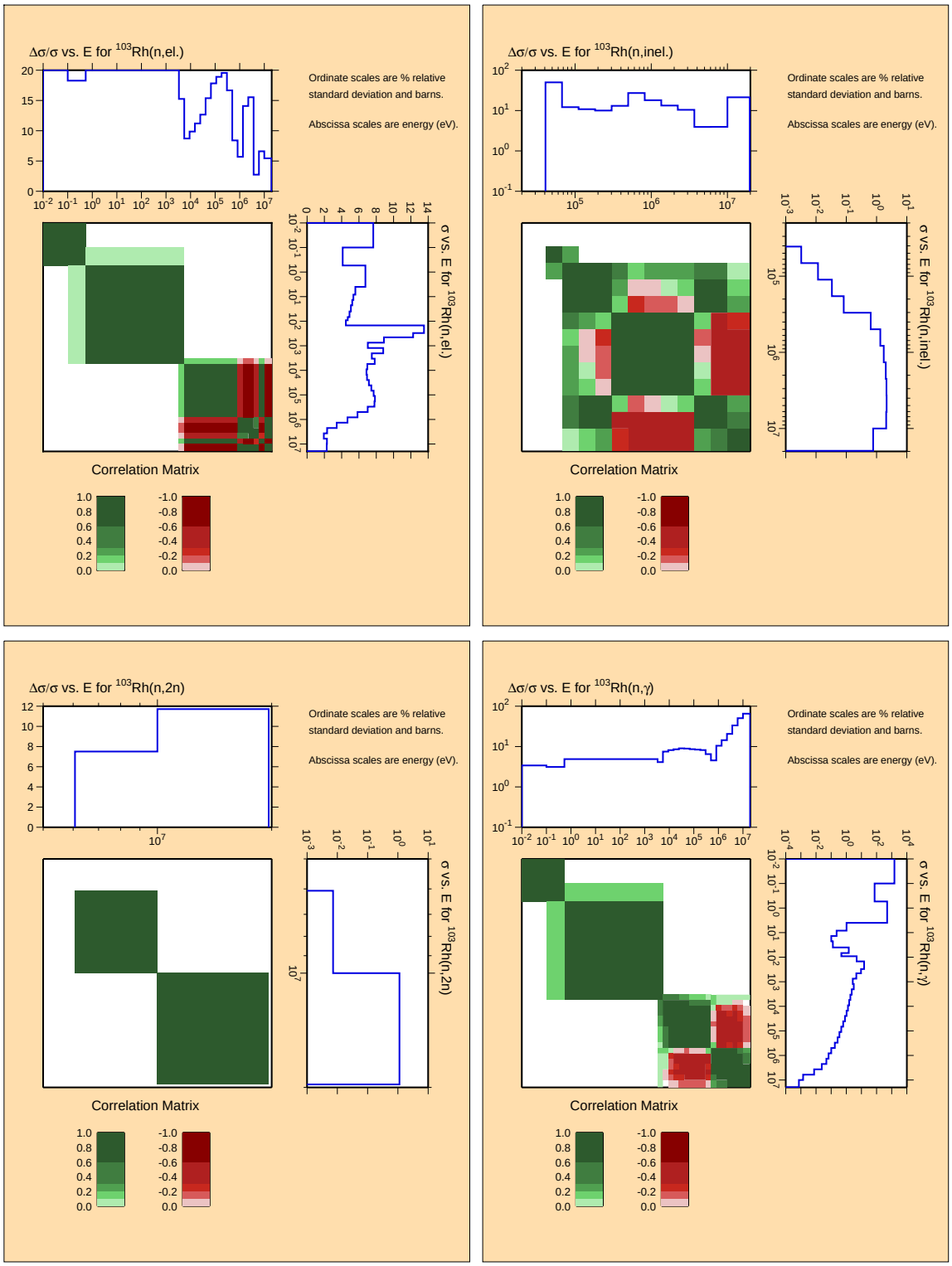

Figure B.39: Covariances for fission product ^{103}Rh.

^{105}Pd

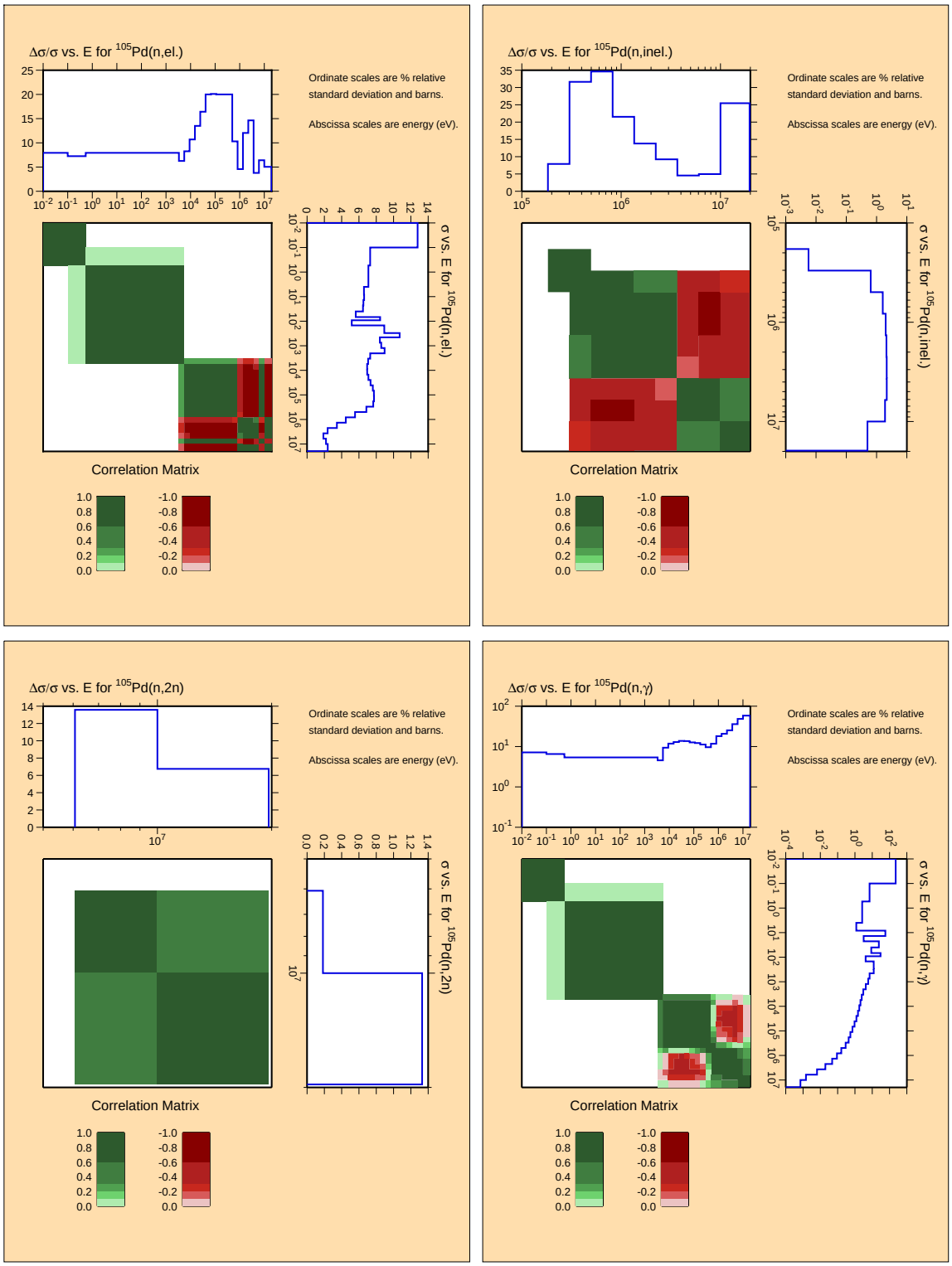

Figure B.40: Covariances for fission product ^{105}Pd.

^{106}Pd

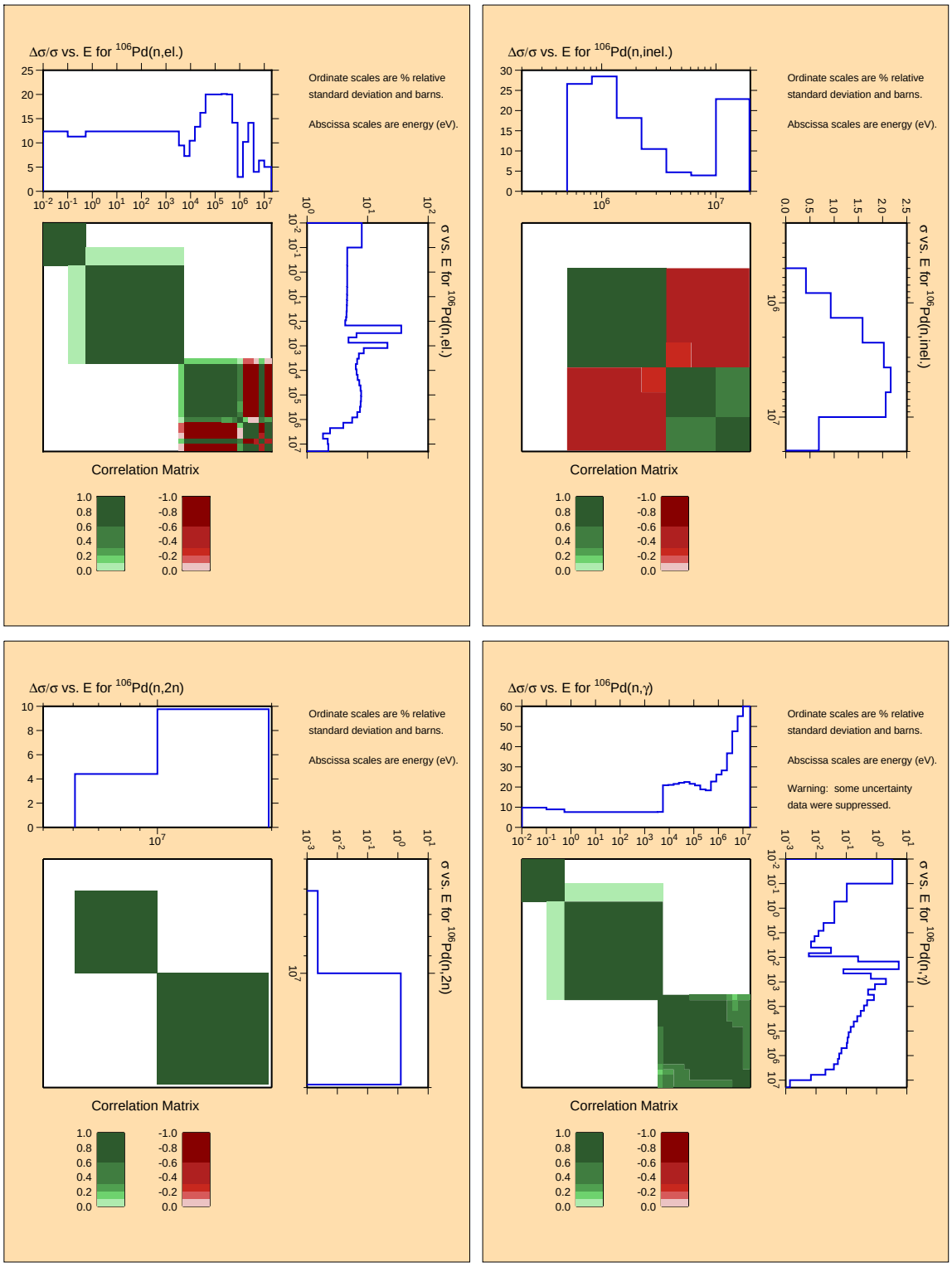

Figure B.41: Covariances for fission product ^{106}Pd.

^{107}Pd

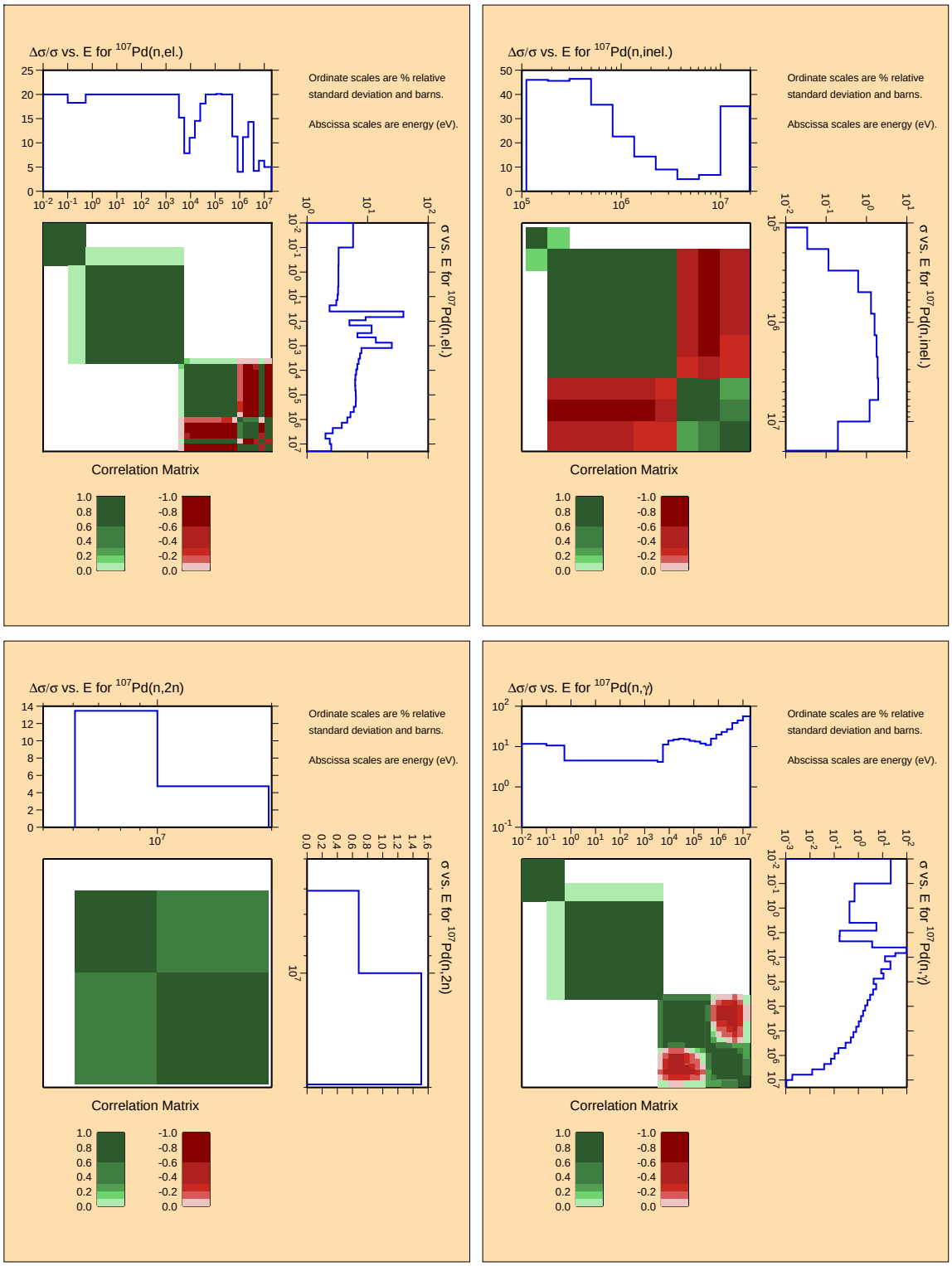

Figure B.42: Covariances for fission product ^{107}Pd.

^{108}Pd

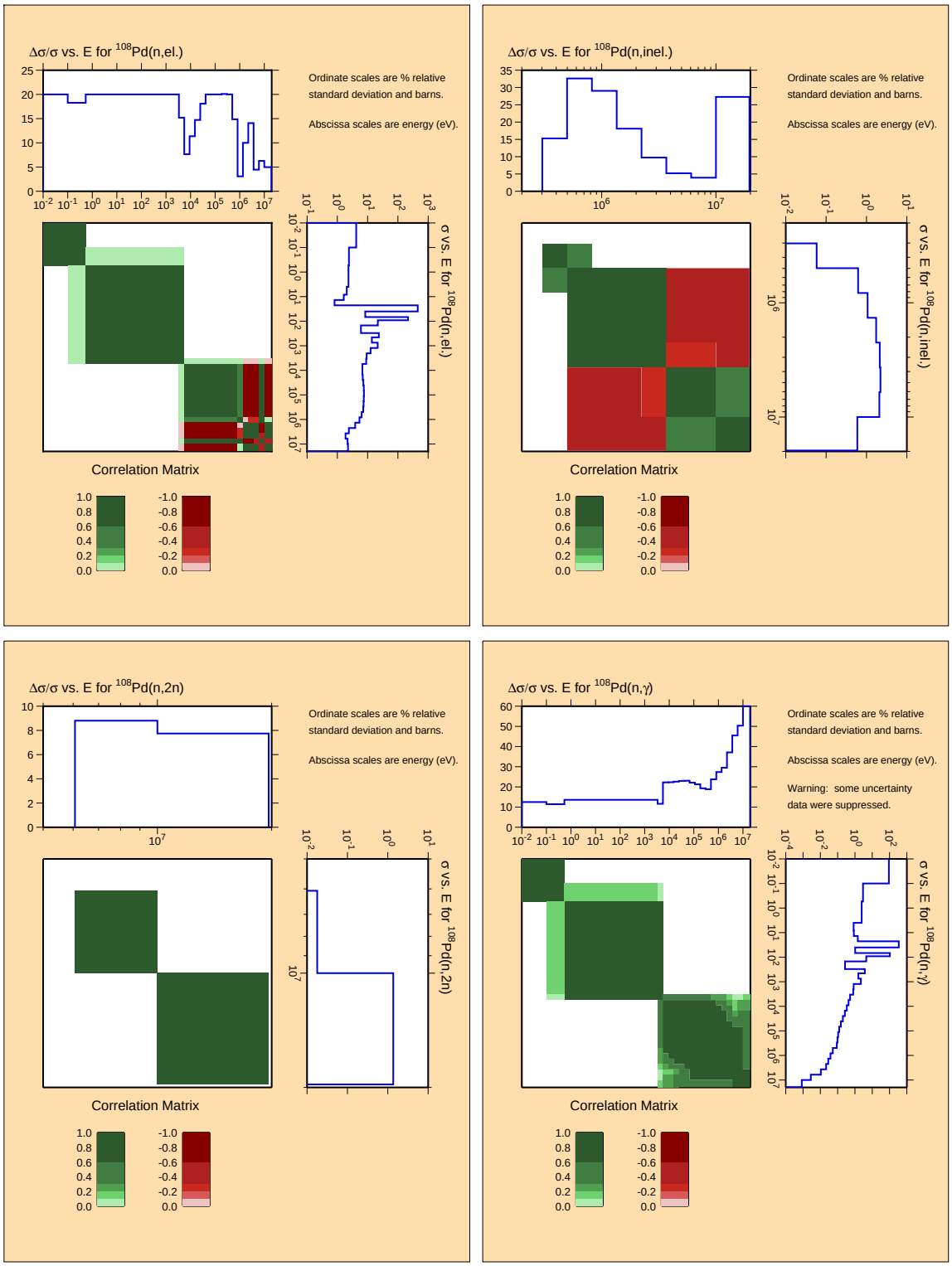

Figure B.43: Covariances for fission product ^{108}Pd.

^{109}Ag

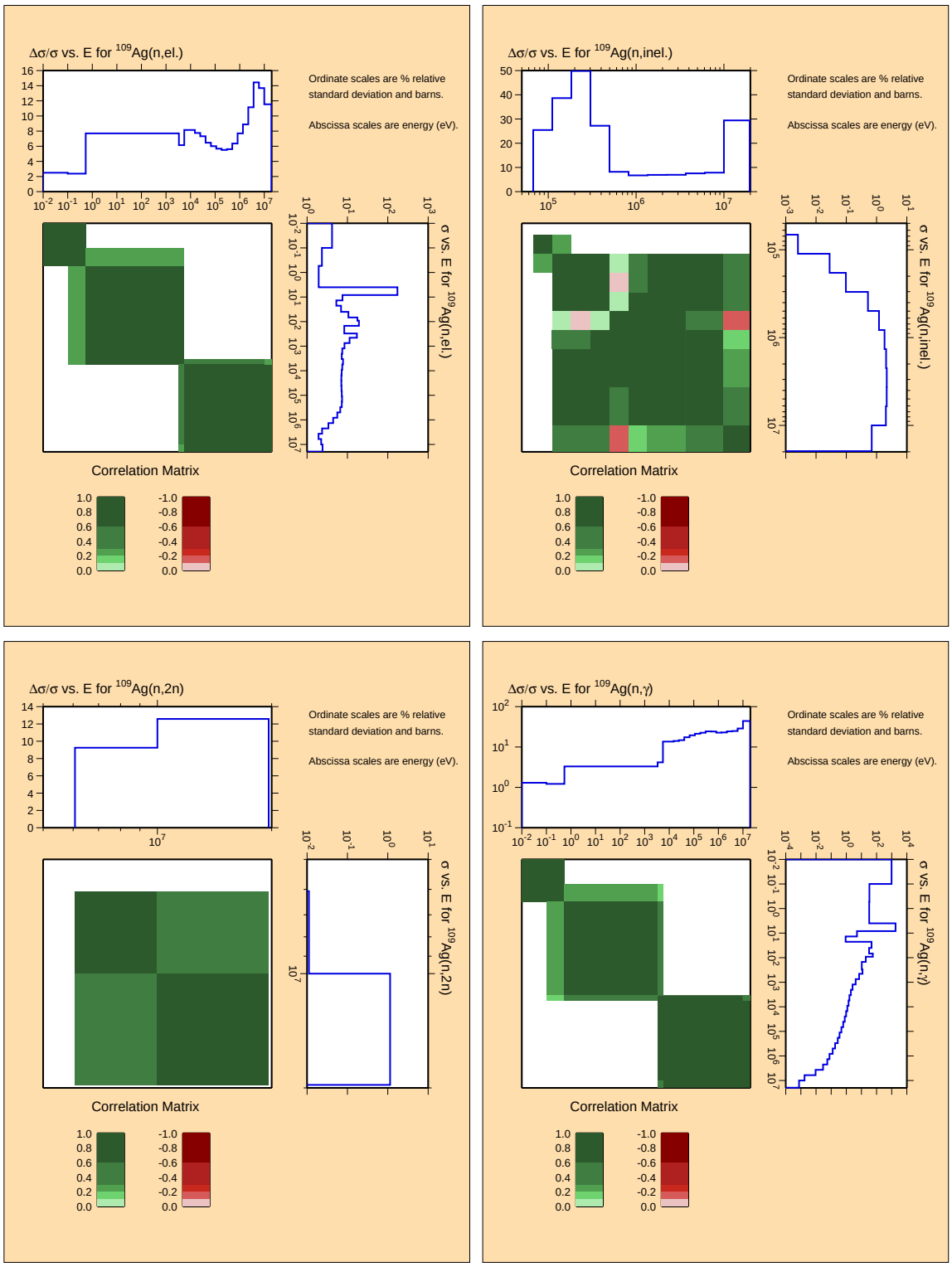

Figure B.44: Covariances for fission product ^{109}Ag.

^{127}I

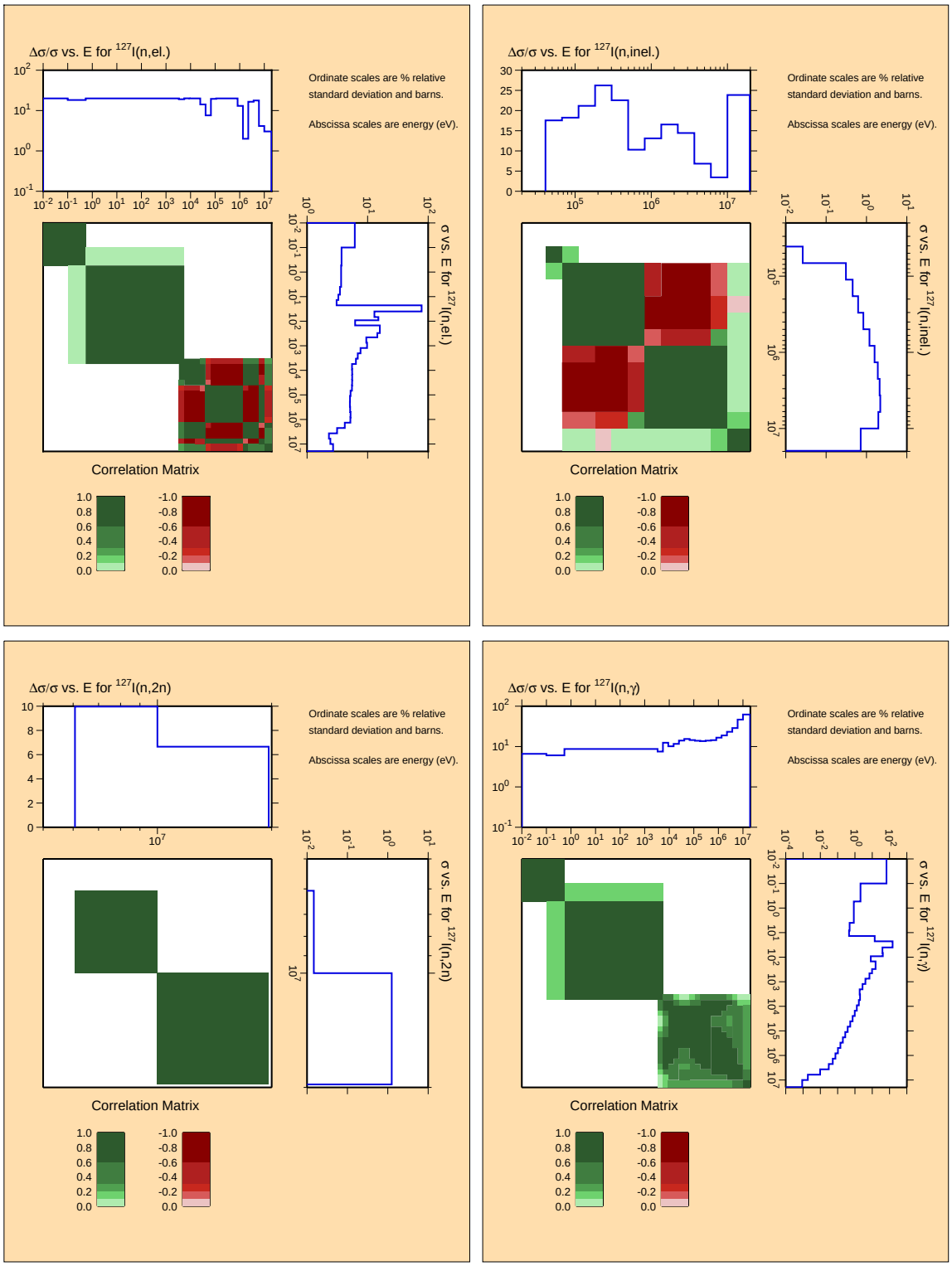

Figure B.45: Covariances for fission product ^{127}I.

^{129}I

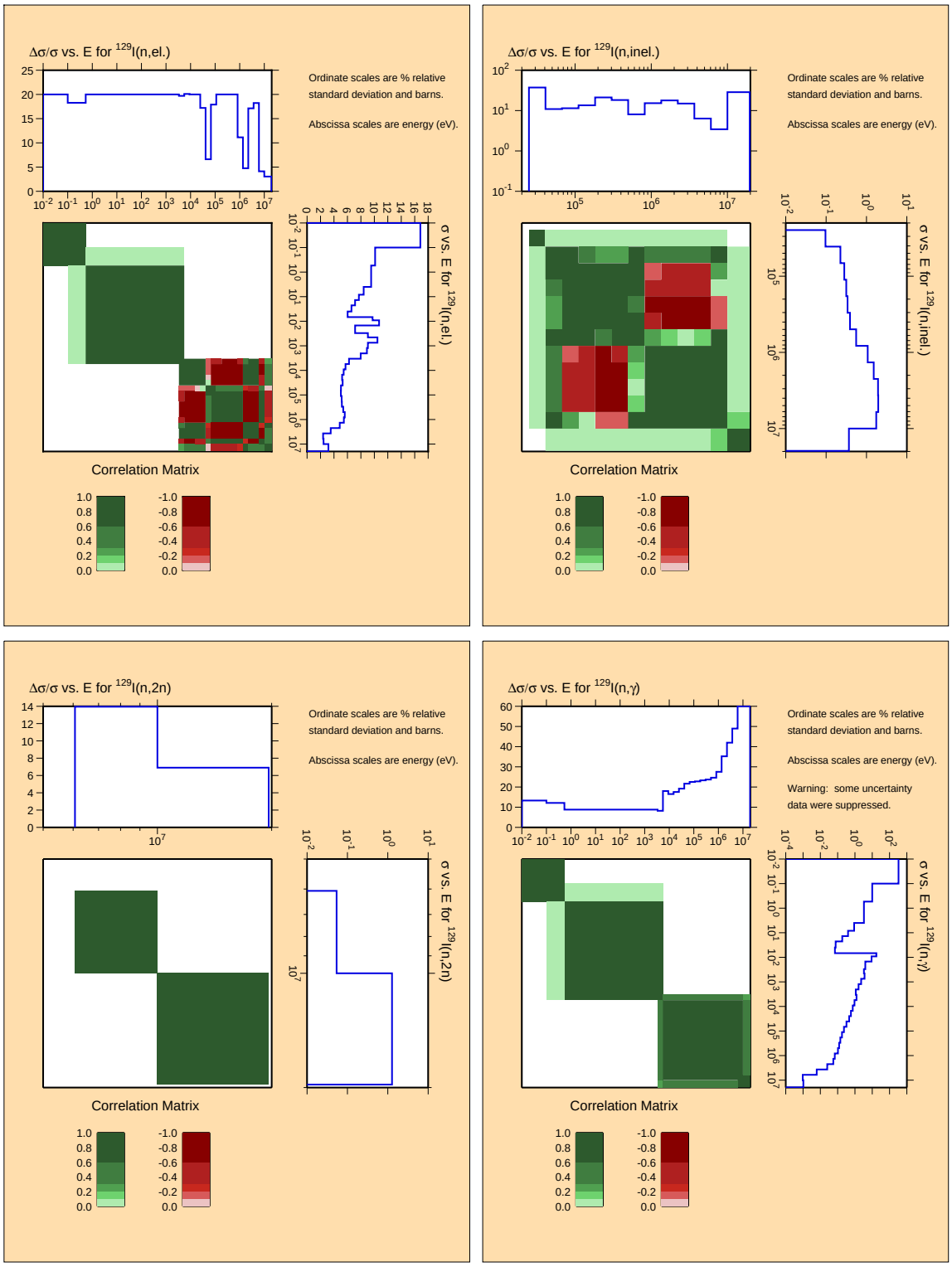

Figure B.46: Covariances for fission product ^{129}I.

^{131}Xe

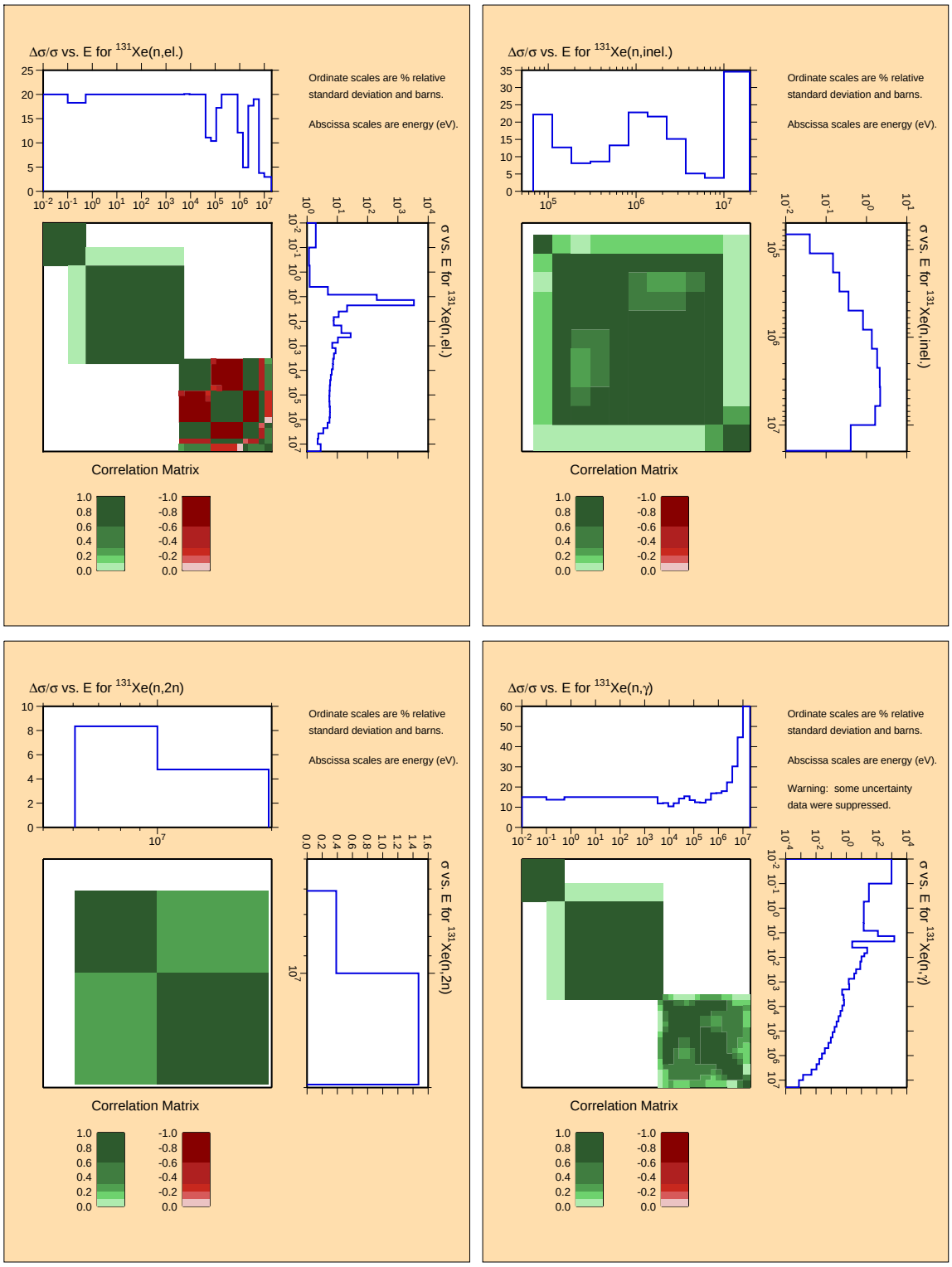

Figure B.47: Covariances for fission product ^{131}Xe.

^{132}Xe

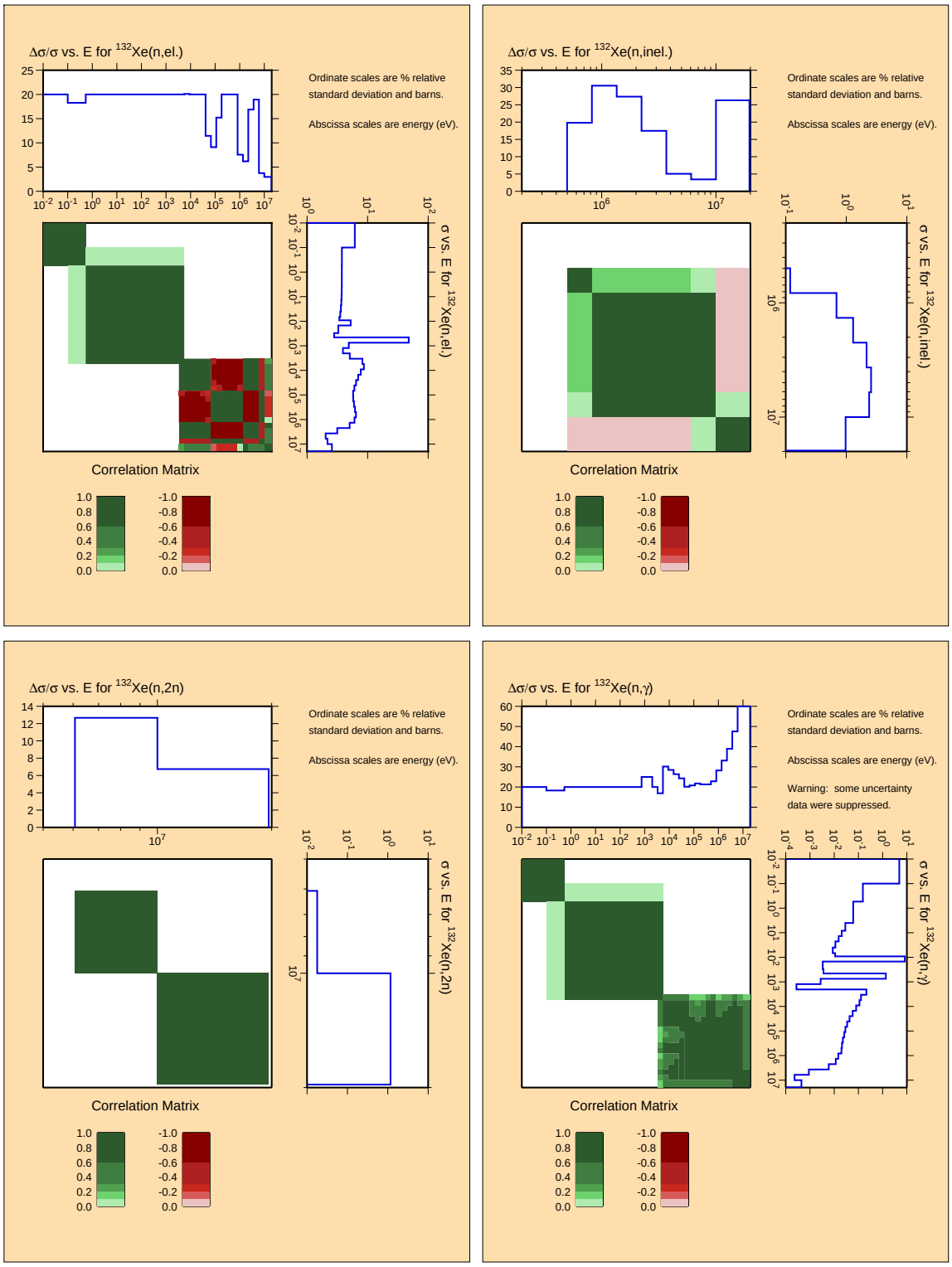

Figure B.48: Covariances for fission product ^{132}Xe.

^{134}Xe

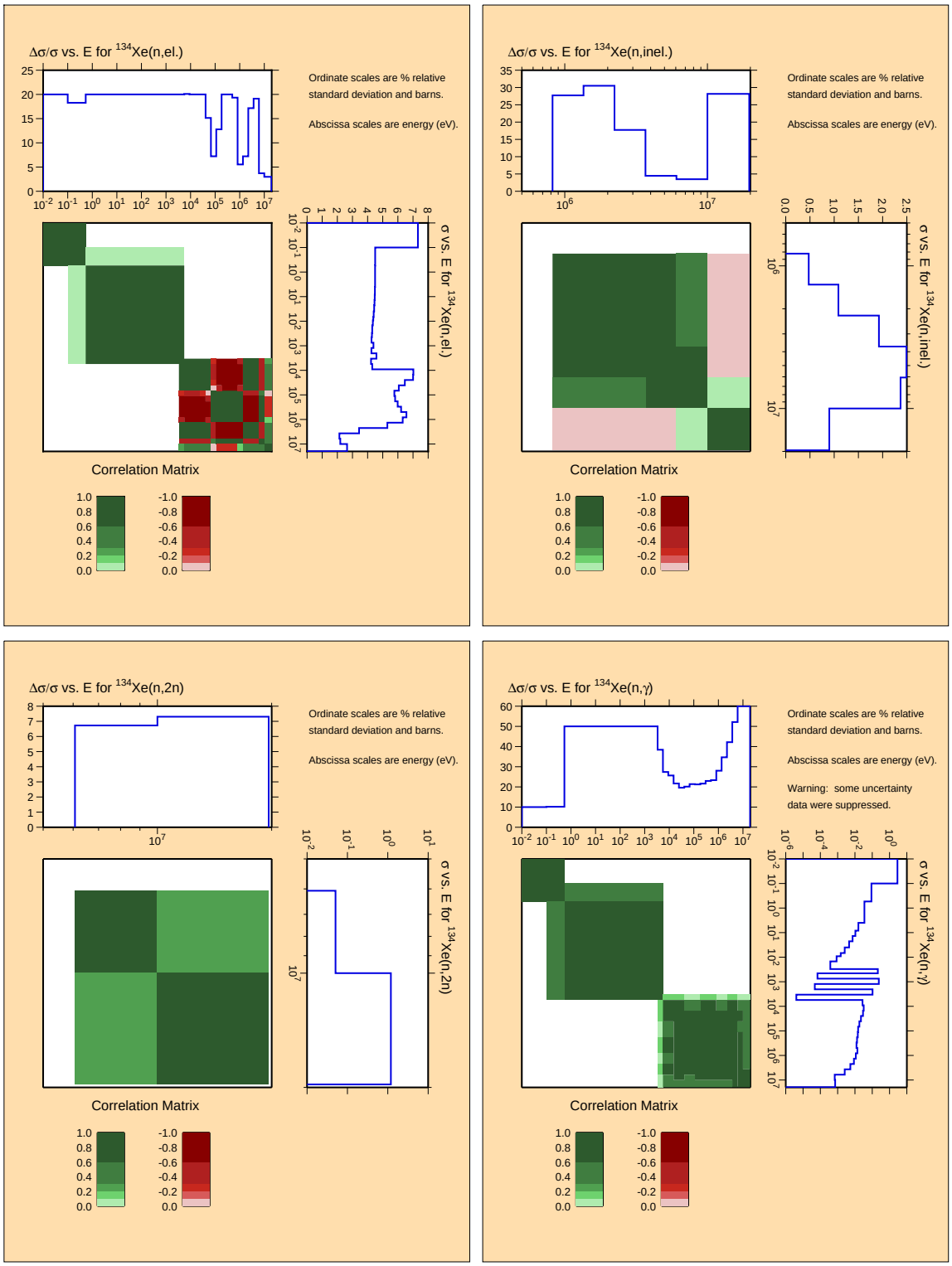

Figure B.49: Covariances for fission product ^{134}Xe.

^{133}Cs

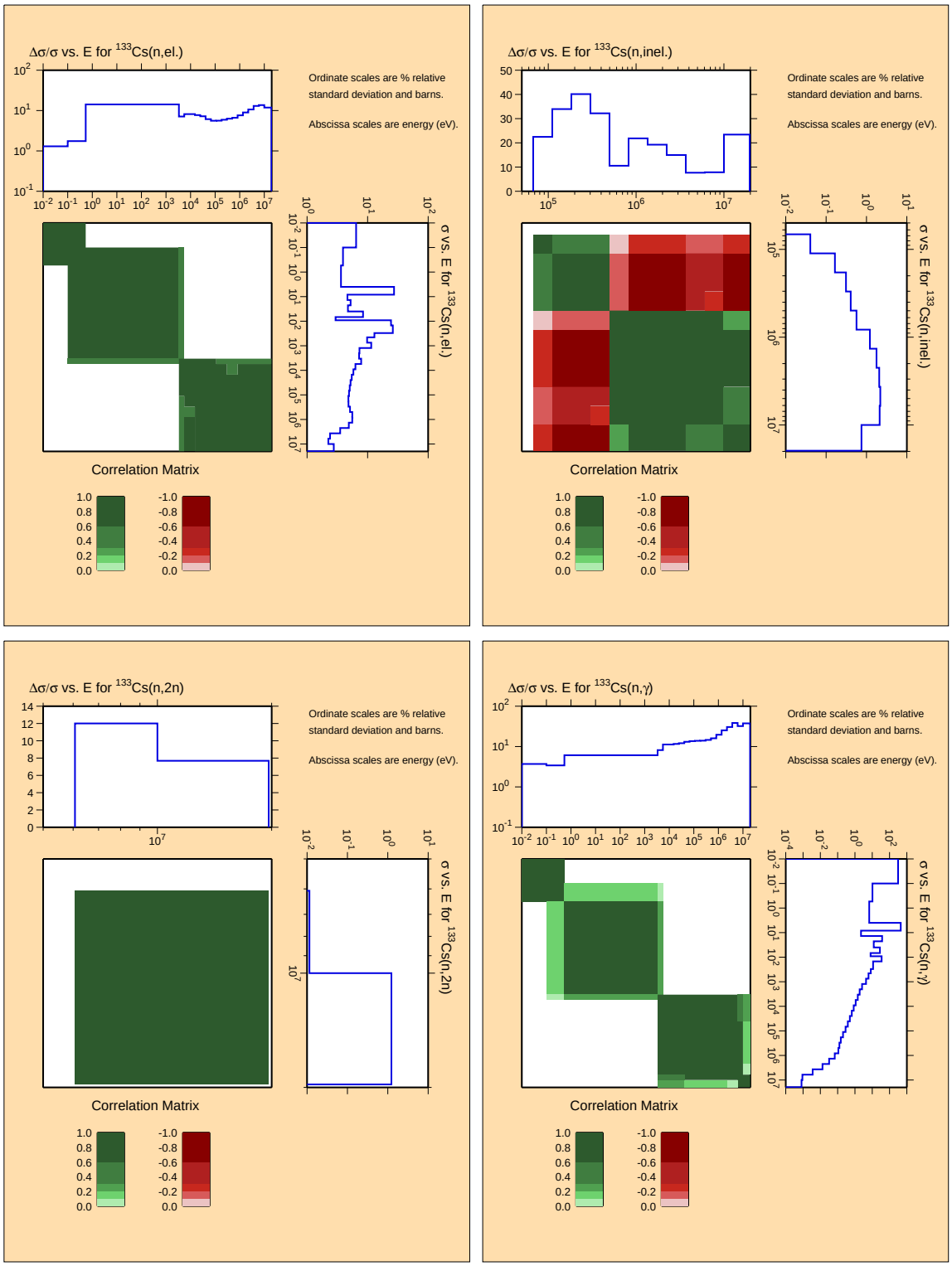

Figure B.50: Covariances for fission product ^{133}Cs.

^{135}Cs

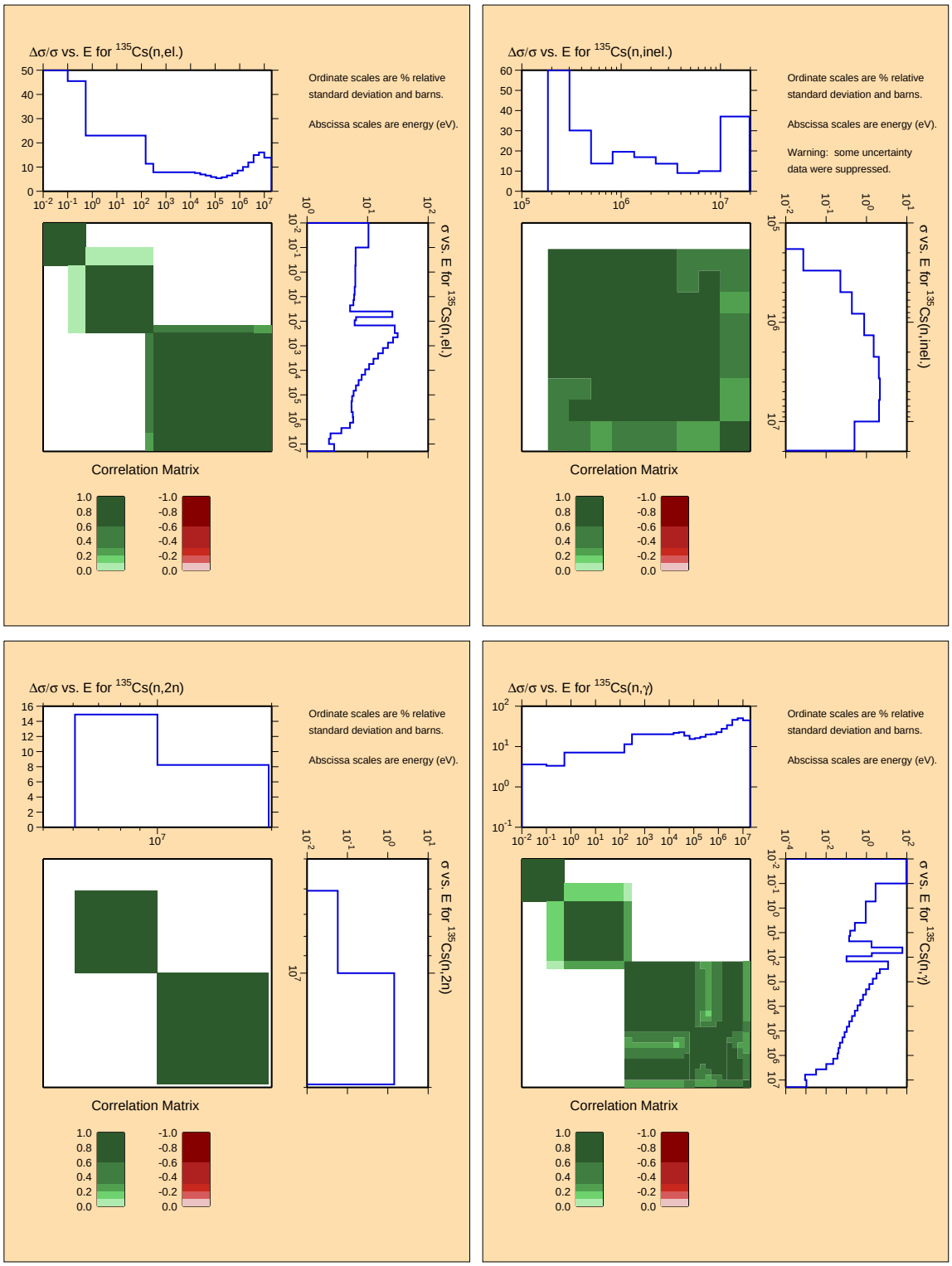

Figure B.51: Covariances for fission product ^{135}Cs.

^{139}La

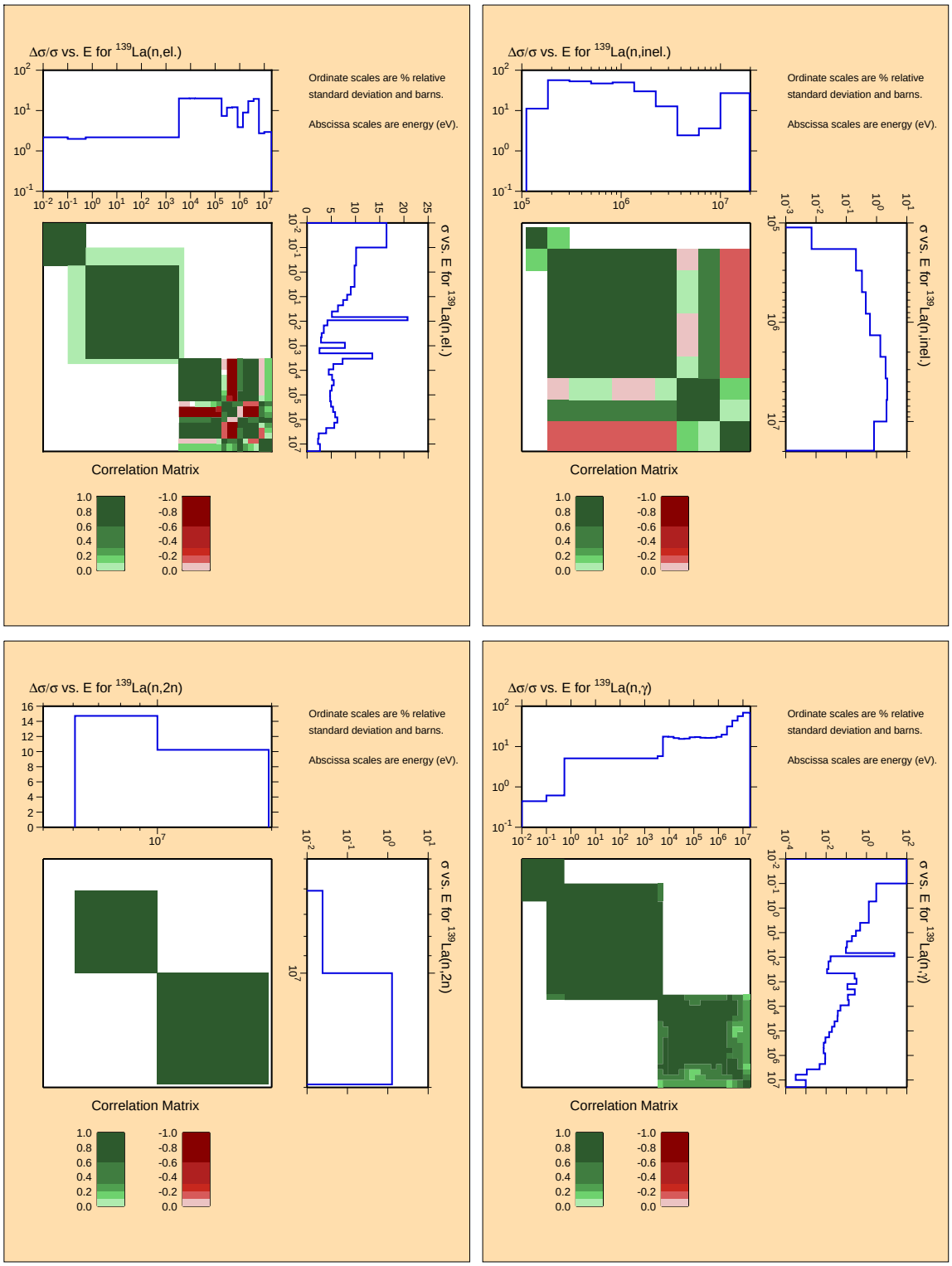

Figure B.52: Covariances for fission product ^{139}La.

^{141}Ce

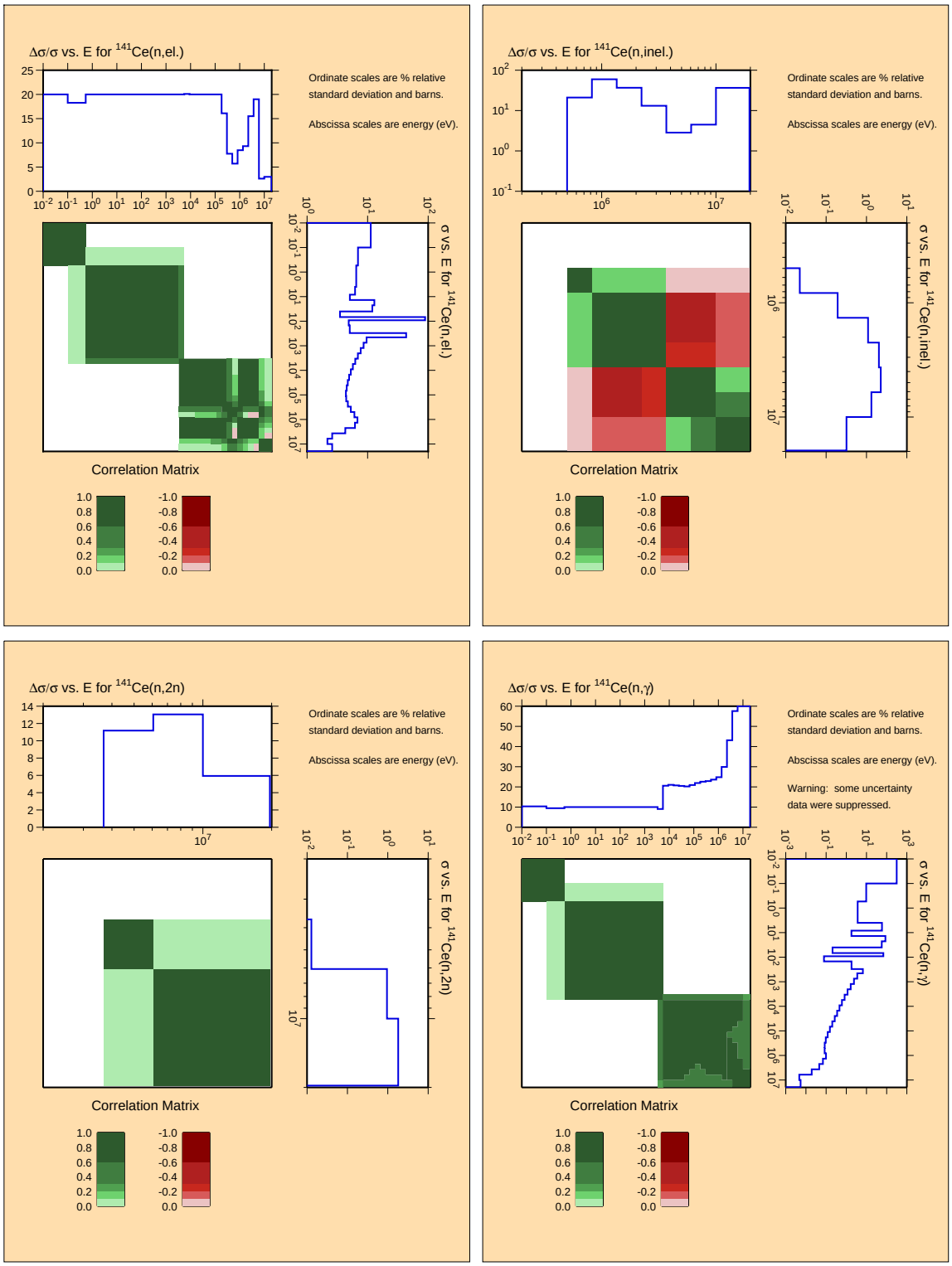

Figure B.53: Covariances for fission product ^{141}Ce.

^{141}Pr

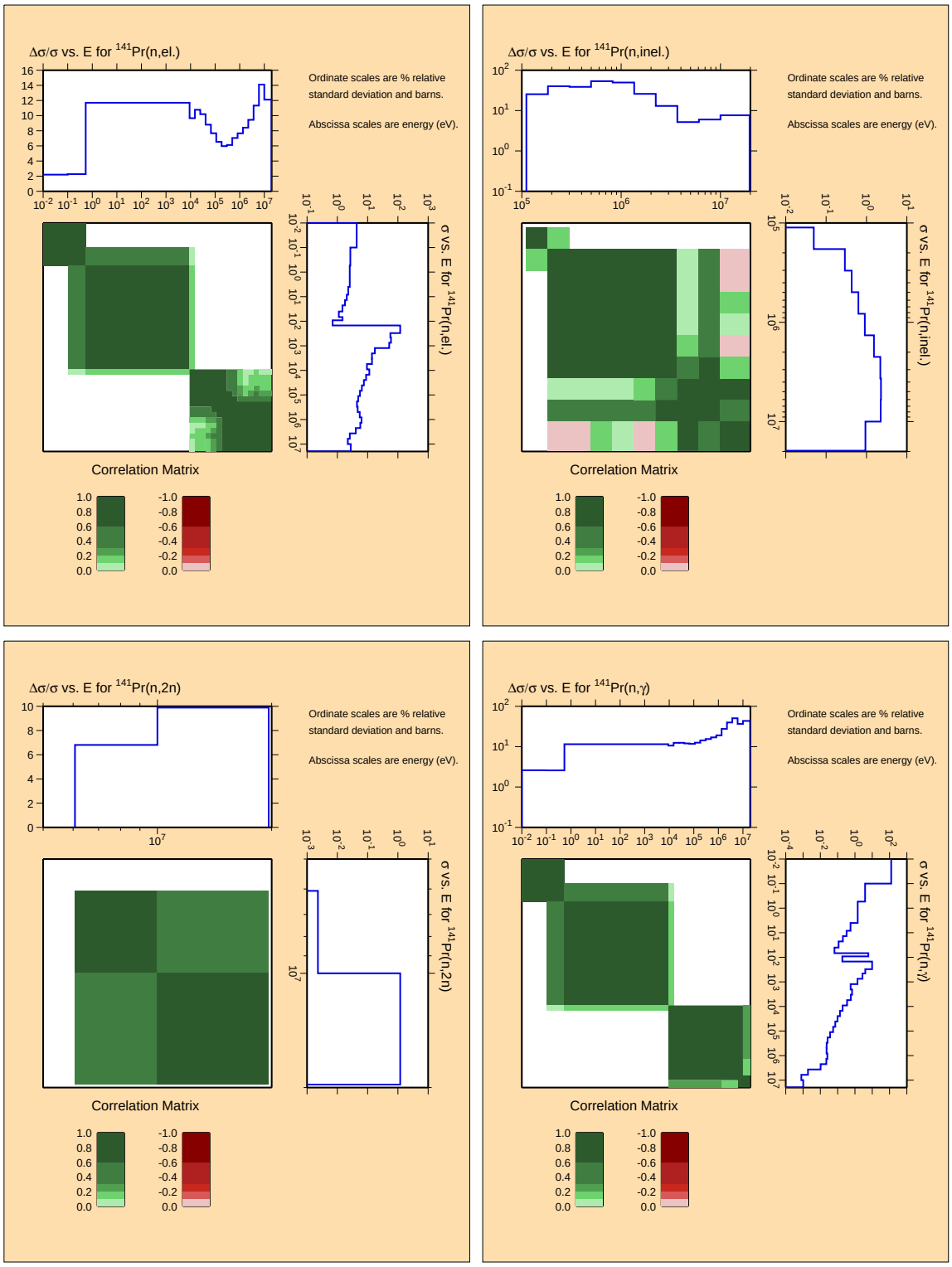

Figure B.54: Covariances for fission product ^{141}Pr.

^{143}Nd

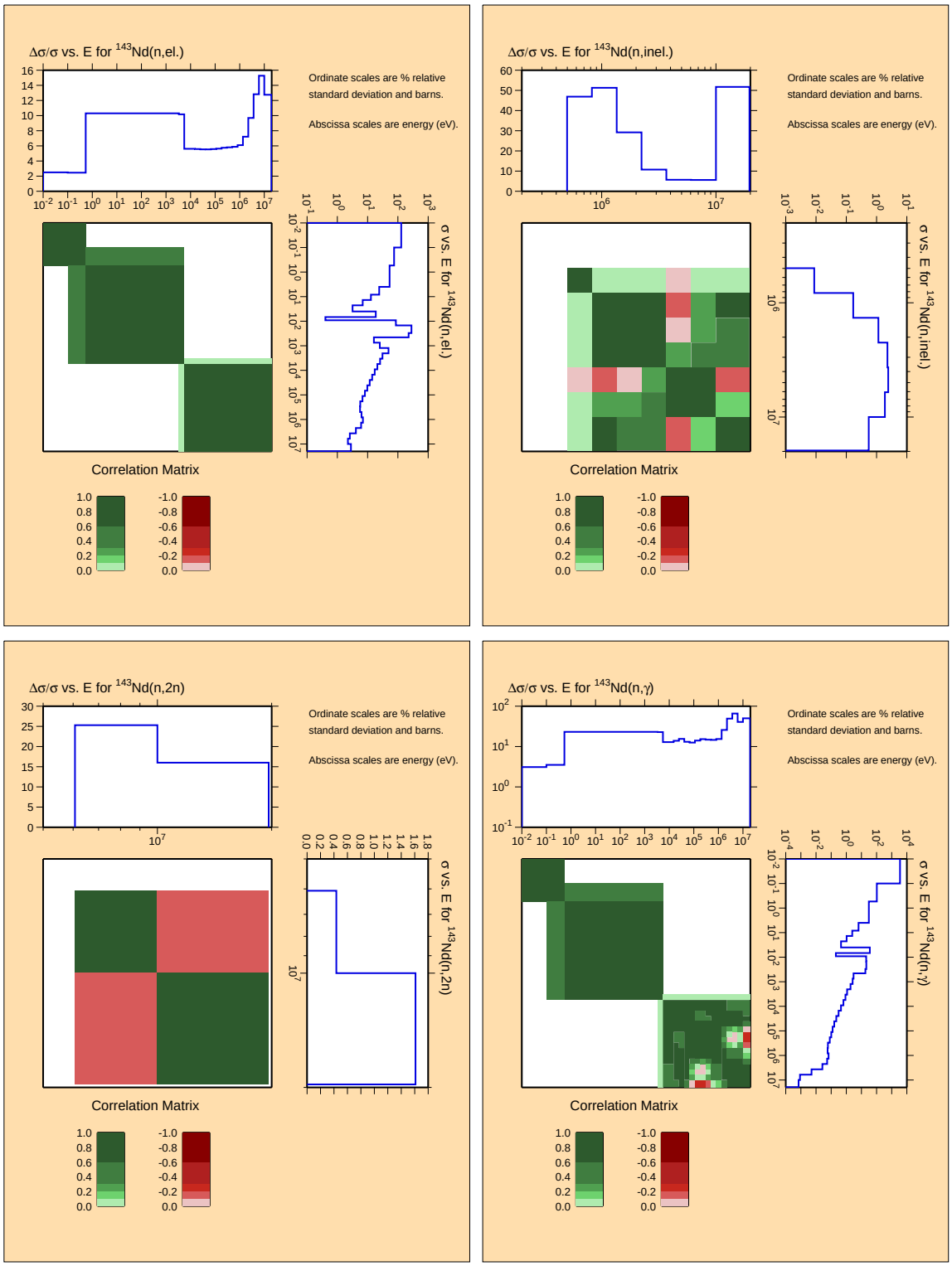

Figure B.55: Covariances for fission product ^{143}Nd.

^{145}Nd

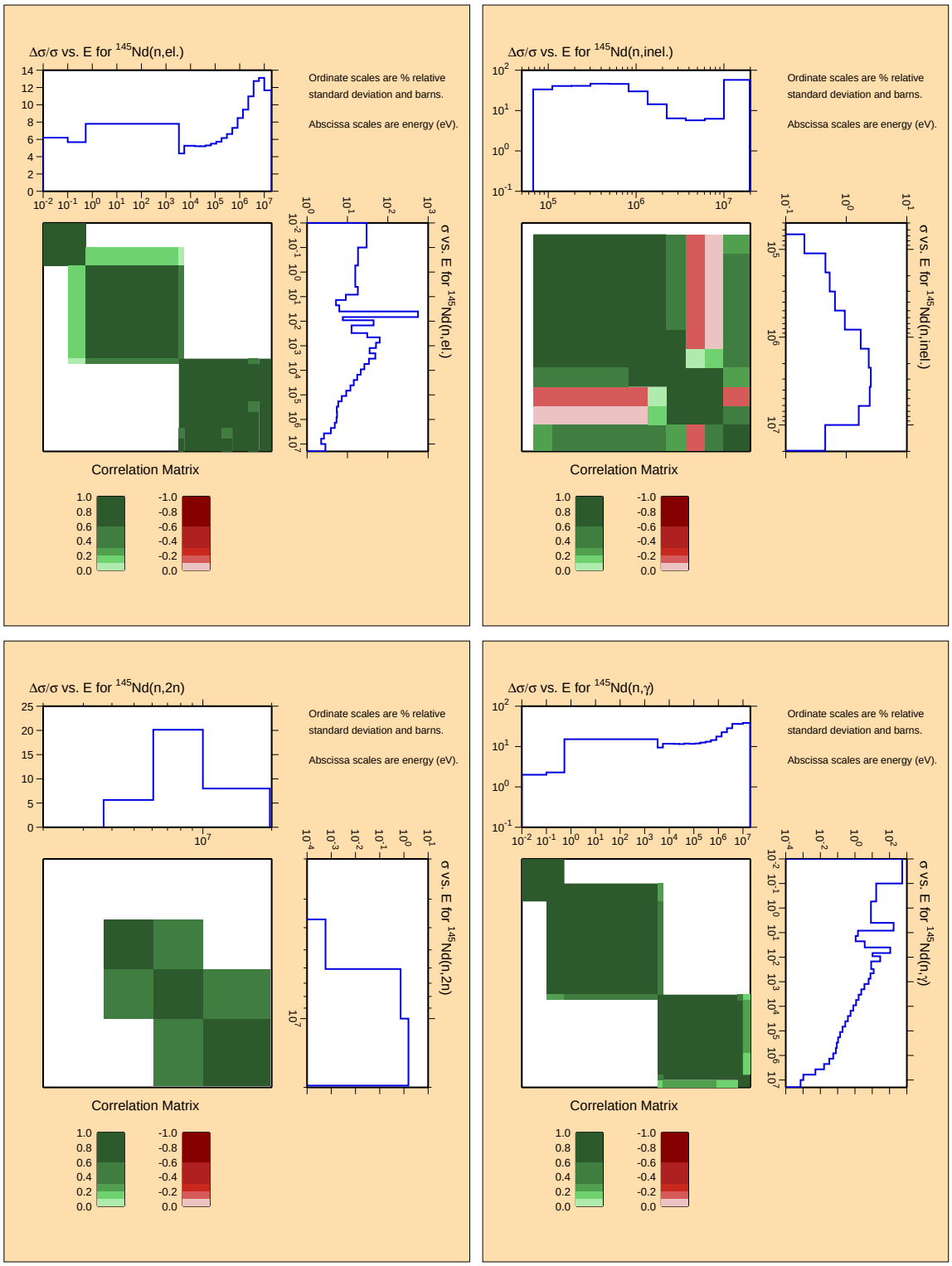

Figure B.56: Covariances for fission product ^{145}Nd.

^{146}Nd

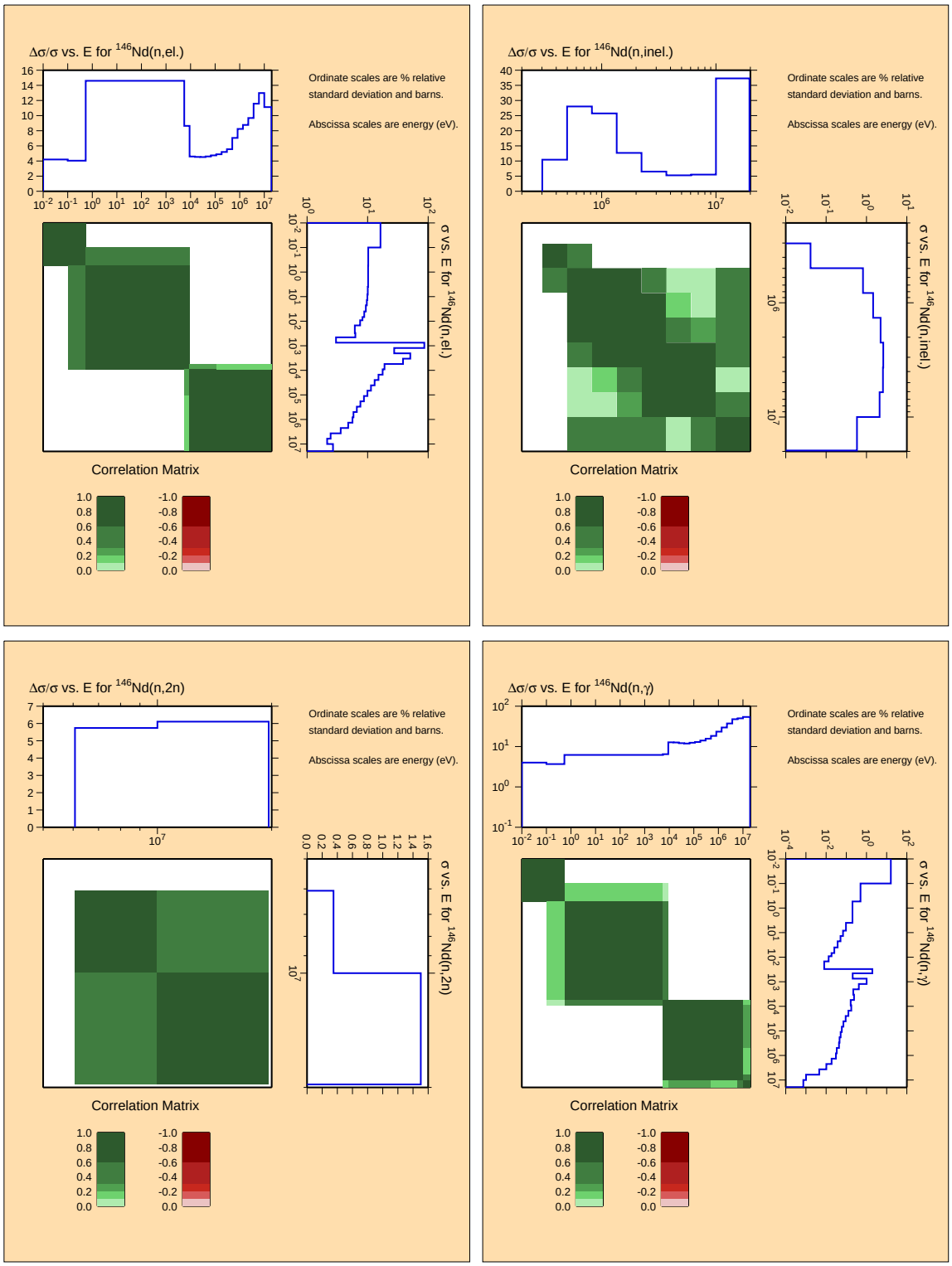

Figure B.57: Covariances for fission product ^{146}Nd.

^{148}Nd

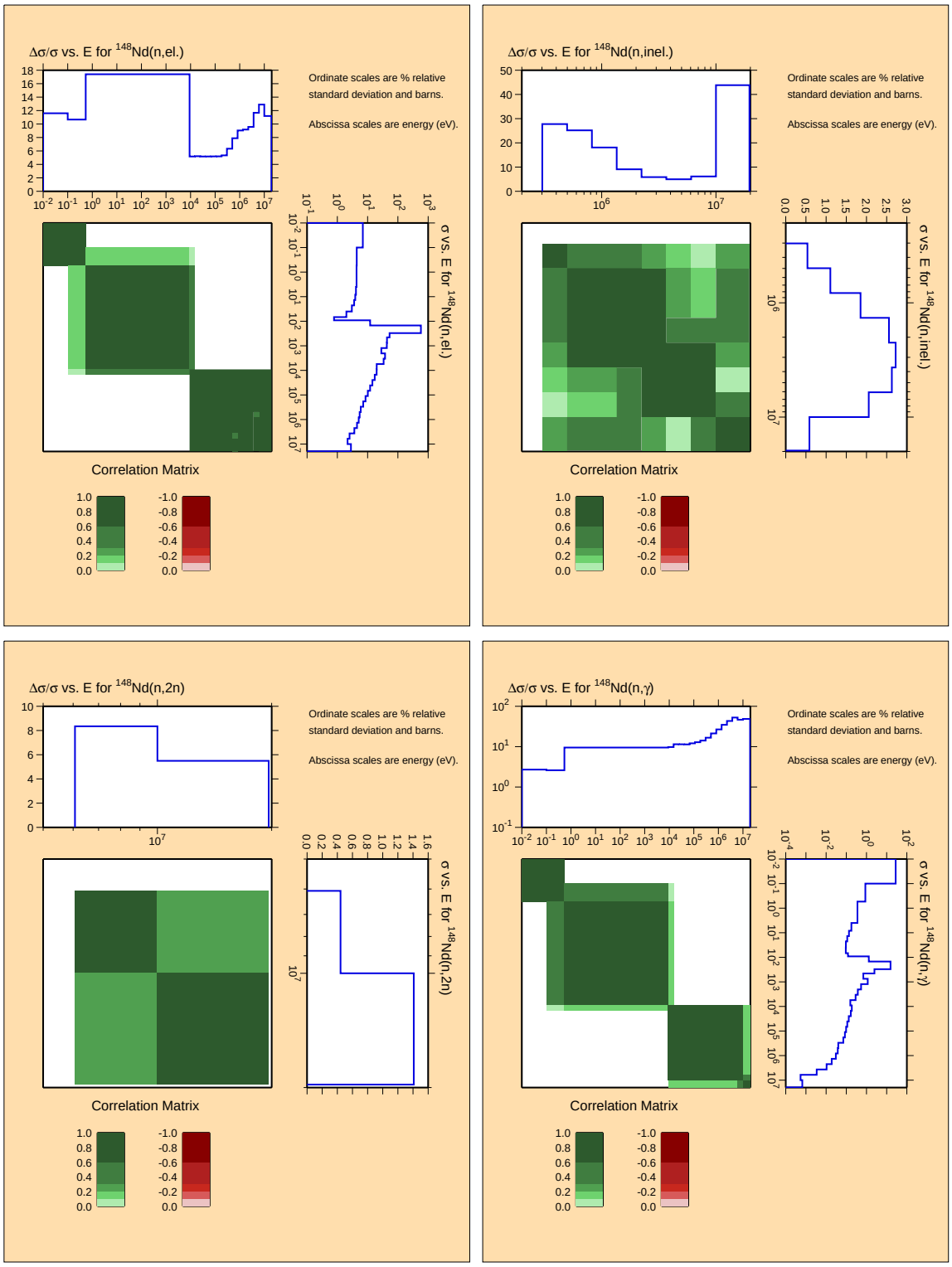

Figure B.58: Covariances for fission product ^{148}Nd.

^{147}Pm

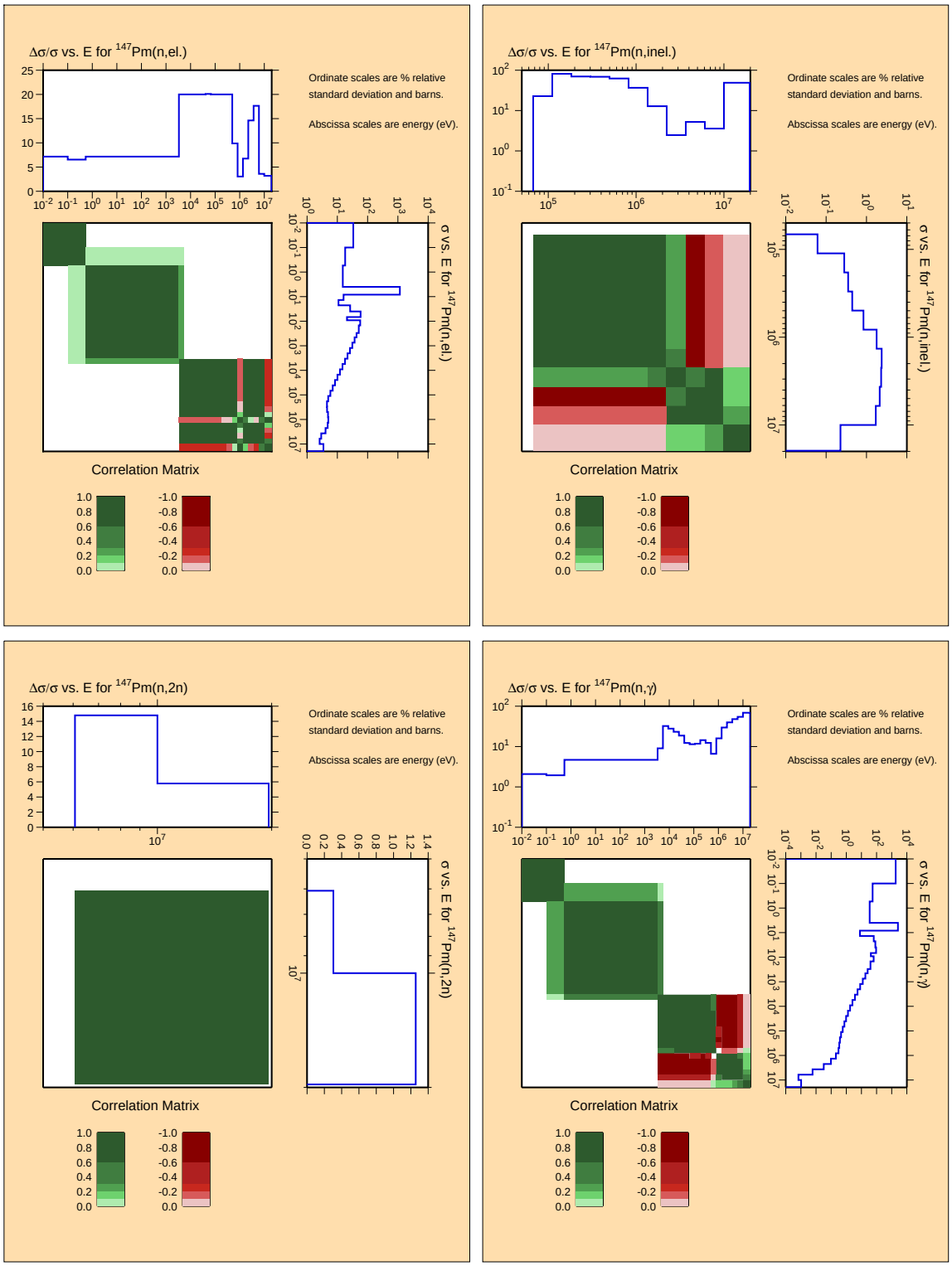

Figure B.59: Covariances for fission product ^{147}Pm.

^{149}Sm

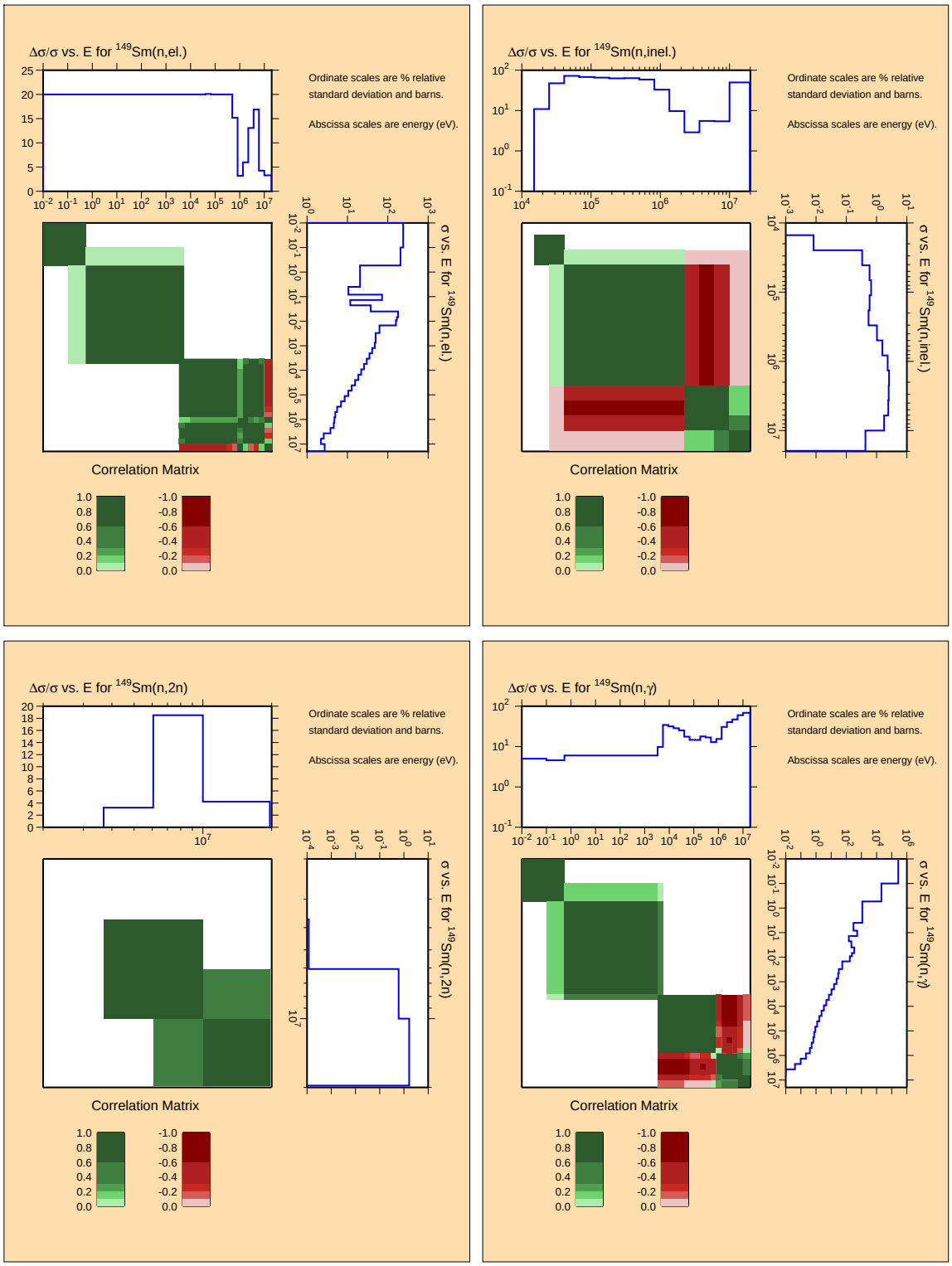

Figure B.60: Covariances for fission product ^{149}Sm.

^{151}Sm

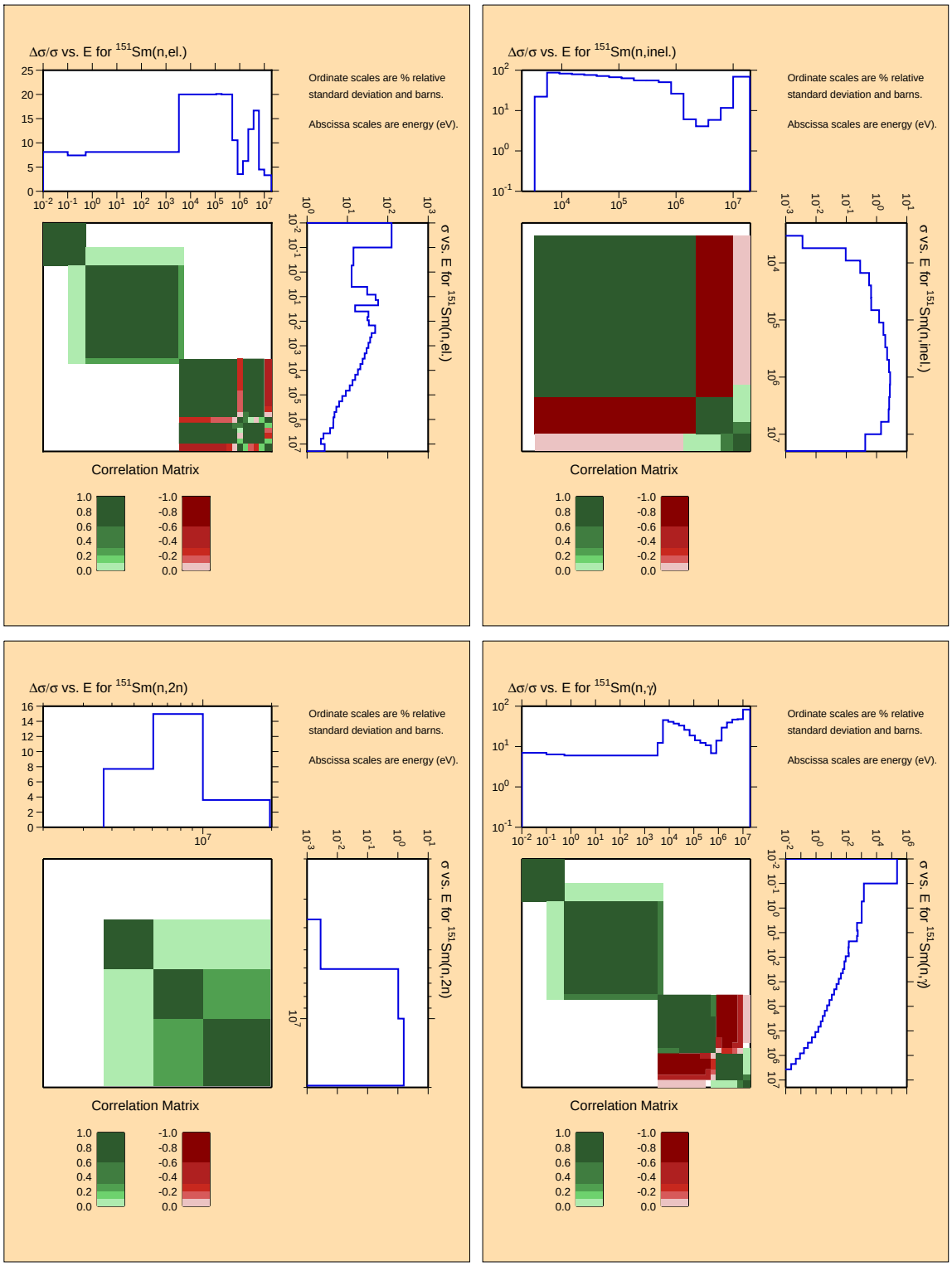

Figure B.61: Covariances for fission product ^{151}Sm.

^{152}Sm

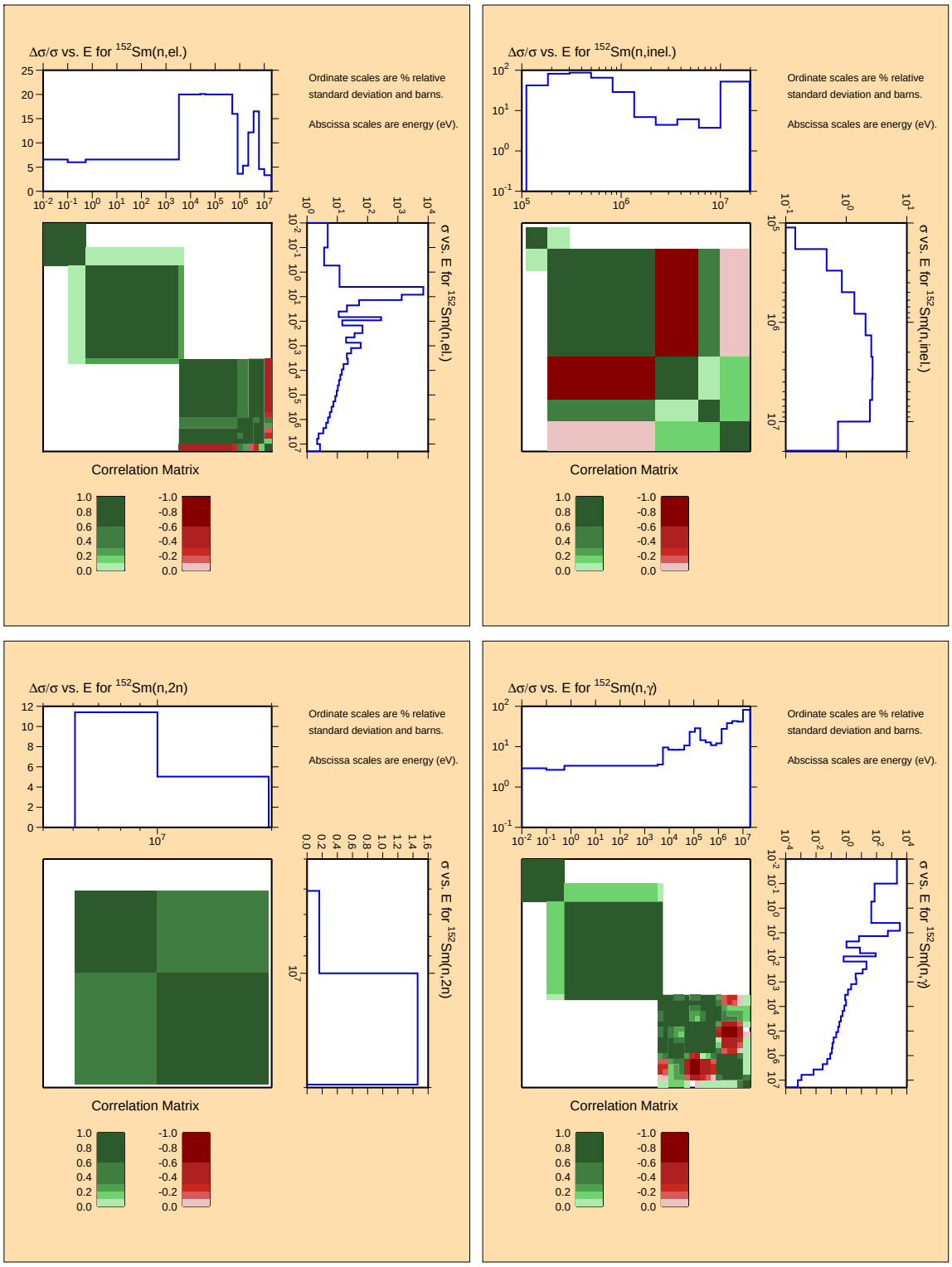

Figure B.62: Covariances for fission product ^{152}Sm.

^{153}Eu

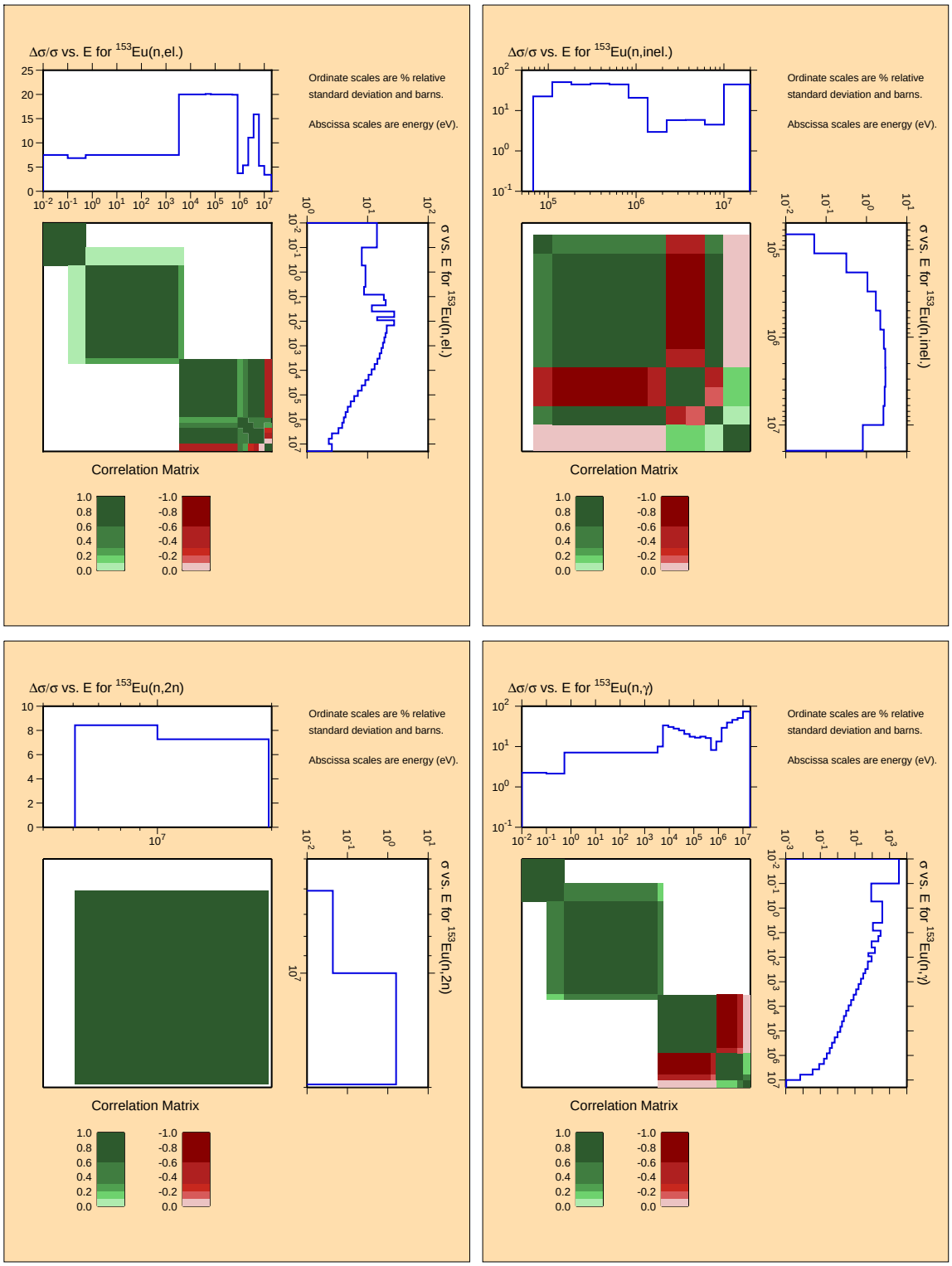

Figure B.63: Covariances for fission product ^{153}Eu.

^{155}Eu

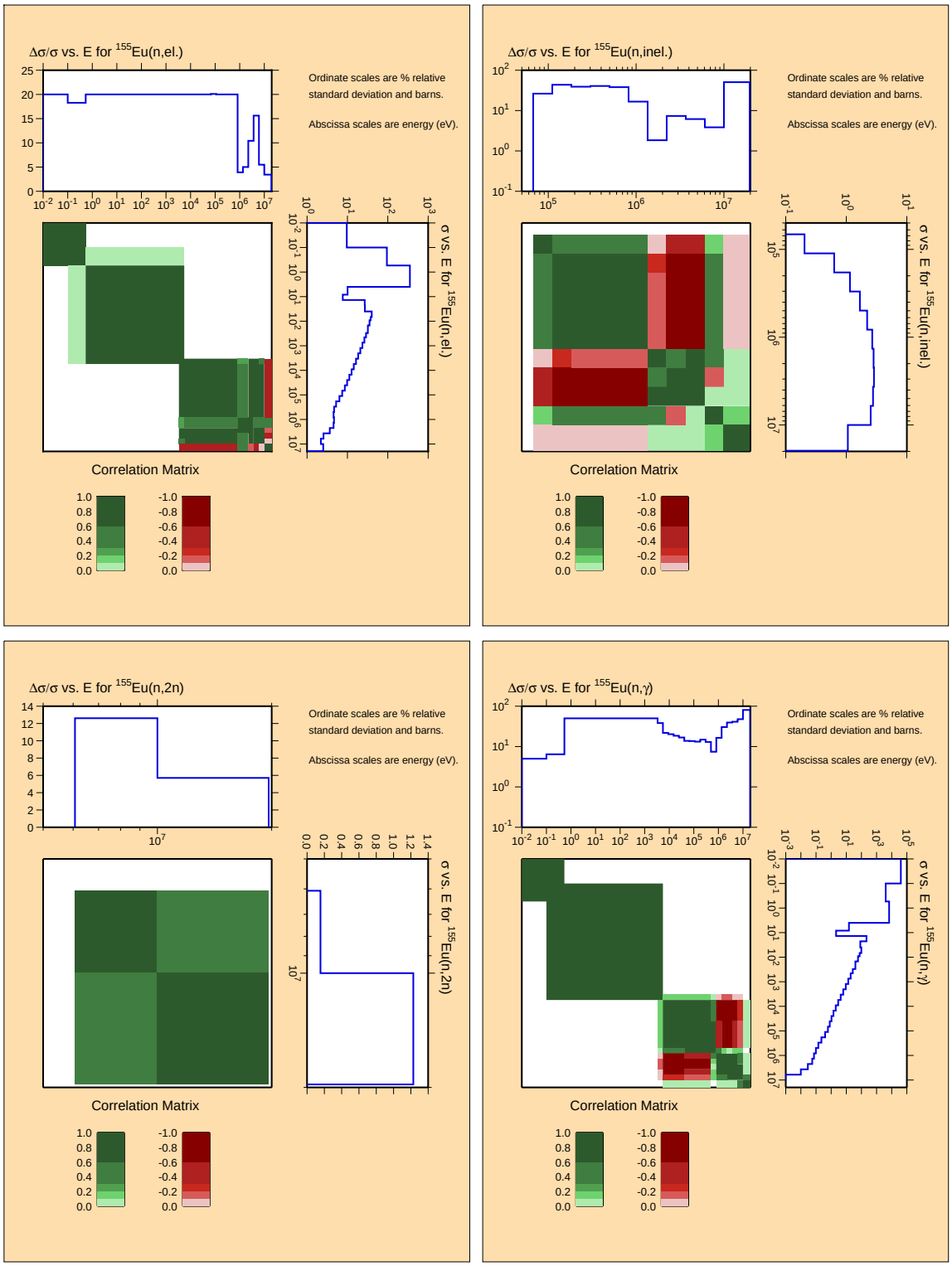

Figure B.64: Covariances for fission product ^{155}Eu.

^{155}Gd

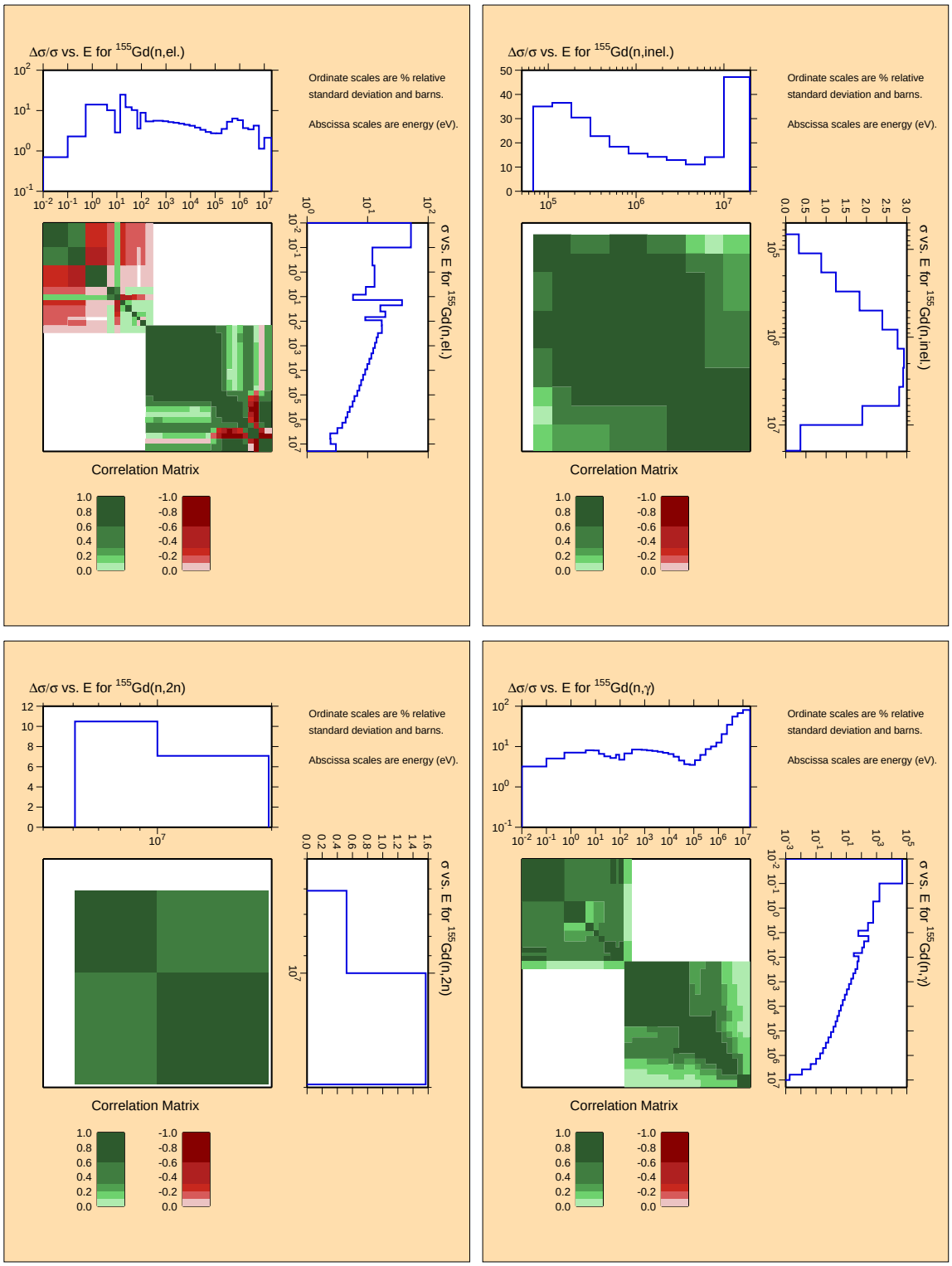

Figure B.65: Covariances for structural material ^{155}Gd.

^{156}Gd

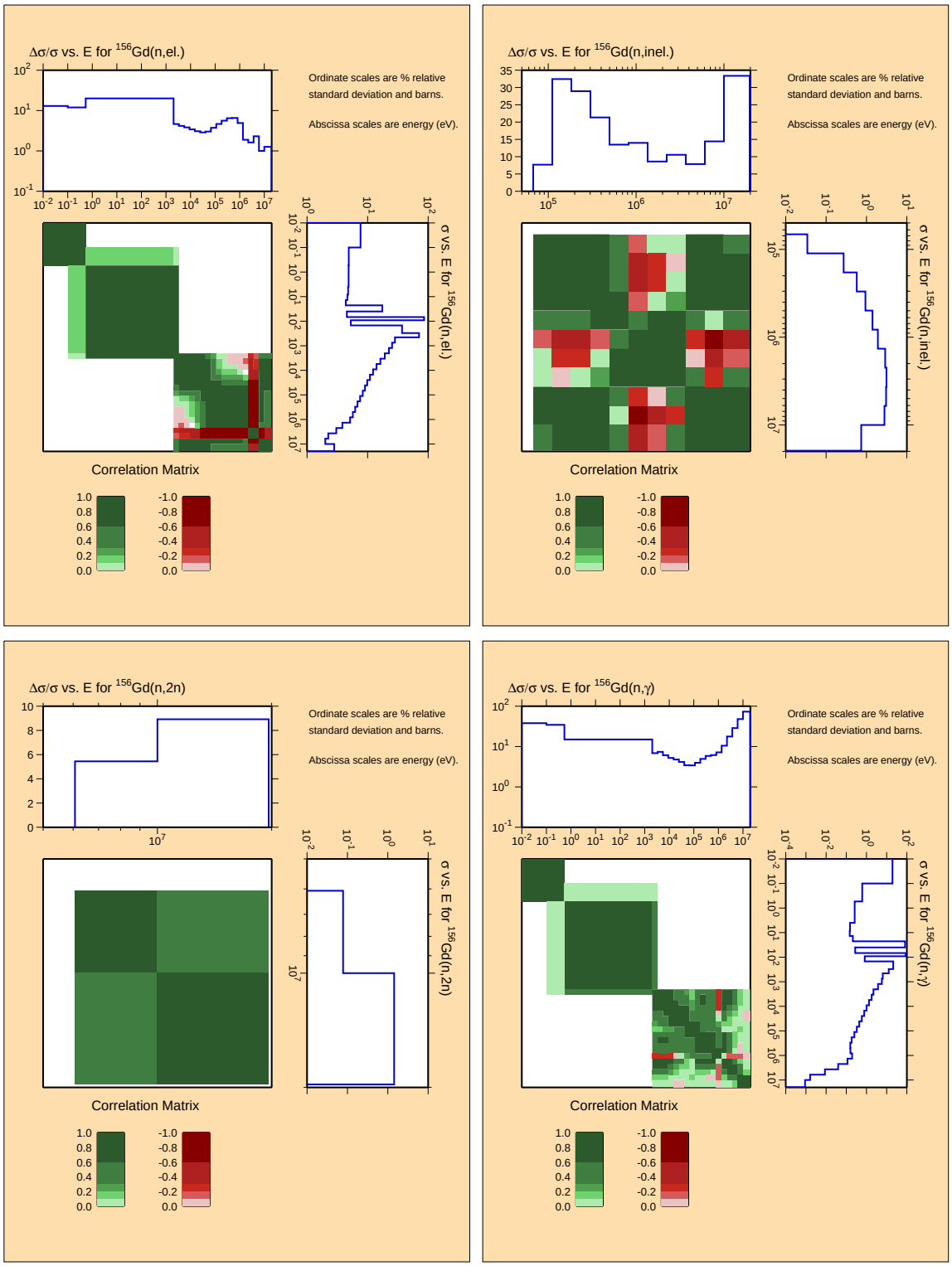

Figure B.66: Covariances for structural material ^{156}Gd.

^{157}Gd

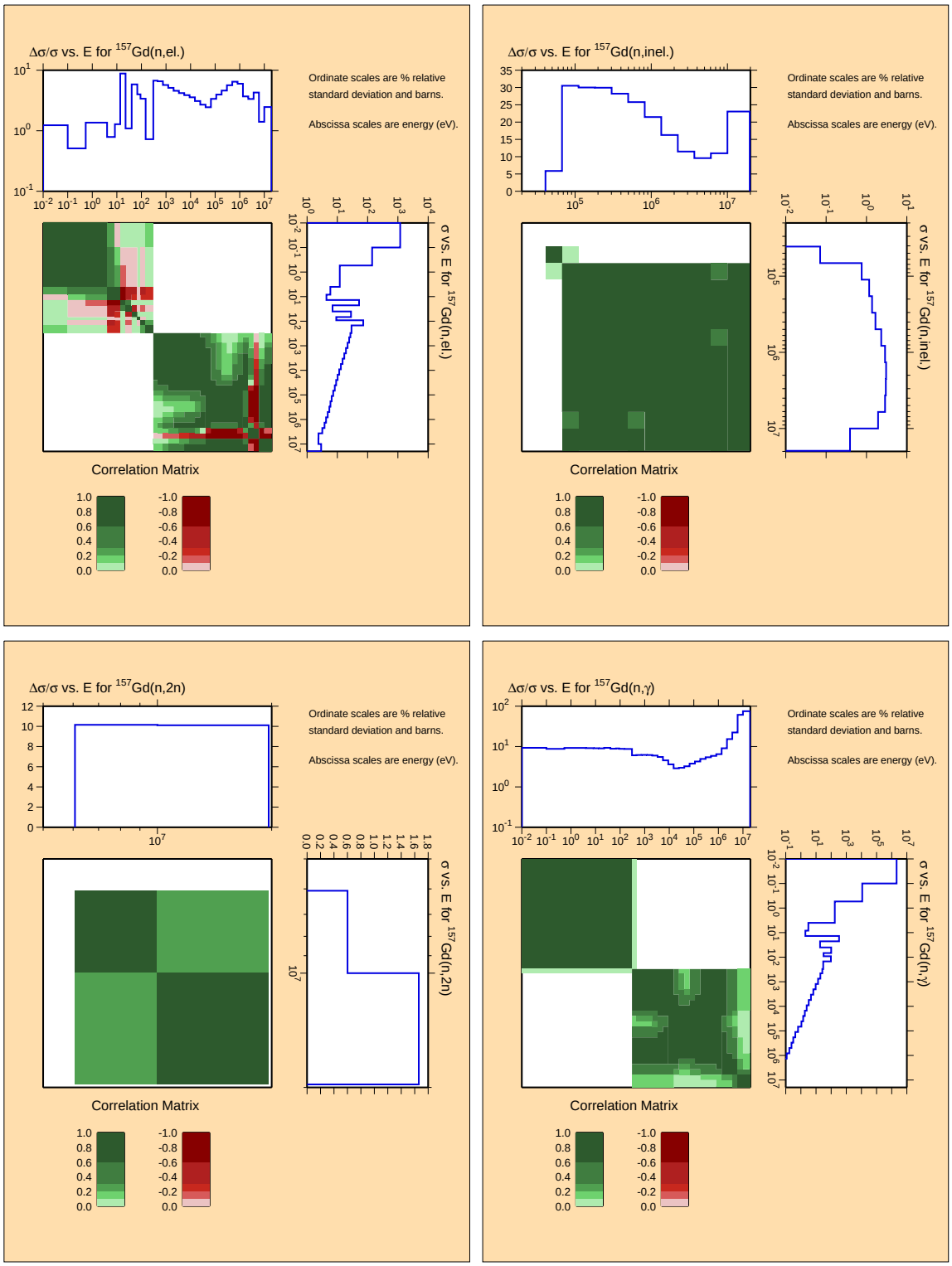

Figure B.67: Covariances for structural material ^{157}Gd.

^{158}Gd

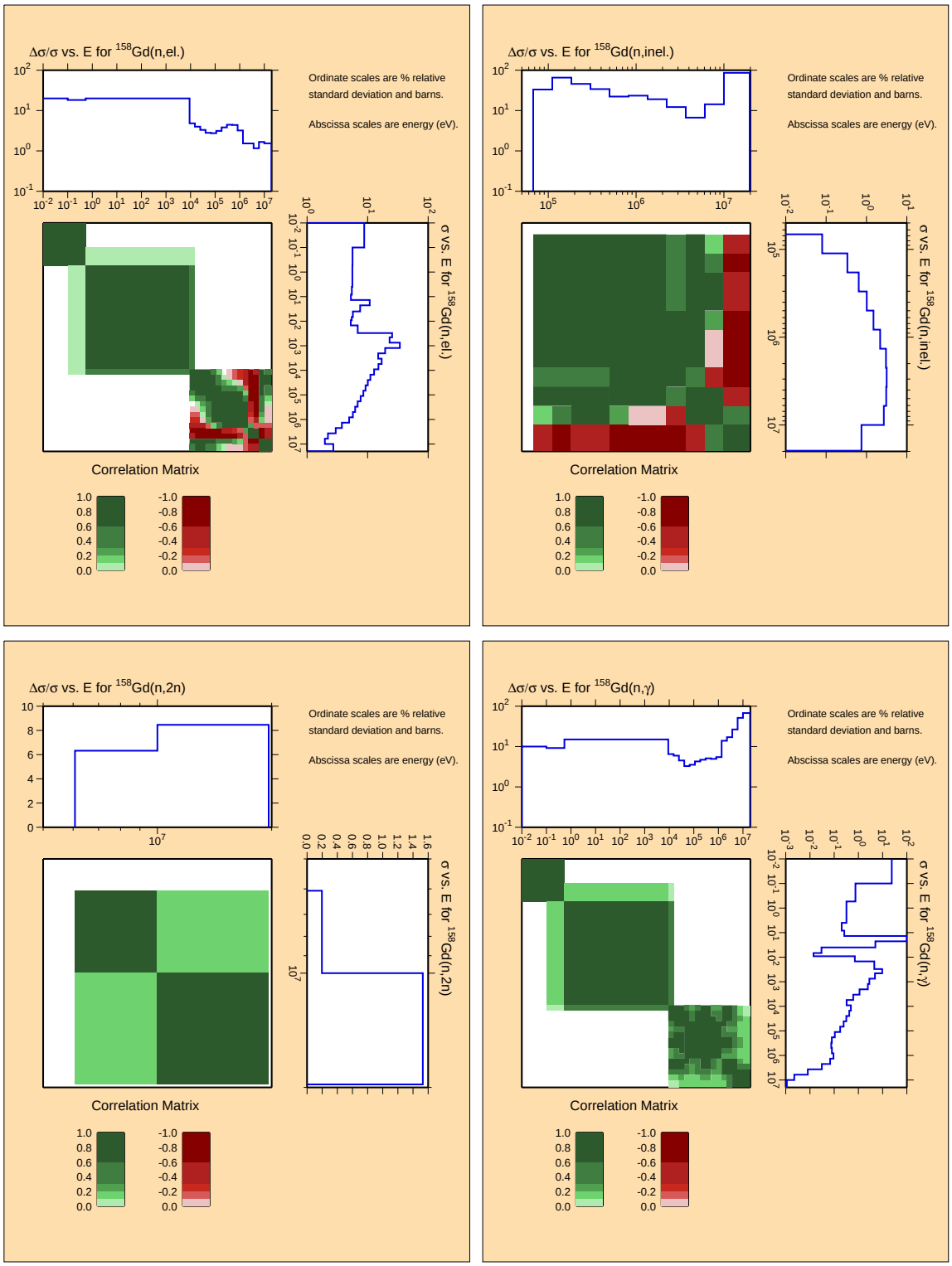

Figure B.68: Covariances for structural material ^{158}Gd.

^{160}Gd

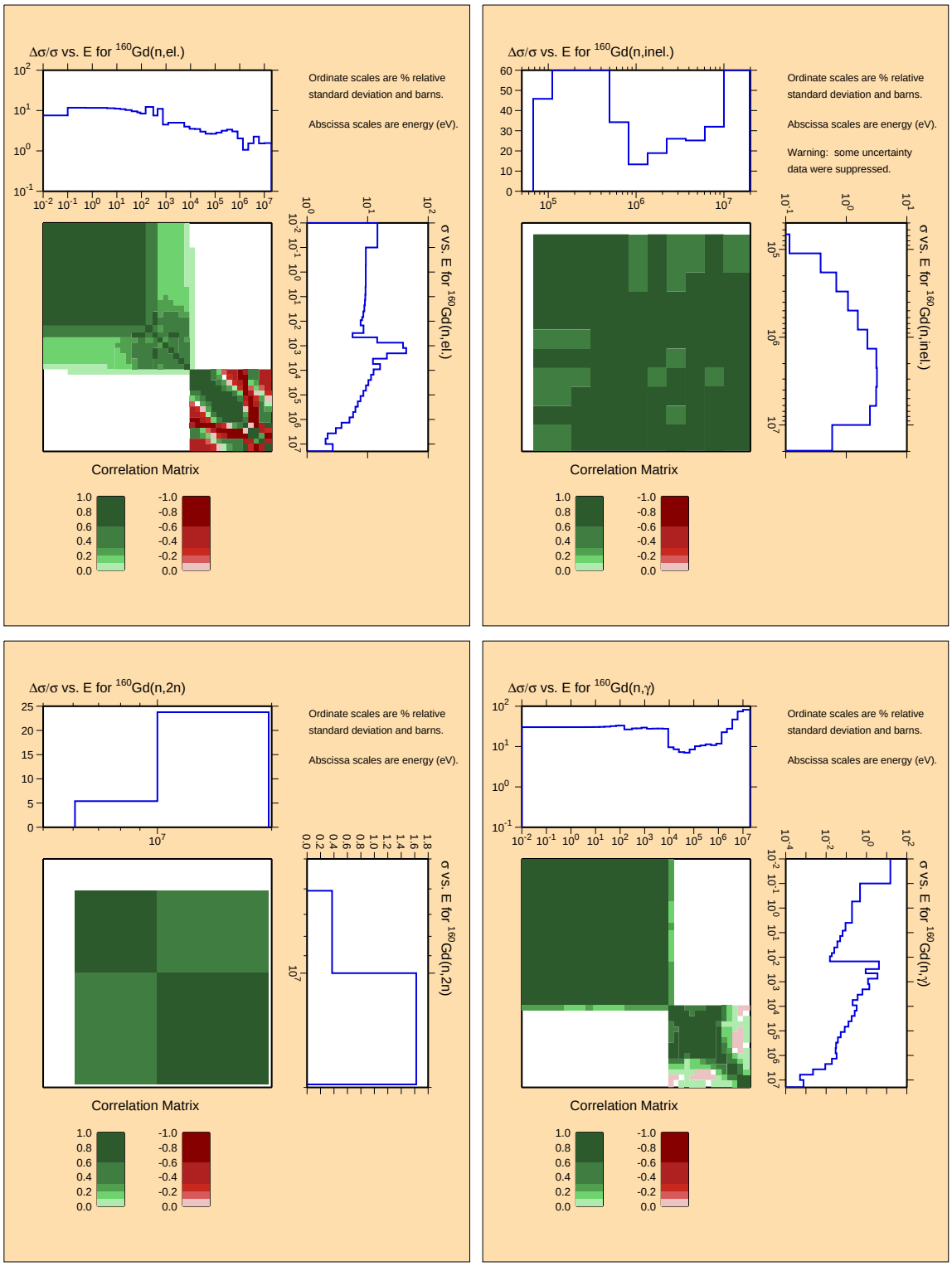

Figure B.69: Covariances for structural material ^{160}Gd.

^{166}Er

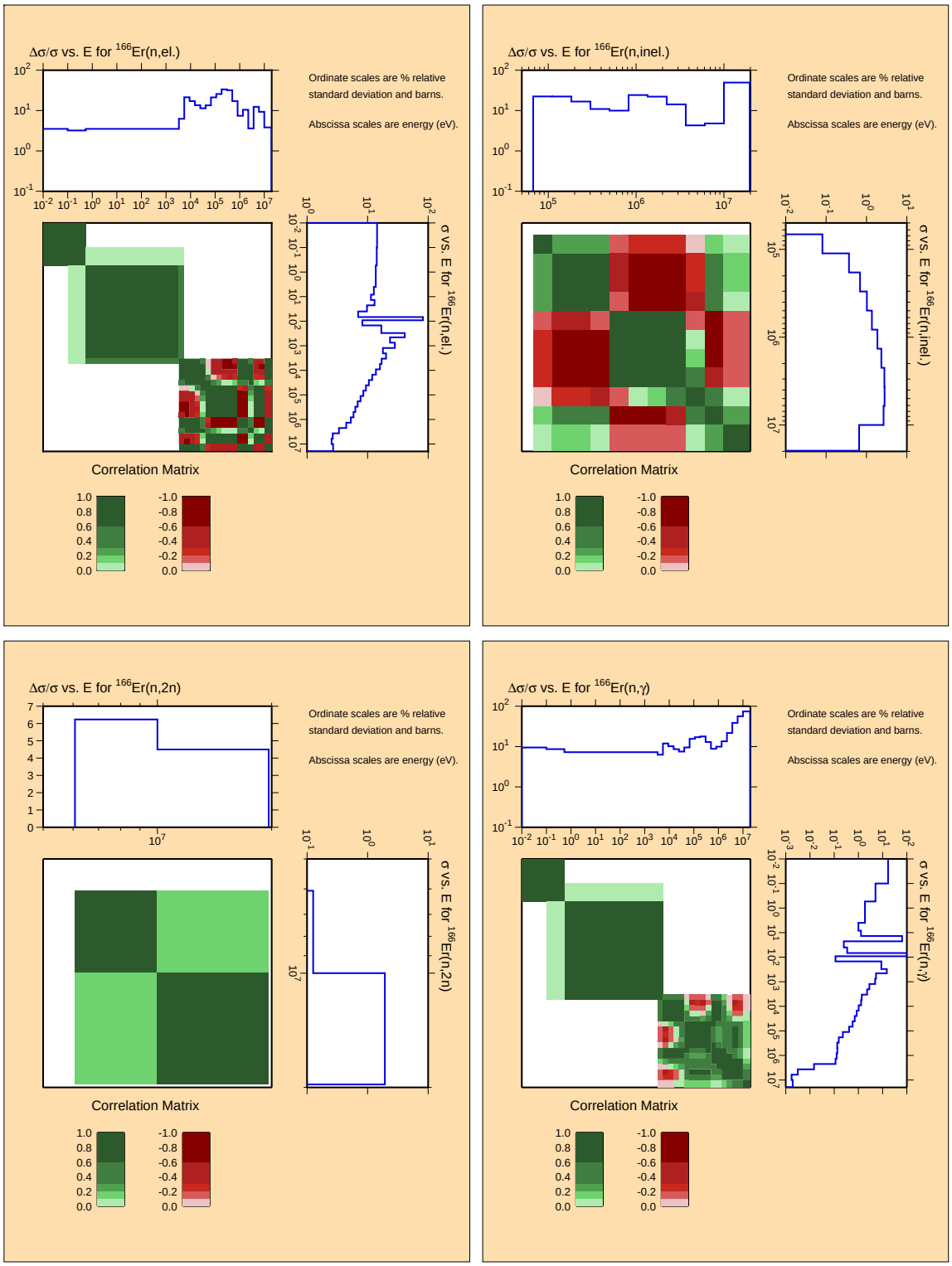

Figure B.70: Covariances for structural material ^{166}Er.

^{167}Er

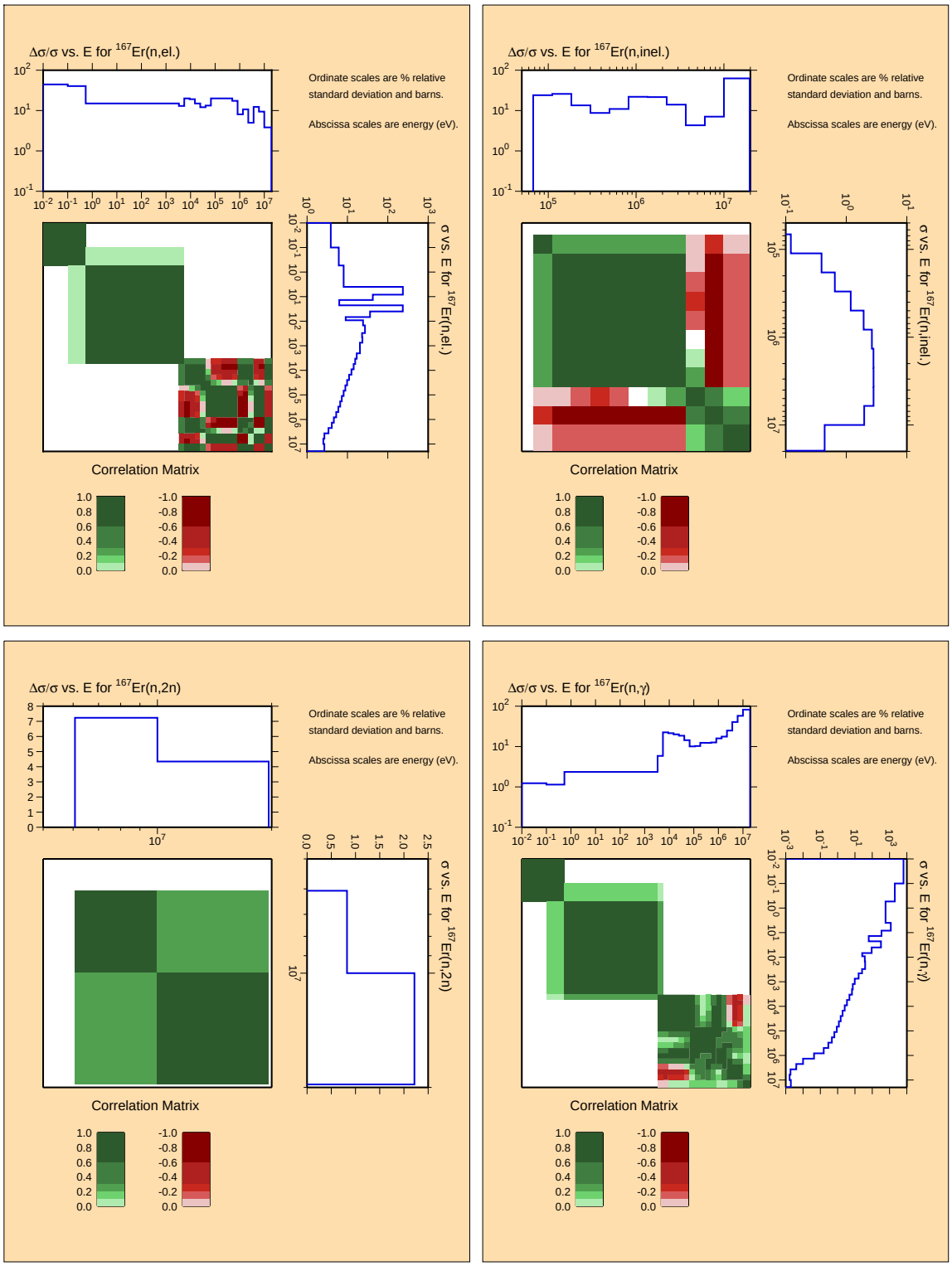

Figure B.71: Covariances for structural material ^{167}Er.

^{168}Er

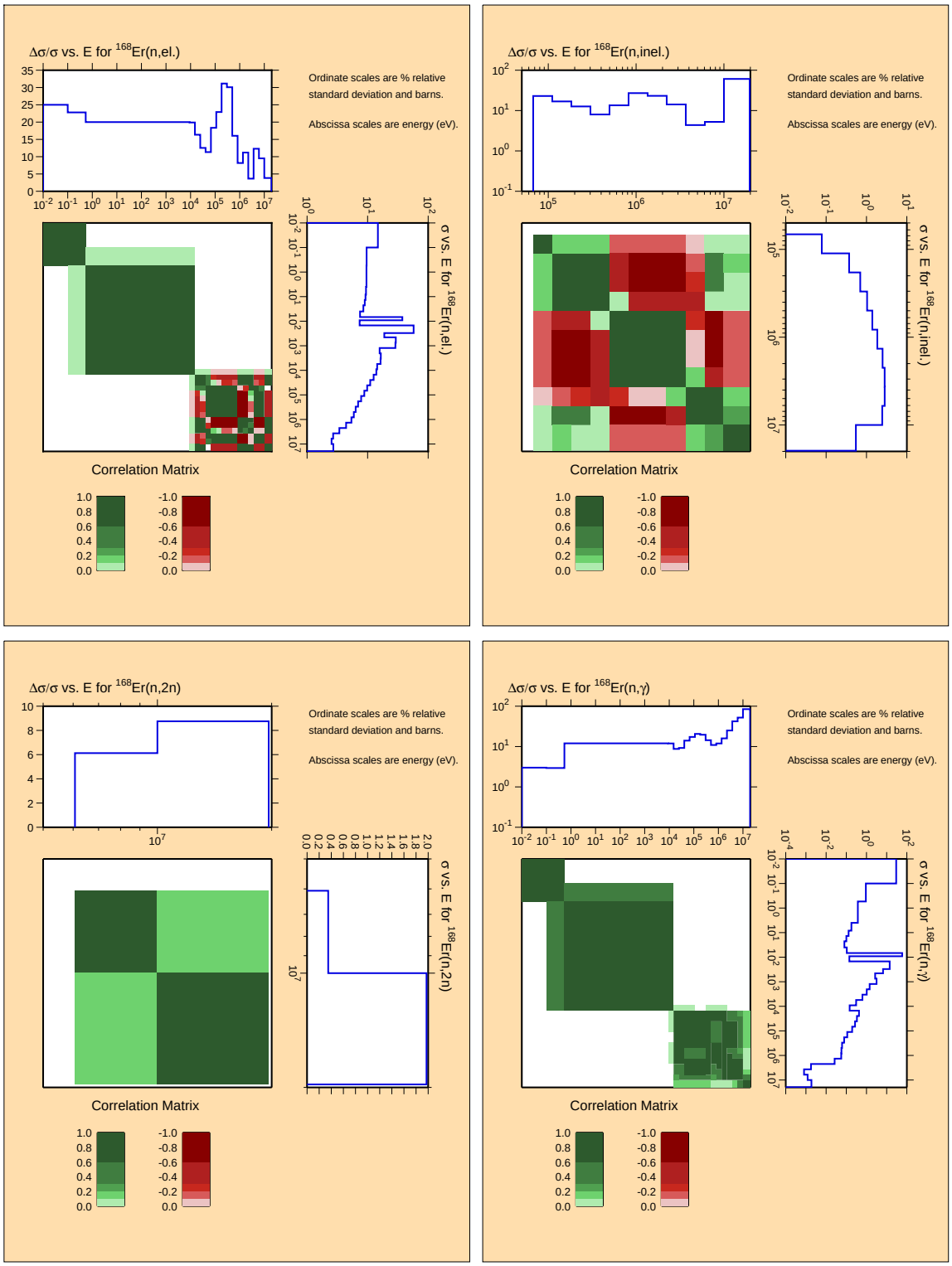

Figure B.72: Covariances for structural material ^{168}Er.

^{170}Er

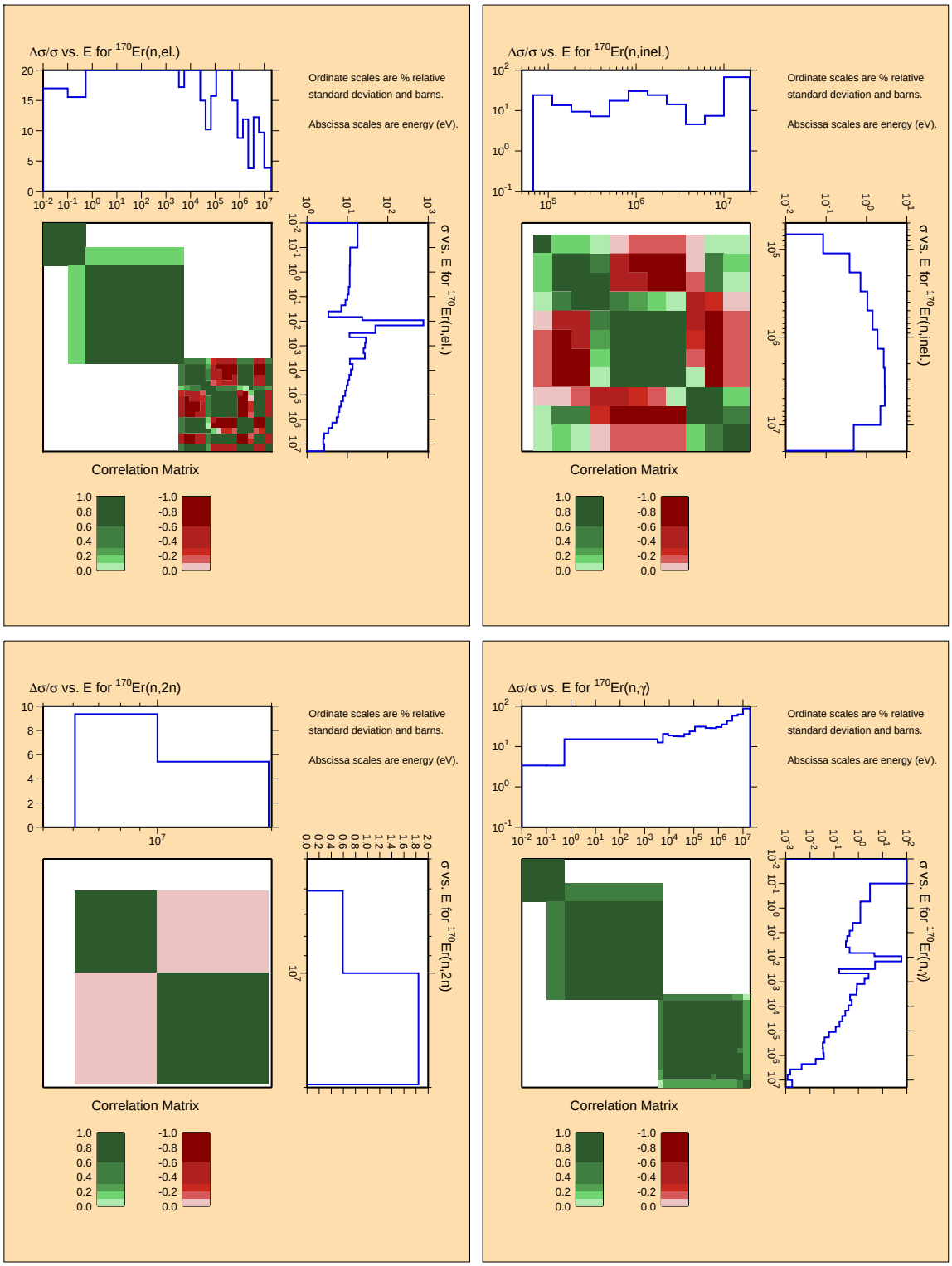

Figure B.73: Covariances for structural material ^{170}Er.

^{204}Pb

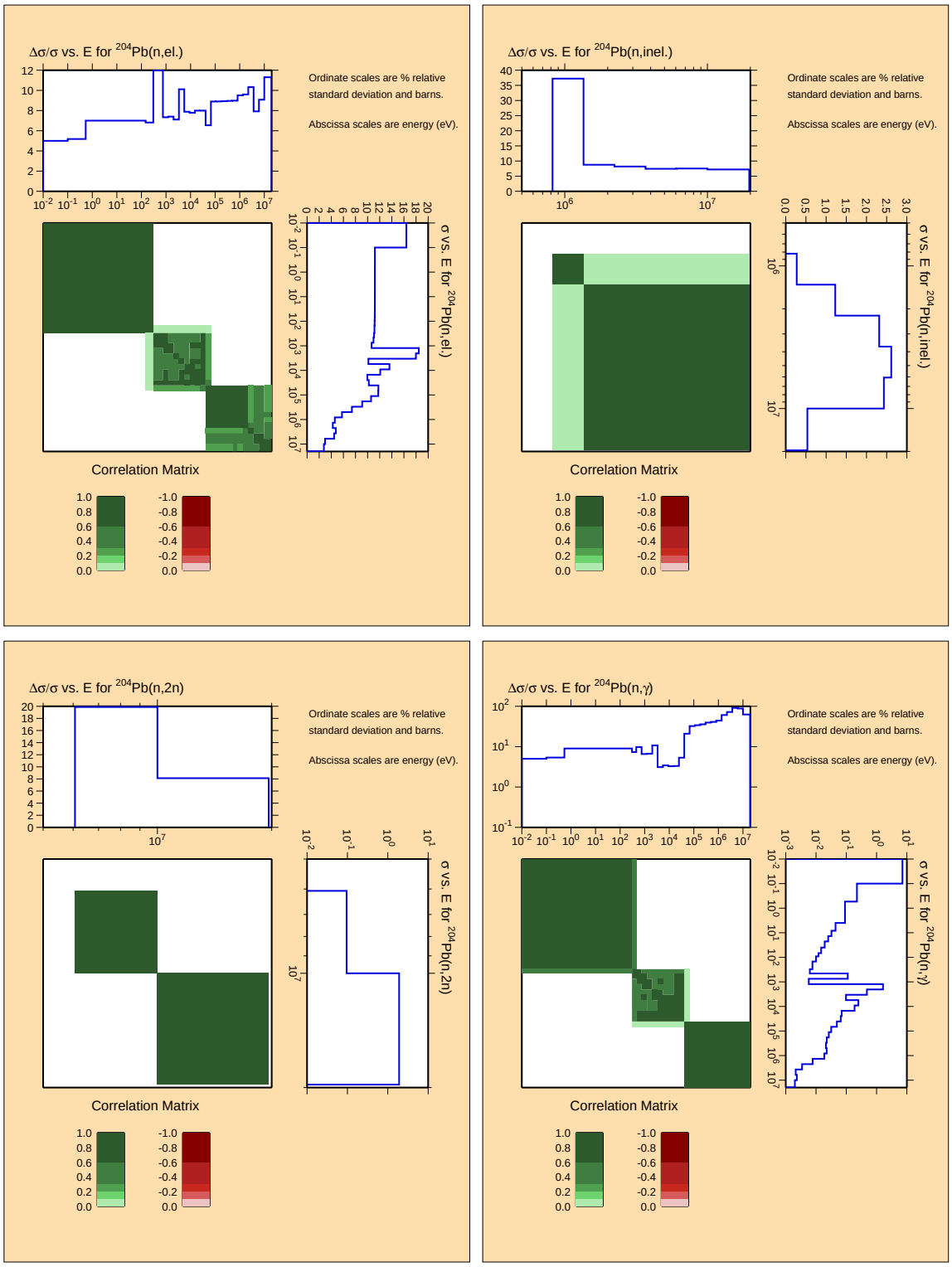

Figure B.74: Covariances for structural material ^{204}Pb.

^{206}Pb

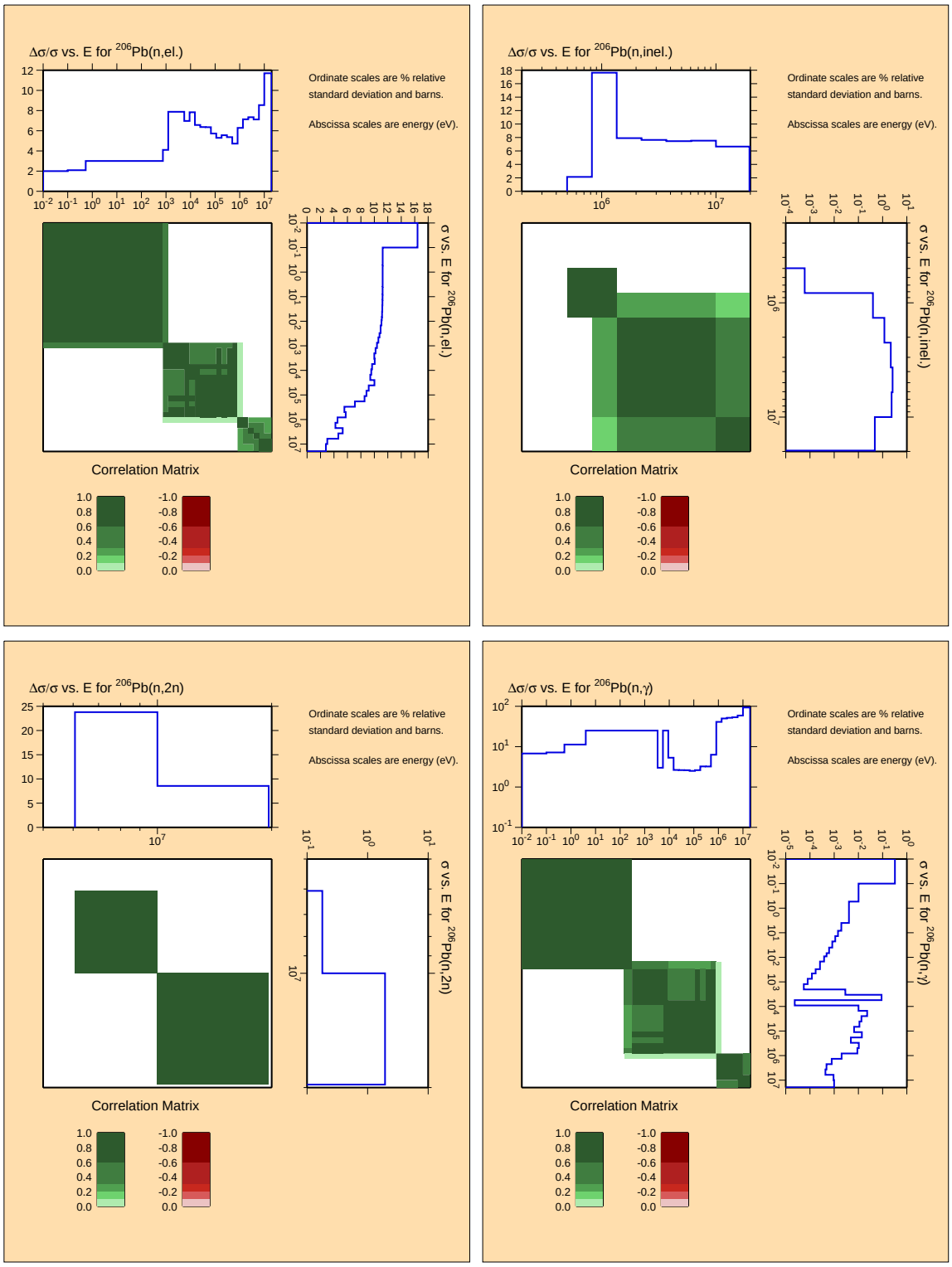

Figure B.75: Covariances for structural material ^{206}Pb.

^{207}Pb

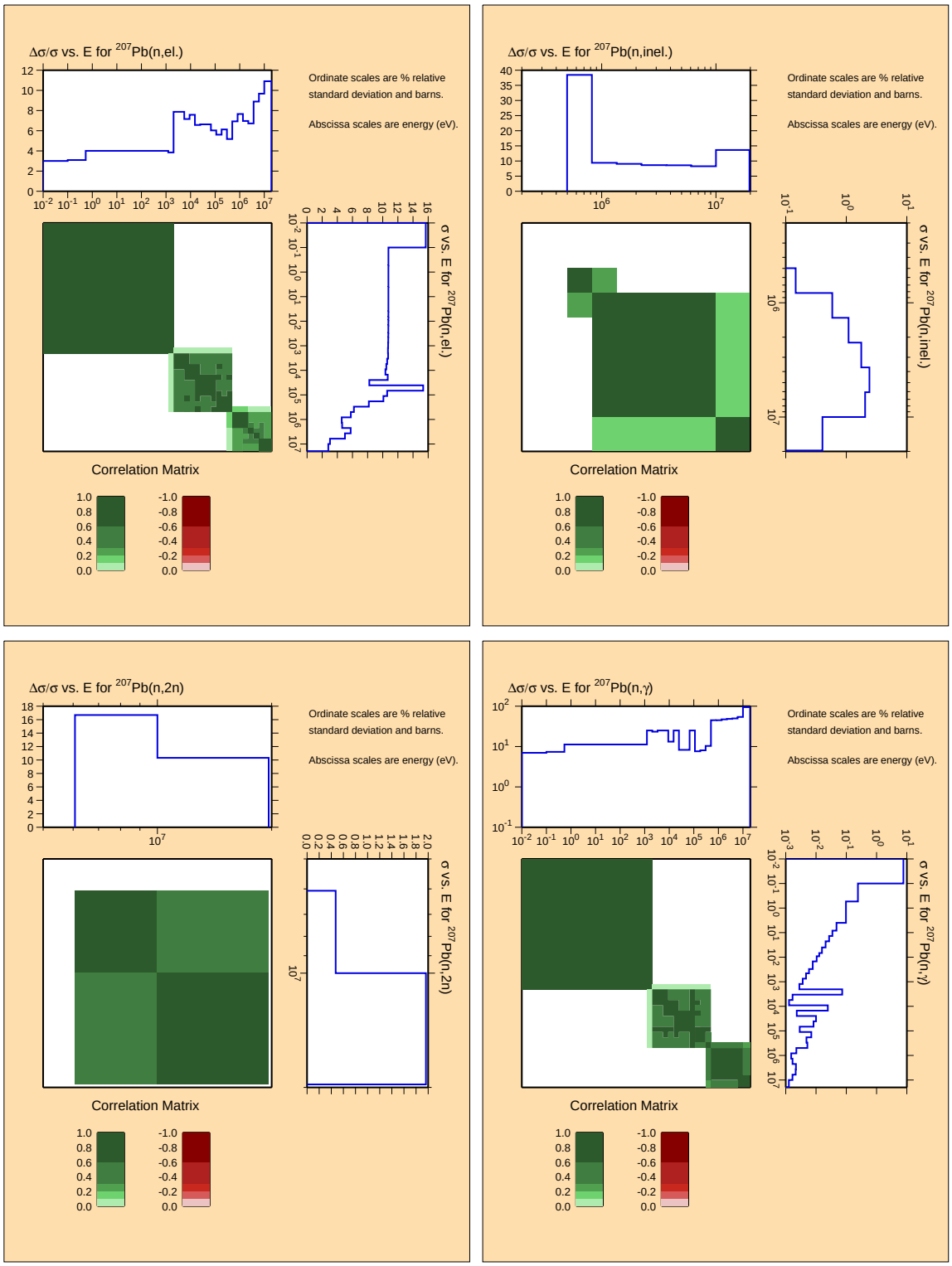

Figure B.76: Covariances for structural material ^{207}Pb.

^{208}Pb

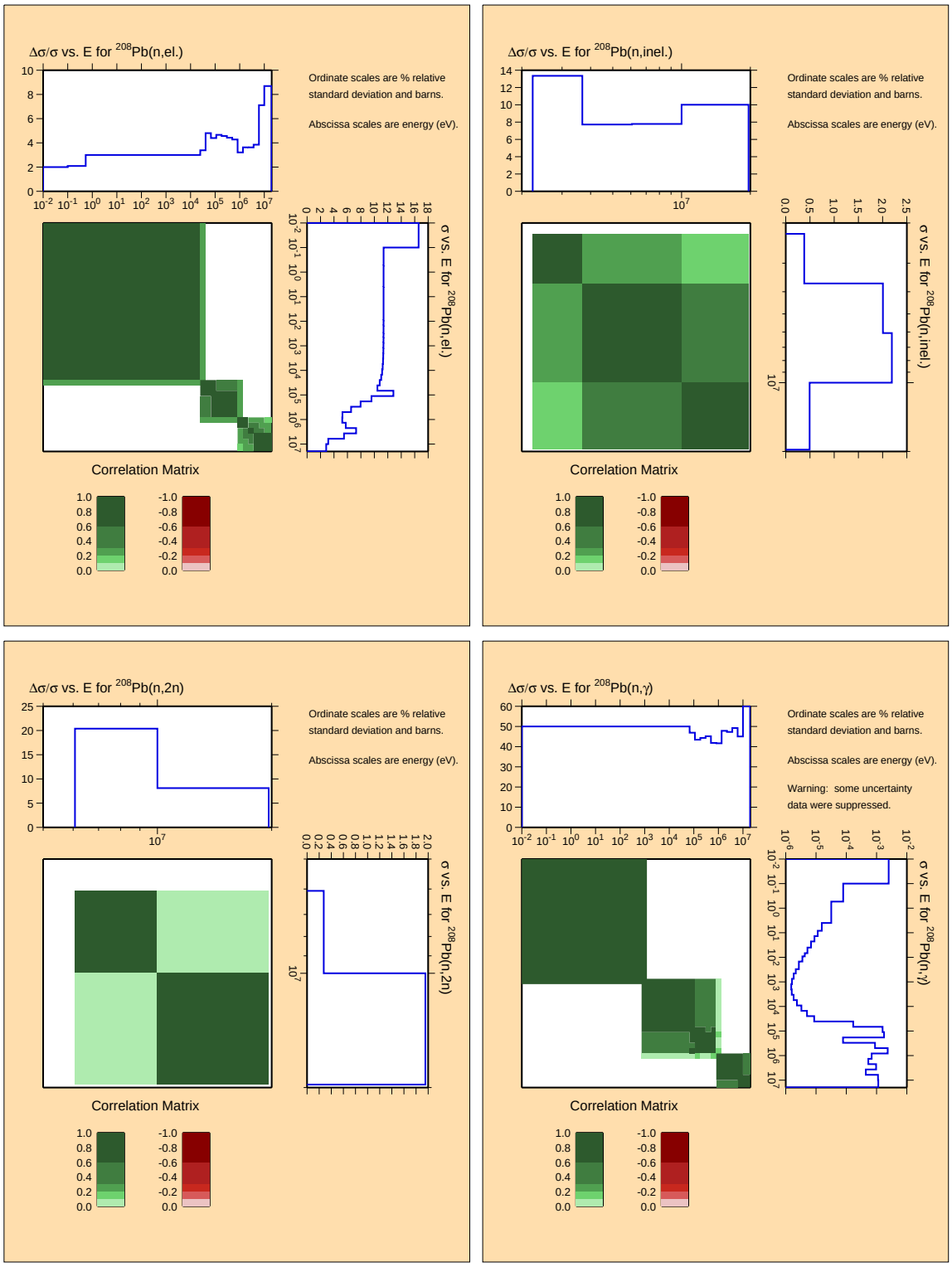

Figure B.77: Covariances for structural material ^{208}Pb.

^{209}Bi

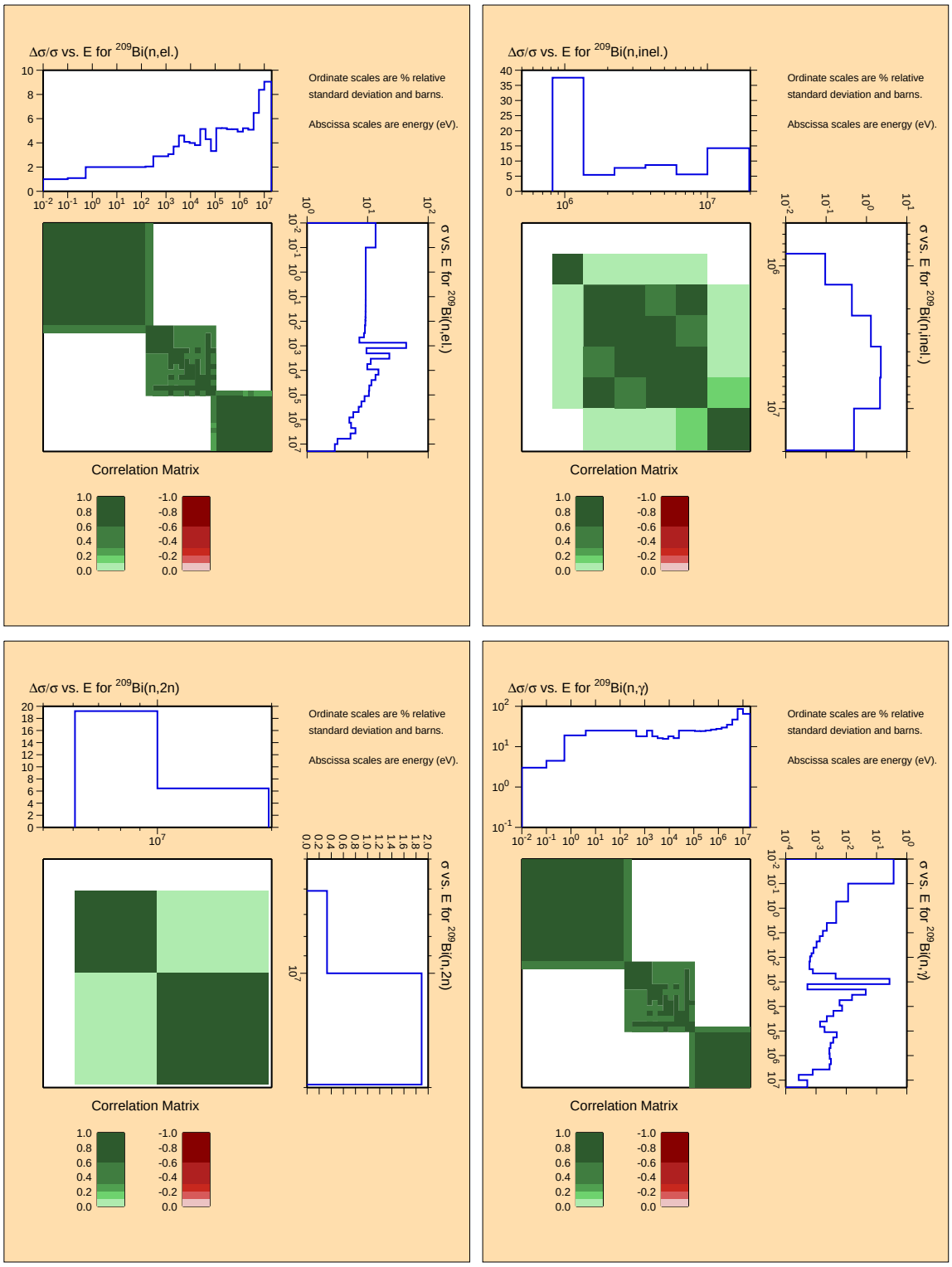

Figure B.78: Covariances for structural material ^{209}Bi.

Appendix C

AFCI 2.0 Covariance Plots

Actinides

(20 materials: cross sections and $\bar{\nu}$)
(3 materials: prompt fission neutron spectra)

^{232}Th

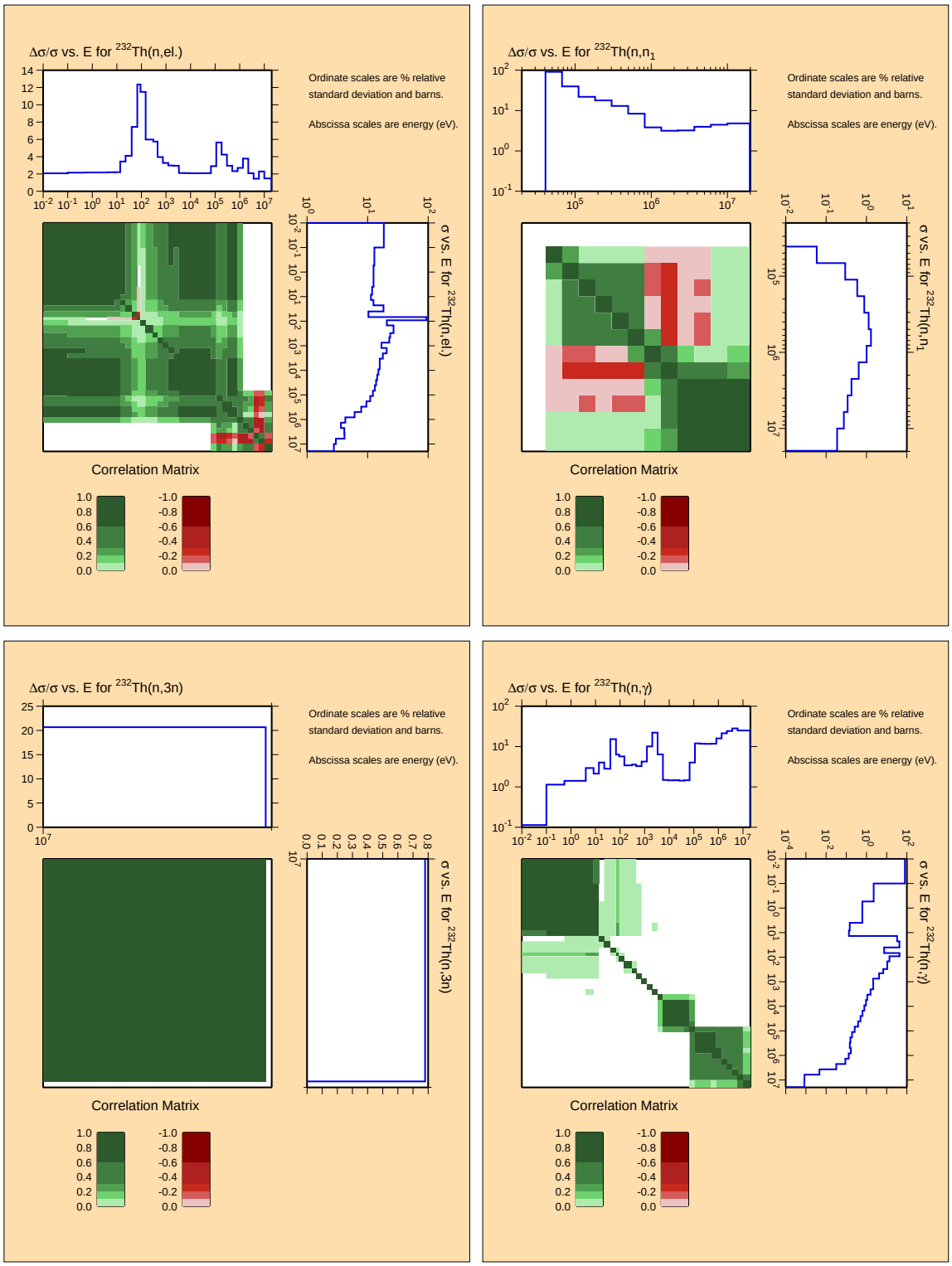

Figure C.1: Covariances for actinide ^{232}Th.

^{232}Th

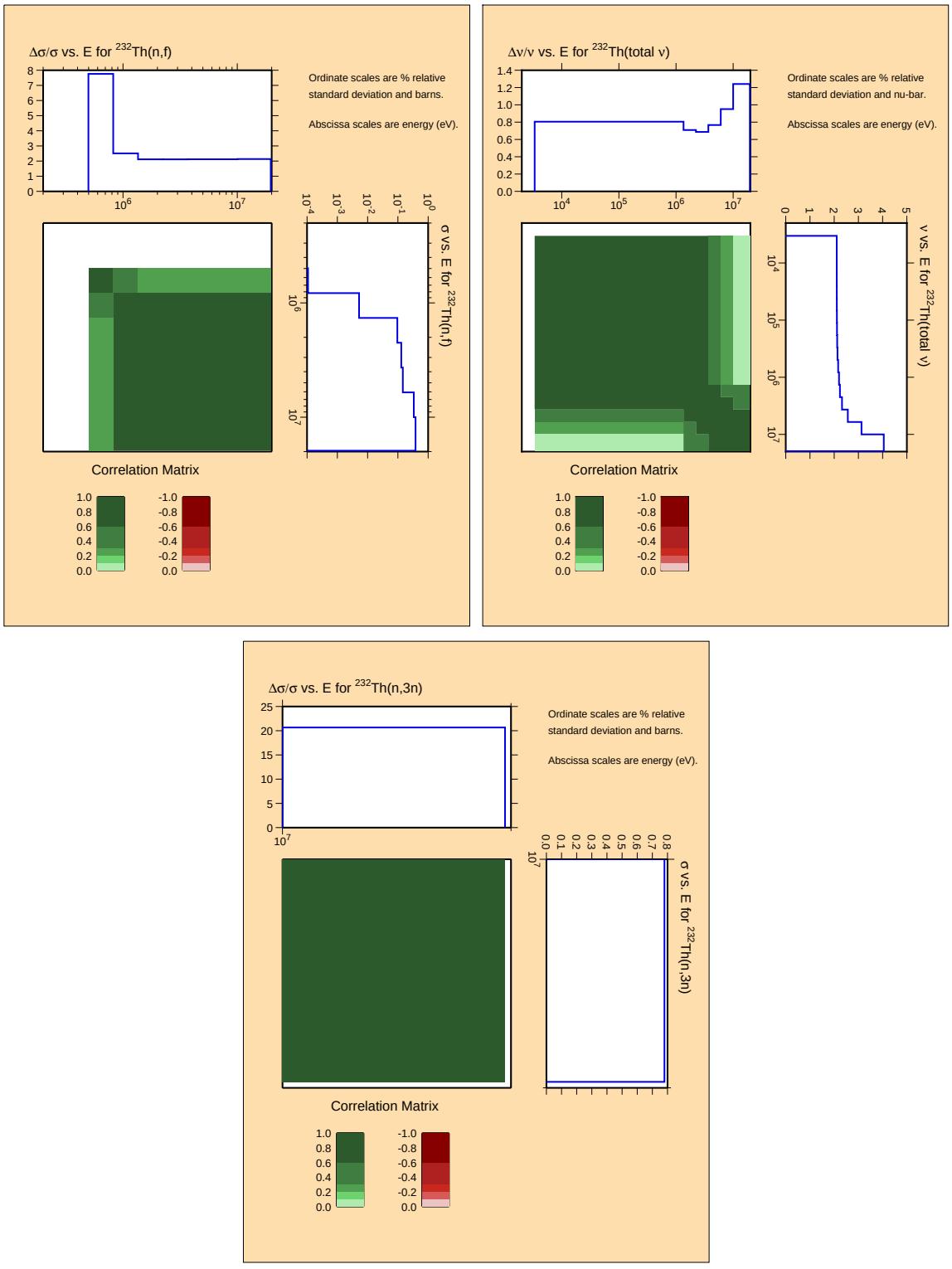

Figure C.2: Covariances for actinide ^{232}Th (continued).

^{233}U

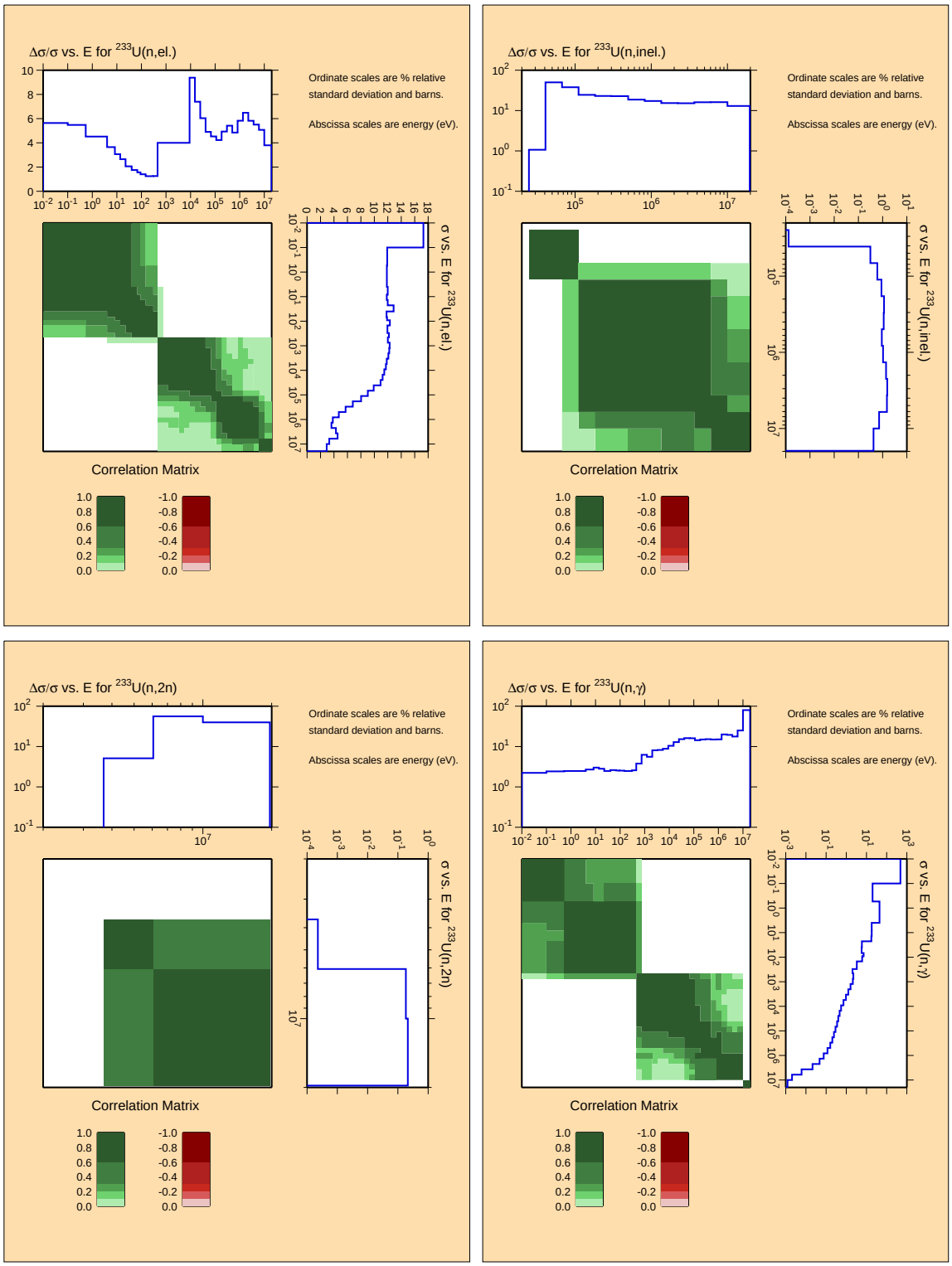

Figure C.3: Covariances for actinide ^{233}U.

^{233}U

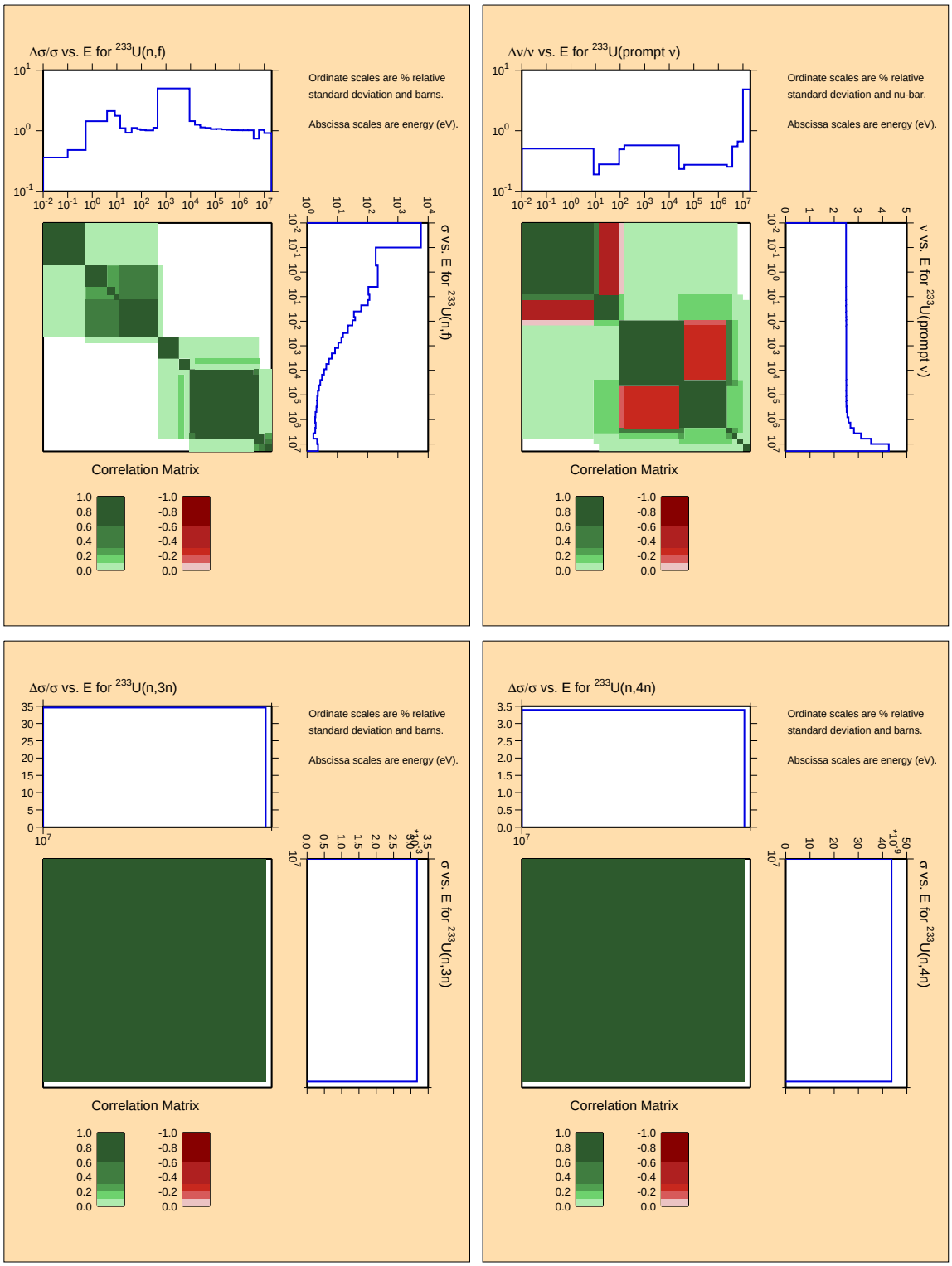

Figure C.4: Covariances for actinide ^{233}U (continued).

^{234}U

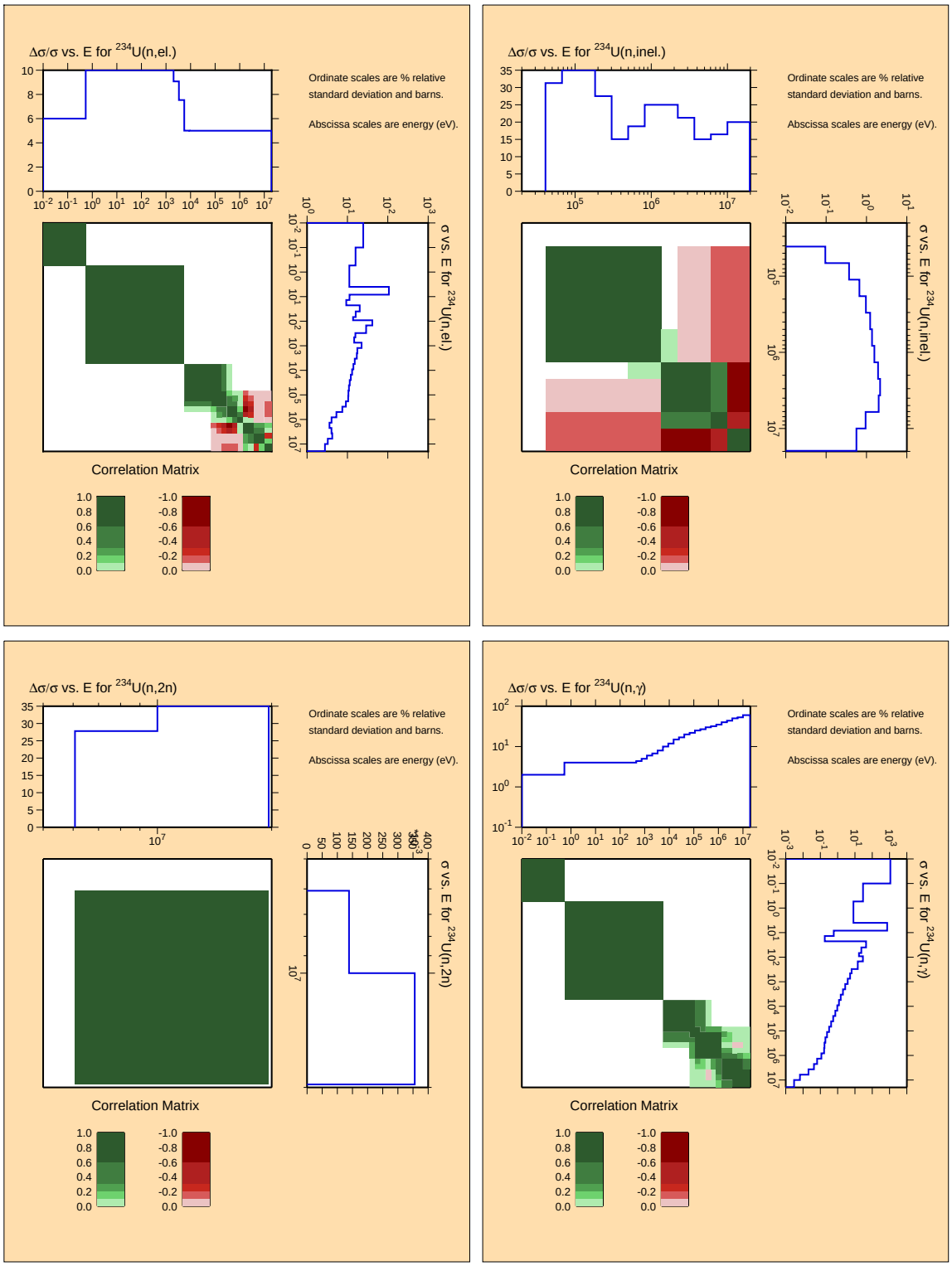

Figure C.5: Covariances for actinide ^{234}U.

^{234}U

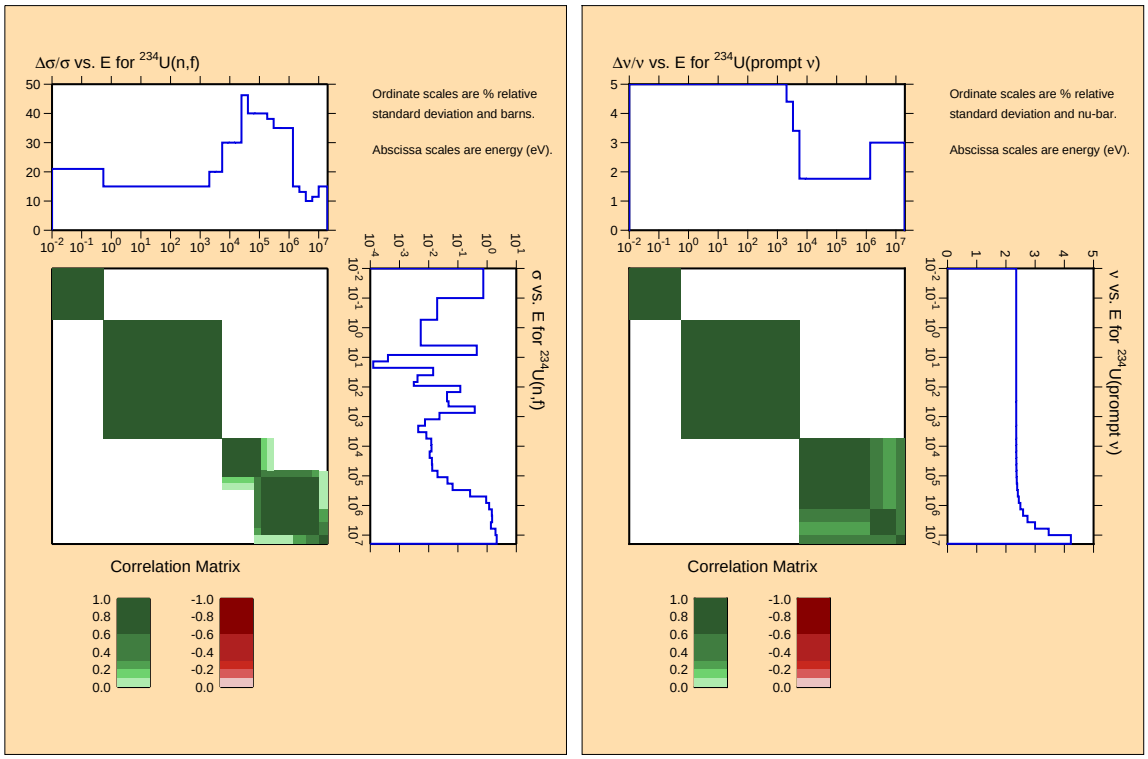

Figure C.6: Covariances for actinide ^{234}U (continued).

^{235}U

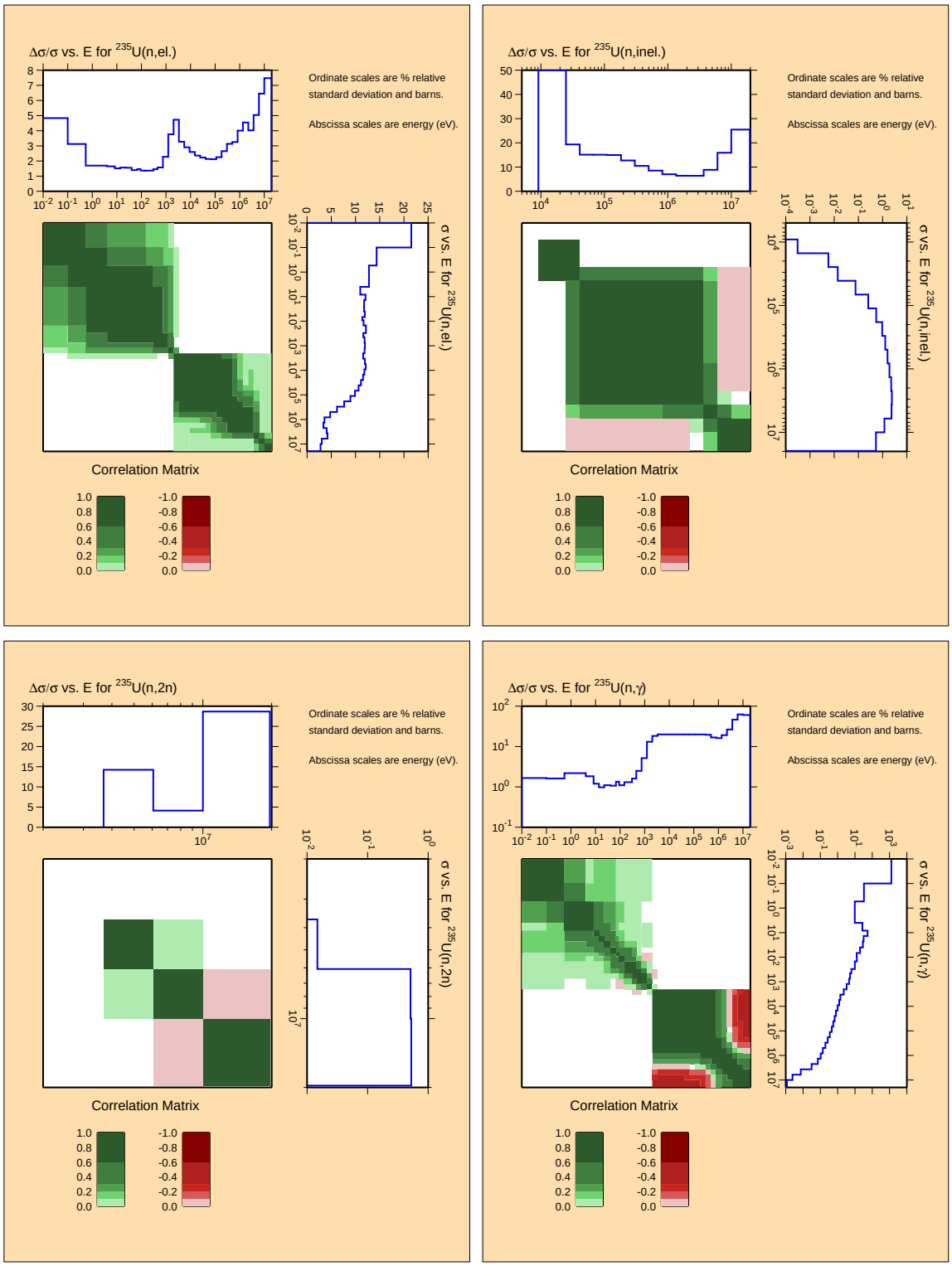

Figure C.7: Covariances for actinide ^{235}U.

^{235}U

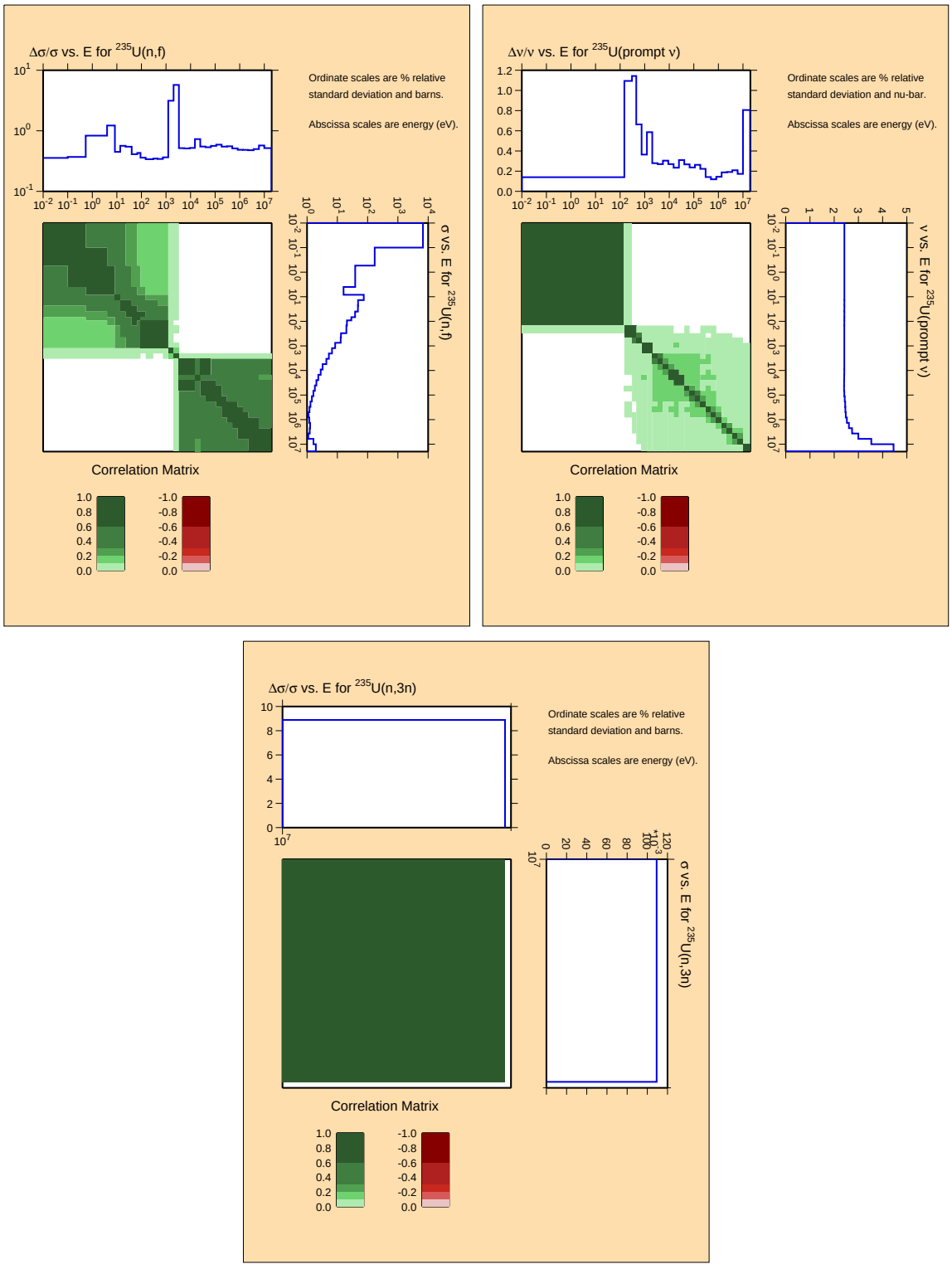

Figure C.8: Covariances for actinide ^{235}U (continued).

^{236}U

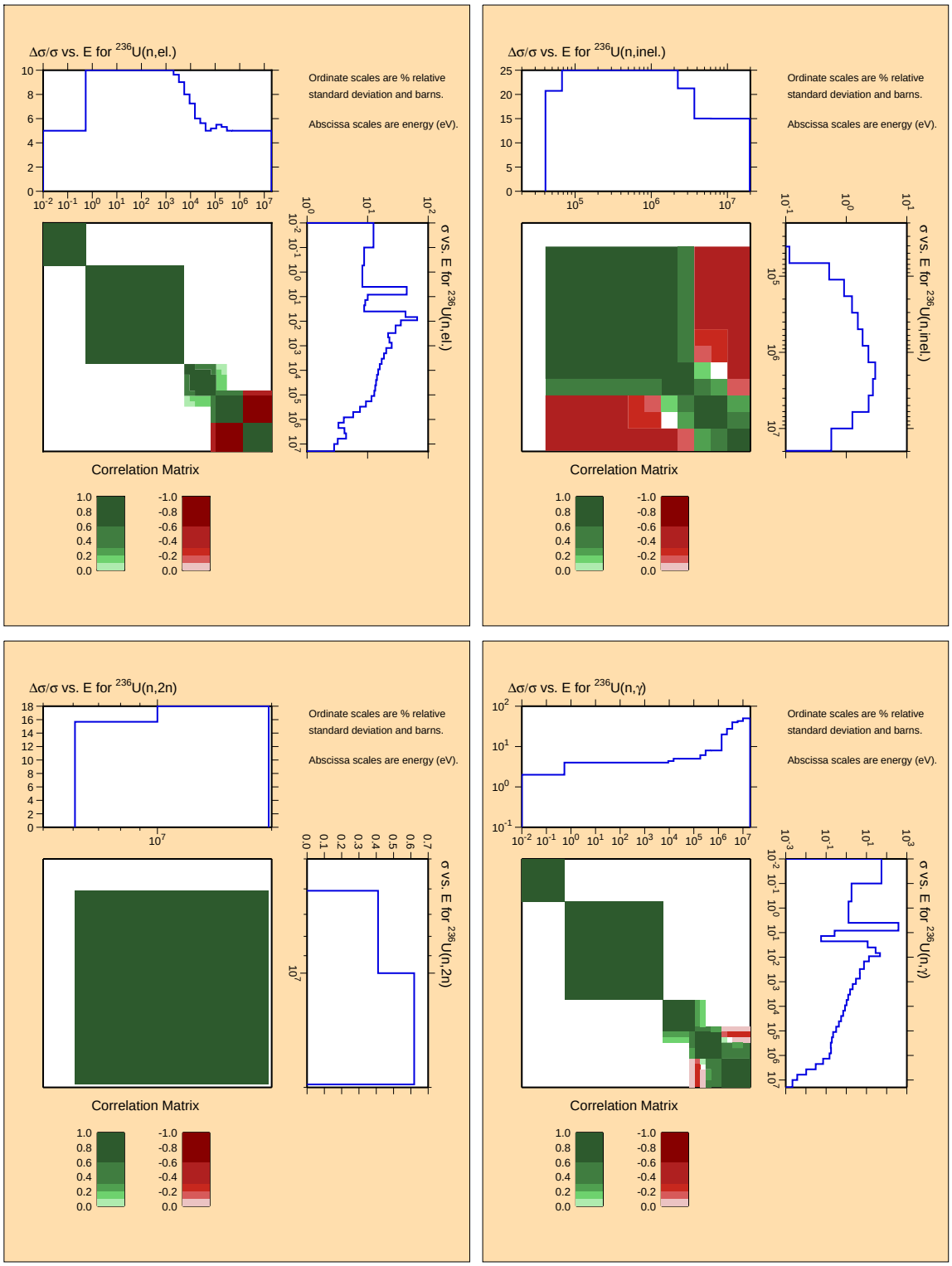

Figure C.9: Covariances for actinide ^{236}U.

^{236}U

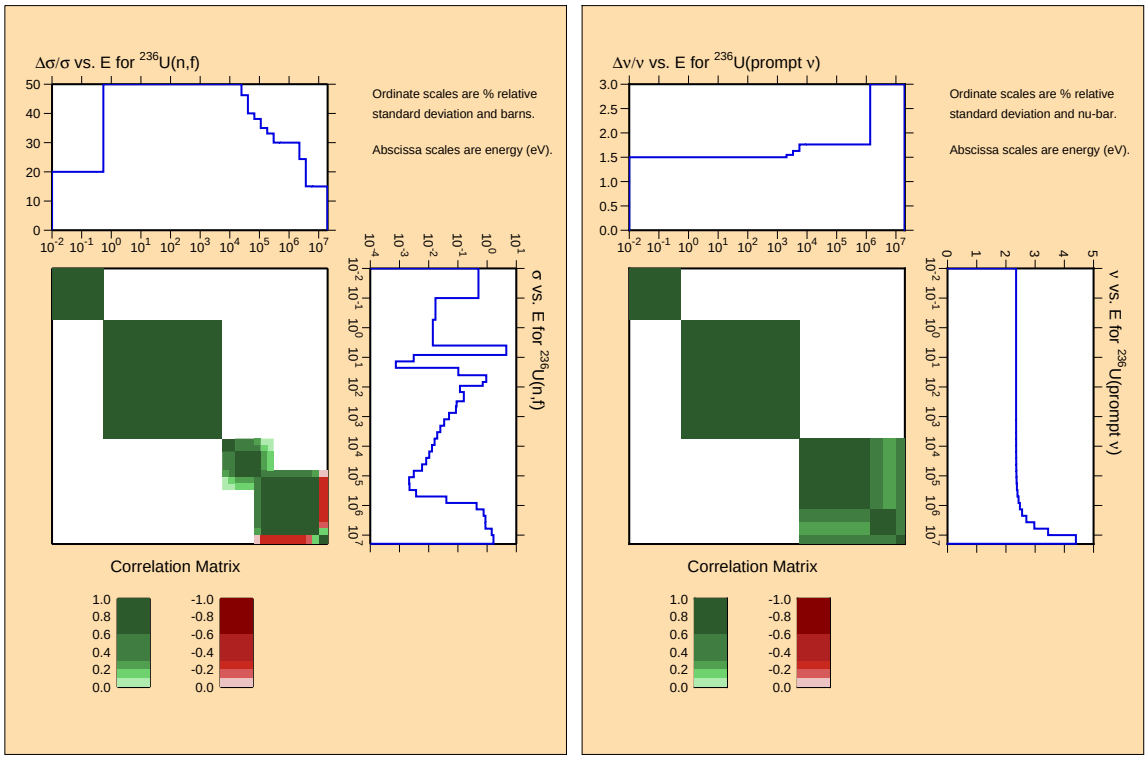

Figure C.10: Covariances for actinide ^{236}U (continued).

^{238}U

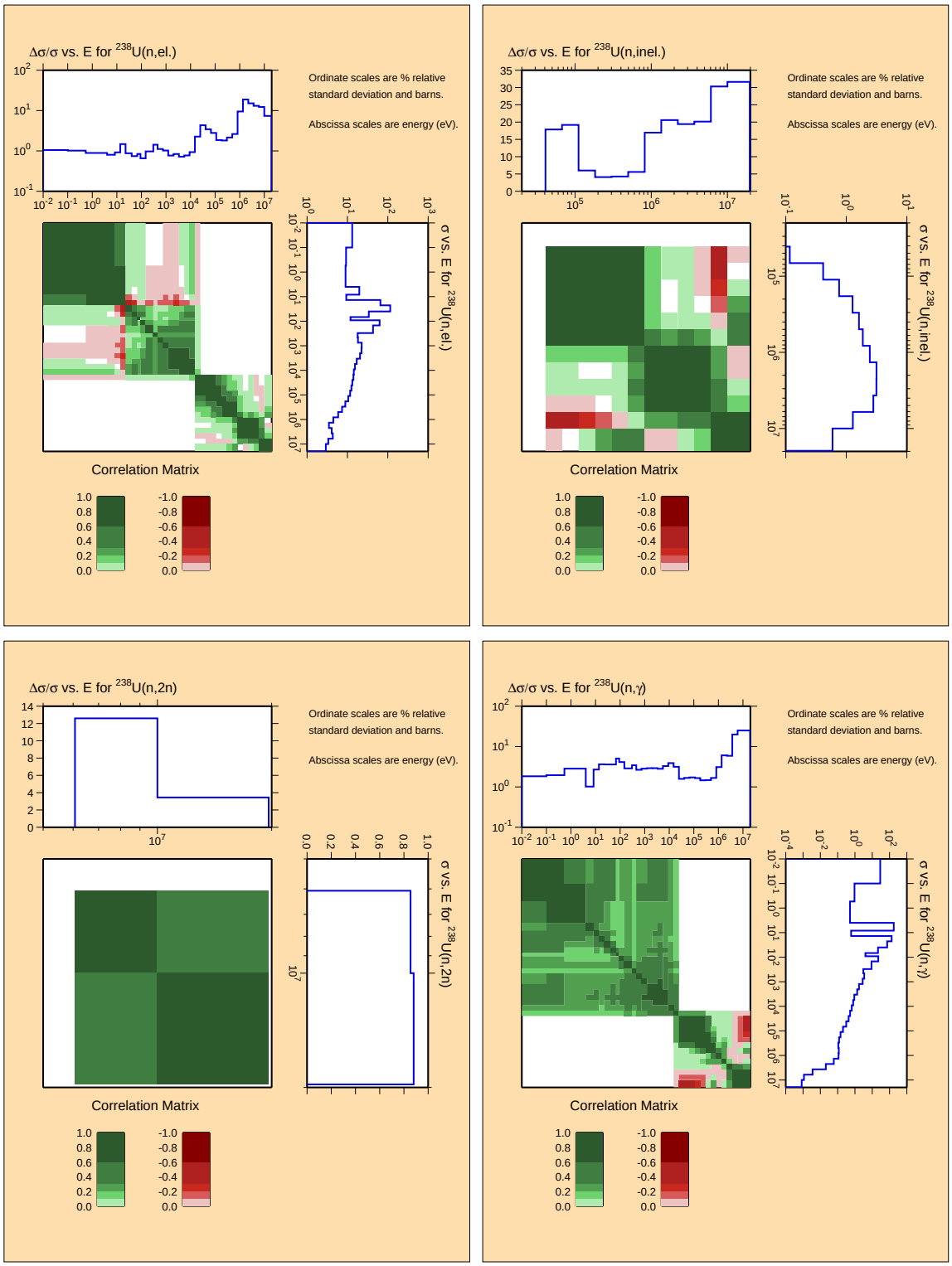

Figure C.11: Covariances for actinide ^{238}U.

^{238}U

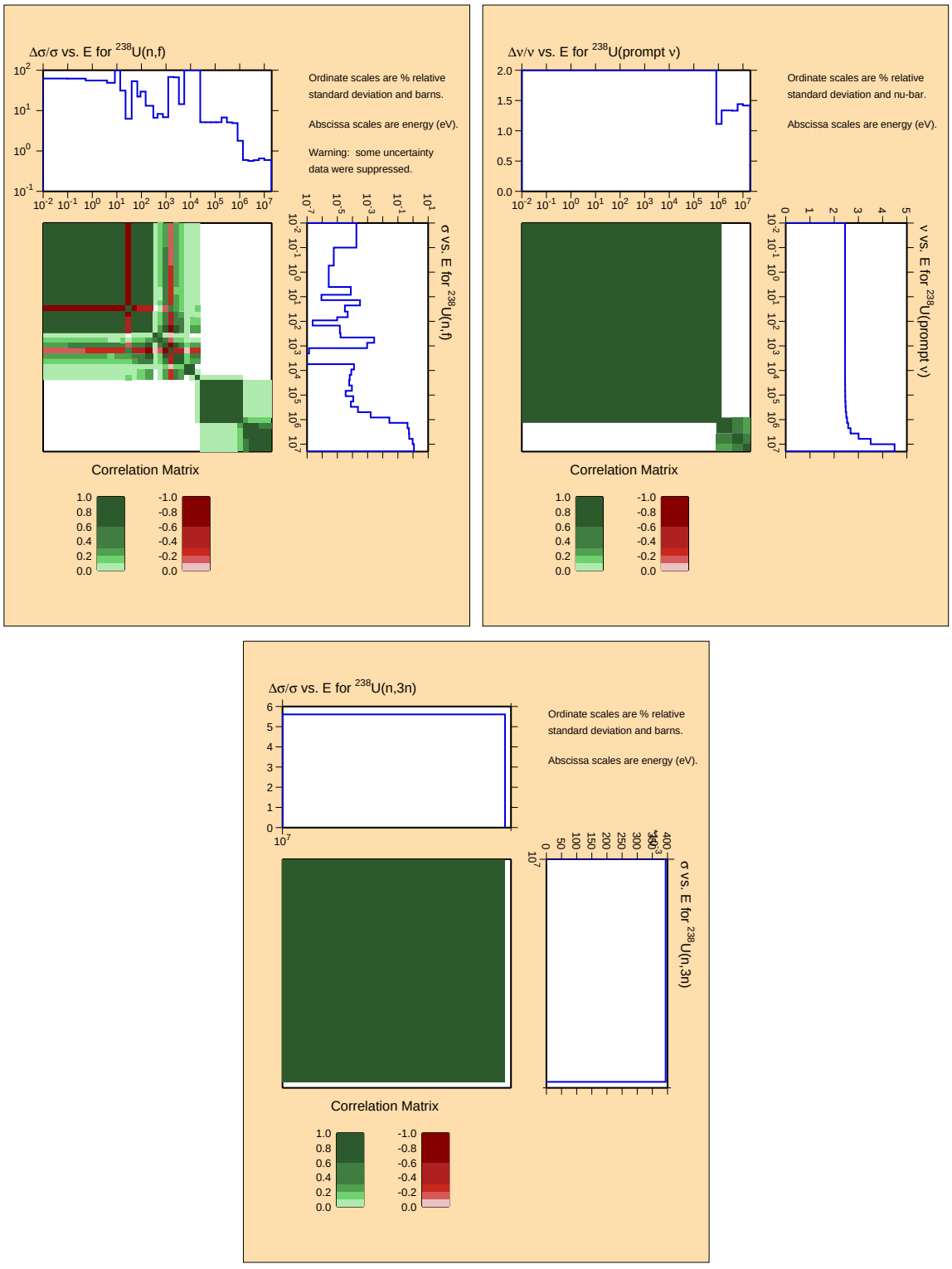

Figure C.12: Covariances for actinide ^{238}U (continued).

^{237}Np

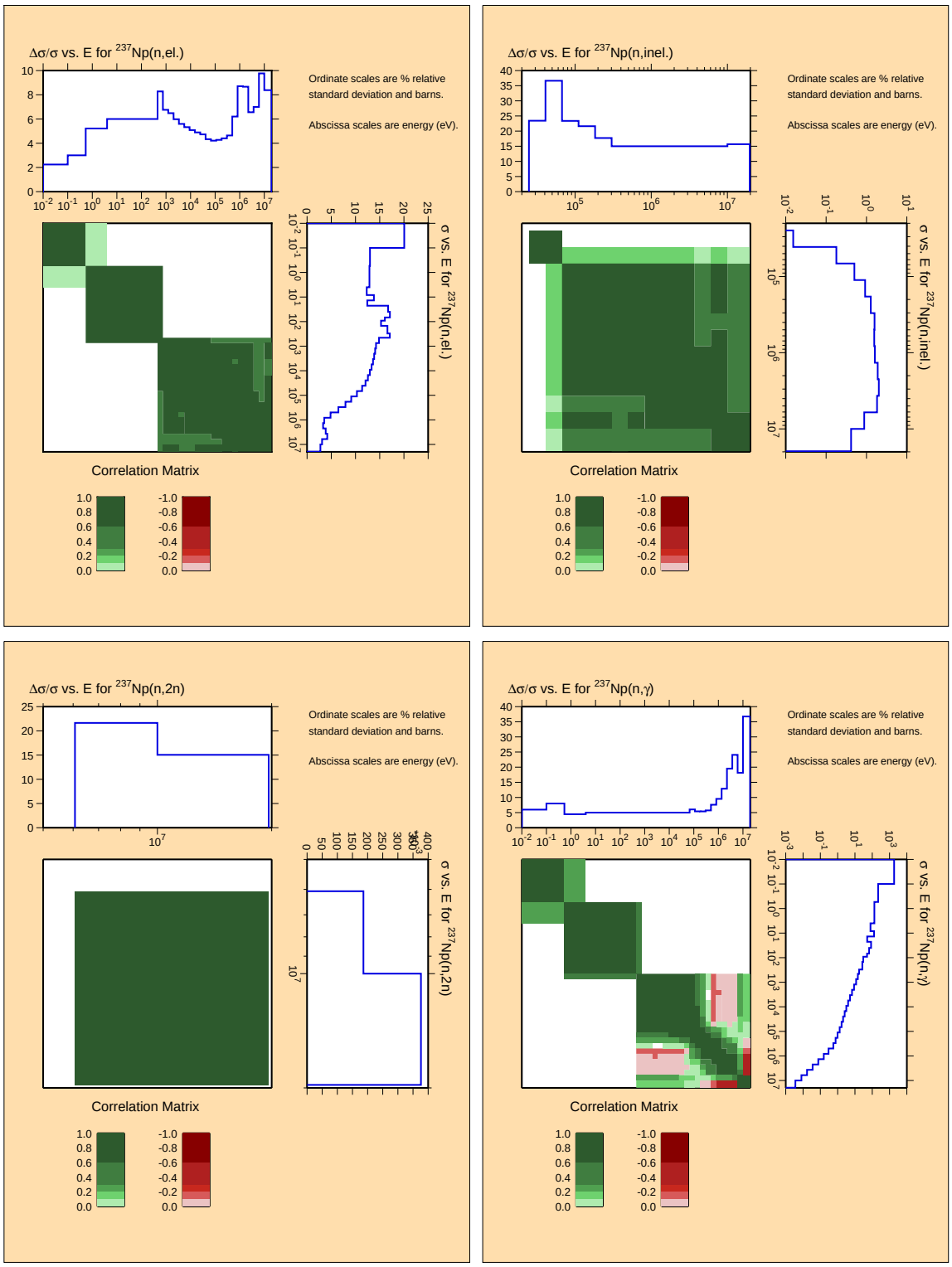

Figure C.13: Covariances for actinide ^{237}Np.

^{237}Np

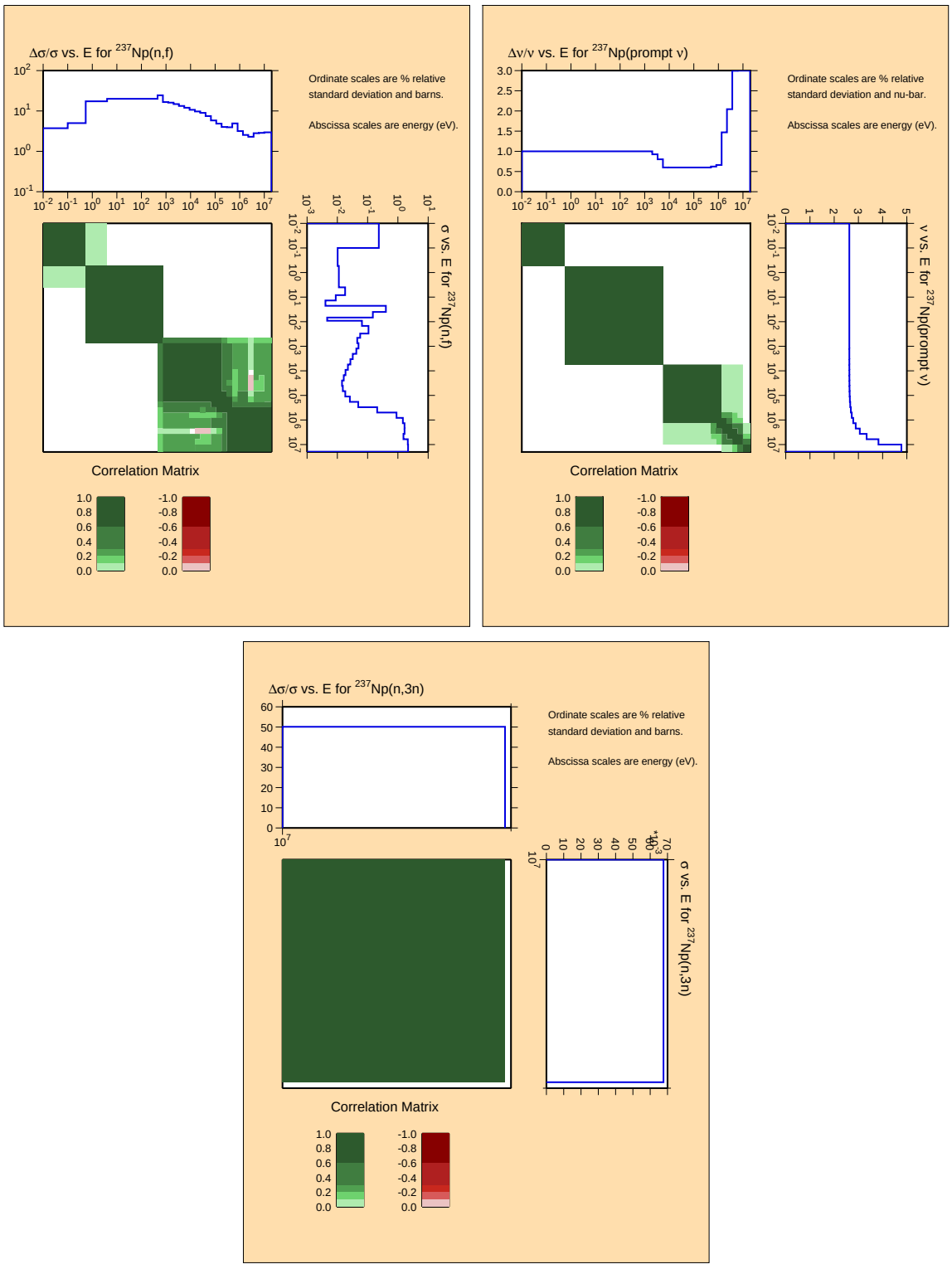

Figure C.14: Covariances for actinide ^{237}Np (continued).

^{238}Pu

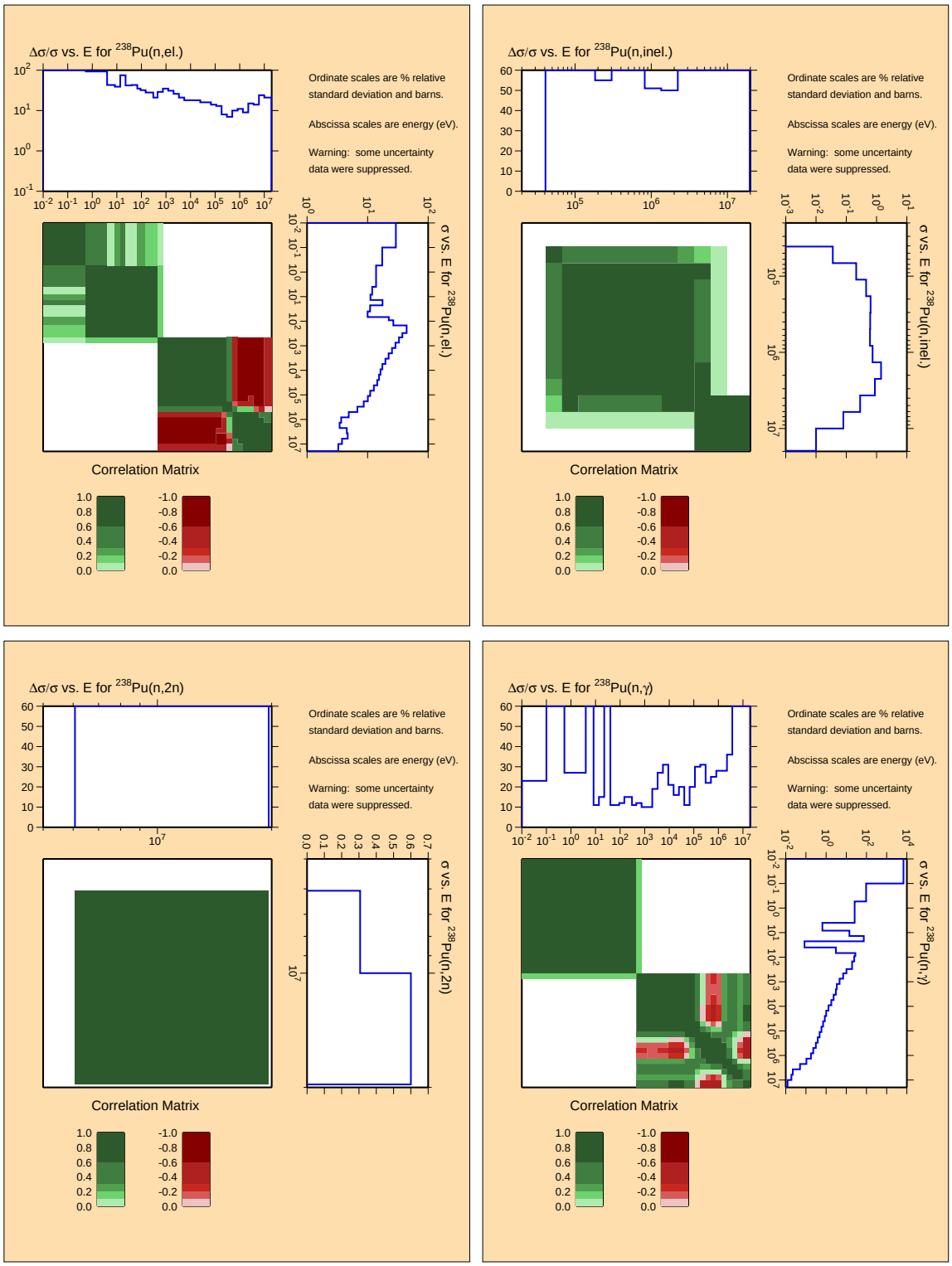

Figure C.15: Covariances for actinide ^{238}Pu.

^{238}Pu

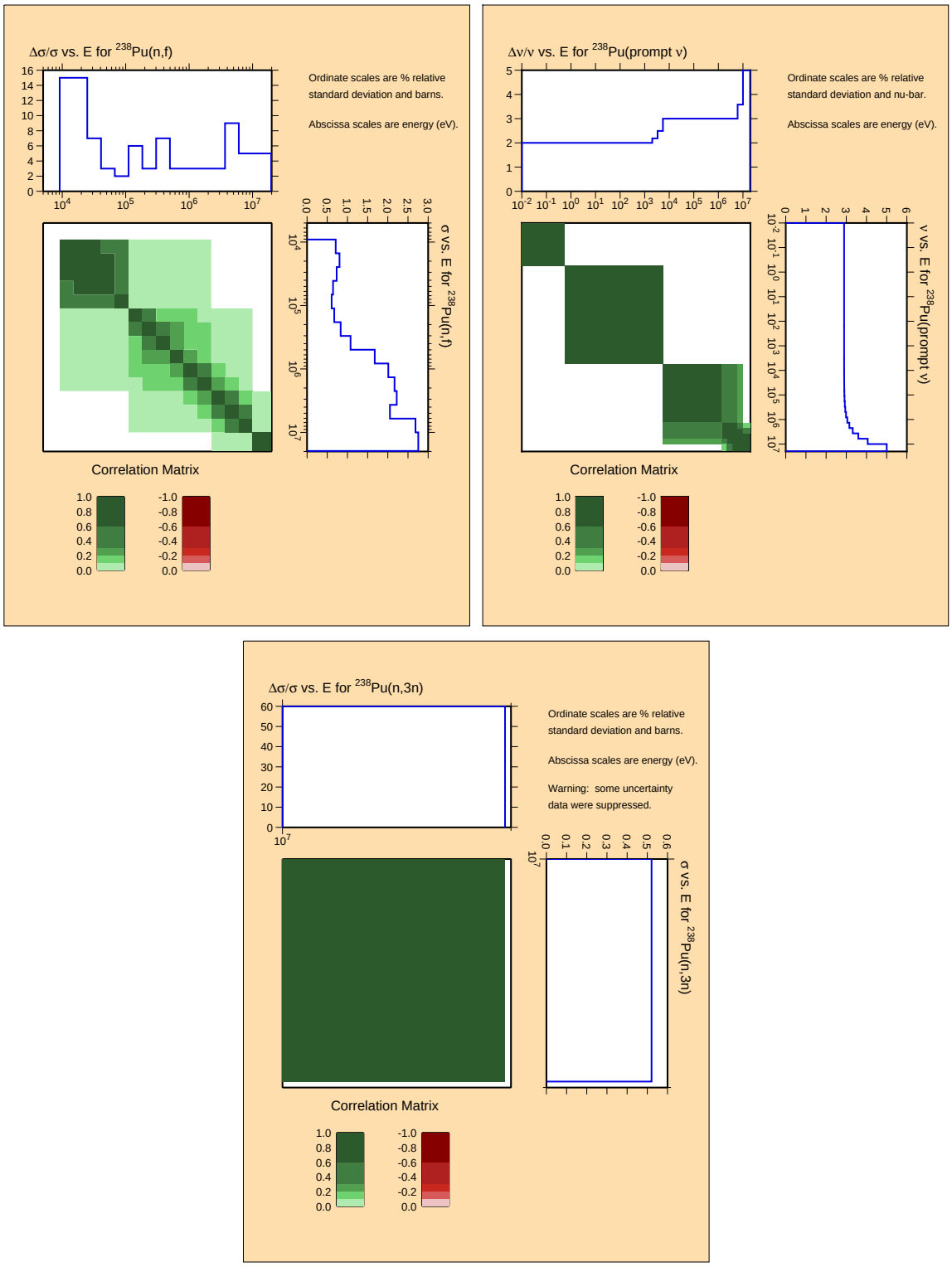

Figure C.16: Covariances for actinide ^{238}Pu (continued).

^{239}Pu

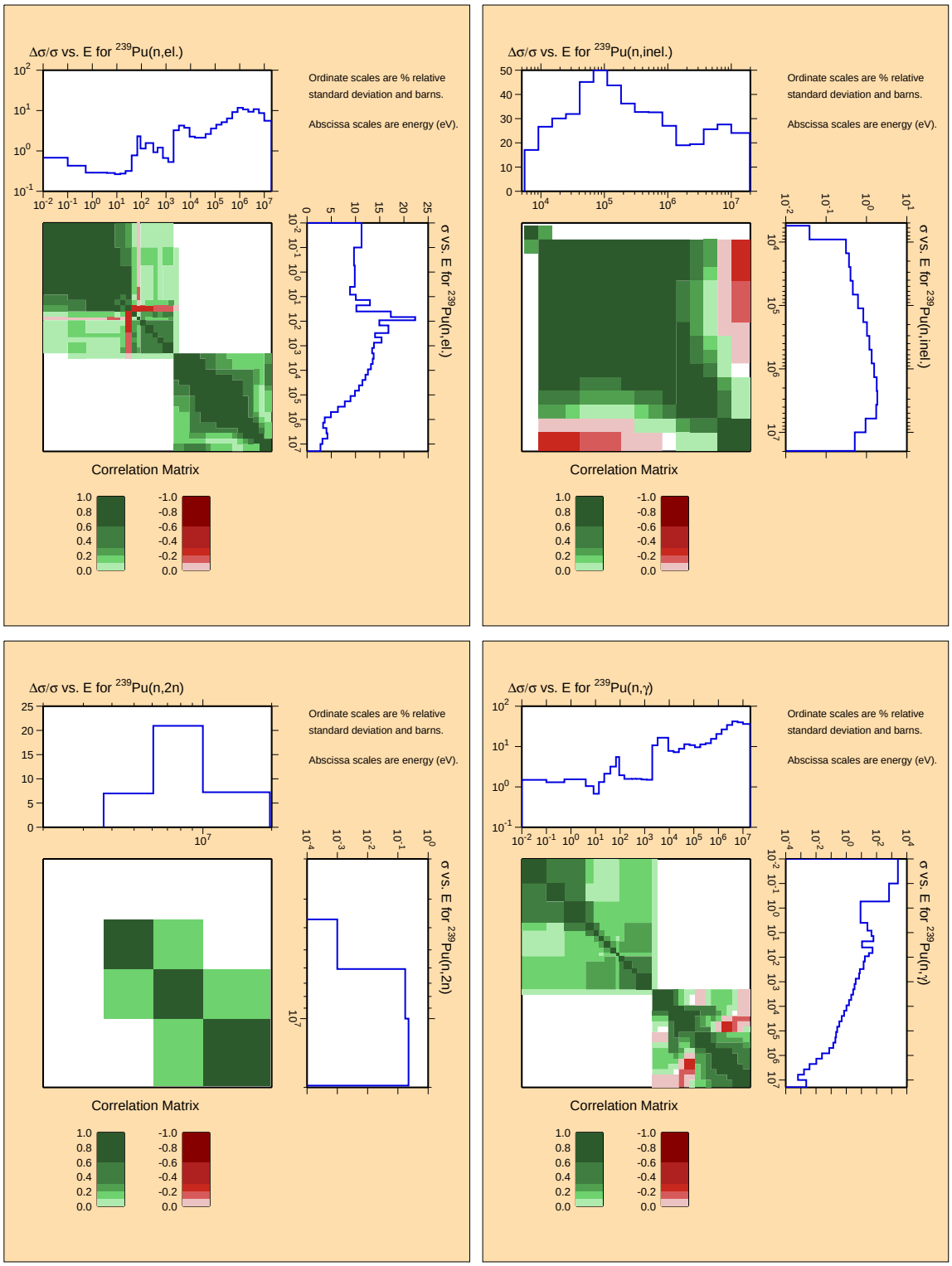

Figure C.17: Covariances for actinide ^{239}Pu.

^{239}Pu

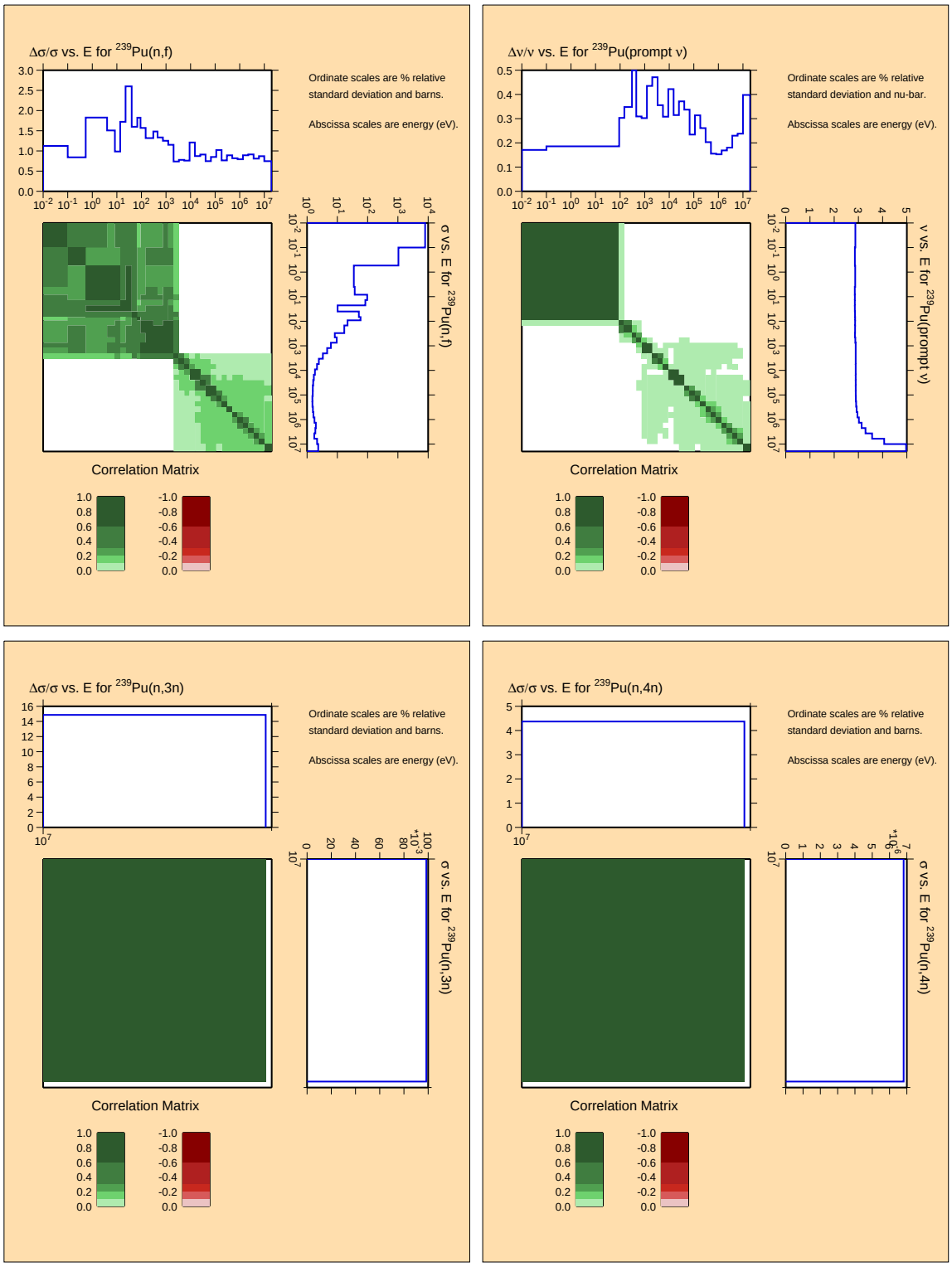

Figure C.18: Covariances for actinide ^{239}Pu (continued).

^{240}Pu

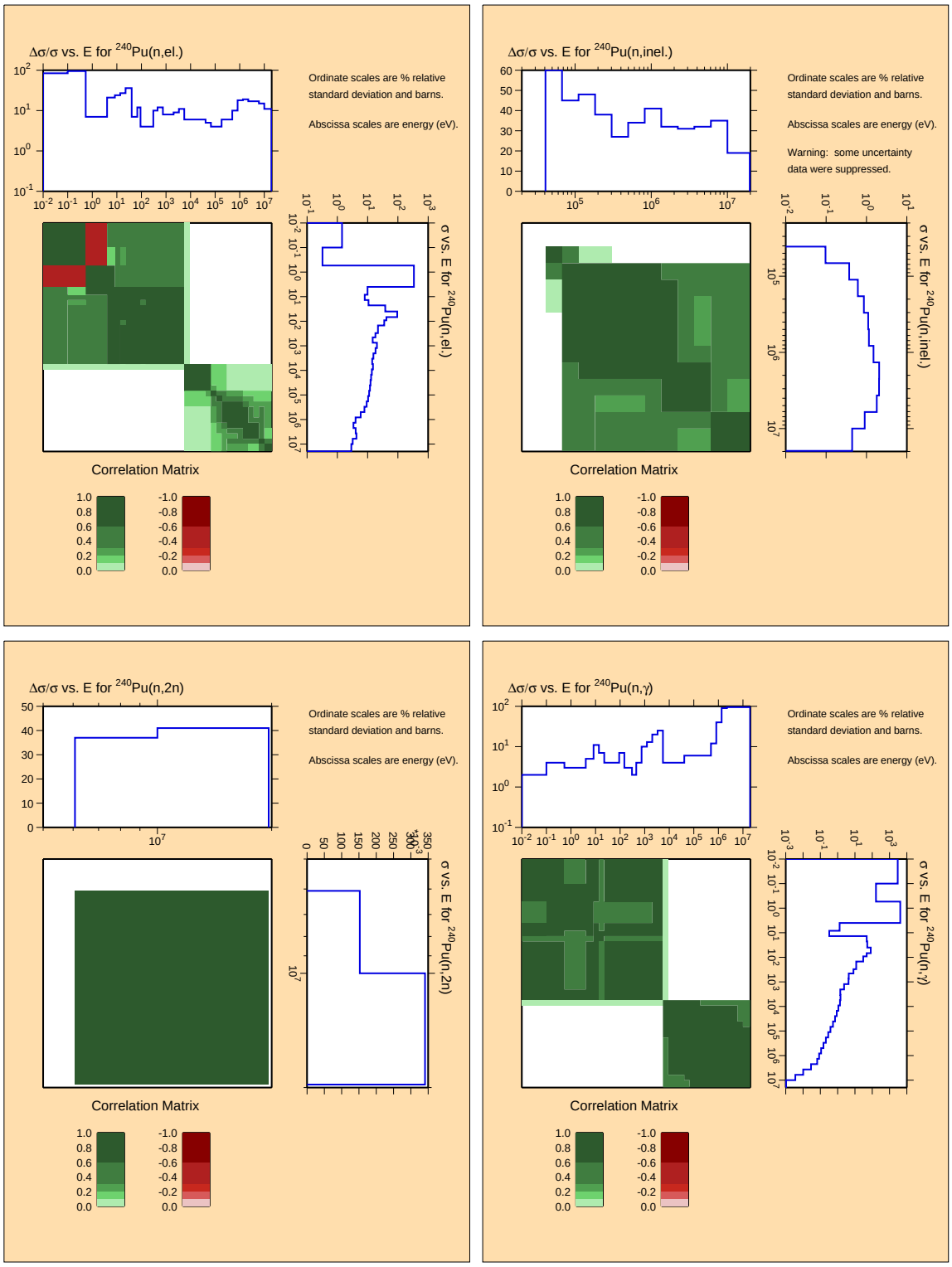

Figure C.19: Covariances for actinide ^{240}Pu.

^{240}Pu

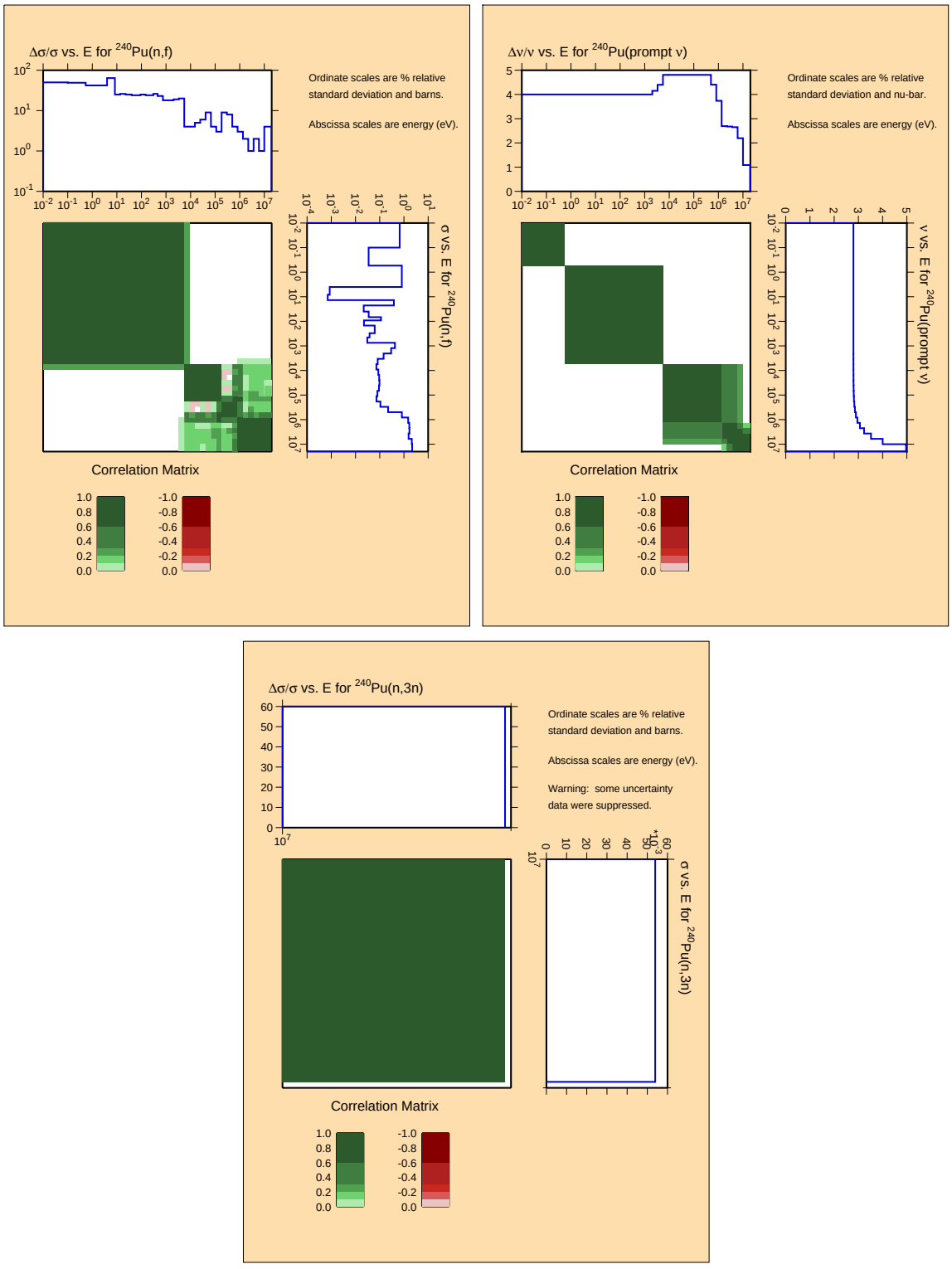

Figure C.20: Covariances for actinide ^{240}Pu (continued).

^{241}Pu

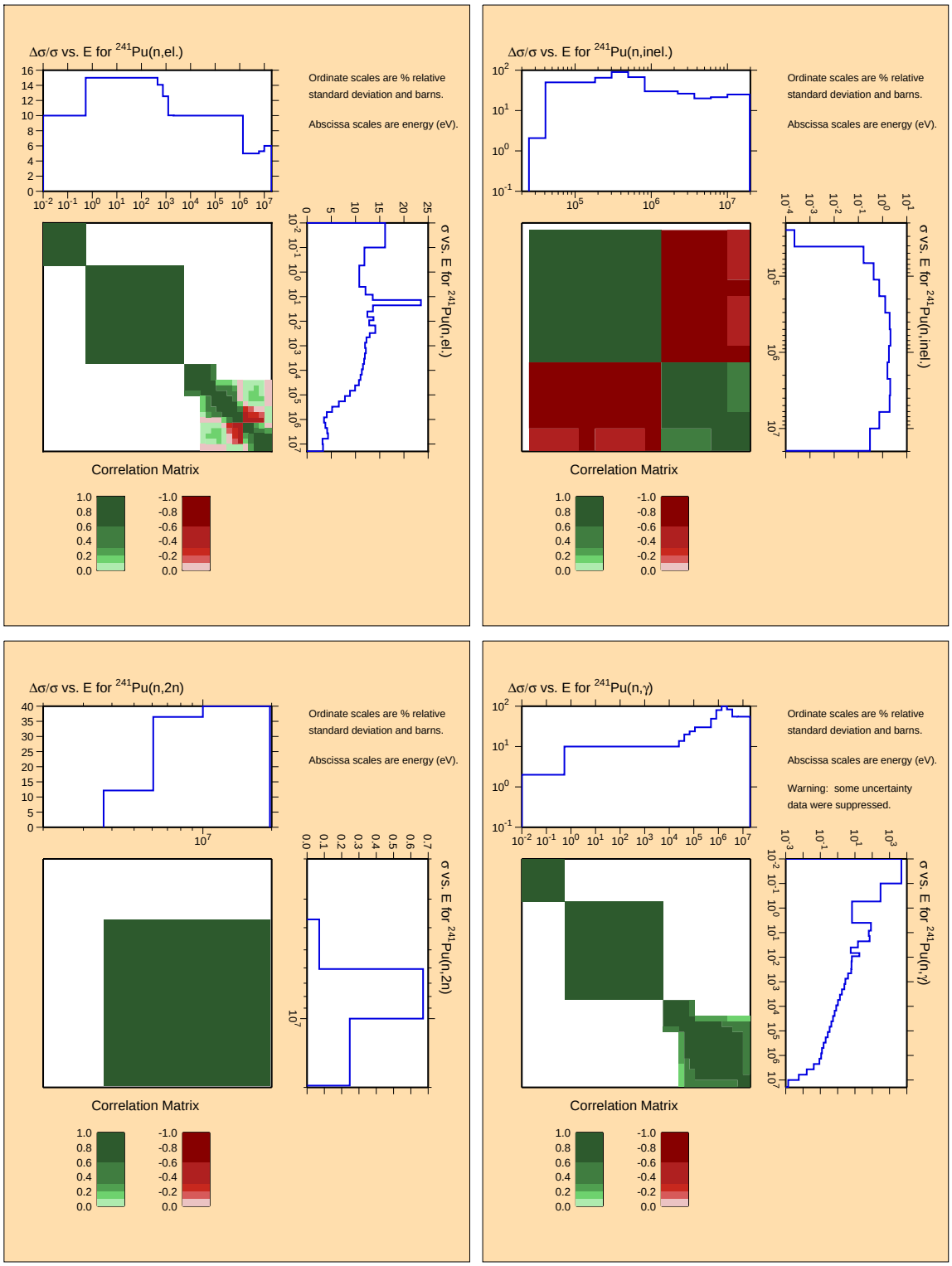

Figure C.21: Covariances for actinide ^{241}Pu.

^{241}Pu

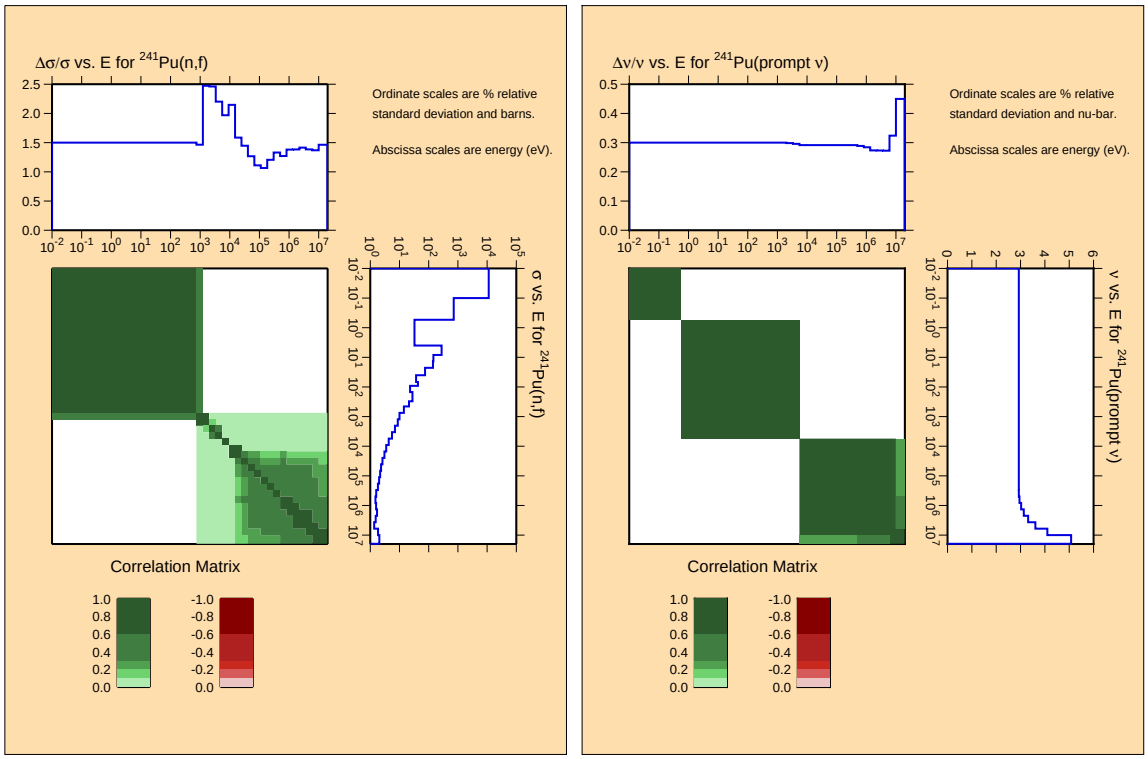

Figure C.22: Covariances for actinide ^{241}Pu (continued).

^{242}Pu

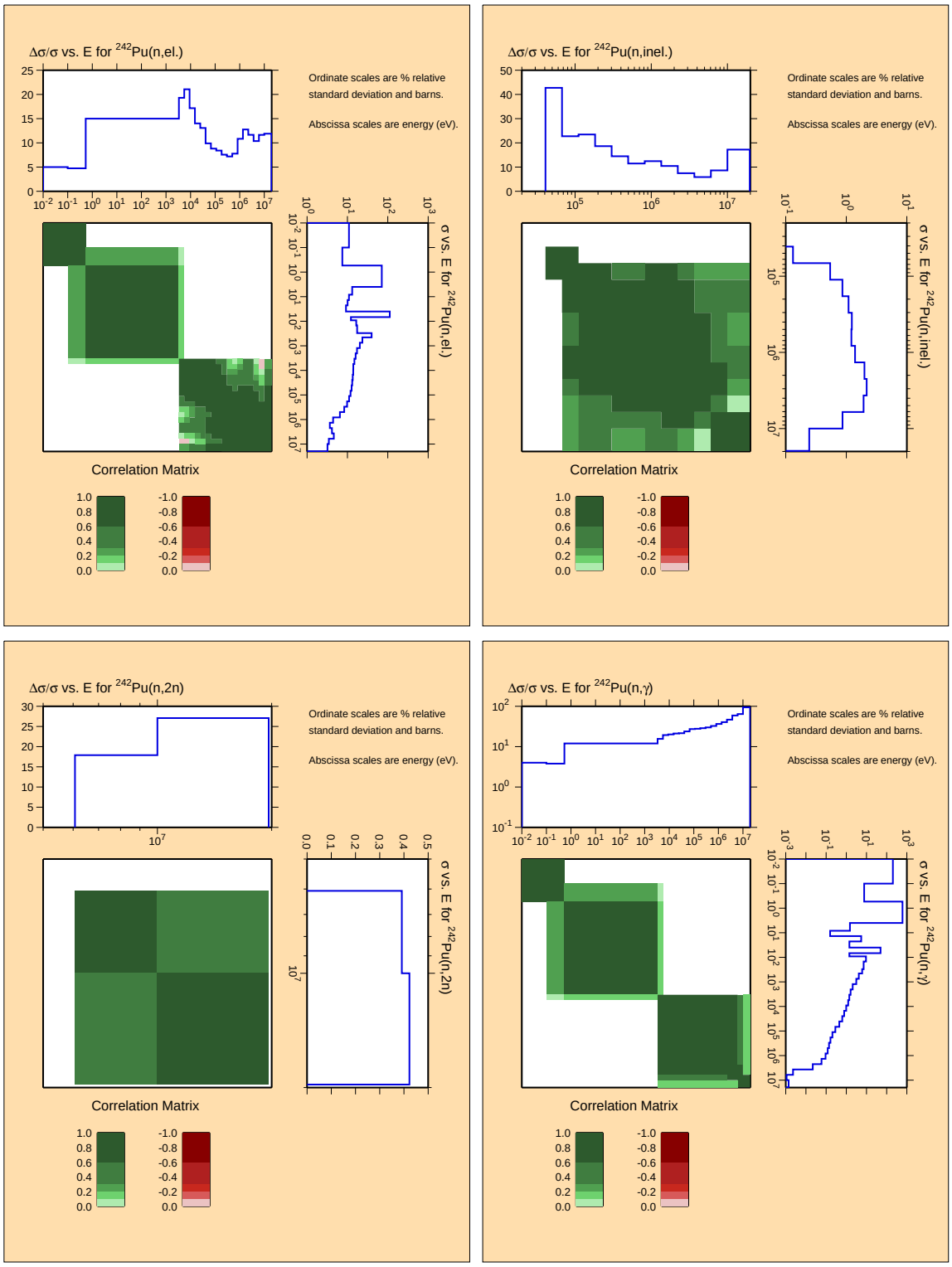

Figure C.23: Covariances for actinide ^{242}Pu.

^{242}Pu

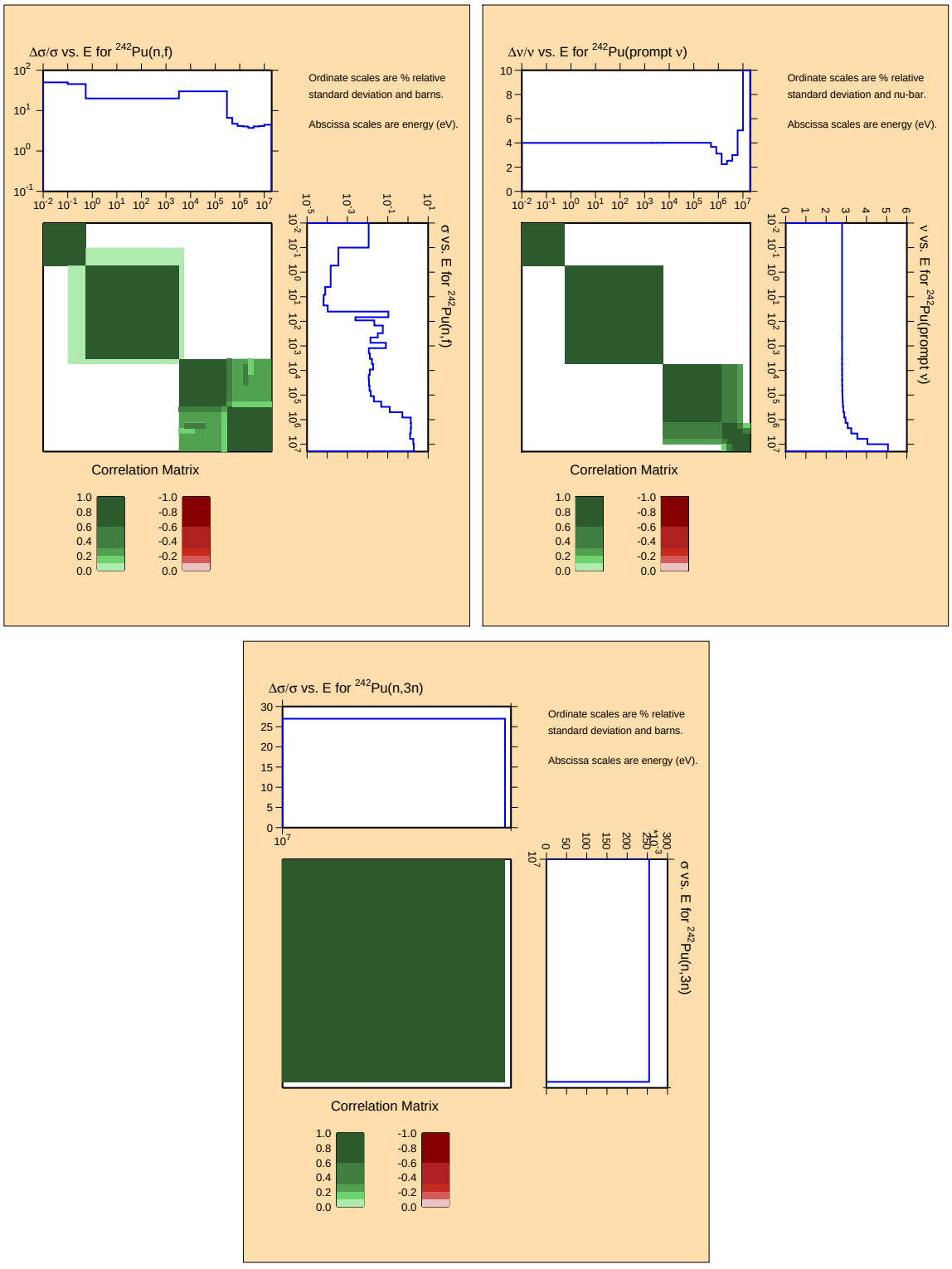

Figure C.24: Covariances for actinide ^{242}Pu (continued).

^{241}Am

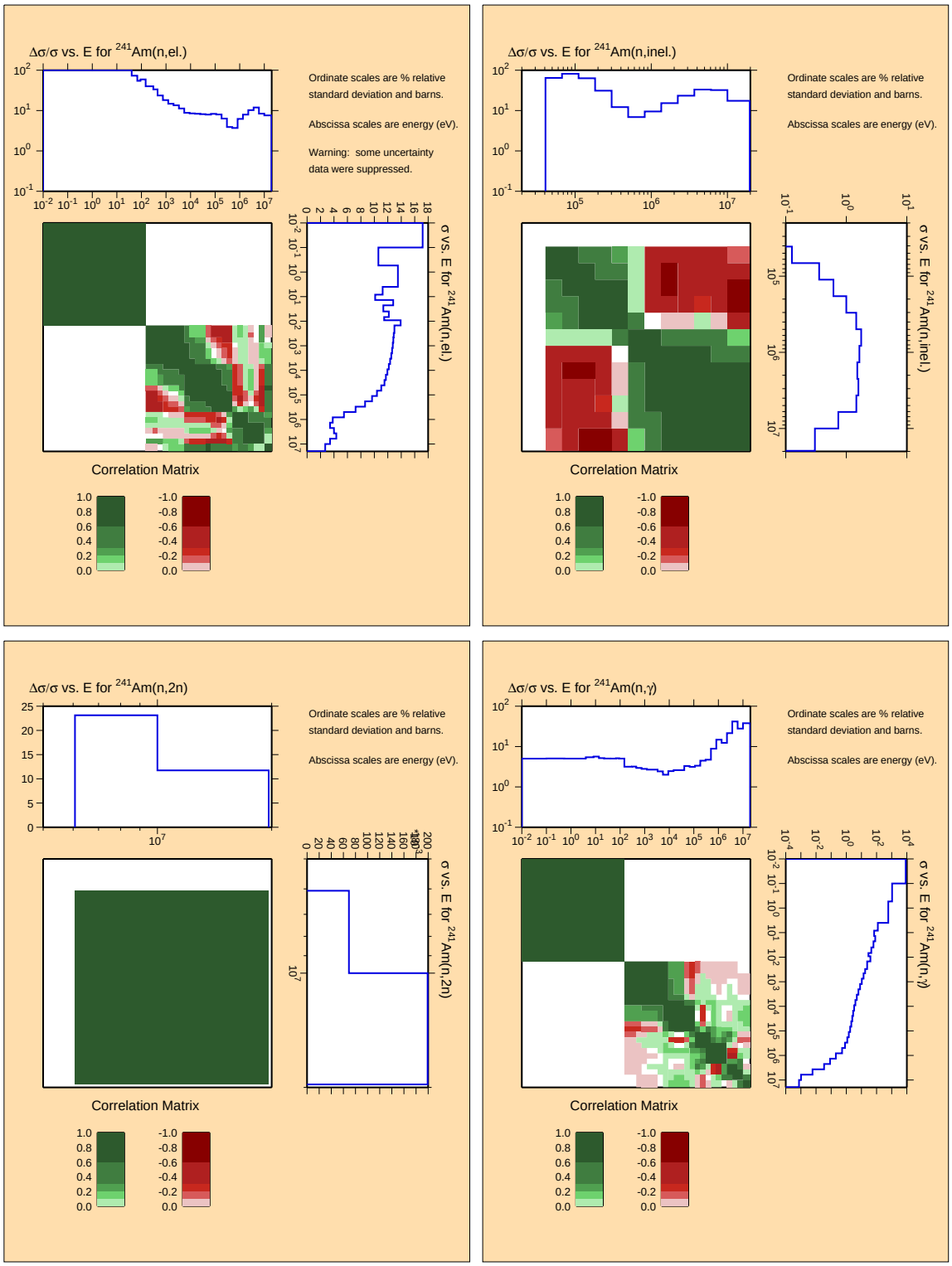

Figure C.25: Covariances for actinide ^{241}Am.

^{241}Am

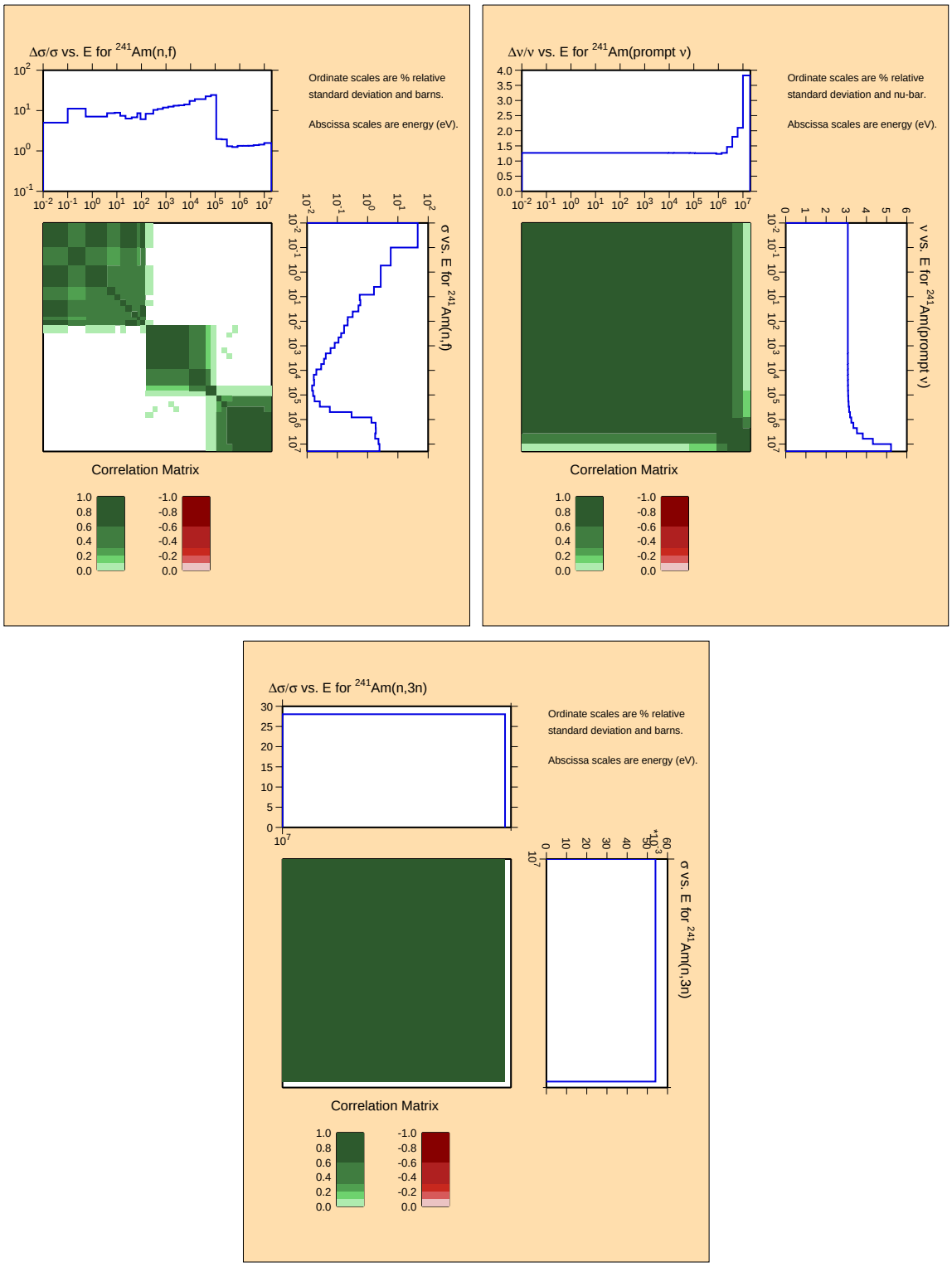

Figure C.26: Covariances for actinide ^{241}Am (continued).

^{242m}Am

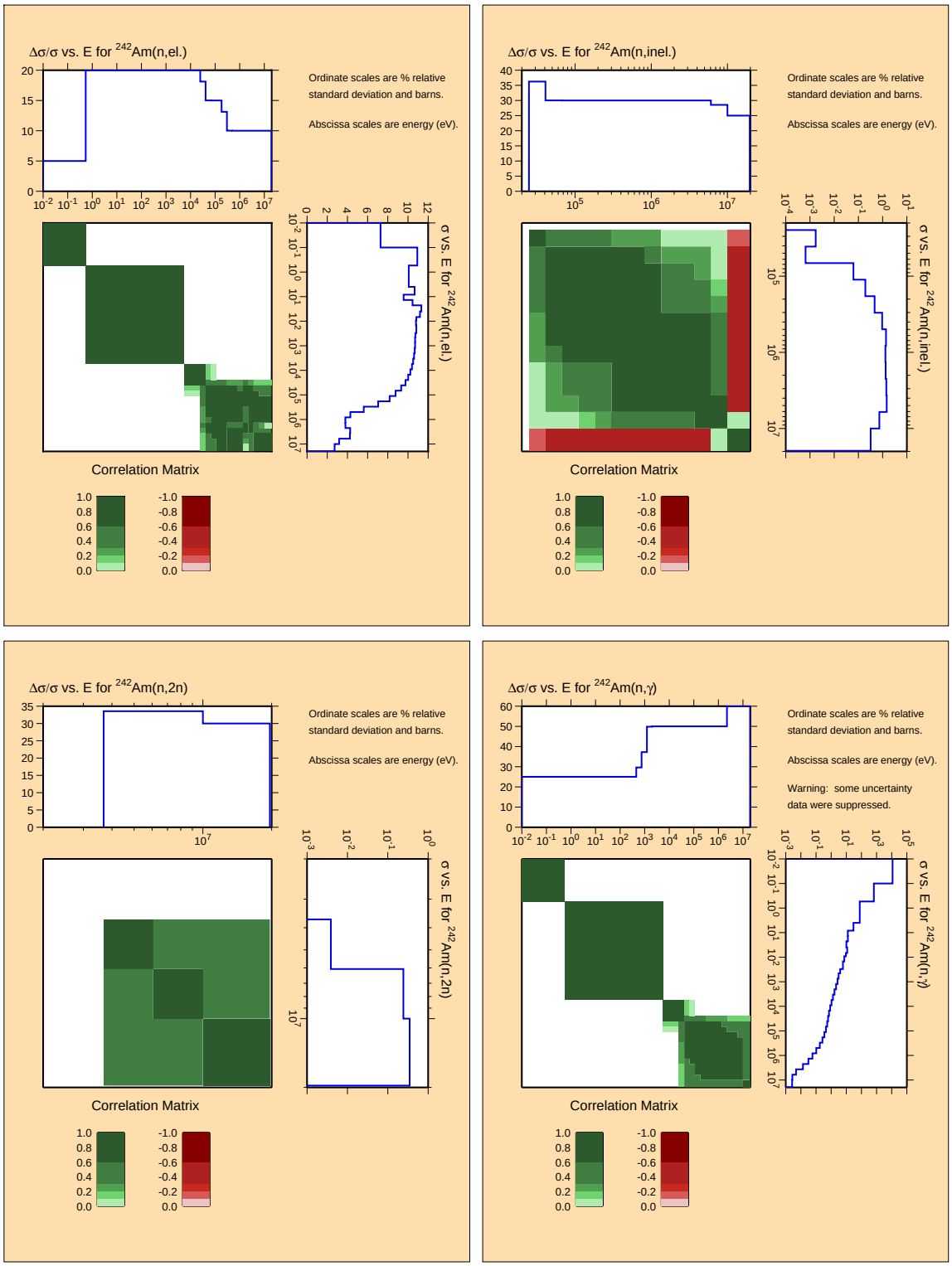

Figure C.27: Covariances for actinide ^{242m}Am.

^{242m}Am

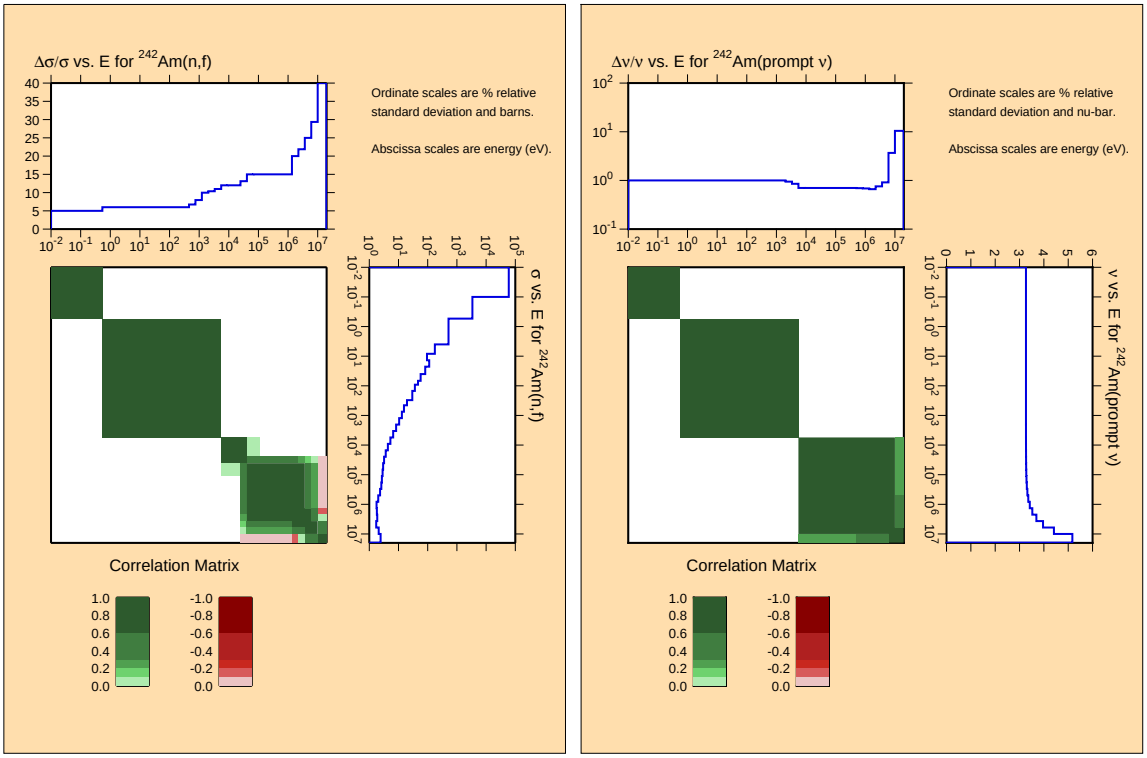

Figure C.28: Covariances for actinide ^{242m}Am (continued).

^{243}Am

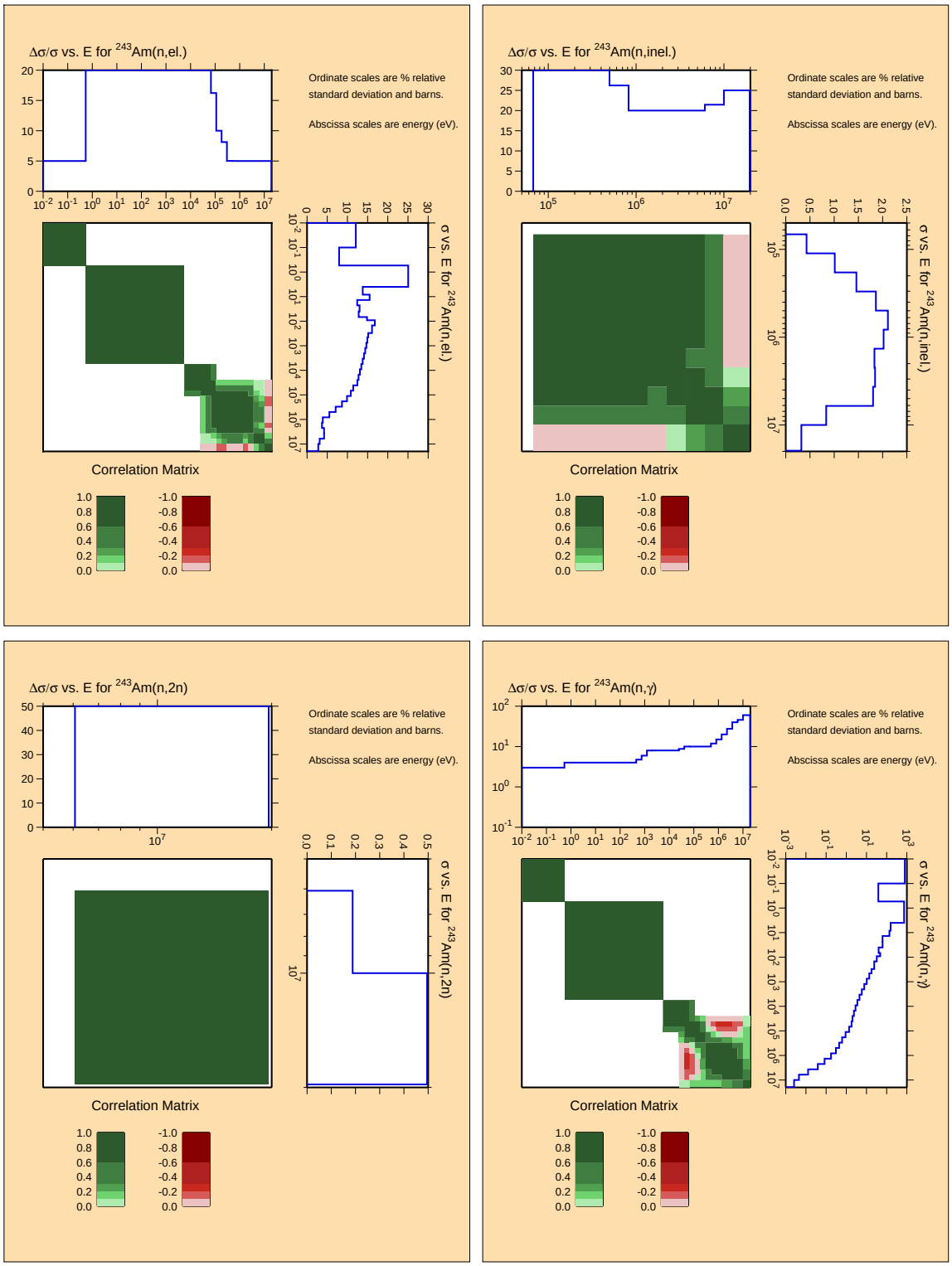

Figure C.29: Covariances for actinide ^{243}Am.

^{243}Am

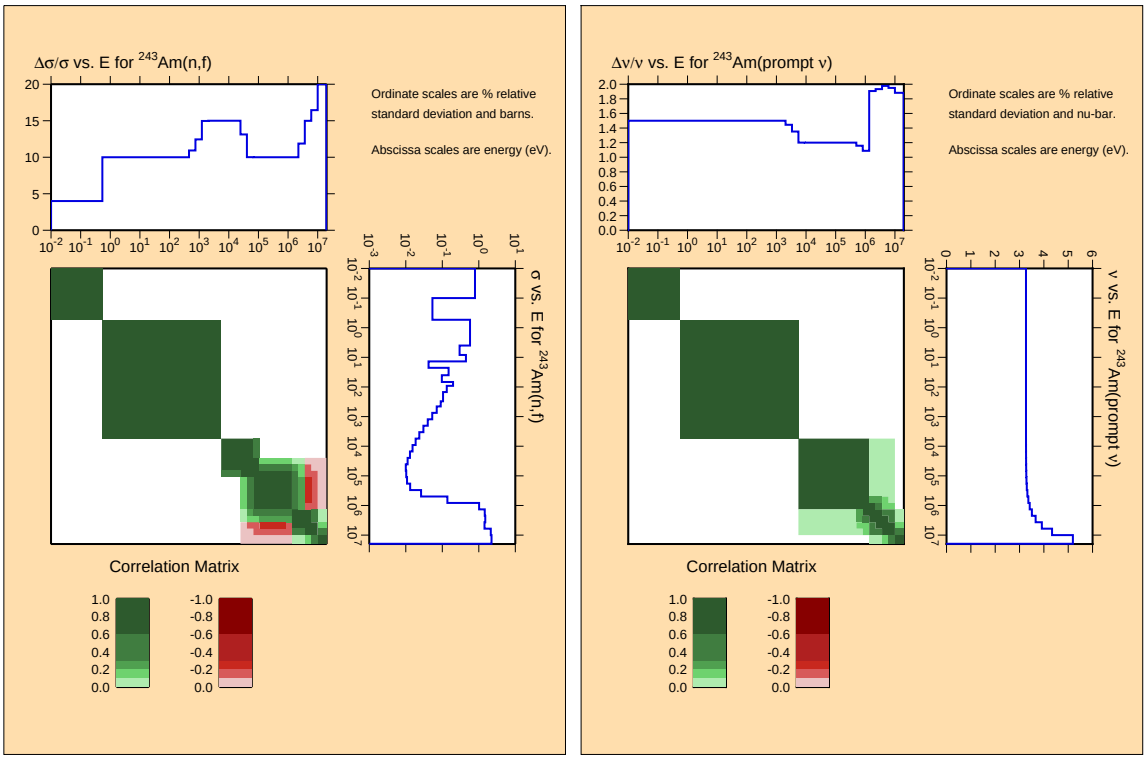

Figure C.30: Covariances for actinide ^{243}Am (continued).

^{242}Cm

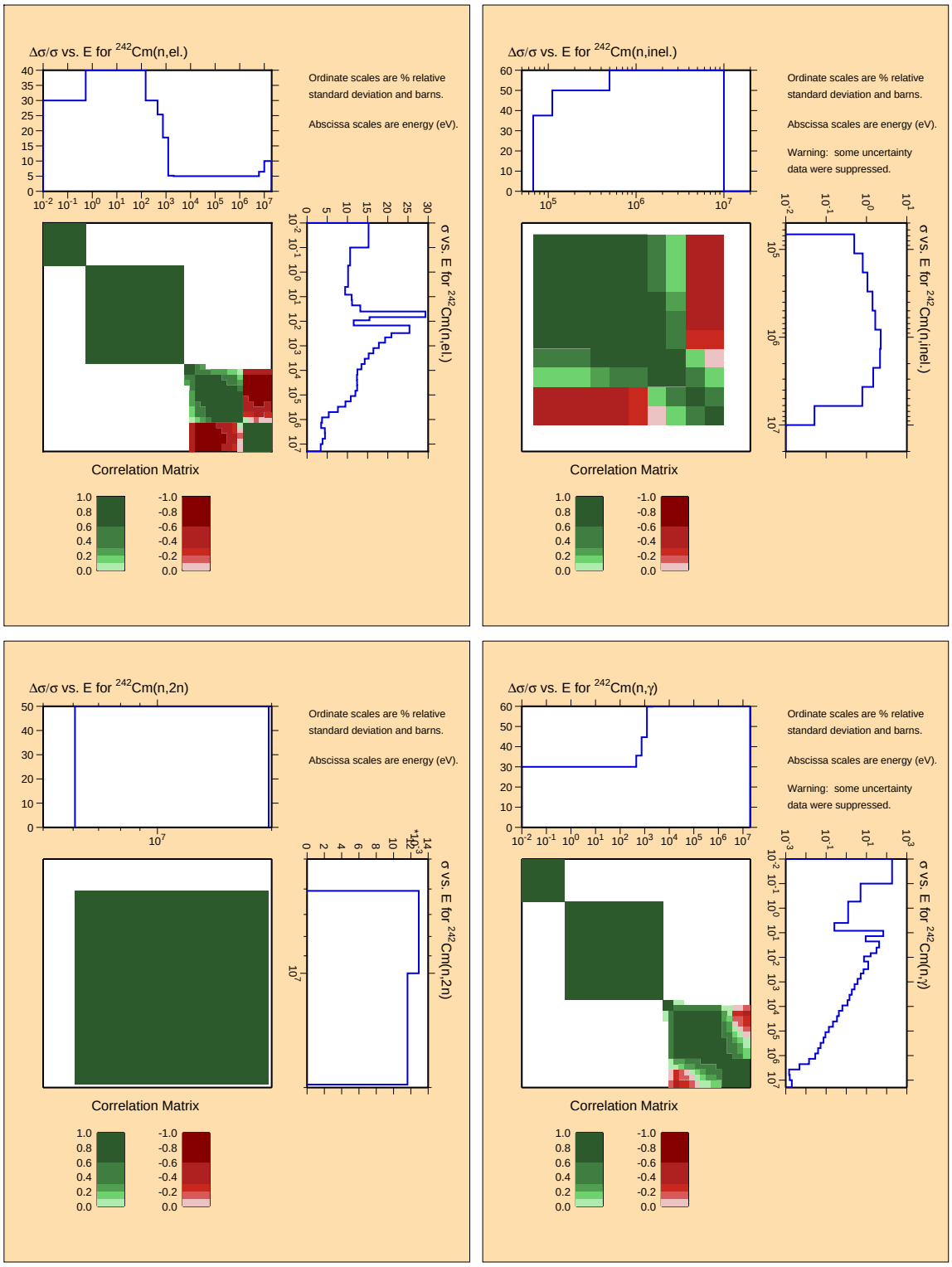

Figure C.31: Covariances for actinide ^{242}Cm.

^{242}Cm

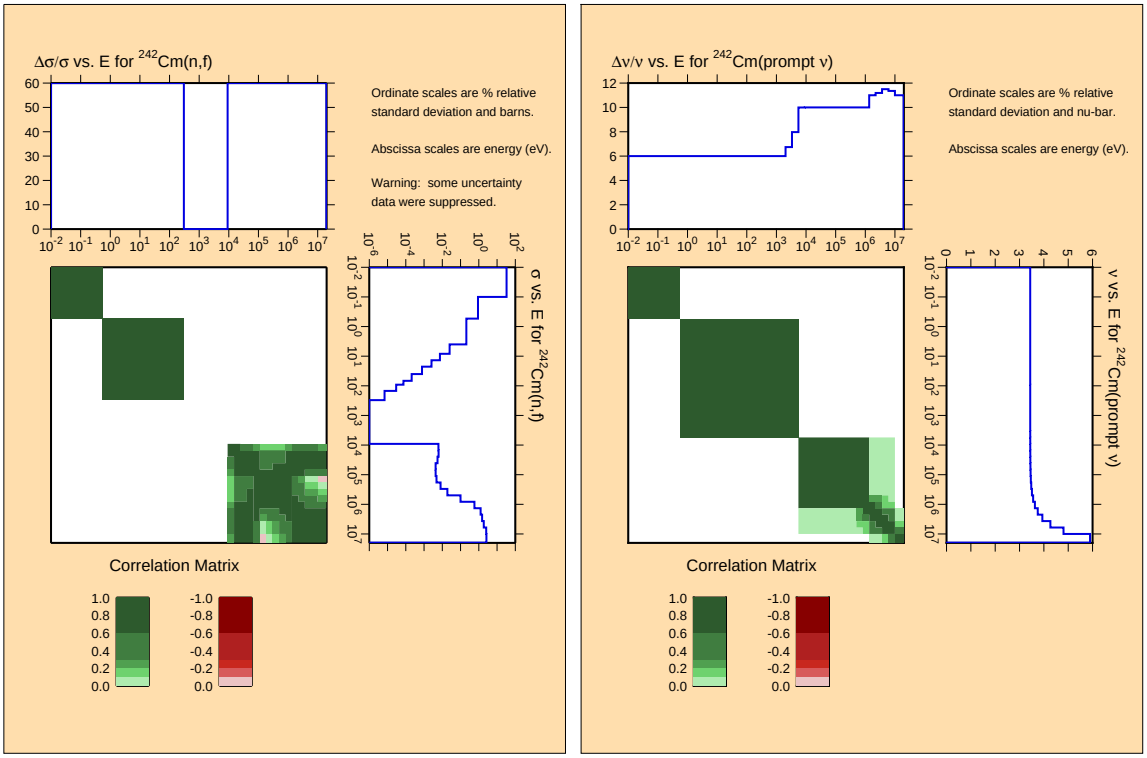

Figure C.32: Covariances for actinide ^{242}Cm (continued).

^{243}Cm

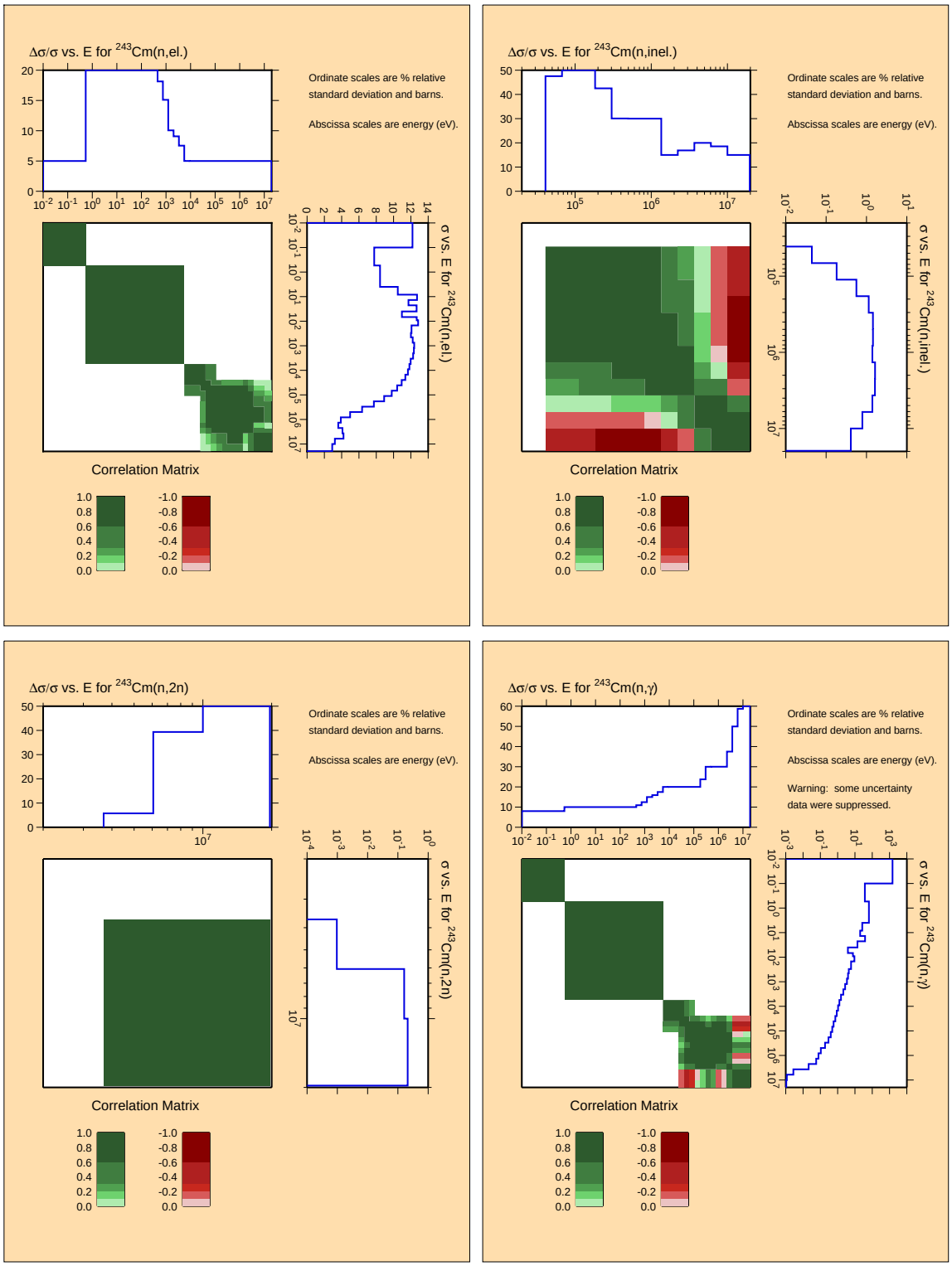

Figure C.33: Covariances for actinide ^{243}Cm.

^{243}Cm

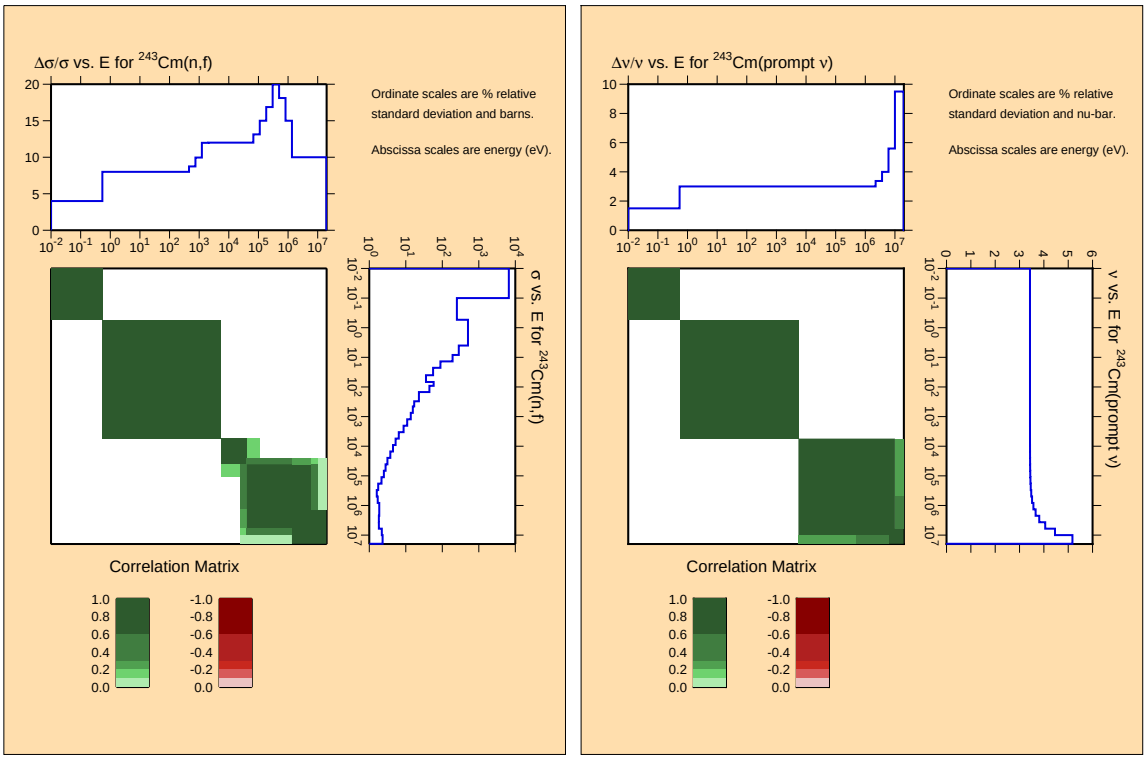

Figure C.34: Covariances for actinide ^{243}Cm (continued).

^{244}Cm

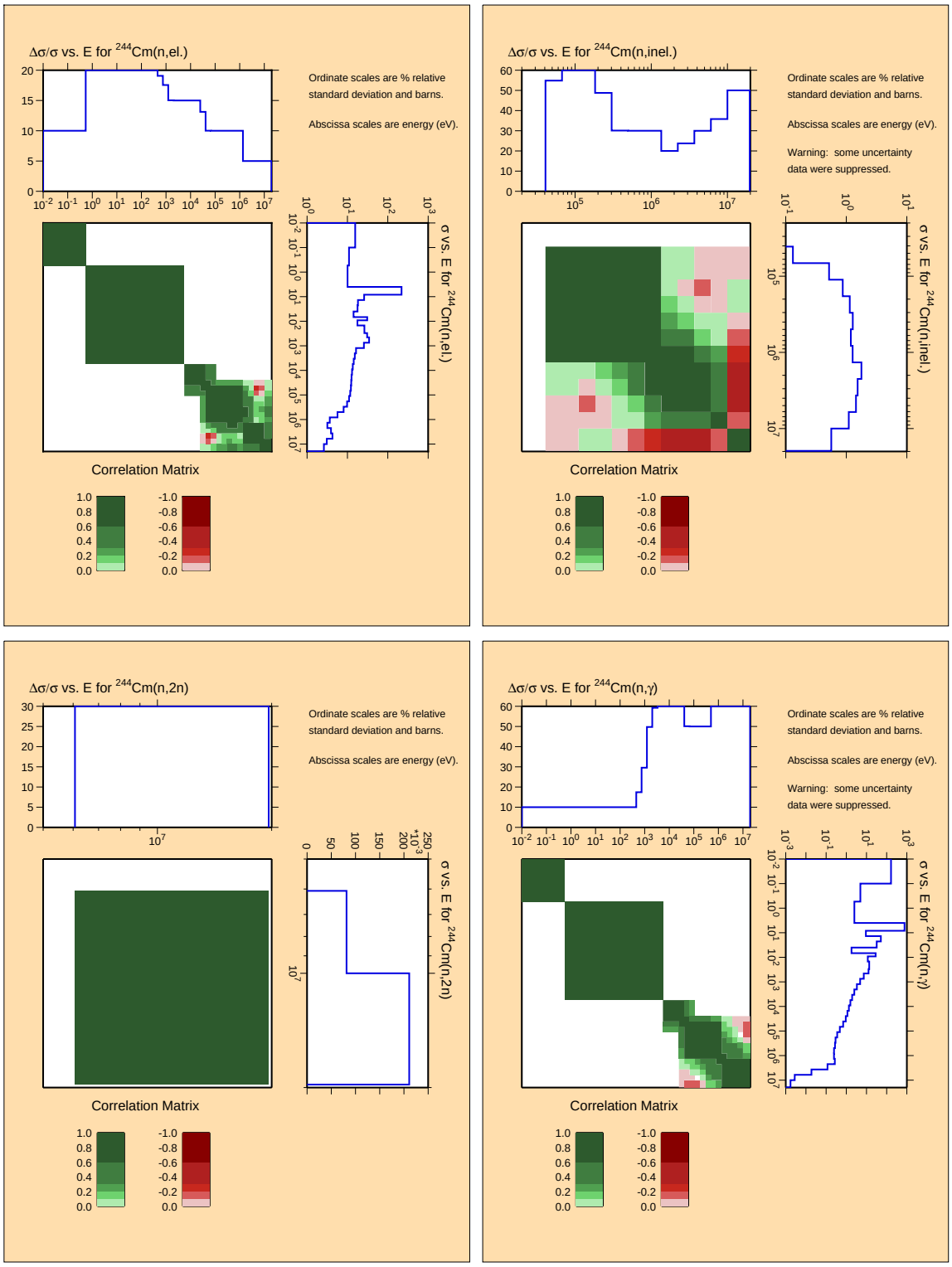

Figure C.35: Covariances for actinide ^{244}Cm.

^{244}Cm

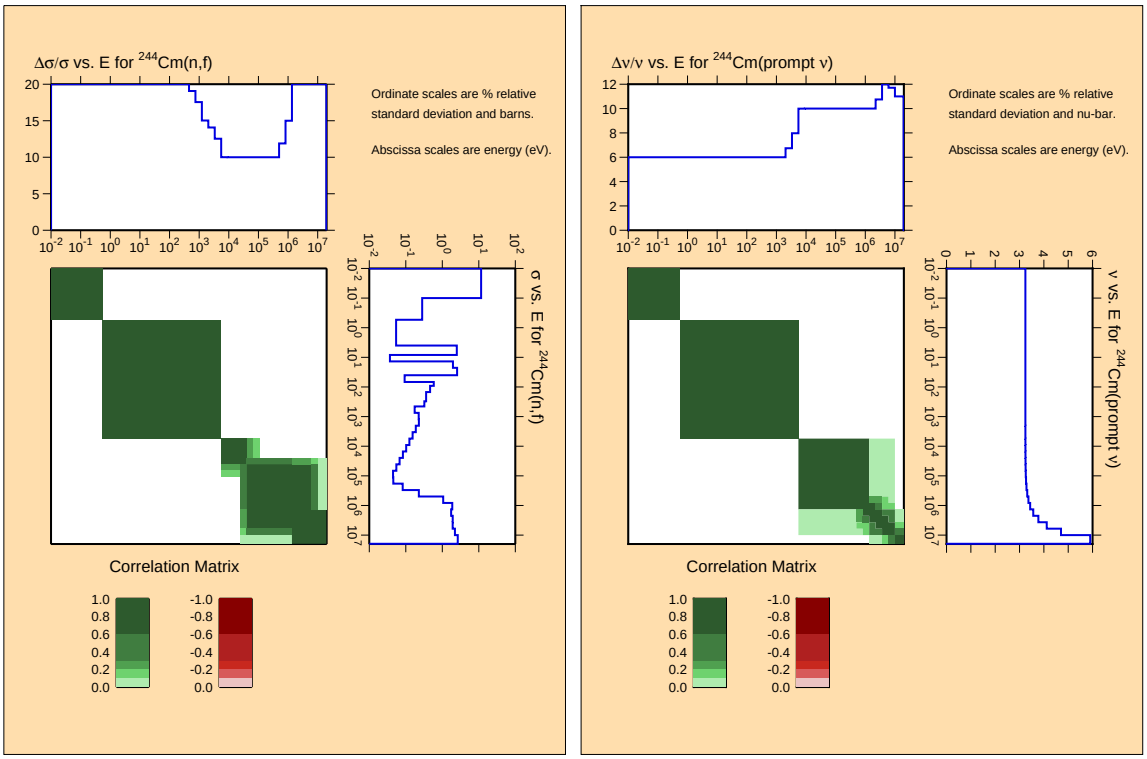

Figure C.36: Covariances for actinide ^{244}Cm (continued).

^{245}Cm

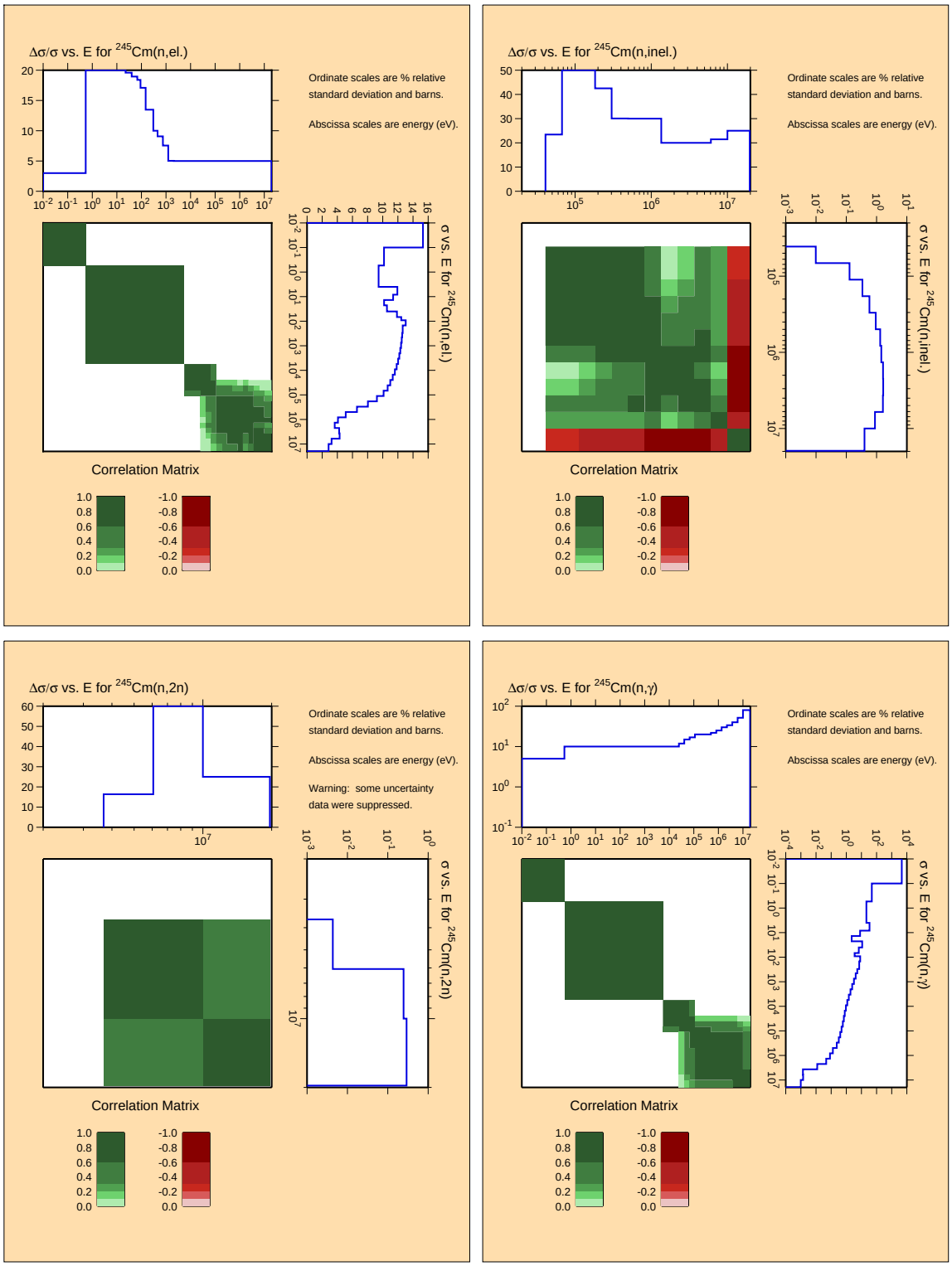

Figure C.37: Covariances for actinide ^{245}Cm.

^{245}Cm

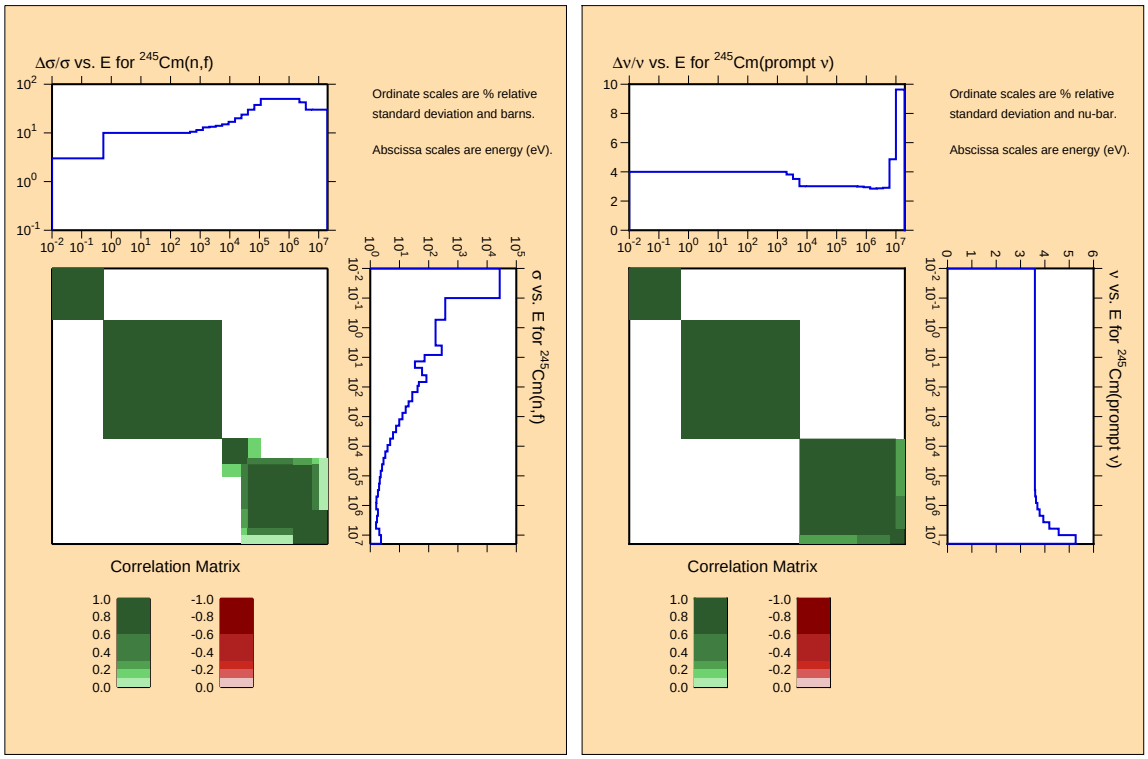

Figure C.38: Covariances for actinide ^{245}Cm (continued).

^{246}Cm

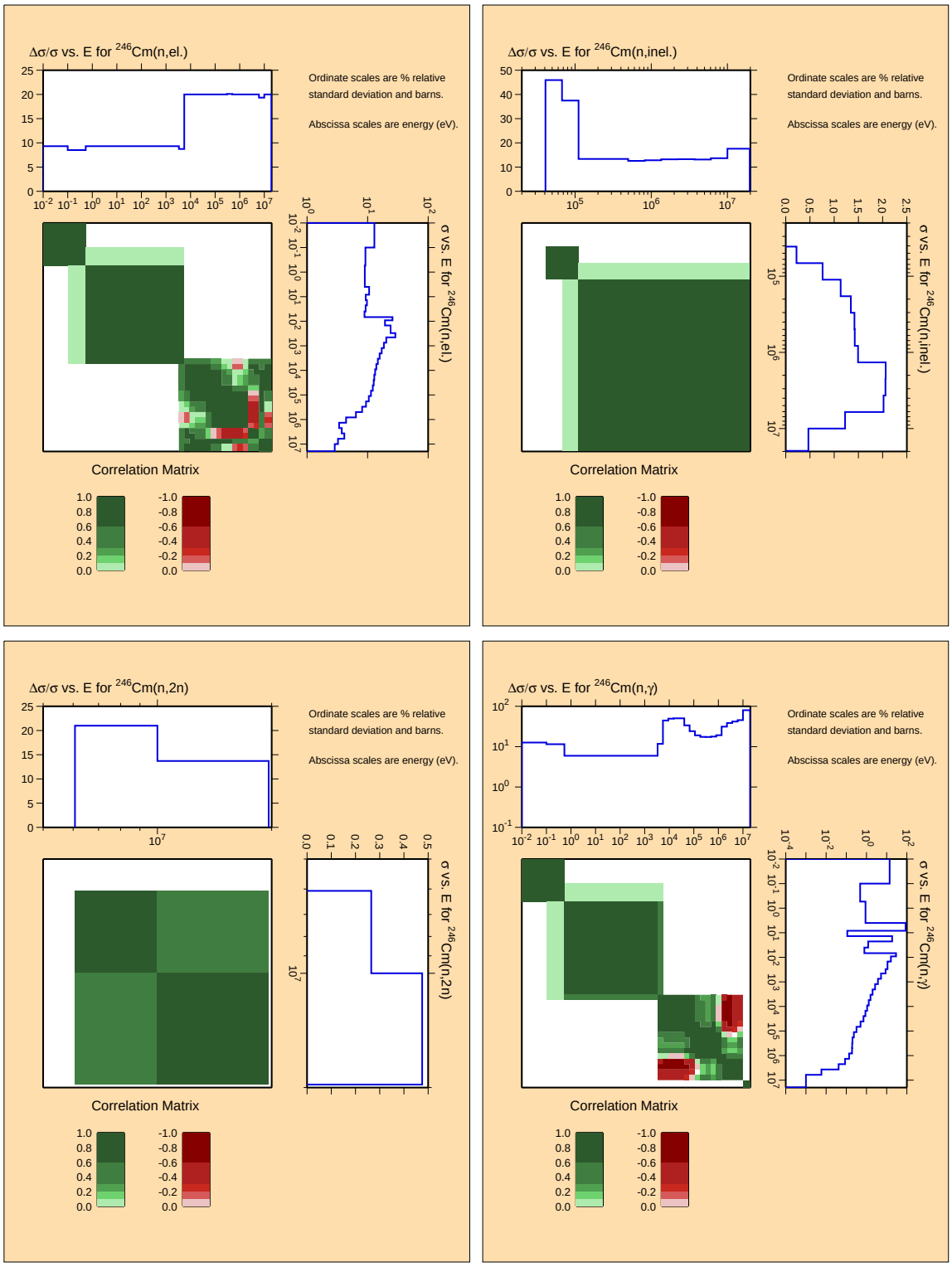

Figure C.39: Covariances for actinide ^{246}Cm.

^{246}Cm

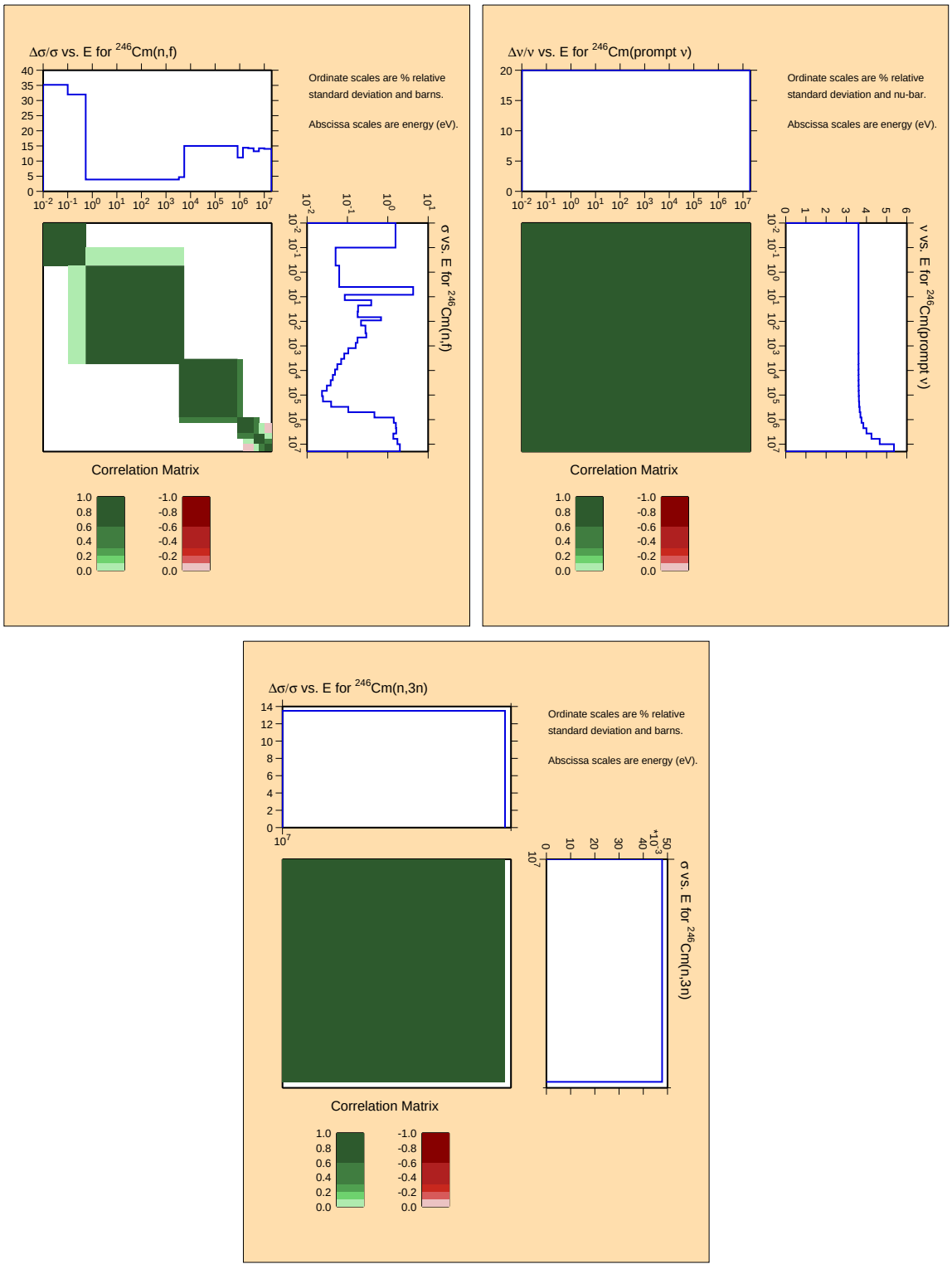

Figure C.40: Covariances for actinide ^{246}Cm (continued).

^{238,239,240}Pu

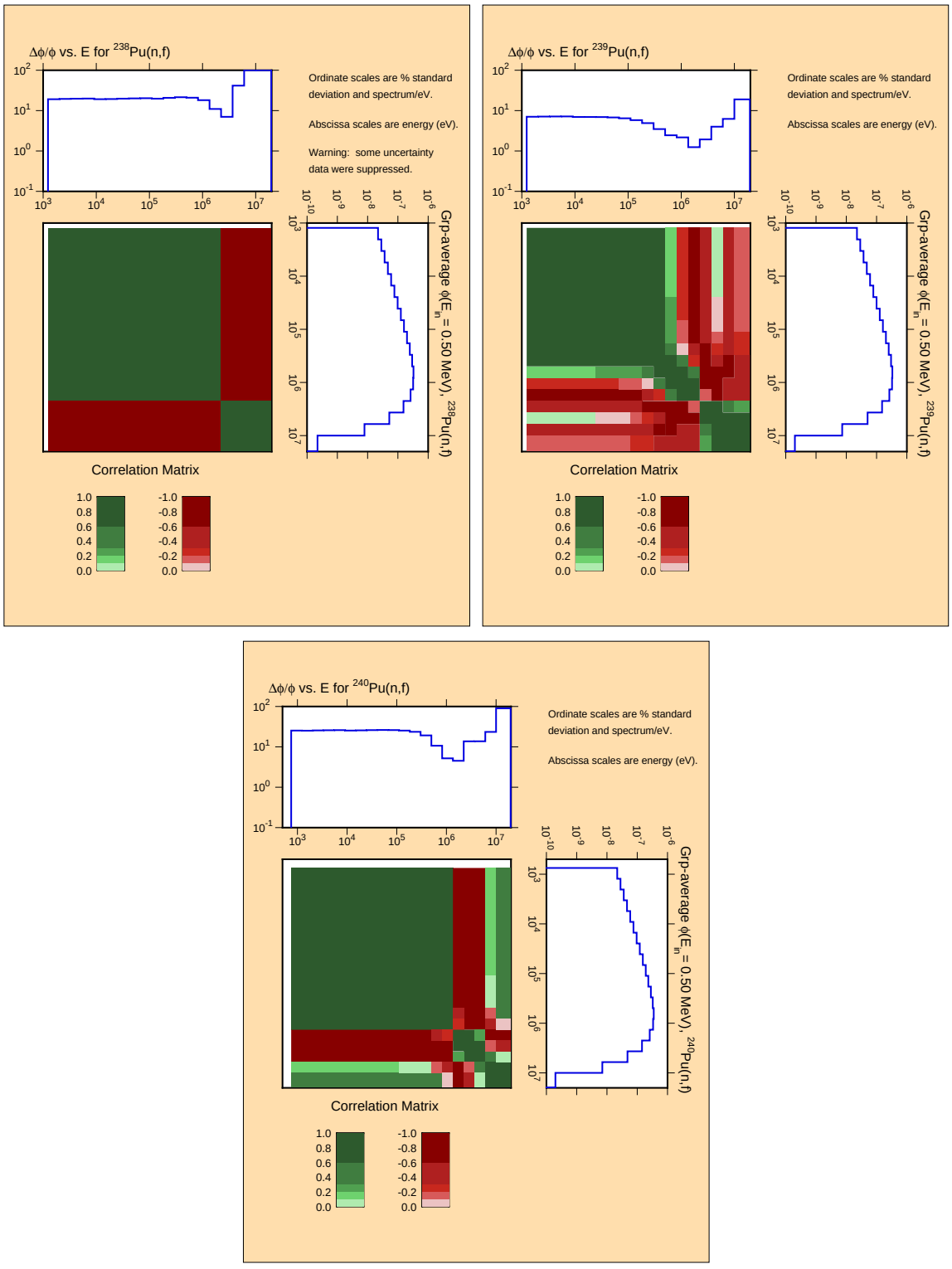

Figure C.41: Covariances for prompt fission neutron spectra.

Appendix D

AFCI 2.0 Covariances for $\bar{\mu}$

(2 materials)

^{23}Na ^{56}Fe

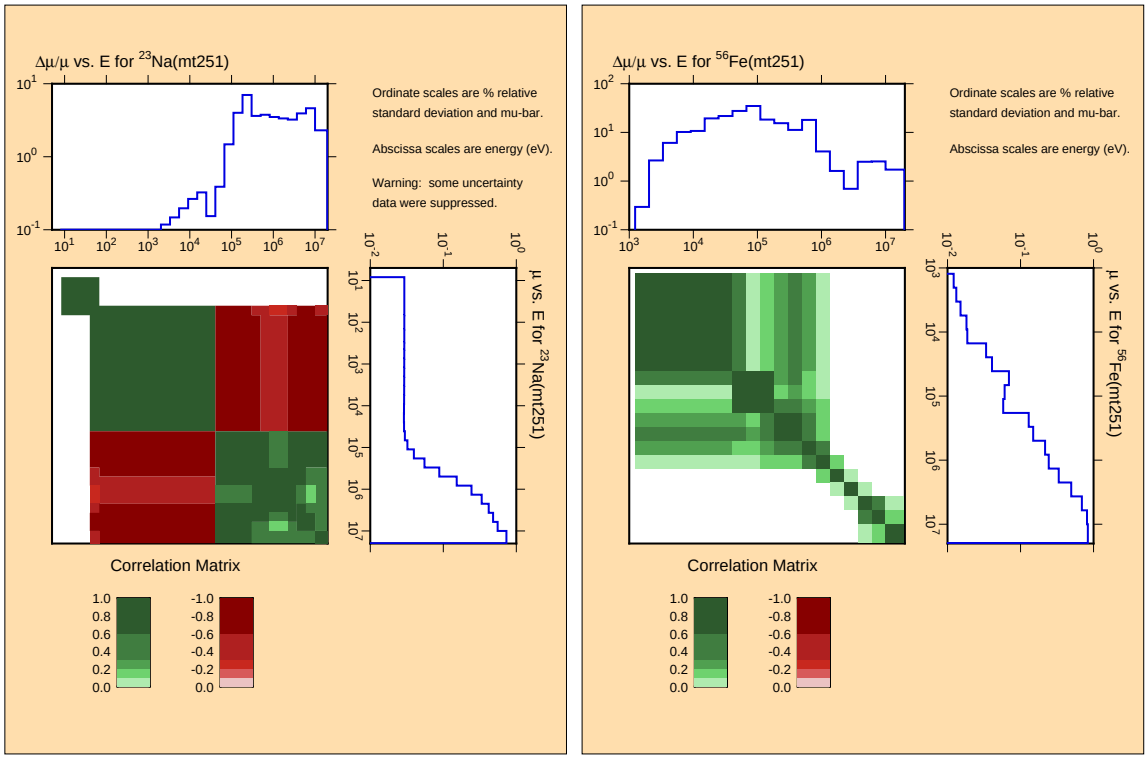

Figure D.1: Covariances for $\bar{\mu}$.